ISSN (1230-0322)
2024, Vol. 74, No. 4

Food

Polish Journal of Food and Nutrition Sciences

formerly Acta Alimentaria Polonica

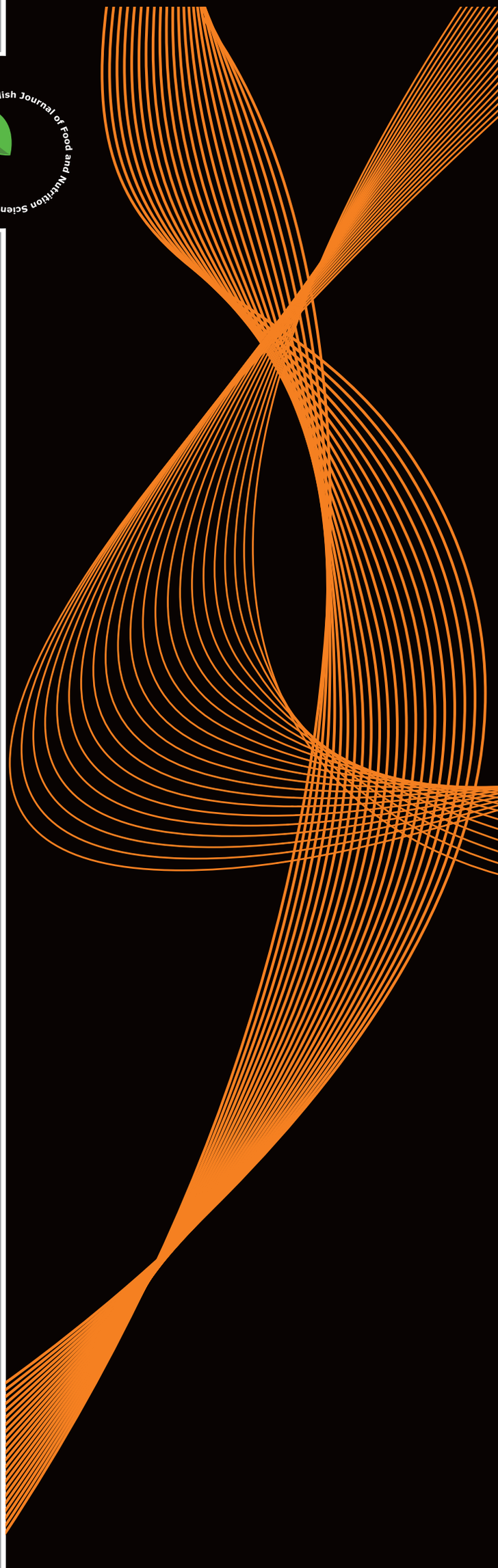

Published

by Institute of Animal Reproduction and Food Research of the Polish Academy of Sciences, Olsztyn

Published since 1957 as
Roczniki Chemii i Technologii Żywności and Acta Alimentaria Polonica (1975–1991)

SCOPE: The Journal covers fundamental and applied research in food area and nutrition sciences with a stress on interdisciplinary studies in the areas of food, nutrition and related subjects.

POLICY: Editors select submitted manuscripts in relation to their relevance to the scope. Reviewers are selected from the Advisory Board and from Polish and international scientific centres. Identity of reviewers is kept confidential.

AUTHORSHIP FORMS referring to Authorship Responsibility, Conflict of Interest and Financial Disclosure, Copyright Transfer and Acknowledgement, and Ethical Approval of Studies are required for all authors.

FREQUENCY: Quarterly – one volume in four issues (March, June, September, December).

COVERED by Web of Science, Current Contents/Agriculture, Biology & Environmental Sciences, Journal Citation Reports and Science Citation Index Expanded, BIOSIS (Biological Abstracts), SCOPUS, FSTA (formerly: Food Science and Technology Abstracts), CAS (Chemical Abstracts), AGRICOLA, AGRO-LIBREX data base, EBSCO, FOODLINE, Leatherhead FOOD RA data base FROSTI, AGRIS and Index Copernicus data bases, Biblioteka Nauki ICM, Biblioteka Narodowa – POLONA, and any www browser; ProQuest: The Summon, Bacteriology Abstracts, Immunology Abstracts.

EDITORIAL AND BUSINESS CORRESPONDENCE: Submit contributions (see Instructions to Authors) and address all communications regarding subscriptions, changes of address, etc. to:

CORRESPONDENCE TO: Ms. Joanna Molga
Polish Journal of Food and Nutrition Sciences
Institute of Animal Reproduction and Food Research
of Polish Academy of Sciences
ul. Tuwima 10, 10-747 Olsztyn, Poland
e-mail: pjfns@pan.olsztyn.pl; http://journal.pan.olsztyn.pl

Polish Journal of Food and Nutrition Sciences

ADVISORY BOARD OF PJFNS 2023–2026

Contents

ORIGINAL PAPERS

covered by CURRENT CONTENTS/AGRICULTURE, BIOLOGY & ENVIRONMENTAL SCIENCES, JOURNAL CITATION REPORTS AND SCIENCE CITATION INDEX EXPANDED, BIOSIS, SCOPUS, IFIS Publishing and CAS abstracts, and AGRO-Librex, FROSTI, PSJC, AGRIS and Index Copernicus data bases

Subscription
2024 – One volume, four issues per volume. Annual subscription rates are: Poland 150 PLN, all other countries 80 EUR. Prices are subject to exchange rate fluctuation. Subscription payments should be made by direct bank transfer to Bank Gospodarki Żywnościowej, Olsztyn, Poland, account No 17203000451110000000452110 SWIFT code: GOPZPLWOLA with corresponding banks preferably. Subscription and advertising offices at the Institute of Animal Reproduction and Food Research of Polish Academy of Sciences, ul. J. Tuwima 10, 10-747 Olsztyn, Poland, tel./fax (48 89) 5234670, fax (48 89) 5240124, e-mail: pjfns@pan.olsztyn.pl; http://journal.pan.olsztyn.pl

Zamówienia prenumeraty: Joanna Molga (e-mail: pjfns@pan.olsztyn.pl)

Wersja pierwotna (referencyjna) kwartalnika PJFNS: wersja papierowa (ISSN 1230–0322)
Nakład: 70 egz.; Ark. wyd. 17; Ark. druk. 15
Skład i druk: ITEM

ORIGINAL ARTICLE
http://journal.pan.olsztyn.pl

Polish Journal of Food and Nutrition Sciences
2024, Vol. 74, No. 4, 313–322
DOI: 10.31883/pjfns/194599
ISSN 1230-0322, e-ISSN 2083-6007

Antioxidant Properties, Texture and Sensory Quality of Sliced Bread Enriched with Leaf Powder from Mango (*Mangifera indica*)

Mónica Pirca-Palomino[1], Yvette I. Malange[2], Fernando Ramos-Escudero[2,3], Ana M. Muñoz[2,4], Keidy Cancino-Chávez[2*]

[1]Career in Agroindustrial Engineering and Agribusiness, Engineering Faculty, San Ignacio de Loyola University, Av. La Fontana 550, 15024 Lima, Perú
[2]Nutrition, Health, Functional Foods and Nutraceuticals Research Unit, San Ignacio de Loyola University (UNUSAN-USIL), Av. La Fontana 550, 15024 Lima, Perú
[3]Career in Nutrition and Dietetic, Health Sciences Faculty, San Ignacio de Loyola University, Av. La Fontana 550, 15024 Lima, Perú
[4]Food Science and Nutrition Institute, San Ignacio de Loyola University (ICAN-USIL), Campus Pachacamac, Sección B, Parcela 1, Fundo La Carolina, Pachacamac, 15823 Lima, Perú

Mango leaf (*Mangifera indica* L.) is used in traditional medicine and more recently in food applications due to its bioactive compounds that promote healthy effects. The objectives of the present study were to develop a sliced bread (SB) enriched with leaf powder from three mango varieties (Kent, Criollo and Edward) and evaluate the total phenolic content, total flavonoid content and antioxidant capacity. The effect of mango leaf powder on the sensory, textural and chromatic parameters of SB was also assessed. The results showed that bread enriched with mango leaf powder (replacing 2%, 6% and 10% of wheat flour in a bread recipe) compared to control SB had a higher total phenolic content (1.16 to 4.03 mg GAE/g) and antioxidant capacity in the DPPH assay (0.15 to 0.76 µmol TE/g) and in the ferric ion-reducing antioxidant power (FRAP) assay (2.33 to 5.36 µmol $FeSO_4$/g). Values of chromatic parameters such as lightness (L^*) decreased from 59.10 to 40.71, when the mango leaf powder percentage in bread increased due to the presence of pigments such as chlorophylls (0.54 to 0.69 mg/g) and carotenoids (2.04 to 2.48 mg/g). Among enriched breads, SBs with 2% mango leaf powder obtained the highest sensory panel scores in terms of color, flavor and odor. The enriched breads were characterized by lower hardness, chewiness and gumminess compared to the control bread. In conclusion, it can be stated that sliced bread enriched with mango leaf powder can be an excellent potential resource of bioactive compounds.

Keywords: antioxidant capacity, bakery product, bread fortification, chromatic parameters, functional food, mango by-product

INTRODUCTION

The mango (*Mangifera indica* L.) belongs to the Anacardiaceae family, it is cultivated in the tropical areas, with temperature being an important factor in its growth and development. Currently, mango is the most consumed fruit worldwide, called the "King fruit" [Jahurul *et al*., 2015]; likewise, it is the third most traded tropical fruit in terms of volume [FAO, 2023]. In Peru, the largest production of mangoes for export is concentrated in the geographical area of Piura. Among them is the Criollo variety, intended for the production of pulp and concentrated juices, and the Haden, Kent, Tommy Atkins and Edward varieties, intended for consumption as fresh fruit. The main export countries of Peruvian mango, for the period 2023/24, were the Netherlands (40% of national production) followed by the United States (30%), Spain (8%), the United Kingdom (6%) and others (16%) [Agencia Agraria de Noticias, 2024]. However, mango leaves are considered

***Corresponding Author:**
e-mail: kcancino@usil.edu.pe, kdcancino@yahoo.com (K. Cancino-Chávez)

Submitted: 28 May 2024
Accepted: 14 October 2024
Published on-line: 4 November 2024

waste material generated mainly by pruning, but they are an important resource for their health benefits due to the abundance of phytochemicals such as mangiferin, phenolic acids, benzophenones, flavonoids, ascorbic acid, carotenoids, tocopherols and chlorophylls [Kumar *et al*., 2021]. These phytochemicals foster high potential in terms of biological and pharmacological activities such as antioxidant, antidiabetic, anti-inflammatory, antimicrobial, antiviral, immunomodulatory, antiobesity, antiallergic, antifungal, antiparasitic, antipyretic, hepatoprotective, antimicrobial, antidiarrheal, antitumor, and others [Batool *et al*., 2018]. Among them, phenolic compounds are very important. Different epidemiological and experimental studies have demonstrated the protective effect of polyphenols against chronic diseases such as cancer, diabetes as well as cardiovascular and neurodegenerative diseases [Rasouli *et al*., 2017]. Polyphenols modulate numerous physiological processes, such enzyme activity, cell proliferation, signal transduction pathways and cellular redox potential to fight chronic pathologies [Luca *et al*., 2020].

Bread is a widely consumed food and is part of an everyday diet in different populations around the world. Making bread basically includes wheat flour, water and a small amount of salt. The impact of industrialization on bread making has allowed the addition of other materials such as food additives and yeast to improve bread quality characteristics. Currently, there is a great interest in the enrichment of formulations with various plant flours in order to improve bread nutritional and bioactive properties. The partial replacement of wheat flour with plant-based ingredients has favorably contributed to the increased contents of protein, polyunsaturated fatty acids, polyphenols, plant pigments, and enhanced bioactivity, *e.g.*, antioxidant capacity [Amoah *et al*., 2022; Kowalski *et al*., 2020].

Kumar *et al*. [2021] considered the mango leaf powder as a potential resource for the development of functional foods due to the bioactive potential. However, there are few research works that have used this by-product as a partial substitute in food products [Yelwande e*t al*., 2022]. An approach to the utilization of mango leaves is based on the development of functionalized edible films made of chitosan/starch with a mango leaf extract, and the development of sustainable preservatives to avoid the perishability of climacteric fruits [Cejudo e*t al*., 2023; Majeed *et al*., 2024].

Therefore, the main objective of the research carried out was to develop a sliced bread (SB) enriched with mango leaf powder (MLP) with enhanced antioxidant capacity and increased phenolic compound content, as well as acceptable sensory and texture properties.

MATERIALS AND METHODS

Plant materials

Leaves of three varieties (Criollo, Kent, and Edward) of *Mangifera indica* L. were collected between February and March 2022 at fruit farms of the Association of Mango Producers of the province of Chulucanas (Piura, Peru). GPS coordinates of the leaf collection site were 5°5'43.692"S and 80°10'10.56"W; at an altitude of 92 m above sea level. Approximately 7 kg of young leaves were taken from the bottom of 6 trees for each mango variety studied.

Mango leaf powder preparation

The preliminary post-harvest operations consisted of leaf selection, washing, disinfection and drying at 60°C for 4 h using a commercial dryer with 15 stainless steel trays. Disinfection was carried out by immersing the leaves for 10 min in a diluted solution (5 mL/L of water) of Bio Organic® (Econo Group E.I.R.L, Lima, Perú). The leaves were then milled using a blade mill with a sieve of 0.5 mm in diameter. The MLP was packed in polythene bags and stored until it was used to produce SB and for chemical analysis.

Sliced bread preparation

Sliced breads (SBs) were prepared with wheat flour (control) and with partial replacement of wheat flour (2%, 6%, and 10%) with MLP. In addition to wheat flour (42%, 46%, 50% and 52%) and MLP (10%, 6%, 2% and 0%, respectively), the breads were made of milk (35%), sugar (2%), yeast (1%), butter (9%), and salt (1%). MLP was mixed with the dry ingredients and then with the rest of the ingredients. The kneading time was 8 min. The dough was then left to rest in containers until doubling in size, *i.e.*, for about 1 h. Subsequently, the dough was placed in the stainless-steel molds of 25×11×6 cm, fermented for 2 h at room temperature (20°C), and then baked at 230°C for 35 min. Finally, SBs were allowed to cool to room temperature and packaged in polypropylene bags. Formulations of SB control (0% MLP); SB+Criollo (2%, 6% and 10% MLP), SB+Kent (2%, 6% and 10% MLP) and SB+Edward (2%, 6% and 10% MLP) were prepared in triplicate, and SBs were made twice – the first time for chemical and texture analyses and the second time for sensory evaluation and color measurements.

Preparation of methanolic extracts of mango leaf powder and sliced bread

For the preparation of methanolic extracts of MLP, the procedure described by Romero-Orejón *et al*. [2023] was followed with some modifications. Approximately 0.5 g of MLP was placed in 15-mL centrifuge tubes, and then 5 mL of a methanol and water mixture (70:30, *v/v*) was added. In the case of SB, 10 g was weighed into a 125-mL Erlenmeyer flask, and 50 mL of a methanol and water mixture (70:30, *v/v*) was added. The extraction was developed in two stages, the first by vortexing at the maximum speed for 30 min, and the second by ultrasound bath (CPXH 2.8 L, Bransonic, Danbury, CT, USA) at 40 kHz and 30°C for 30 min. Subsequently, the extracts were centrifuged at 4,000×g for 15 min, and the supernatant was recovered and stored at 5°C until further analyzed.

Determination of total phenolic content

The total phenolic content (TPC) was determined following the conventional method with a Folin-Ciocalteu reagent [Singleton & Rossi, 1965] with some modifications made by Martínez & Ramos-Escudero [2024]. A 50-µL aliquot of MLP or SB extract was reacted with 0.38 mL of the Folin-Ciocalteu phenol reagent (0.2 M). The reaction was developed for 5 min, and subsequently 0.38 mL of 7.5% sodium carbonate was

added. The blue color complex was allowed to develop for 2 h, after this time the absorbance readings were collected at 765 nm using an Orion™ AquaMate 8100 UV-Visible spectrophotometer (Thermo Scientific, Waltham, MA, USA). The results were expressed in mg of gallic acid equivalent *per* g of MLP or SB (mg GAE/g).

Determination of total flavonoid content

The total flavonoid content (TFC) was determined by the method described by Miliauskas *et al*. [2004] with some modifications. A 10-µL aliquot of MLP or SB extract was mixed with 0.1 mL of aluminum chloride hexahydrate (80 mM) and then diluted with 1 mL of distilled water. Absorbance readings were recorded at 415 nm after 15 min at room temperature. The total flavonoid content was expressed as mg of rutin equivalent *per* g of MLP or SB (mg RE/g).

Determination of plant pigment content

The plant pigments of the samples were determined following the methodology described by Lichtenthaler & Buschmann [2001]. Approximately 0.1 g of MLP or SB was weighed and then hydrated with 0.2 mL of water for 3 min. Then, the extraction of chlorophylls and carotenoids was developed by the addition of 5 mL of an acetone and water mixture (80:20, *v/v*). The extraction continued with stirring by vortex and ended with centrifugation at 4,000×g for 15 min. The supernatant was separated and the spectrum in the wavelength range of 400–700 nm was recorded using an Orion AquaMate 8100 UV-visible spectrophotometer (Thermo Scientific). The wavelengths selected for quantification of chlorophylls were 646 and 664 nm, whereas carotenoids were quantified at the wavelength of 470 nm. The total content of individual pigment types was calculated using equations described by Lichtenthaler & Buschmann [2001]. The total content of chlorophylls and carotenoids was expressed in mg *per* g of MLP or SB.

Determination of ferric ion-reducing antioxidant power

Ferric ion-reducing antioxidant power (FRAP) of MLP or SB was determined following the method described by Benzie & Strain [1996] with some modifications. A 0.75-mL aliquot of a solution containing a mixture of 2.5 mL of 2,4,6-tris(2-pyridyl)-*s*-triazine (10 mM in 40 mM HCl), 2.5 mL ferric chloride (20 mM), and 25 mL of sodium acetate (300 mM adjusted to pH 3.6) was added to a 2-mL Eppendorf tube, and then 0.12 mL of a previously diluted MLP or SB extract was added. Absorbance readings were collected at 593 nm. Results were expressed in µmol $FeSO_4$/g of MLP or SB.

Determination of 2,2-diphenyl-1-picrylhydrazyl radical scavenging activity

2,2-Diphenyl-1-picrylhydrazyl (DPPH) assay was carried out following the procedure described by Brand-Williams *et al*. [1995]. An amount of 10 µL of an MLP or SB extract diluted with 40 µL of a methanol and water mixture (70:30, *v/v*) was reacted with 950 µL of the DPPH radical solution (100 µM). Absorbance readings were collected at 515 nm after 10 min of reaction. DPPH radical scavenging activity was expressed as µmol Trolox equivalent *per* g of MLP or SB (µmol TE/g).

Color measurements

Color measurements of the SB crumb were carried out by image analysis following the procedure described by Zegarra *et al*. [2019]. The samples were placed in a portable photo studio (Puluz Technology Limited, Shenzhen, China) containing 64 LED lights with an output power of 30 W and a color temperature of 5,500 K. The photographic images were acquired using a digital camera (Canon, Power Shot SX60 HS, full HD 65X optical zoom, Tokyo, Japan). The photographs were saved on a memory card, and then the RGB color squares were obtained by means of the ImageJ-1.51k software (National Institutes of Health by Wayne Rasband, USA). The L^* (darkness/whiteness), a^* (greenness/redness) and b^* (blueness/yellowness) values were obtained using the color matching tool (Nix Sensor) (**https://www.nixsensor.com/free-color-converter/**), while the total color difference (ΔE) was estimated from Equation (1):

$$\Delta E = \sqrt{(\Delta L^*)^2+(\Delta a^*)^2+(\Delta b^*)^2} \quad (1)$$

where: ΔL^*, Δa^*, and Δb^* are the differences in the L^*, a^* and b^* coordinates, respectively, between SB control and SB enriched with MLP.

Evaluation of sensory properties

A sensory analysis of bread samples was conducted 3 to 5 h after baking with a panel of 15 trained judges from the academic program of food industry engineering and agribusiness, consisting of 6 men and 9 women aged 25 to 45. They evaluated attributes like color, taste, and odor for nine coded treatments, scoring preferences from 9 (best) to 1 (worst). The Friedman classification test was used for discrimination between the samples. Judges signed informed consent, and the study adhered to the ethical principles of the Declaration of Helsinki.

Texture profile analysis

Texture profile analysis (TPA) assessed attributes such as hardness, cohesiveness, springiness, adhesiveness, chewiness, and gumminess, using an analyzer from Ametek (Middleborough, MA, USA). A plexiglass probe with a 25 mm diameter and 35 mm height was employed. The settings included a pretest speed of 1.0 mm/s, a test speed of 2.0 mm/s, a firing force of 0.05 N, and 60% strain, conducted over two compression cycles with a 5-s pause. Five slices from each SB formulation, each 15 mm thick, were evaluated, with data collected at three points *per* slice. The equipment utilized TexturePro CT Advanced Edition software (21 CFR, Ametek), for data analysis.

Statistical analysis

Results were presented as the mean and standard deviation (SD). An analysis of variance (ANOVA) followed by Fisher's least

significant difference (LSD) test was used to compare means between varieties of MLP and in SBs with different formulations. Differences were considered significant at $p<0.05$. For sensory evaluation, multiple non-parametric comparisons were used using Friedman classification test and Kendall's coefficient of agreement (KCC) to measure agreement among judges; and the Newman-Keuls statistical test (N-K) was used to evaluate differences between formulations [Meilgaard *et al*., 1999; Scheff, 2016]. The statistical package STATISTICA, version 8.0 (StatSoft, Inc., Tulsa, OK, USA), was used to analyze all data.

RESULTS AND DISCUSSION

Bioactive compound contents and antioxidant capacity of mango leaf powder

The content of bioactive compounds in MLP is shown in **Table 1**. The TPC of the leaf powder from three mango varieties varied between 63.93 to 76.52 mg GAE/g, and no significant difference ($p\geq0.05$) was found between the varieties Edward and Kent; the variety Criollo was the one that presented lower value. In this regard, Fernández-Ponce *et al*. [2016] found a TPC of ~12 mg GAE/g in dehydrated mango leaves of the Kent variety, however, Sultana *et al*. [2012] found values of 86.62 and 93.18 mg GAE/g of mango leaves of Langra and Chonsa varieties, respectively. Likewise, Kingne *et al*. [2018] indicated that the state of maturity of mango leaves influenced the TPC, demonstrating that it varied between 40 to 90 mg GAE/g with the youngest leaves featuring a higher TPC content compared to the mature leaves. The results of this research demonstrate that leaves of Criollo, Kent and Edward varieties had a high TPC and when compared to other species were slightly similar to cat's claw leaves (~65 mg GAE/g), green tea (~89 mg GAE/g) [Chacaliaza-Rodríguez *et al*., 2016], leaves of different grape varieties (~27 to ~76 mg GAE/g) [Pantelić *et al*., 2017], and superior to quinoa leaves (~10 mg GAE/g), and *Erythroxylum coca* var. coca leaf (~33.02 mg GAE/g) [Chacaliaza-Rodríguez *et al*., 2016].

The TFC, in the mango leaves evaluated, was in the range of 37.36 to 65.14 mg RE/g (**Table 1**). The MLP from Criollo variety presented higher TFC compared to the Edward and Kent varieties. These results differed from the findings reported in other studies. For example, Ghosh *et al*. [2022] reported TFC of mature leaves from various mango varieties between ~0.5 and ~3.5 mg quercetin equivalent (QE)/g. In addition to using another reference than in our study (quercetin *vs*. rutin), they mentioned that the recovery capacity of the flavonoid, which is associated with the type of solvent used for extraction, influenced the determined flavonoid content of mango leaves. The extraction with methanol was more effective than the extraction with acetone and petroleum benzine, indicating that the flavonoids of mango leaves have polar characteristics. Kingne *et al*. [2018] found that the total flavonoid content of young and mature mango leaves varied from 6 to 14 mg catechin equivalent (CE)/g, thus demonstrating that the young leaves presented higher values than the mature leaves. On the contrary, Sultana *et al*. [2012] reported TFC between 76.54 and 83.67 mg CE/g of leaves for Langra and Chonsa varieties, respectively. The TFC of mango leaves of Kent, Edward and Criollo varieties, determined in our study, was superior compared to other edible leaf species, like for example, leaves of different mint species (3.65 to 16.83 mg QE/g dry weight, dw) [Ćavar Zeljković *et al*., 2021], basil (~12 mg QE/g dw), chard (~11 mg QE/g dw), parsley (~15 mg QE/g dw) and red kale (~7 mg QE/g dw) [Chandra *et al*., 2014]. The main flavonoids identified in mango leaves were catechin, rutin, kaempferol 3-*O*-rutinoside, isoquercitrin, hyperin, quercetin 3-*O*-glucoside and quercetin [Kumar *et al*., 2021; Sferrazzo *et al*., 2022].

The plant pigments, including especially carotenoids and chlorophylls, were mainly responsible for the color in MLP. The total carotenoid content ranged from 0.54 to 0.69 mg/g, while the total chlorophyll content ranged from 2.04 to 2.48 mg/g (**Table 1**). The total carotenoid content showed significant differences ($p<0.05$) between the varieties of Kent, Edward, and Criollo, while in respect to the total chlorophyll content, the varieties of Kent and Edward were statistically similar ($p\geq0.05$). Sousa [2022] have mentioned that the leaves of edible plants contain significant amounts of plant pigments, and that the most common are chlorophyll, carotenoids, and anthocyanins. In addition, plant pigments have demonstrated multiple biological effects including antitumor, anti-atherogenic, and anti-inflammatory activity [Magalhães *et al*., 2024]. Mango leaves of Kent, Edward, and Criollo varieties were slightly lower in plant pigment content than leaves of quinoa varieties, showing from ~0.64 to ~0.91 mg/g of carotenoids and from 2.02 to 3.91 mg/g of chlorophylls [Chacaliaza-Rodríguez *et al*., 2016]. Likewise, the content of total plant pigments was reported at ~0.42 to ~2.41 mg/g sample in the commercial samples of coca leaves, lemon verbena, cats' claw, and green tea [Chacaliaza-Rodríguez *et al*., 2016].

The antioxidant capacity of MLP from different mango varieties determined by the DPPH and FRAP assays is shown

Table 1. Contents of total phenolics, total flavonoids and plant pigments of leaf powders from three mango varieties.

Mango leaf powder	Total phenolics (mg GAE/g)	Total flavonoids (mg RE/g)	Total carotenoids (mg/g)	Total chlorophylls (mg/g)
var. Criollo	63.93±1.73^{b}	65.14±2.39^{a}	0.69±0.01^{a}	2.04±0.00^{b}
var. Kent	76.52±3.98^{a}	37.36±0.15^{c}	0.54±0.00^{c}	2.48±0.01^{a}
var. Edward	72.57±2.26^{a}	44.82±1.16^{b}	0.57±0.00^{b}	2.47±0.01^{a}

Values (mean ± standard deviation, $n=3$) with different letters in the same column indicate a significant difference at $p<0.05$, according to Fisher's LSD test. GAE, gallic acid equivalent; RE, rutin equivalent.

Table 2. Antioxidant capacity of leaf powders from three mango varieties.

Mango leaf powder	DPPH assay (μmol TE/g)	FRAP (μmol $FeSO_4$/g)
var. Criollo	19.09±1.33^b	80.25±1.41^c
var. Kent	47.45±2.03^a	107.71±1.50^a
var. Edward	19.75±0.64^b	84.48±2.57^b

Values (mean ± standard deviation, n=3) with different letters in the same column indicate a significant difference at p<0.05, according to Fisher's LSD test. DPPH assay, assay with 2,2-diphenyl-1-picrylhydrazyl radical; FRAP, ferric ion-reducing antioxidant power; TE, Trolox equivalent.

in **Table 2**. For the DPPH assay, values varied from 19.09 to 47.45 μmol TE/g, while the FRAP fluctuated between 80.25 to 107.71 μmol $FeSO_4$/g. Regarding antioxidant capacity, the mango leaf varieties presented the following order: Kent > Edward > Criollo. Results of the DPPH assay were similar to those determined for other edible leaves such as spinach, mustard, and moringa (21.8 to 60.6 μmol TE/g), while for chili leaves and lettuce red coral they ranged from 197.3 to 380.6 μmol TE/g [Manaois *et al*., 2020]. The antioxidant capacity of mango leaves confirmed the results of a previous study by Sferrazzo *et al*. [2022], who stated that mango leaves are an excellent source of phenolic compounds that contribute to their antioxidant properties and can scavenge free radicals.

Total phenolic content, total flavonoid content, and antioxidant capacity of sliced bread enriched with mango leaf powder

The TPC, TFC, and antioxidant capacity determined through DPPH and FRAP assays of sliced breads produced from different recipes are summarized in **Table 3**. The TPC and TFC of the control SB without MLP were 0.58 mg GAE/g and 0.08 mg RE/g, respectively, and the antioxidant capacity determined by DPPH and FRAP assays was 0.02 μmol TE/g and 0.25 μmol $FeSO_4$/g, respectively. These values were significantly (p<0.05) higher for the breads enriched with MLP and increased with increasing MLP content in the bread recipe. Moreover, it was observed that among SBs produced with the highest percentage of MLP in the recipe (10%), the MLP from Kent variety allowed obtaining the most advantageous product in terms of TPC, TFC and antioxidant capacity.

Leaves from plant sources have been used for bread fortification to achieve healthier foods rich in plant metabolites such as carotenoids, chlorophylls, and flavonoids [Amoah *et al*., 2022]. For example, quercetin and kaempferol derivatives have been detected in slices of bread enriched with pea leaf, while slices of bread enriched with lupine leaves have been found rich in chrysoeriol and genistein that could elicit health benefits, especially in the treatment of women's diseases [Klopsch *et al*., 2018; Yu *et al*., 2021]. Another report mentioned that the enrichment of bakery products with stinging nettle leaves (*Urtical dioica*) contributed to an increase in lutein, β-carotene, and total phenolics content and also in antioxidant activity [Maietti *et al*., 2021]. These findings indicate that the fortification of bakery products with plant sources improves their nutritional and functional properties.

There is a little evidence in the scientific literature on the commercial application of the use of MLP even though the MLP extract has been shown to provide excellent antioxidant capacity and antimicrobial activity towards *Pseudomonas fluorescens*, *Staphylococcus haemolyticus*, and *Staphylococcus aureus* [Sferrazzo *et al*., 2022]. On the other hand, an *in vitro* cytotoxicity study with human hepatic stellate cell (LX-2) and macrophages (U937) has not shown the evidence of cell viability at concentrations between 35 to 150 μg/mL [Sferrazo *et al*., 2022]. One approach for the use of the MLP extract in the food industry is the development of active packaging based on films composed

Table 3. Total phenolic content, total flavonoid content and antioxidant capacity of wheat flour sliced bread (SB control) and sliced breads (SB) enriched with leaf powders (replacement of 2%, 6%, and 10% of wheat flour) from three mango varieties (Criollo, Kent and Edward).

Bread	Total phenolics (mg GAE/g)	Total flavonoids (mg RE/g)	DPPH assay (μmol TE/g)	FRAP (μmol $FeSO_4$/g)
SB control	0.58±0.01^g	0.08±0.01^h	0.02±0.00^h	0.25±0.01^h
SB+Criollo 2%	1.58±0.20^e	1.91±0.33^f	0.25±0.01^f	2.79±0.00^f
SB+Criollo 6%	3.36±0.05^c	7.38±0.36^c	0.65±0.00^c	4.14±0.23^c
SB+Criollo 10%	3.62±0.05^{bc}	11.49±0.98^b	0.76±0.00^a	4.35±0.17^{bc}
SB+Kent 2%	1.29±0.06^f	0.51±0.21^{gh}	0.15±0.00^g	2.33±0.03^g
SB+Kent 6%	2.69±0.06^d	3.22±0.56^e	0.53±0.02^d	3.69±0.13^d
SB+Kent 10%	4.03±0.14^a	17.90±0.65^a	0.76±0.01^a	5.36±0.26^a
SB+Edward 2%	1.16±0.05^f	1.26±0.40^{fg}	0.16±0.05^g	2.46±0.02^g
SB+Edward 6%	2.57±0.06^d	4.35±0.31^d	0.53±0.01^d	3.68±0.12^d
SB+Edward 10%	3.71±0.20^b	7.97±0.78^c	0.72±0.03^b	4.46±0.02^b

Values (mean ± standard deviation. n=3) with different letters in the same column indicate a significant difference at p<0.05, according to Fisher's LSD test. GAE, gallic acid equivalent; RE, rutin equivalent; DPPH assay, assay with 2,2-diphenyl-1-picrylhydrazyl radical; FRAP, ferric ion-reducing antioxidant power; TE, Trolox equivalent.

Table 4. Chromatic parameters of wheat flour sliced breads (SB control) and sliced bread (SB) enriched with leaf powders (replacement of 2%, 6%, and 10% of wheat flour) from three mango varieties (Criollo, Kent and Edward).

Bread	*L**	*a**	*b**	Δ*E*
SB control	65.26±1.12^{a}	0.93±0.45^{b}	43.92±1.84^{a}	
SB+Criollo 2%	58.05±4.48^{b}	1.67±1.17^{b}	31.41±3.93^{d}	15.23
SB+Criollo 6%	49.79±3.08^{cd}	4.22±1.58^{a}	41.97±1.77^{ab}	16.06
SB+Criollo 10%	40.71±4.82^{f}	4.55±1.34^{a}	35.66±3.30^{c}	26.32
SB+Kent 2%	51.79±2.64^{c}	1.43±0.79^{b}	33.56±3.35^{cd}	17.47
SB+Kent 6%	48.01±3.30^{cd}	1.17±0.78^{b}	40.63±2.58^{ab}	17.71
SB+Kent 10%	45.64±5.90^{de}	−1.85±2.08^{c}	39.44±4.22^{b}	21.07
SB+Edward 2%	59.10±5.50^{ab}	0.11±1.06^{bc}	32.25±1.40^{cd}	13.90
SB+Edward 6%	52.34±2.49^{c}	2.13±2.34^{b}	32.87±1.99^{cd}	17.33
SB+Edward 10%	42.60±6.93^{ef}	1.20±2.30^{b}	39.04±3.87^{b}	23.36

Values (mean ± standard deviation, n=10) with different letters in the same column indicate a significant difference at p<0.05, according to Fisher's LSD test. *L**, darkness/whiteness; *a**, greenness/redness; *b**, blueness/yellowness; Δ*E*, total color difference.

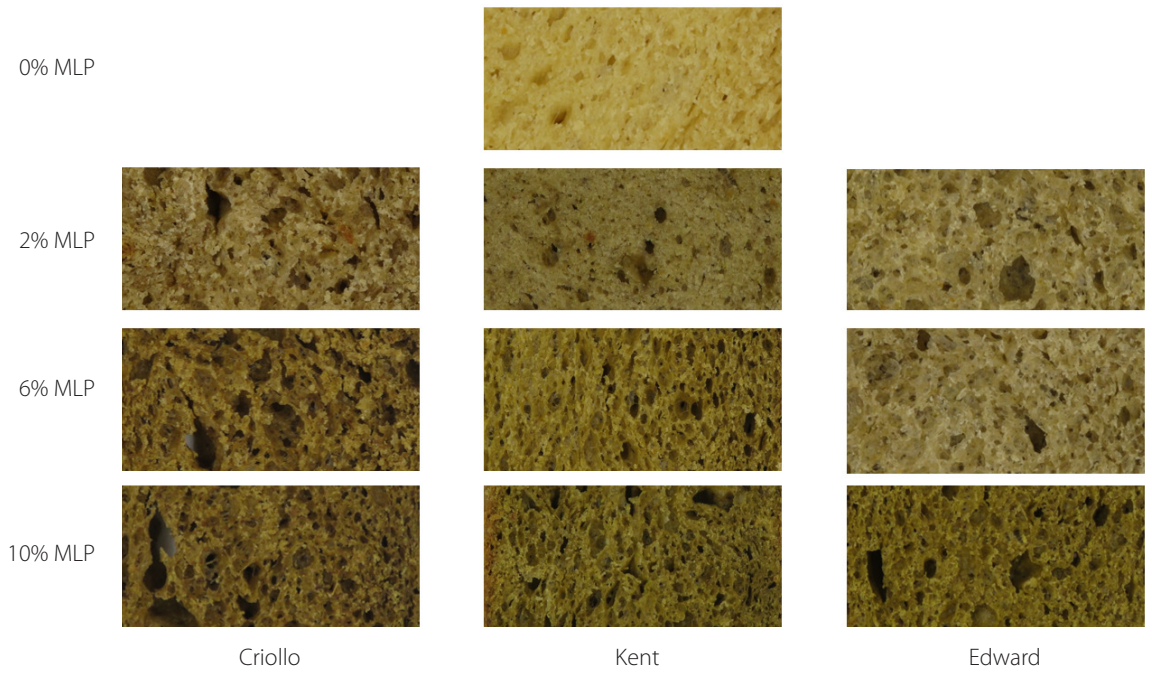

Figure 1. Appearance of wheat flour sliced bread (control, 0% MLP) and sliced breads enriched with MLP (replacement of 2%, 6%, and 10% of wheat flour) from three mango varieties (Criollo, Kent and Edward). MLP, mango leaf powder.

of polymers and polyphenols of MLP for the extension of the shelf life of food products [Cejudo-Bastante *et al.*, 2021, 2022].

Chromatic parameters of sliced bread enriched with mango leaf powder

Color is one of the most important parameters in determining the acceptability of food by consumers. The chromatic parameters of SB enriched with MLP are shown in **Table 4**, and photos showing SB appearance are presented in **Figure 1**. Lightness was higher for SB control (65.26) in comparison with SBs enriched with MLP (40.71 to 59.10). However, the SB+Edward 2% did not differ significantly (p≥0.05) from SB control. *L** values of SB enriched with 2% MLP ranged from 51.79 to 59.10, while those of SB with 6% MLP ranged from 48.01 to 52.34. The color of the SB darkened with increasing percentage of MLP in the bread recipe. This relationship was also observed in biscuits enriched with 1% and 2% of *Spirulina* biomass with *L** values of 42.86 and 36.62, respectively [Şahin, 2020]. The reduction

Table 5. Sensory scores of sliced breads (SB) enriched with leaf powders (replacement of 2%, 6%, and 10% of wheat flour) from three mango varieties (Criollo, Kent and Edward).

Bread	Sum of color attribute ranks	Color	Sum of taste attribute ranks	Taste	Sum of odor attribute ranks	Odor
SB+Criollo 2%	108	7.20 ± 2.04^{a}	109	7.26 ± 2.34^{a}	86	5.80 ± 2.56^{ab}
SB+Kent 2%	113	7.53 ± 1.40^{a}	97	6.46 ± 1.99^{ab}	92	6.13 ± 2.58^{ab}
SB+Edward 2%	113	7.53 ± 1.88^{a}	103	6.86 ± 2.09^{a}	113	7.53 ± 1.84^{a}
SB+Criollo 6%	78	5.20 ± 2.33^{b}	91	6.06 ± 1.98^{abc}	77	5.13 ± 2.69^{bc}
SB+Kent 6%	71	4.73 ± 1.38^{b}	73	4.86 ± 2.16^{bcd}	76	5.20 ± 2.62^{bc}
SB+Edward 6%	72	4.80 ± 1.61^{b}	67	4.46 ± 1.95^{cde}	59	4.00 ± 2.32^{bc}
SB+Criollo 10%	34	2.26 ± 1.16^{c}	54	3.60 ± 1.99^{de}	59	3.93 ± 2.21^{bc}
SB+Kent 10%	56	3.73 ± 1.75^{b}	42	2.80 ± 1.89^{e}	66	4.40 ± 2.16^{bc}
SB+Edward 10%	30	2.00 ± 1.30^{c}	39	2.60 ± 1.95^{e}	45	3.00 ± 1.55^{c}
Friedman X^2		71.804		49.546		29.958
p-value*		0.000		0.000		0.0002
KCC		0.569		0.371		0.249

Results are expressed as mean ± standard deviation. Mean with different letters in the same column indicates a significant difference ($p<0.05$) according to the Newman-Keuls test. *Friedman's rank test. KCC, Kendall's coefficient of concordance.

in lightness affected the other color parameters. The chromatic coordinate *a** ranged from 0.93 (SB control) to 4.55 (SB+Criollo 10%) except for the formulation SB+Kent 10% that presented a negative value (–1.85) (**Table 4**). The *a** value was significantly ($p<0.05$) higher compared to the control only for two samples (SB+Criollo 6% and SB+Criollo 10%). The value of *a** did not differ significantly ($p\geq0.05$) between most of samples. In this section, it is important to emphasize that the MLP color presented negative *a** values ranging from –6.98 to –9.75 (data no shown), indicating a greenish color. It is possible that the positive *a** values of most SBs were due to the depletion of plant pigments; hence, the formation of pheophytin [Klopsch *et al*., 2018]. For the chromatic parameter *b**, it was observed to be lower in SBs with MLP (31.41 to 41.97) compared to the control SB (43.92). These results are consistent with those reported by Cacak-Pietrzak *et al*. [2023] who found a decrease in *b** values when 1% to 6% of freeze-dried pomace from black chokeberry (*Aronia melanocarpa* L.) was added to bread. The same decrease was observed in food matrices rich in chlorophyll as in biscuits enriched with *Spirulina* biomass, while biscuits enriched with *Dunaliella* biomass rich in β-carotene showed an increase in *b** values [Şahin, 2020]. Finally, the total color difference showed an increase when increasing the proportion of 2%, 6%, and 10% of MLP in SB recipe with values that fluctuated between 13.90 and 26.32.

Sensory properties of sliced bread enriched with mango leaf powder

The sensory evaluation determined the degree of acceptance of breads enriched with MLP according to the attributes of color, flavor, and odor, *i.e.*, features that determine consumer choice when purchasing bread. **Table 5** shows the values assigned to SBs in their sensory evaluation. The results shown for the attributes of color, taste, and odor indicate significant differences between the products, finding greater acceptability of SBs enriched with 2% of MLP in the recipe. Regarding color, the judges preferred lighter and less greenish colors that were intensified by carotenoids and chlorophylls, with an increase in the percentage of wheat flour substitution by MLP in the SB recipe. However, in the evaluation of taste and odor, there were no significant ($p\geq0.05$) differences between the SBs with 2% and 6% of MLP from the Criollo and Kent varieties. This may be because dark breads tend to be associated with a burnt bread taste and green hue of bread is associated with a bitter taste.

SBs enriched with 10% of MLP from all varieties received the lowest score for the sensory attributes, particularly in taste. This could be due to the bitter and astringent taste of the major phenolic compounds contained in mango leaves, such as phenolic acids, xanthones, benzophenones, tannins, and flavonoids [Rasouli *et al*., 2017].

Texture profile of sliced bread enriched with mango leaf powder

The texture parameters of SBs enriched with MLP and control SB are shown in **Table 6**. The control SB had higher hardness, chewiness, and gumminess values in all breads evaluated. The high hardness of the control bread may be due to not having additional fiber unlike the enriched breads. Fiber absorbing water changes the structure of dough and thus reduces the hardness of bread. Bourekoua *et al*. [2018] obtained similar results; their control bread presented a greater hardness than these with the *Moringa oleifera* leaf powder. However, an excess of fiber

Table 6. Texture profile of wheat flour sliced breads (SB control) and sliced bread (SB) enriched with leaf powders (replacement of 2%, 6%, and 10% of wheat flour) from three mango varieties (Criollo, Kent and Edward).

Bread	Hardness (N)	Cohesiveness (–)	Springiness (m)	Adhesiveness (mJ)	Chewiness (mJ)	Gumminess (N)
SB control	22.84±2.39^{a}	0.40±0.00^{a}	0.012±0.00^{b}	0.07±0.07^{b}	7.31±0.75^{a}	9.140±0.94^{a}
SB+Criollo 2%	12.67±2.02^{ef}	0.33±0.06^{bc}	0.012±0.00^{b}	0.05±0.02^{b}	3.32±0.13^{c}	4.151±0.16^{d}
SB+Criollo 6%	14.99±1.99^{cde}	0.30±0.00^{c}	0.011±0.00^{c}	0.08±0.07^{b}	3.31±0.64^{c}	4.497±0.60^{cd}
SB+Criollo 10%	16.37±0.75^{bc}	0.30±0.00^{c}	0.009±0.00^{d}	0.25±0.25^{a}	3.41±0.72^{c}	4.911±0.22^{cd}
SB+Kent 2%	12.48±0.62^{ef}	0.40±0.00^{a}	0.014±0.00^{a}	0.02±0.01^{b}	4.49±0.22^{b}	4.993±0.25^{cd}
SB+Kent 6%	13.45±0.66^{def}	0.40±0.00^{a}	0.012±0.00^{b}	0.04±0.01^{b}	4.30±0.21^{bc}	5.383±0.27^{bc}
SB+Kent 10%	16.85±1.55^{bc}	0.36±0.06^{ab}	0.012±0.00^{b}	0.08±0.04^{b}	5.04± 1.03^{b}	6.30±1.29^{b}
SB+Edward 2%	13.38±0.83^{def}	0.40±0.00^{a}	0.012±0.00^{b}	0.03 ±0.00^{b}	4.28±0.27^{bc}	5.35±0.33^{bc}
SB+Edward 6%	15.82±0.86^{bcd}	0.33±0.06^{bc}	0.012±0.00^{b}	0.03±0.02^{b}	4.22±0.79^{bc}	5.28±0.99^{bcd}
SB+Edward 10%	17.87±1.51^{b}	0.30±0.00^{c}	0.012±0.00^{b}	0.09±0.05^{b}	4.12±0.58^{bc}	5.36±0.45^{bc}

Values (mean ± standard deviation, n=15) with different letters in the same column indicate a significant difference at p<0.05, according to Fisher's LSD test.

can have a negative effect on hardness, as seen in the case of SB enriched with 10% of MLP (significantly higher value than for SB enriched with 2% of MLP, **Table 6**). In this regard, Mau *et al.* [2020] demonstrated that a relationship must be found between the percentage of potato leaf powder and the amount of water added to the formulation to maintain or improve the texture characteristics of sliced bread.

As mentioned above, the findings indicate that MLP incorporation reduced the hardness of SB when compared to the control SB. However, increasing the amount of MLP had a directly proportional effect on the hardness of the tested breads. Khan *et al.* [2023] observed an inverse relationship; hardness and springiness of wheat flour leavened bread significantly decreased with rises in supplementation levels of *Moringa oleifer*a leaf powder. However, gumminess exhibited a slightly increasing tendency as compared to that of control. According to Cao *et al.* [2023], hardness, chewiness, and gumminess adversely affect bread quality, while springiness and cohesion improve it. These traits were noted in all SBs enriched with 10% of MLP and the control SB. In contrast, the SB enriched with 2% and 6% of MLP from Criollo and Kent varieties provided the best texture profile, as confirmed by sensory evaluations.

A greater springiness index indicates the freshness and elasticity of bread, as it shows the sample's capacity to revert to its initial shape after being stretched; qualities generally valued by consumers [Cornejo & Rosell, 2015]. In this context, the samples with the highest springiness index included SB Kent 2%, followed by SB Edward at 2% and 6%, as well as SB Kent at 2% and 6% formulations (**Table 6**).

CONCLUSIONS

Mango leaf powder contained high levels of phenolic compounds and plant pigments and had high antioxidant capacity. Therefore, the partial replacement of wheat flour with MLP (2%, 6%, and 10%) in the preparation of sliced bread improved its total phenolic content, total flavonoid content and antioxidant capacity. The enrichment of bread with MLP modified the chromatic parameters, and the total color difference from the sliced control bread increased with the increase in MLP percentage in the bread recipe. Sliced bread enriched with 2% of mango leaf powder achieved higher scores according to the sensory panel. In summary, mango leaf powder has the potential to be used in the preparation of sliced bread and other products derived from the baking industry, since it can enrich them in phenolic compounds and improve their antioxidant capacity and their sensory attributes of color, taste, and odor.

ACKNOWLEDGEMENTS

The authors would like to thank the Facultad de Administración Hotelera, Turismo y Gastronomía, Universidad San Ignacio de Loyola and the Instituto de Investigación de Bioquímica y Biología Molecular (UNALM) for their support in the textural analysis.

RESEARCH FUNDING

The author(s) received no financial support for the research, authorship, and/or publication of this article.

CONFLICT OF INTERESTS

The authors declare that they have no conflict of interests.

ORCID IDs

K. Cancino-Chávez https://orcid.org/0000-0003-1953-534X
Y.I. Malange https://orcid.org/0009-0002-7621-0816
A.M. Muñoz https://orcid.org/0000-0003-3080-9823
M. Pirca-Palomino https://orcid.org/0009-0008-0642-9277
F. Ramos-Escudero https://orcid.org/0000-0002-6907-3166

REFERENCES

1. Agencia Agraria de Noticias. (2024). Mango fresco peruano llegó a 36 mercados en la campaña 2023/2024. Available at: https://agraria.pe/noticias/mango-fresco-peruano-llego-a-36-mercados-en-la-campana-2023--35680#:~:text=Los%20principales%20destinos%20del%20

mango,%25)%3B%20Reino%20Unido%20con%206%25%20 (accessed: 25 September 2024).
2. Amoah, I., Cairncross, C., Osei, E.O., Yeboah, J.A., Cobbinah, J.C., Rush, E. (2022). Bioactive properties of bread formulated with plant-based functional ingredients before consumption and possible links with health outcomes after consumption – A review. *Plant Foods for Human Nutrition, 77*, 329–339. https://doi.org/10.1007/s11130-022-00993-0
3. Batool, N., Ilyas, N., Shabir, S., Saeed, M., Mazhar, R. (2018). A mini-review of therapeutic potential of *Mangifera indica* L. *Pakistan Journal of Pharmaceutical Sciences, 31*(4), 1441–1448.
4. Benzie, I.F.F., Strain, J.J. (1996). The ferric reducing ability of plasma (FRAP) as a measure of "antioxidant power": the FRAP assay. *Analytical Biochemistry, 239*(1), 70–76. https://doi.org/10.1006/abio.1996.0292
5. Bourekoua, H., Różyło, R., Gawlik-Dziki, U., Benatallah, L., Zidoune, M.N., Dziki, D. (2018). Evaluation of physical, sensorial, and antioxidant properties of gluten-free bread enriched with *Moringa oleifera* leaf powder. *European Food Research and Technology, 244*, 189–195. https://doi.org/10.1007/s00217-017-2942-y
6. Brand-Williams, W., Cuvelier, M.E., Berset, C. (1995). Use of a free radical method to evaluate antioxidant activity. *LWT – Food Science and Technology, 28*(1), 25–30. https://doi.org/10.1016/S0023-6438(95)80008-5
7. Cacak-Pietrzak, G., Dziki, D., Gawlik-Dziki, U., Parol-Nadłonek, N., Kalisz, S., Krajewska, A., Stępniewska, S. (2023). Wheat bread enriched with black chokeberry (*Aronia melanocarpa* L.) pomace: Physicochemical properties and sensory evaluation. *Applied Sciences, 13*(12), art. no. 6936. https://doi.org/10.3390/app13126936
8. Cao, H., Gao, F., Shen, H., Su, Q., Guan, X., Sun, Z., Yu, Z. (2023). Influence of partial substitution of wheat flour with sprouted oat flours on physicochemical and textural characteristics of wheat bread. *Journal of Cereal Science, 110*, art. no. 103649. https://doi.org/10.1016/j.jcs.2023.103649
9. Ćavar Zeljković, S., Šišková, J., Komzáková, K., De Diego, N., Kaffková, K., Tarkowski, P. (2021). Phenolic compounds and biological activity of selected Mentha species. *Plants, 10*(3), art. no. 550. https://doi.org/10.3390/plants10030550
10. Cejudo, C., Ferreiro, M., Romera, I., Casas, L., Mantell, C. (2023). Functional, physical, and volatile characterization of chitosan/starch food films functionalized with mango leaf extract. *Foods, 12*(15), art. no. 2977. https://doi.org/10.3390/foods12152977
11. Cejudo-Bastante, C., Silva, N.H.C.S., Casas Cardoso, L., Mantell Serrano, C., Martínez de la Ossa, E.J., Freire, C.S.R., Vilela, C. (2021). Biobased films of nanocellulose and mango leaf extract for active food packaging: Supercritical impregnation *versus* solvent casting. *Food Hydrocolloids, 117*, art. no. 106709. https://doi.org/10.1016/j.foodhyd.2021.106709
12. Cejudo-Bastante, C., Verano-Naranjo, L., Toro-Barrios, N., Pereyra, C., Mantell, C., Casas, L. (2022). Structural modification of polymers functionalized with mango leaf extract by supercritical impregnation: Approaching of further food and biomedical applications. *Polymers, 14*(12), art. no. 2413. https://doi.org/10.3390/polym14122413
13. Chacaliaza-Rodríguez, L., Espinoza-Begazo, G., Ramos-Escudero, F., Servan, K. (2016). Proximate chemical composition and content of biologically active components in leaves of two quinoa cultivars (Salcedo and Altiplano) produced in Peru. *Research Journal of Medicinal Plants, 10*(8), 450–456. https://doi.org/10.3923/rjmp.2016.450.456
14. Chandra, S., Khan, S., Avula, B., Lata, H., Yang, M.H., ElSohly, M.A., Khan, I.A. (2014). Assessment of total phenolic and flavonoid content, antioxidant properties, and yield of aeroponically and conventionally grown leafy vegetables and fruit crops: A comparative study. *Evidence-Based Complementary and Alternative Medicine, 2014*, art. no. 253875. https://doi.org/10.1155/2014/253875
15. Cornejo, F., Rosell, C.M. (2015). Physicochemical properties of long rice grain varieties in relation to gluten free bread quality. *LWT – Food Science and Technology, 62*(2), 1203–1210. https://doi.org/10.1016/j.lwt.2015.01.050
16. FAO, Food and Agriculture Organization. (2023 Main tropical fruits. Market analysis 2022. Food and Agriculture Organization of the United Nations. Rome, Italy: FAO.
17. Fernández-Ponce, M.T., Parjikolaei, B.R., Lari, H. N., Casas, L., Mantell, C., Martínez de la Ossa, E.J. (2016). Pilot-plant scale extraction of phenolic compounds from mango leaves using different green techniques: Kinetic and scale up study. *Chemical Engineering Journal, 299*, 420–430. https://doi.org/10.1016/j.cej.2016.04.046
18. Ghosh, B., Majumder, S., Acharyya, S., Ghosh, A., Saha, S., Sarkar, S., Chakraborty, S., Bhattacharya, M. (2022). Comparative phytochemical analysis of mature mango leaves from nineteen cultivars of Murshidabad district, India. *Asian Journal of Natural Product Biochemistry, 20*(2), 48–55. https://doi.org/10.13057/biofar/f200202
19. Jahurul, M.H.A., Zaidul, I.S.M., Ghafoor, K., Al-Juhaimi, F.Y., Nyam, K.L., Norulaini, N.A.N., Sahena, F., Mohd Omar, A.K. (2015). Mango (*Mangifera indica* L.) by-products and their valuable components: A review. *Food Chemistry, 183*, 173–180. https://doi.org/10.1016/j.foodchem.2015.03.046
20. Khan, M.A., Shakoor, S., Ameer, K., Farooqi, M.A., Rohi, M., Saeed, M., Asghar, M.T., Irshad, M.B., Waseem, M., Tanweer, S., Ali, U., Ahmed, I.A.M., Ramzan, Y. (2023). Effects of dehydrated moringa (*Moringa oleifera*) leaf powder supplementation on physicochemical, antioxidant, mineral, and sensory properties of whole wheat flour leavened bread. *Journal of Food Quality, 2023*, art. no. 473000. https://doi.org/10.1155/2023/4473000
21. Kingne, F.K., Djikeng, F.T., Tsafack, H.D., Karuna, M.S.L., Womeni, H.M. (2018). Phenolic content and antioxidant activity of young and mature mango (*Mangifera indica*) and avocado (*Persea americana*) leave extracts. *International Journal of Phytomedicine, 10*(4), 181-190. https://doi.org/10.5138/09750185.2289
22. Klopsch, R., Baldermann, S., Voss, A., Rohn, S., Schreiner, M., Neugart, S. (2018). Bread enriched with legume microgreens and leaves — ontogenetic and baking-driven changes in the profile of secondary plant metabolites. *Frontiers in Chemistry,* 6, art. no. 322. https://doi.org/10.3389/fchem.2018.00322
23. Kowalski, S., Mikulec, A., Pustkowiak, H. (2020). Sensory assessment and physicochemical properties of wheat bread supplemented with chia seeds. *Polish Journal of Food and Nutrition Sciences, 70*(4), 387–397. https://doi.org/10.31883/pjfns/129015
24. Kumar, M., Saurabh, V., Tomar, M., Hasan, M., Changan, S., Sasi, M., Maheshwari, C., Prajapati, U., Singh, S., Prajapat, R.K., Dhumal, S., Punia, S., Amarowicz, R., Mekhemar, M. (2021). Mango (*Mangifera indica* L.) leaves: Nutritional composition, phytochemical profile, and health-promoting bioactivities. *Antioxidants, 10*(2), art. no. 299. https://doi.org/10.3390/antiox10020299
25. Lichtenthaler, H.K., Buschmann, C. (2001). Chlorophylls and carotenoids: Measurement and characterization by UV-VIS spectroscopy. *Current Protocols in Food Analytical Chemistry, 1*, F4.3.1–F4.3.8. https://doi.org/10.1002/0471142913.faf0403s01
26. Luca, S.V., Macovei, I., Bujor, A., Miron, A., Skalicka-Woźniak, K., Aprotosoaie, A.C., Trifan, A. (2020). Bioactivity of dietary polyphenols: The role of metabolites. *Critical Reviews in Food Science and Nutrition, 60*(4), 626–659. https://doi.org/10.1080/10408398.2018.1546669
27. Magalhães, D., Gonçalves, R., Rodrigues, C.V., Rocha, H.R., Pintado, M., Coelho, M.C. (2024). Natural pigments recovery from food by-products: Health benefits towards the food industry. *Foods, 13*(14), art. no. 2276. https://doi.org/10.3390/foods13142276
28. Maietti, A., Tedeschi, P., Catani, M., Stevanin, C., Pasti, L., Cavazzini, A., Marchetti, N. (2021). Nutrient composition and antioxidant performances of bread-making products enriched with stinging nettle (*Urtica dioica*) leaves. *Foods, 10*(5), art. no. 938. https://doi.org/10.3390/foods10050938
29. Majeed, H., Iftikhar, T., Zohaib, M. (2024). Extension of guava shelf life through the application of edible coating formulated with mango and lemon leaves extracts. *Industrial Crops and Products, 216*, art. no. 118671. https://doi.org/10.1016/j.indcrop.2024.118671
30. Manaois, R.V., Zapater, J.E.I., Morales, A.V. (2020). Phytochemical content and antioxidant capacities of hydrophilic extracts of vegetables commonly consumed in the Philippines. *Philippine Journal of Science, 149*(4), 1045–1057. https://doi.org/10.56899/149.04.04
31. Martínez, E., Ramos-Escudero, F. (2024). Valorization of flours from cocoa, sinami and sacha inchi by-products for the reformulation of Peruvian traditional flatbread ('Pan Chapla'). *International Journal of Gastronomy and Food Science, 36*, art. no. 100930. https://doi.org/10.1016/j.ijgfs.2024.100930
32. Mau, J.-L., Lee, C.-C., Yang, C.-W., Chen, R.-W., Zhang, Q.-F., Lin, S.-D. (2020). Physicochemical, antioxidant and sensory characteristics of bread partially substituted with aerial parts of sweet potato. *LWT – Food Science and Technology, 117*, art. no. 108602. https://doi.org/10.1016/j.lwt.2019.108602
33. Meilgaard, M., Civille, G.V., Carr, B.T. (1999). Attribute differences test. III. Pairwise ranking test: Friedman analysis. In M.C. Meilgaard, B.T. Carr, G.V. Civille (Eds.), *Sensory Evaluation Techniques*. 3rd edition, CRC Press, Boca Raton, USA, pp. 103–106. https://doi.org/10.1201/9781003040729
34. Miliauskas, G., Venskutonis, P.R., Van Beek, T.A. (2004). Screening of radical scavenging activity of some medicinal and aromatic plant extracts. *Food Chemistry, 85*(2), 231–237. https://doi.org/10.1016/j.foodchem.2003.05.007
35. Pantelić, M.M., Dabić Zagorac, D.Č., Ćirić, I.Ž., Pergal, M.V., Relić, D.J., Todić, S.R., Natić, M.M. (2017). Phenolic profiles, antioxidant activity and minerals in leaves of different grapevine varieties grown in Serbia. *Journal of Food Composition and Analysis, 62*, 76–83. https://doi.org/10.1016/j.jfca.2017.05.002

36. Rasouli, H., Farzaei, M.H., Khodarahmi, R. (2017). Polyphenols and their benefits: A review. *International Journal of Food Properties, 20*(sup2), 1700–1741. **https://doi.org/10.1080/10942912.2017.1354017**
37. Romero-Orejón, F.L., Huaman, J., Lozada, P., Ramos-Escudero, F., Muñoz, A.M. (2023). Development and functionality of sinami (*Oenocarpus mapora*) seed powder as a biobased ingredient for the production of cosmetic products. *Cosmetics, 10*(3), art. no. 90. **https://doi.org/10.3390/cosmetics10030090**
38. Şahin, O.I. (2020). Functional and sensorial properties of cookies enriched with *SPIRULINA* and *DUNALIELLA* biomass. *Journal of Food Science and Technology, 57*(10), 3639–3646. **https://doi.org/10.1007/s13197-020-04396-4**
39. Scheff, S.W. (2016). Chapter 8 – Nonparametric statistics. In S. Scheff (Ed.), *Fundamental Statistical Principles for the Neurobiologist: A Survival Guide.* Academic Press, pp. 157–182. **https://doi.org/10.1016/B978-0-12-804753-8.00008-7**
40. Sferrazzo, G., Palmeri, R., Restuccia, C., Parafati, L., Siracusa, L., Spampinato, M., Carota, G., Distefano, A., Di Rosa, M., Tomasello, B., Costantino, A., Gulisano, M., Li Volti, G., Barbagallo, I. (2022). *Mangifera indica* L. leaves as a potential food source of phenolic compounds with biological activity. *Antioxidants, 11*(7), art. no. 1313. **https://doi.org/10.3390/antiox11071313**
41. Singleton, V.L., Rossi, J.A. (1965) Colorimetry of total phenolics with phosphomolybdic-phosphotungstic acid reagent. *American Journal of Enology and Viticulture, 16*, 144–158. **http://www.ajevonline.org/content/16/3/144.full.pdf+html**
42. Sousa, C. (2022). Anthocyanins, carotenoids and chlorophylls in edible plant leaves unveiled by tandem mass spectrometry. *Foods, 11*(13), art. no. 1924. **https://doi.org/10.3390/foods11131924**
43. Sultana, B., Hussain, Z., Asif, M., Munir, A. (2012). Investigation on the antioxidant activity of leaves, peels, stems bark, and kernel of mango (*Mangifera indica* L.). *Journal of Food Science, 77*(8), C849–C852. **https://doi.org/10.1111/j.1750-3841.2012.02807.x**
44. Yelwande, S., Wagh, J., Late, P., Habeeba, S., Shete, S. (2022). Studies on value addition of nutritional food product by incorporation of mango (*Mangifera indica*) leaves. *Emerging Trends in Nutraceuticals, 1*(3), 8–21. **http://dx.doi.org/10.18782/2583-4606.112**
45. Yu, L., Rios, E., Castro, L., Liu, J., Yan, Y., Dixon, D. (2021). Genistein: Dual role in women's health. *Nutrients, 13*(9), art. no. 3048. **https://doi.org/10.3390/nu13093048**
46. Zegarra, S., Muñoz, A.M., Ramos-Escudero, F. (2019). Elaboration of a gluten-free bread based on cañihua (*Chenopodium pallidicaule* Aellen) flour and sensory acceptability evaluation. *Revista Chilena de Nutrición, 46*, 561–570 (in Spanish, English abstract). **http://dx.doi.org/10.4067/S0717-75182019000500561**

ORIGINAL ARTICLE
http://journal.pan.olsztyn.pl

Polish Journal of Food and Nutrition Sciences
2024, Vol. 74, No. 4, 323–339
DOI: 10.31883/pjfns/194650
ISSN 1230-0322, e-ISSN 2083-6007

Biogenic Amine Content and Shelf-Life of Salmon Fillets Packaged in Modified Atmospheres of Low-Level Carbon Monoxide and Different Carbon Dioxide Concentrations

Esra Akkaya[1]*, Hilal Colak[1], Hamparsun Hampikyan[2], Ayse S. Engin[3], Enver B. Bingol[1]

[1]Department of Food Hygiene and Technology, Faculty of Veterinary Medicine, İstanbul University-Cerrahpaşa, 34500 Buyukcekmece, İstanbul, Turkey
[2]Department of Gastronomy and Culinary Arts, Faculty of Fine Arts, İstanbul Beykent University, 34500 Buyukcekmece, İstanbul, Turkey
[3]Department of Gastronomy and Culinary Arts, Faculty of Fine Arts, İstanbul Gelisim University, 34310 Avcilar, İstanbul, Turkey

The objective of this study was to determine the biogenic amine levels and quality parameters of Atlantic salmon fillets packaged with a low level of carbon monoxide and varied concentrations of carbon dioxide and stored at 1°C. For this purpose, ambient air packaging and modified atmosphere packaging (MAP) with gas mixtures of CO, CO_2 and N_2 (in a ratio of 0.4/30/69.6); CO_2, N_2 and O_2 (in the ratios of 40/30/30, 50/30/20, and 60/30/10); and CO_2 and N_2 (in a ratio of 40/60) were applied. Salmon fillets were analyzed for biogenic amine contents and chemical, microbiological and sensorial properties during 27-day cold storage. The study results indicate that salmon fillets stored in cold storage undergo a deterioration process depending on storage time and packaging conditions. The thiobarbituric acid reactive substances, total volatile basic nitrogen and trimethylamine nitrogen values, and biogenic amine levels were lower in CO-MAP and 60% CO_2-MAP compared to the air-packaged samples in extended storage period. Furthermore, 1.5–2 log bacterial inhibition was recorded in CO-MAP and 60% CO_2-MAP, which allowed the products to be consumed up to day 21. However, the shelf-life of air-packaged salmon was limited to one week due to the signs of deterioration. In conclusion, modified atmosphere packaging with 0.4% CO and 60% CO_2 significantly extended the shelf-life of cold-stored salmon fillets by maintaining quality characteristics of the products. These alternative gas concentrations can also be effective in the preservation of other fatty fish species under cold storage.

Keywords: Atlantic salmon, cold storage, packaging, quality parameters, sensory attributes

INTRODUCTION

Fish and other seafood are one of the most perishable food items because of their high water, protein and fatty acid content, which the spoilage microflora need to growth [Chan *et al*., 2021a; Surówka *et al*., 2021]. Atlantic salmon (*Salmo salar L*.) is a substantial aquacultural fish species, with its high nutritional value making it a popular food for consumers worldwide. However, this nutritient content can also limit the shelf-life of the product [Chan *et al*., 2021b; Kritikos *et al*., 2020]. The biochemical and enzymatic reactions which occur in fresh salmon from the time of capture trigger autolysis, oxidation and enhanced microbial growth, all leading to a rapid spoilage [Chan *et al*., 2021a]. The lipid oxidation of polyunsaturated fatty acids, the oxidation of protein and non-protein nitrogenous compounds, and growth of spoilage organisms are the main factors reducing the shelf-life of fresh salmon, thereby generating off-flavor and off-odor that influence the consumer's acceptance [Merlo *et al*., 2019]. Furthermore, the formation of biogenic amines in fish is directly related to the growth of spoilage microorganisms [Çelebi Sezer *et al*., 2022; Houicher *et al*., 2021].

***Corresponding Author:**
e-mail: esra.akkaya@iuc.edu.tr (Dr. E. Akkaya)

Submitted: 11 August 2024
Accepted: 15 October 2024
Published on-line: 5 November 2024

Biogenic amines are nitrogenous compounds with heterocyclic, aromatic and aliphatic chemical structures generated by microbial decarboxylation of free amino acids [Arulkumar *et al*., 2023; Çelebi Sezer *et al*., 2022]. Histamine, cadaverine, putrescine, tryptamine, phenylethylamine, tyramine, spermine and spermidine are the most important biogenic amines found in food. *Enterobacteriaceae*, *Clostridium* spp., *Aeromonas* spp., *Aerobacter* spp., *Pseudomonas* spp., *Shewanella* spp., *Lactobacillus* spp., *Photobacterium* spp., *Morganella morganii*, yeast and mold are among the microorganisms responsible for the deterioration of salmon and the formation of biogenic amines [Arulkumar *et al*., 2023; Powell & Tamplin, 2012]. The composition of food, the microbial flora and parameters (*i.e.,* temperature) that promote bacterial growth, packaging and storage time, influence the amount and type of biogenic amines formed [Dadáková *et al*., 2009]. Therefore, it is imperative to use chilling methods in order to preserve the quality of fresh fish from the moment it is caught until it is offered for consumption [Surówka *et al*., 2021].

Packaging techniques applied in combination with low-temperature storage offer an effective practice for extending the shelf-life of fresh fish and fishery products [Chan *et al*., 2021a; Kritikos *et al*., 2020]. Modified atmosphere packaging (MAP) is the most preferred preservation method allowing to manipulate the content of gas mixtures (O_2, CO_2, N_2, *etc.*) in the packages before sealing them with a permeable film to retard the enzymatic and chemical reactions [Chan *et al*., 2021b]. Studies conducted so far have shown that, depending on fish species and storage temperatures, modified atmosphere packaging extends the shelf-life of seafood and its products compared to air packaging [Powell & Tamplin, 2012; Sivertsvik *et al*., 2003; Tsironi & Taoukis, 2018; Zhang *et al*., 2022]. Besides all these, the composition of a gas mixture used in MAP is critical to ensure a high-quality product and varies depending on the species of fish [Cooksey, 2014]. For fatty fish species such as salmon, the use of higher CO_2 levels with lower or without O_2 is inevitable to reduce oxidative rancidity and the growth of bacteria [Chan *et al*., 2021b; Merlo *et al*., 2019]. In addition, carbon monoxide (CO) is an alternative gas used at low levels (0.3 to 0.5%) with 60 to 70% CO_2 and 30 to 40% N_2 in modified atmosphere packaging to ensure color stability, suppress microbial growth, prevent oxidation and discoloration of the bones, and improve flavor acceptability [Cooksey, 2014; Cornforth & Hunt, 2008; Djenane & Roncalés, 2018].

Therefore, the aim of this study was to evaluate the biogenic amine contents and quality parameters affecting the shelf-life of Atlantic salmon fillets packaged with a low level of CO (0.4%) and varied concentrations of CO_2 during 27-day cold storage at 1°C.

MATERIAL AND METHODS

Preparation of salmon samples

Atlantic salmon (*Salmo salar* L.) was purchased from a chain branch of an international company that sells fish in three independent dates and transported to the laboratories within 2 h in polystyrene boxes containing dry ice. A total of 36 whole salmons (each weighing about 6–7 kg) were obtained 24–48 h post-catch and kept under cold storage until processing.

Each batch of 12 whole salmons was manually filleted after the tail, head, belly and backflaps were removed. Then, the filleted salmon samples were portioned into equal portions weighing approximately 200±50 g. Approximately 300 slices of salmon were randomly selected and placed on trays with two slices of salmon each.

Packaging salmon fillets

The salmon fillets of each group were placed on low O_2 permeable (8–12 cm^3/m^2/24 h at standard temperature and pressure, STP) polyethylene terephthalate trays in portions of approximately 400±50 g (two slices of salmon *per* tray) and were heat-sealed with a low O_2 permeable (3 cm^3/m^2/24 h) lidding film (Wrap Film Systems, London, UK) using a Ponapack VTK 40 SC Tray sealer (Ponapack, İstanbul, Turkey).

The ambient air was used for air packaging, while gas mixtures of CO, CO_2 and N_2 (in the percentage ratio of 0.4/30/69.6); CO_2, N_2 and O_2 (in the percentage ratios of 40/30/30, 50/30/20, and 60/30/10); and CO_2 and N_2 (in the percentage ratio of 40/60), purchased in Linde Gas (Kocaeli, Turkey), were applied for modified atmosphere packaging. Codes of salmon fillet groups corresponding to each gas mixture used in packing are given in **Table 1**. All packages were stored at 1±1°C for up to 27 days, and salmon fillets were analyzed on days 3, 6, 9, 12, 15, 18, 21, 24 and 27. On each analysis day, a total of 2 packages were allocated, one tray for sensory analysis and other tray for quality analysis. The gas ratios of all packages were measured before opening on each analysis day using a PDI Dansensor A/B gas meter (PBI-Dansensor A/B, Ronnedevaj 18, DK 410, Ringsted, Denmark). Each experimental trial was performed in triplicate on different times.

Microbiological analyses

Total aerobic mesophilic bacteria (TAMB), total psychrotrophic bacteria (PsB), *Enterobacteriaceae*, lactic acid bacteria (LAB), *Pseudomonas* spp., *Brochothrix thermosphacta* and yeast-mold counts were determined in accordance with the related International

Table 1. Composition of gas mixtures used in the packaging of salmon fillets.

Group	Gas mixture composition
Air	Ambient air (21% O_2, 78% N_2, 1% other gases)
CO-MAP	0.4% CO, 30% CO_2, 69.6% N_2
30% O_2-MAP	30% O_2, 40% CO_2, 30% N_2
20% O_2-MAP	20% O_2, 50% CO_2, 30% N_2
10% O_2-MAP	10% O_2, 60% CO_2, 30% N_2
60% CO_2-MAP	60% CO_2, 40% N_2
40% CO_2-MAP	40% CO_2, 60% N_2

MAP, modified atmosphere packaging.

Organization for Standardization method no. 6887-1 [ISO, 2017a]. Microbiological analyses were performed using 25 g of salmon samples for each group mixed with 225 mL of sterile peptone water in stomacher bags. After homogenization, serial dilutions were prepared to analyze relevant microorganisms.

Total aerobic mesophilic and psychrotrophic bacteria counts of salmon fillets were enumerated on plate count agar (Oxoid, CM0463, Basingstoke, Hampshire, UK) using ISO methods no. 4833-1 [ISO, 2013] and no. 17410 [ISO, 2019], respectively. *Enterobacteriaceae* counts were detected on violet red bile glucose agar (Oxoid, CM0485), lactic acid bacteria on de Man, Rogosa and Sharpe (MRS) agar (Oxoid, CM0361), *Pseudomonas* spp. on Pseudomonas agar (Oxoid, CM0559 and SR0103) supplemented with cetrimide-fucidin-cephalosporin (CFC), *B. thermosphacta* on streptomycin tallous acetate actidione (STAA) agar (Oxoid, CM0881) with STAA selective supplement and yeast-mold counts on dichloran rose Bengal chloramphenicol (DRBC) agar (Oxoid, CM0727) according to ISO methods no. 21528-2 [ISO, 2017b], no. 15214 [ISO, 1998], no. 13720 [ISO, 2010], no. 13722 [ISO, 2017c] and no. 21527-1 [ISO, 2008], respectively. Microbial counts were expressed as log CFU/g.

Determination of biogenic amine content

The content of biogenic amines (histamine, cadaverine, putrescine, tryptamine, phenylethylamine, tyramine, spermine, spermidine) was detected by high performance liquid chromatography (HPLC) using the Agilent system (Agilent Technologies, St. Clara, CA, USA) equipped with a diode array detector (G1315B DAD), in accordance with the method described by Bogdanović *et al*. [2020].

The reagents, all eight biogenic amines and analytical column were purchased from Sigma-Aldrich (St. Louis, MO, USA) and all were of HPLC grade (purity 98–99%). A homogenized salmon sample (5 g) was extracted with 0.4 M perchloric acid, and the filtrate was alkalized by the addition of 200 µL of a 2 M NaOH solution. After subsequent steps, 2 mL of a dansyl chloride solution was added, and the mixture was incubated (at 40°C for 45 min). The remaining dansyl chloride was removed and kept in darkness (45 min). The total volume was made up to 5 mL with acetonitrile, and the mixture was filtered through a 0.45 µm syringe filter (Sartorius, Gottingen, Germany). The separation of biogenic amines was carried out using a LiChrospher C18 analytical column (250×4.0 mm, particle size 5 µm) with an injection volume of 20 µL. HPLC conditions were applied according to the procedures described by Bogdanović *et al*. [2020]. The calibration curves covering eight concentrations ranging from 0.25 mg/kg to 500 mg/kg were used to quantify biogenic amines. The mean content of individual amines in salmon fillets was expressed as mg/kg.

Chemical analyses

Measurement of pH, water activity and moisture content

The pH of salmon fillets was measured with a digital pH meter (Hanna HI-9321, Woonsocket, RI, USA) calibrated with pH 4.0 and 7.0 solutions at room temperature. The water activity (a_w) of salmons was determined by using an a_w meter (Decagon AquaLab LITE, Washington, USA). The moisture content of salmon fillets was specified by drying a homogeneous mixture at 105±2°C to a constant weight [AOAC, 2005].

Determination of thiobarbituric acid reactive substance value

The thiobarbituric acid reactive substance (TBARS) value of salmon fillets was detected by measuring the absorbance of color developed at 530 nm using a T80+ UV/VIS spectrometer (PG Instruments Ltd., London, UK). In accordance with the method described by Shrestha & Min [2006], the samples were extracted with trichloroacetic acid (TCA) and then treated with a thiobarbituric acid (TBA) reagent. The TBARS value was expressed as mg of malondialdehyde (MDA) *per* kg.

Determination of trimethylamine nitrogen value

Trimethylamine nitrogen (TMA-N) content of salmon fillets was determined according to the AOAC [2000] procedure by homogenizing salmon samples (10 g) with 20 mL of a 7.5% TCA (*w/v*) solution and then centrifuging at 1,008×*g* for 15 min. After the subsequent analysis steps had been completed in accordance with the relevant method, the final content was measured at 410 nm using a spectrophotometer (PG Instruments Ltd). Results of TMA-N level determination were expressed as mg/100 g salmon fillet.

Determination of total volatile basic nitrogen value

The determination of total volatile basic nitrogen (TVB-N) levels of salmon fillets was performed in accordance with the procedure described by Esteves *et al*. [2021] using the microdiffusion method of Conway & Byrne [1933]. Results of TVB-N level determination were expressed as mg N/100 g salmon fillet.

Instrumental color analysis

The surface color of skinless salmon fillets was measured by using a Color Flex HunterLab apparatus (Hunter Associates Laboratory Inc., Reston, VA, USA). Color coordinate values for L^* (lightness), a^* (redness) and b^* (yellowness) were recorded on the average of four different areas (3×3 cm) of salmon fillets using diffuse illumination (D65 2° observer) with an 8 mm aperture and a 25 mm port size [AMSA, 2012]. The total color difference (ΔE) was calculated using Equation (1):

$$\Delta E = [(L^* - L_0^*)^2 + (a^* - a_0^*)^2 + (b^* - b_0^*)^2]^{1/2} \quad (1)$$

where: L^* indicates lightness value at storage time and L_0^* indicates the initial lightness value of the sample; a^* indicates redness value at storage time and a_0^* indicates the initial redness value of the sample; b^* indicates yellowness value at storage time and b_0^* indicates the initial yellowness value of the sample.

Sensory evaluation

The sensory evaluation of salmon fillets was carried out with a panel consisting of 12 panelists (age between 28 to 47 years,

7 men and 5 women) trained according to the ISO method no. 8586 [ISO, 2012] and experienced in seafood evaluation. Before the sensorial assessment, a preliminary session (1 h) was organized to define the sensory attributes in a round-table discussion using a standardized procedure no. 13299 [ISO, 2016] in two separate sessions. An open-discussion session was then held to familiarize the panelists with the attributes and the scale to be used.

The panelists evaluated four sensory attributes (color intensity, off-odor, appearance and tenderness) using a 9-cm unstructured linear scale, in which 1 (left side) referred to "pale color, putrid odor, stale and dull appearance, soft and pasty texture" and 9 (right side) referred to "strong color, typical fresh salmon odor, fresh and bright appearance, firm and succulent texture" for color intensity, off-odor, appearance and tenderness, following the method of Ouahioune *et al.* [2022].

The sessions were performed in individual booths under standardized laboratory conditions equipped in accordance with the ISO standard no. 8589 [ISO, 2007] on days 1, 3, 9, 15, 21 and 27 of salmon fillets storage. In each storage time, two salmon fillet samples of each of the seven packaging groups were served monadically as raw and coded with a three-digit number in randomized order.

The panelists received 7 independent sample sets, which included salmon samples served in closed cups immediately after the trays were opened for the evaluation of off-odor characteristics and samples on a plate for the assessment of other characteristics, on each day of analysis. Sensory panel was conducted in triplicate in two sessions.

Statistical analysis

The general linear model (GLM) procedure from SPSS 16.0 (SPSS Inc., Chicago, IL, USA) program was used to analyze the data for each parameter. The one-way analysis of variance (ANOVA) was conducted for each variable to determine the effects of packaging conditions and storage time. A Duncan's test was used to check the significance of differences between and within groups for different days of storage, and differences were found significant at $p<0.05$. The data collected for sensorial evaluation was subjected to a Friedman test followed by a least significant difference test. The model used included the fixed effects of packaging conditions and storage time. All results were presented as means and standard errors (SE). Each experimental trial was repeated in triplicate on different times.

RESULTS AND DISCUSSION

Physicochemical properties

The initial gas composition of packages contained 30.08%, 39.24%, 50.98%, 59.34%, 59.28%, 39.46% CO_2 and 69.08%, 29.48%, 28.58%, 30.07%, 40.72%, 60.54% N_2 for CO, 30% O_2, 20% O_2, 10% O_2, 60% CO_2 and 40% CO_2 MAP groups, respectively. The CO_2 level in the headspace composition of packages maintained relatively stable during storage time. On day 15 and 27 of storage, the CO_2 levels of packages decreased to 24.62% and 21.49% for CO-MAP, to 50.43% and 45.79% for 60% CO_2-MAP, to 34.28% and 29.65% for 40% CO_2-MAP, while the CO_2 concentrations increased to 43.45% and 47.76% for 30% O_2-MAP, to 54.01% and 56.75% for 20% O_2-MAP, and to 63.16% and 65.98% for 10% O_2-MAP. The O_2 concentrations were negligible under anaerobic conditions (CO and 40-60% CO_2), while a slight decrease was observed in packages with low O_2. The O_2 level in gas composition of air packages decreased throughout the storage, resulting in an increase in CO_2 concentration in the headspace (19.58% O_2/2.46% CO_2 on the first day to 12.56% O_2/6.83% CO_2 on day 27).

The pH of salmon fillets showed an increase parallel to the deterioration process during 27-day cold storage (**Table 2**). There was a significant ($p<0.05$) difference between packaging conditions in pH values throughout storage time except the 12th day. The samples packaged under CO-MAP and 60% CO_2-MAP had significantly lower pH values than those packaged in air and 30% O_2-MAP atmosphere ($p<0.001$). The pH value of air-packaged salmon showed a steady increase from 6.52 on day 15 to 6.94 at the end of storage, while the lowest value was recorded as 6.5 at the end of storage in 60% CO_2-MAP and CO-MAP. The pH value, which starts to decrease in the *post-mortem* process due to *rigor mortis*, decreases further with CO_2 decomposition in the package atmosphere. Subsequently, depending on storage time, an increase in pH value occurs due to microbial spoilage. This change in the pH value recorded in our study is similar to the observations made in other studies of Atlantic salmon packaged in a modified atmosphere [Fletcher *et al.*, 2002; Milne & Powell, 2014; Sivertsvik *et al.*, 2003]. The study of Chan *et al.* [2021b] also reported that modified atmosphere-packaged salmon samples had a significantly lower pH than the air-packaged ones, which is in line with our findings.

The water activity values and moisture content of salmons decreased through cold storage period in all packages (**Table 2**), with salmons packaged with air and 30% O_2-MAP having lower a_w values and moisture content than those packaged in 60% CO_2-MAP and CO-MAP. There was a significant ($p<0.05$) difference between the air-packaged and MAP-packaged salmon throughout storage time.

Microbiological changes

Microbiological changes in salmon samples during cold storage are presented in **Figure 1**. The initial bacterial loads of salmon fillets were 3.00 log CFU/g, 3.81 log CFU/g, 0.69 log CFU/g, 4.20 log CFU/g, 3.74 log CFU/g, 3.58 log CFU/g and 3.00 log CFU/g for TAMB, PsB, *Enterobacteriaceae*, LAB, *Pseudomonas* spp., *B. thermosphacta* and yeast-mold counts, respectively.

There was a significant difference between the air-packaged and modified atmosphere-packaged samples throughout storage time for psychrotrophic and mesophilic bacteria counts ($p<0.001$). The TAMB counts of modified atmosphere-packaged samples reached 5.90–7.30 log CFU/g at the end of the 27-day storage, while the PsB count reached 5.14–6.11 log CFU/g (**Figure 1**). The air-packaged samples had mesophilic and psychrotrophic bacteria counts of 7.89 and 7.64 log CFU/g, respectively, whereas a 2-log inhibition was recorded in those packaged in CO-MAP and 60% CO_2-MAP. There was also a significant difference in *Enterobacteriaceae*

Table 2. Physicochemical properties of salmon fillets packaged in air and modified atmosphere during storage period.

Characteristic	Group	Day 0	Day 1	Day 3	Day 6	Day 9	Day 12	Day 15	Day 18	Day 21	Day 24	Day 27	*p*
pH	Air	5.92±0.01^{H}	6.05±0.01^{aG}	6.14±0.01^{aG}	6.27±0.02^{aF}	6.36±0.01^{aEF}	6.40±0.06^{E}	6.52±0.01^{aD}	6.59±0.06^{aCD}	6.68±0.06^{aC}	6.82±0.03^{aB}	6.94±0.02^{aA}	***
	CO-MAP	5.92±0.01^{G}	5.96±0.01^{dG}	6.00±0.06^{bcFG}	6.08±0.01^{cdEF}	6.13±0.01^{dDE}	6.20±0.03^{CD}	6.24±0.02^{deC}	6.30±0.06^{dC}	6.41±0.06^{cB}	6.49±0.01^{bAB}	6.53±0.02^{cA}	***
	30% O_2-MAP	5.92±0.01^{G}	6.01±0.01^{bFG}	6.09±0.02^{abF}	6.23±0.02^{abE}	6.31±0.02^{bDE}	6.34±0.06^{D}	6.48±0.01^{abC}	6.53±0.05^{abBC}	6.62±0.01^{aB}	6.79±0.06^{aA}	6.86±0.01^{abA}	***
	20% O_2-MAP	5.92±0.01^{F}	5.99±0.01^{cEF}	6.07±0.03^{abcE}	6.20±0.03^{abD}	6.27±0.01^{bD}	6.30±0.06^{D}	6.44±0.02^{bC}	6.51±0.05^{abcBC}	6.59±0.06^{abB}	6.73±0.06^{aA}	6.81±0.01^{bA}	***
	10% O_2-MAP	5.92±0.01^{G}	5.98±0.01^{cFG}	6.04±0.02^{bcF}	6.16±0.02^{bcE}	6.22±0.02^{cDE}	6.25±0.05^{DE}	6.31±0.01^{cCD}	6.36±0.03^{bcdC}	6.47±0.05^{bcB}	6.52±0.02^{bAB}	6.58±0.02^{cA}	***
	60% CO_2-MAP	5.92±0.01^{F}	5.95±0.01^{dEF}	5.99±0.01^{cEF}	6.06±0.04^{dDE}	6.11±0.01^{dCD}	6.17±0.02^{BCD}	6.21±0.01^{eBC}	6.28±0.03^{dB}	6.39±0.03^{cA}	6.46±0.01^{bA}	6.50±0.06^{cA}	***
	40% CO_2-MAP	5.92±0.01^{H}	5.98±0.01^{cH}	6.00±0.02^{bcGH}	6.10±0.06^{cdFG}	6.15±0.03^{dEF}	6.23±0.01^{DE}	6.28±0.02^{cdD}	6.33±0.04^{cdCD}	6.43±0.02^{cBC}	6.50±0.02^{bAB}	6.55±0.03^{cA}	***
	p	NS	***	*	***	***	NS	***	*	**	***	***	
a_w	Air	0.999±0.010^{A}	0.996±0.001^{cdA}	0.992±0.001^{cB}	0.989±0.001^{cB}	0.983±0.002^{eC}	0.979±0.001^{fD}	0.975±0.001^{dE}	0.965±0.001^{dF}	0.964±0.001^{dF}	0.962±0.001^{dF}	0.962±0.001^{dF}	***
	CO-MAP	0.999±0.010^{A}	0.998±0.001^{abA}	0.996±0.001^{aAB}	0.994±0.001^{abBC}	0.993±0.002^{aBC}	0.991±0.001^{abC}	0.986±0.001^{abD}	0.976±0.001^{bE}	0.973±0.002^{bF}	0.972±0.001^{bF}	0.971±0.001^{aF}	***
	30% O_2-MAP	0.999±0.010^{A}	0.995±0.001^{dB}	0.991±0.001^{cC}	0.989±0.002^{cC}	0.984±0.001^{deD}	0.980±0.001^{efE}	0.976±0.001^{dF}	0.971±0.001^{cG}	0.969±0.001^{bcGH}	0.967±0.001^{cHI}	0.966±0.001^{cI}	***
	20% O_2-MAP	0.999±0.010^{A}	0.996±0.001^{cdB}	0.992±0.001^{cC}	0.989±0.001^{cD}	0.987±0.001^{cdD}	0.982±0.001^{dE}	0.979±0.002^{cdF}	0.972±0.001^{cG}	0.970±0.001^{cGH}	0.969±0.001^{bcH}	0.968±0.001^{bcH}	***
	10% O_2-MAP	0.999±0.010^{A}	0.997±0.001^{bcA}	0.993±0.001^{bcB}	0.990±0.001^{cC}	0.988±0.001^{bcCD}	0.986±0.001^{cD}	0.978±0.001^{dEF}	0.973±0.001^{bcG}	0.970±0.001^{bcG}	0.970±0.001^{bcG}	0.968±0.001^{bcG}	***
	60% CO_2-MAP	0.999±0.010^{A}	0.999±0.001^{aA}	0.997±0.001^{aAB}	0.996±0.001^{aABC}	0.994±0.001^{aBC}	0.993±0.001^{aC}	0.989±0.002^{aD}	0.980±0.001^{aE}	0.979±0.001^{aEF}	0.976±0.001^{aF}	0.972±0.001^{aG}	***
	40% CO_2-MAP	0.999±0.010^{A}	0.998±0.001^{abA}	0.995±0.001^{abB}	0.992±0.001^{bcC}	0.991±0.001^{abC}	0.989±0.001^{bC}	0.983±0.002^{bcD}	0.973±0.002^{bcE}	0.971±0.001^{bcE}	0.970±0.001^{bcE}	0.970±0.001^{abE}	***
	p	NS	***	***	**	***	***	***	***	**	***	***	
Moisture content (g/100 g)	Air	49.63±0.02^{A}	49.01±0.01^{bB}	48.51±0.23^{cC}	46.56±0.23^{dD}	43.15±0.09^{fE}	40.56±0.17^{fF}	39.64±0.11^{eG}	37.79±0.06^{dH}	37.18±0.10^{eI}	35.65±0.17^{cJ}	34.45±0.12^{K}	***
	CO-MAP	49.63±0.02^{A}	49.55±0.17^{aA}	49.12±0.07^{abB}	48.23±0.13^{bC}	46.41±0.12^{bD}	43.75±0.12^{bE}	41.99±0.11^{bF}	39.08±0.05^{bG}	38.58±0.17^{bH}	36.92±0.01^{abI}	36.03±0.02^{bJ}	***
	30% O_2-MAP	49.63±0.02^{A}	49.42±0.12^{aA}	48.76±0.12^{bcB}	46.36±0.12^{dC}	44.29±0.12^{eD}	42.52±0.12^{eE}	39.85±0.06^{eF}	38.24±0.14^{cG}	37.46±0.06^{eH}	35.33±0.11^{cI}	34.91±0.06^{dJ}	***
	20% O_2-MAP	49.63±0.02^{A}	49.45±0.17^{aA}	48.65±0.12^{bcB}	47.23±0.13^{cC}	44.88±0.06^{dD}	42.95±0.11^{dE}	40.49±0.17^{dF}	38.51±0.11^{cG}	37.84±0.06^{dH}	35.43±0.11^{cI}	35.03±0.06^{dJ}	***
	10% O_2-MAP	49.63±0.02^{A}	49.54±0.12^{aA}	48.68±0.12^{bcB}	47.34±0.12^{cC}	45.52±0.17^{cD}	43.21±0.12^{cdE}	40.68±0.06^{dF}	38.88±0.06^{bG}	38.11±0.06^{cdH}	36.36±0.17^{bcI}	35.48±0.02^{cJ}	***
	60% CO_2-MAP	49.63±0.02^{A}	49.60±0.06^{aA}	49.44±0.25^{aA}	48.77±0.06^{aB}	47.17±0.10^{aC}	44.16±0.10^{aD}	43.32±0.18^{aE}	39.69±0.12^{aF}	39.03±0.17^{aG}	37.41±0.11^{abH}	37.15±0.09^{aI}	***
	40% CO_2-MAP	49.63±0.02^{A}	49.59±0.06^{aA}	49.34±0.20^{aA}	48.01±0.06^{bB}	46.36±0.06^{bC}	43.42±0.11^{bcD}	41.22±0.13^{cE}	38.97±0.12^{bF}	38.21±0.12^{cFG}	37.96±0.71^{aG}	36.91±0.06^{aH}	***
	p	NS	*	**	***	***	***	***	***	***	**	***	

Composition of gas mixtures used in MAP of different groups of salmon fillets are shown in Table 1. Results are presented as mean ± standard error. Means within a column with different letters (a–e) are significantly different ($p<0.05$). Means within a row with different letters (A–H) are significantly different ($p<0.05$). *, $p<0.05$; **, $p<0.01$; ***, $p<0.001$; NS, not significant; a_w, water activity; MAP, modified atmosphere packaging.

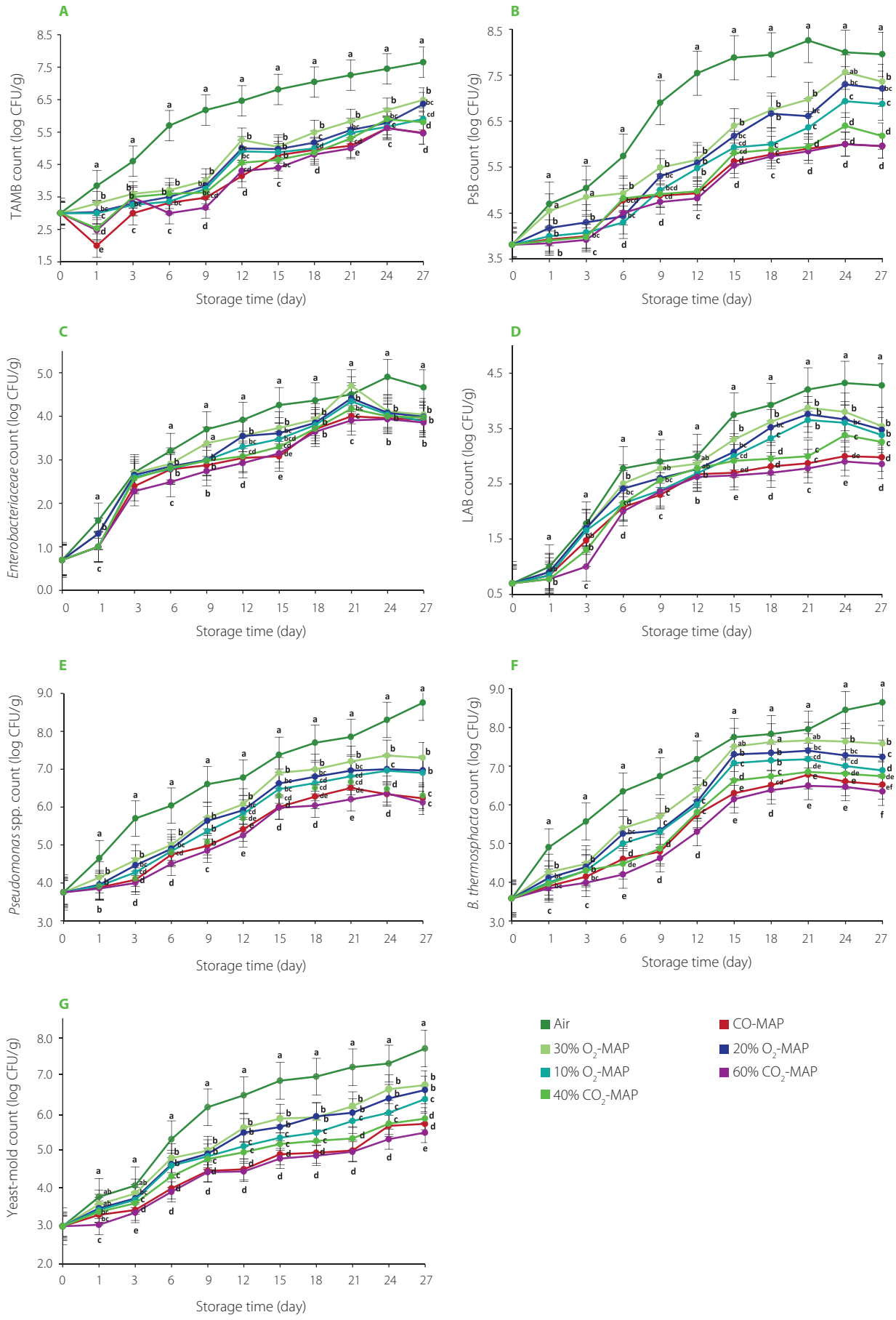

Figure 1. Counts of total aerobic mesophilic bacteria, TAMB (**A**), total psychrotrophic bacteria, PsB (**B**), *Enterobacteriaceae* (**C**), lactic acid bacteria, LAB (**D**), *Pseudomonas* spp. (**E**), *Brochothrix thermosphacta* (**F**) and yeast-mold (**G**) of salmon fillets packaged in air and modified atmosphere during storage period. Different letters for each storage day indicate significant differences ($p<0.05$). Details regarding modified atmosphere packaging (MAP) are presented in Table 1.

counts between the packaging groups ($p<0.001$) during storage except the 3rd day ($p\geq0.05$), while an inhibition of 0.5 log was recorded in CO and 60% CO_2-MAP compared to air packaging at the end of storage. The changes in LAB counts were close to each other during the 27-day storage period, but there was a significant difference of about 1 log between the air-packaged and modified atmosphere-packaged groups ($p<0.05$). The *Pseudomonas* spp. count of salmon fillets packaged with ambient air and 30% O_2 exceeded 7 log CFU/g on days 15 and 24, respectively, while salmon packaged with 60% CO_2 and CO did not reach this value even at the end of storage. The CO-MAP and 60% CO_2-MAP samples had 1 log CFU/g lower bacterial count than the samples packaged with high O_2, which was significantly different ($p<0.001$). A similar change was determined in *B. thermosphacta* counts of salmon fillets, and the bacterial counts of air-packaged samples were 1.0–2.3 log CFU/g higher than these recorded for the other groups at the end of storage ($p<0.001$). Yeast-mold counts reached 7.7 log CFU/g with a rise noted in the air-packaged samples during storage time, and an inhibition at a level of 2.0–2.2 log recorded in the CO-MAP and 60% CO_2-MAP samples ($p<0.001$).

The study results indicate that salmon fillets stored in cold storage conditions undergo a deterioration process depending on storage time and packaging conditions. The salmon fillets packaged with ambient air entered a faster spoilage process than the products packaged with modified gas mixtures. This process was relatively slower in the samples packaged with high CO_2 and low CO (<0.5%). Since fish and fishery products are highly susceptible to contamination and spoilage, storage in ambient air leads to a rise in microbial activity, especially when temperature increases [Chan *et al*., 2021b]. There are many studies supporting this scientific view that storage in ambient air accelerates microbiological activity in salmon, and this can be slowed down by modified atmosphere packaging resulting in product's shelf-life extension [Fernandez *et al*., 2009; Qian *et al*., 2022; Saraiva *et al*., 2017; Sivertsvik *et al*., 2003].

Similarly to our study, Fernandez *et al*. [2009] reported that the changes in total bacterial counts of salmon packaged in modified atmosphere with different gas combinations were lower than those observed for the samples packaged with ambient air, which was also demonstrated by Qian *et al*. [2022]. The shortest shelf-life recorded for salmon was 16 days in 25% CO_2/75% N_2 package, while the longest shelf-life reached 22 days in 75% CO_2/25% N_2 packages [Fernandez *et al*., 2009]. Beside this, Qian *et al*. [2022] highlighted that CO_2 content above 40% was found to effectively inhibit the growth of mesophilic bacteria. However, higher CO_2 contents, such as 100% and 80%, did not have a greater inhibitory effect on bacteria as higher CO_2 concentrations contribute to bacterial growth by increasing the solubility of muscle proteins [Qian *et al*., 2022]. In addition, similar changes in the count of psychrophilic bacteria were recorded with an effective suppression under a gas composition of 60% CO_2/10% O_2/30% N_2 [Qian *et al*., 2022].

Likewise, Sivertsvik *et al*. [2003] observed enhanced bacterial growth in air-packaged Atlantic salmons compared to the modified atmosphere-packaged samples. In turn, Saraiva *et al*. [2017] found that the bacterial load of air-packaged salmon samples reached 7.16 log CFU/g on day 9 of storage, while the modified atmosphere-packaged samples remained below (6.36 log CFU/g) this level even on the 13th day. In this regard, the use of CO_2 in modified atmosphere packaging retards microbiological growth by prolonging the lag phase and reducing the accumulation of degradation compounds, such as TVB-N and hypoxanthine [Chan *et al*., 2021b]. Moreover, De la Hoz *et al*. [2000] reported that the shelf-life of salmon steaks packaged under different CO_2 concentrations was extended by 6 and 15 days for 20% and 40% CO_2, respectively, compared to air packaging, and stated that the primary bacterial group responsible for the spoilage of salmon was *Pseudomonas*/*Shewanella* and the second one was *Enterobacteriaceae*. Saraiva *et al*. [2017] detected the yeast-mold counts at 7.23 log CFU/g on day 9 of storage in air-packaged salmon, while this level could not be overpassed (4.06 log CFU/g) in modified atmosphere packaging even on the 13th day of storage. Conformably, *Brochothrix* spp. and *Carnobacterium* spp. were reported to be the main bacterial groups detected in salmon packaged under 60% CO_2 modified atmosphere and cold stored for 18 days. The high CO_2 levels used in MAP reduce the count of aerobic bacteria, while CO_2 levels in packages promote the growth of lactic acid bacteria, which are one of the organisms responsible for spoilage in salmon stored under modified atmosphere [Merlo *et al*., 2019].

Biogenic amine formation

The histamine, cadaverine, putrescine, tryptamine, phenylethylamine, tyramine, spermine and spermidine contents of salmon fillets packaged under modified atmosphere with different gas mixtures determined during the cold storage for 27 days are given in **Figure 2**. The levels of the mentioned biogenic amines increased significantly at the end of storage. Modified atmosphere packaging with different gas mixtures had significant effects on the formation of biogenic amines compared with air packaging ($p<0.001$). The lowest levels of the analyzed biogenic amines were found in the CO-MAP and 60% CO_2-MAP samples, respectively.

Cadaverine, tryptamine and tyramine were not detected in the salmon samples until the 6th day of storage, while histamine was detected only in the air-packaged samples; and putrescine, phenylethylamine, spermine and spermidine were detected in the modified atmosphere-packaged salmon except CO-MAP and 60% CO_2-MAP samples on the 3rd day of storage. The histamine content of the air-packaged salmon samples exceeded 100 mg/kg on day 21 of cold storage, whereas this value was not reached even on day 27 of storage in CO-MAP and 60% CO_2-MAP (**Figure 2**). Cadaverine was not detected in the CO-MAP and 60% CO_2-MAP samples until the 9th day of storage, while it was detected at 61.84, 71.15 and 85.71 mg/kg in the CO-MAP, 60% CO_2-MAP and 40% CO_2-MAP samples, respectively, at the end of storage. For the air-packaged samples, this value reached 144.58 mg/kg on the last day. Even though the quantity of putrescine was below 50 mg/kg in all groups until day 15 of storage, it was recorded as 85 mg/kg in the air-

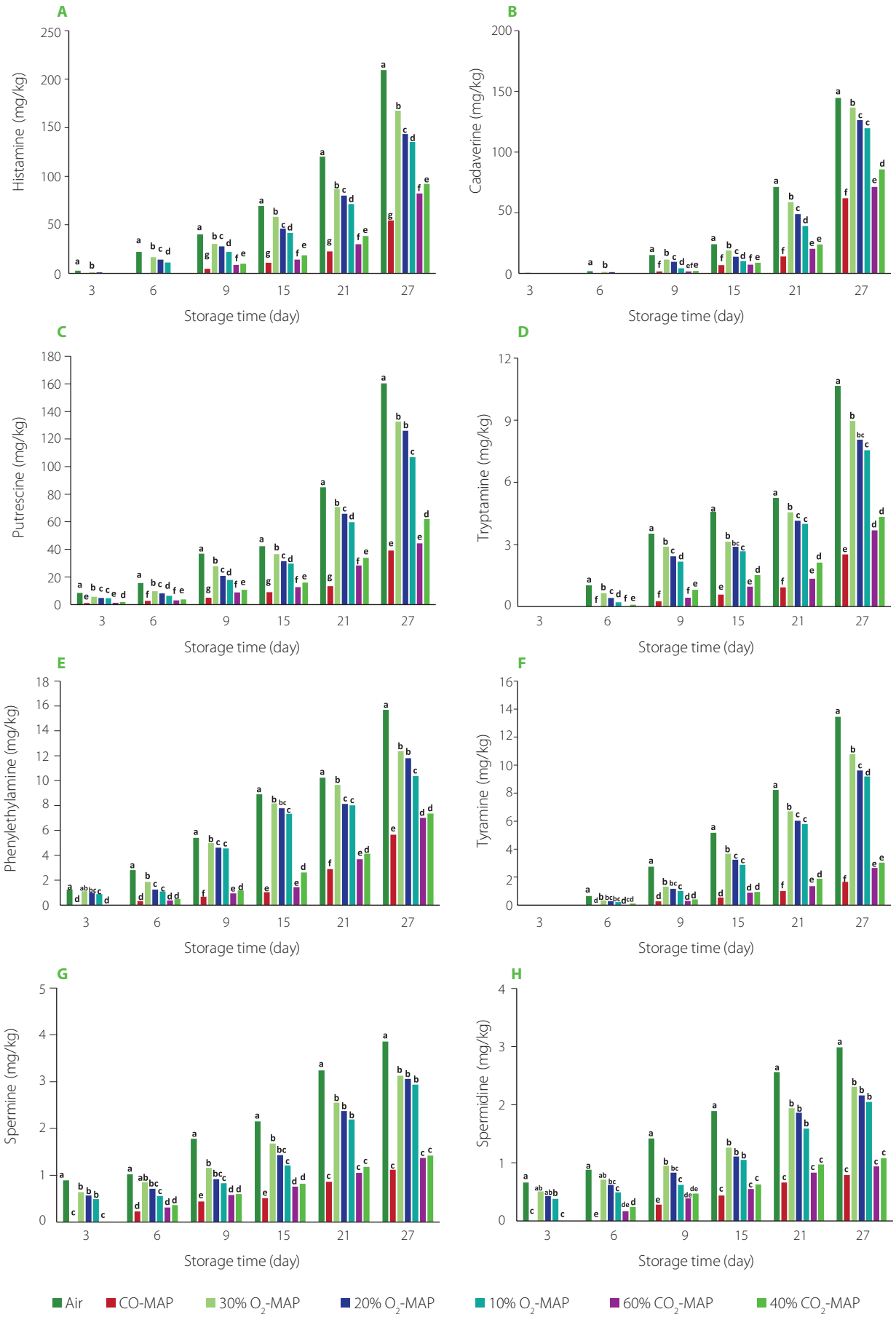

Figure 2. Biogenic amine contents including histamine (**A**), cadaverine (**B**), putrescine (**C**), tryptamine (**D**), phenylethylamine (**E**), tyramine (**F**), spermine (**G**), spermidine (**H**) of salmon fillets packaged in air and modified atmosphere during storage period. Different letters for each storage day indicate significant differences ($p<0.05$). Details regarding modified atmosphere packaging (MAP) are presented in Table 1.

-packaged salmon and as 60–70 mg/kg in the 20% and 30% O_2-MAP samples on day 21. Meanwhile, putrescine content was above 100 mg/kg on the last day of storage in the CO-MAP, 60% CO_2-MAP and 40% CO_2-MAP samples with a value of 39.19, 44.42 and 62.02 mg/kg, respectively. The amount of tryptamine remained below 10 mg/kg in all MA-packaged samples until the end of storage, only in the air-packaged samples it was recorded as 10.66 mg/kg on day 27. Phenylethylamine showed a similar change to tryptamine, reaching a value of 15.68 mg/kg on the 27th day of storage in the air-packaged salmon. The highest content of phenylethylamine recorded in the CO-MAP sample was 5.66 mg/kg, while values of 7.01 mg/kg and 7.36 mg/kg were determined in the 40% and 60% CO_2-MAP samples, respectively. Similarly to phenylethylamine and tryptamine, the tyramine contents were determined as 13.44 mg/kg and 10.79 mg/kg on the last day of storage in the air-packaged and 30% O_2-MAP samples, respectively. However, the amounts of tyramine remained below 10 mg/kg in the 10% and 20% O_2-MAP samples, whereas in the salmon samples packaged with CO and high CO_2 they were in the range of 1.66 to 3.03 mg/kg until the end of storage. The spermine and spermidine contents did not reach even 4 mg/kg until the end of storage in all packages, with values determined in the CO-MAP and high CO_2-MAP samples below 1.5 mg/kg even at the end of storage.

The formation of biogenic amines can be affected by many factors such as handling, processing and storage conditions, as well as the existing bacterial load in seafood, *i.e.*, raw material quality [Houicher *et al*., 2021]. Although it is accelerated by temperature, it also occurs at low storage temperatures (4°C). Therefore, biogenic amine formation, which may continue throughout the cold storage period depending on the type and count of microorganisms, especially due to the activity of biogenic amine-producing psychrophilic bacteria, is an important indicator affecting the quality of the products and a sign of breaking the cold chain during the processing and storage stages of foods [Çelebi Sezer *et al*., 2022]. It is also largely dependent on fish species. Fish with dark-colored muscles (tuna, mackerel, herring, sardines named as scombroid fish) show higher biogenic amine formation compared to white-muscled fish (cod, hake, sea bass, sea bream, trout, salmon) due to a higher histidine level [Prester *et al*., 2009]. Free histidine levels in the scombroid fish range from 5,000 mg/kg to 20,000 mg/kg, while Atlantic salmon which belongs to the Salmonidae family has 10 to 200 times lower free histidine levels (less than 1000 mg/kg) than the scombroid fish [FAO/WHO, 2018].

Biogenic amines such as histamine, cadaverine and putrescine are used to indicate deterioration. Due to its toxicological effects, histamine is currently the only biogenic amine for which maximum levels have been set in the EU and USA. According to the U.S. Food and Drug Administration (USFDA), food is considered spoilt when the histamine level reaches 50 ppm [FDA, 2005]. Therefore, Codex Alimentarius standard recognizes histamine level as a spoilage and hygiene indicator for fish. According to the EU legislation, the histamine level in fish offered for consumption should not exceed 100 mg/kg for tuna, mackerel and sardines, and 200 mg/kg for cod and salmon [EU, 2013]. In turn, the European Food Safety Authority (EFSA) stipulated the acceptable level of histamine below 200 mg/kg for chilled and frozen fish [EFSA, 2011].

Modified atmosphere packaging, used for the preservation of seafood to prolong shelf-life by reducing the microbiological growth and retarding the enzymatic degradation, proves to be an effective treatment for slowing down the formation of biogenic amines in salmon [Çelebi Sezer *et al*., 2022; Qian *et al*., 2022]. The inhibitory effect of MAP on the formation of biogenic amines has been associated with the antimicrobial effects of carbon dioxide on decarboxylase producing microorganisms [Çelebi Sezer *et al*., 2022]. De la Hoz *et al*. [2000] reported that the biogenic amine levels of salmon fillets packaged in modified atmosphere with CO_2 at different rates increased during cold storage. The levels of cadaverine and histamine in CO_2-packaged samples were found to be half of those found in the air-packaged samples. The levels of spermine and spermidine remained almost close to the initial values in all packages, while no significant change was observed in phenylethylamine and tryptamine values. Tryptamine recorded for the first time on day 5 of storage was similar to the present study.

A significant correlation was reported between the counts of certain microorganisms and the formation of biogenic amines. Particularly, a positive correlation was found between mesophilic bacteria and tryptamine, putrescine, tyramine and histamine, as well as between psychrophilic bacteria and putrescine, tyramine, tryptamine and spermidine, between *Enterobacteriaceae* and putrescine, cadaverine and histamine, and between *Pseudomonas* and putrescine and cadaverine [Arulkumar *et al*., 2023].

Oxidative changes

The TBARS values that indicated the fatty acid oxidation of salmon fillets are given in **Table 3**. The gas composition in MAP had a significant effect on lipid oxidation inhibition. The TBARS values of salmon fillets were close to 1 mg MDA/kg in the air-packaged group after 6th day of cold storage, while this value was exceeded on day 24 in the CO-MAP and 60% CO_2-MAP samples. A significant difference was recorded between the air and other packaging conditions during storage (p<0.001). Besides, the difference between samples in O_2 containing and non-containing packages was found to be significant (p<0.001), showing the lowest oxidation in CO and 60% CO_2 packages.

Amanatidou *et al*. [2000] stated that TBARS values of salmon increased significantly after 14 days of storage at 5°C. Zhang *et al*. [2022] emphasized that modified atmosphere packaging effectively inhibited lipid oxidation in seafood fillets and that TBARS values of air-packaged samples increased rapidly after a slow increase on the first days of storage. However, a slow increase was determined in MAP products over the storage period, indicating that the 70% CO_2/30% N_2 gas mixture most effectively inhibited lipid oxidation. Also, it was highlighted that the increase in CO_2 resulted in lower TBARS values, probably due to limited microbial growth and release of lipolytic enzyme. Similarly, in the present study, higher O_2 concentrations led to an increase in TBARS value,

Table 3. Oxidative changes in salmon fillets packaged in air and modified atmosphere during storage period.

Characteristic	Group	Day 0	Day 1	Day 3	Day 6	Day 9	Day 12	Day 15	Day 18	Day 21	Day 24	Day 27	*p*
TBARS (mg MDA/kg)	Air	0.02 ± 0.01^{H}	0.08 ± 0.01^{aH}	0.44 ± 0.04^{aG}	0.97 ± 0.01^{aF}	1.21 ± 0.06^{aEF}	1.31 ± 0.06^{aDE}	1.51 ± 0.12^{aCD}	1.67 ± 0.17^{aC}	2.14 ± 0.06^{aB}	2.22 ± 0.06^{aAB}	2.40 ± 0.12^{aA}	***
	CO-MAP	0.02 ± 0.01^{H}	0.02 ± 0.01^{dH}	0.18 ± 0.01^{dG}	0.36 ± 0.01^{fF}	0.46 ± 0.01^{eE}	0.56 ± 0.06^{deD}	0.62 ± 0.01^{cD}	0.82 ± 0.06^{cC}	0.96 ± 0.02^{dB}	1.05 ± 0.03^{cB}	1.17 ± 0.06^{cA}	***
	30% O_2-MAP	0.02 ± 0.01^{I}	0.06 ± 0.03^{bI}	0.30 ± 0.01^{bH}	0.61 ± 0.02^{bG}	0.73 ± 0.02^{bFG}	0.87 ± 0.02^{bEF}	1.03 ± 0.02^{bDE}	1.23 ± 0.12^{bCD}	1.40 ± 0.12^{bBC}	1.54 ± 0.12^{bAB}	1.73 ± 0.12^{bA}	***
	20% O_2-MAP	0.02 ± 0.01^{H}	0.06 ± 0.03^{bH}	0.25 ± 0.02^{cG}	0.58 ± 0.02^{cF}	0.67 ± 0.01^{bcEF}	0.76 ± 0.02^{bcDE}	0.88 ± 0.06^{bD}	1.05 ± 0.03^{bcC}	1.24 ± 0.12^{bcB}	1.47 ± 0.12^{bA}	1.63 ± 0.06^{bA}	***
	10% O_2-MAP	0.02 ± 0.01^{F}	0.04 ± 0.06^{cF}	0.23 ± 0.03^{cE}	0.51 ± 0.01^{dD}	0.61 ± 0.06^{cdD}	0.69 ± 0.06^{cdD}	0.87 ± 0.06^{bC}	1.02 ± 0.01^{bcBC}	1.19 ± 0.06^{bcB}	1.43 ± 0.11^{bA}	1.59 ± 0.12^{bA}	***
	60% CO_2-MAP	0.02 ± 0.01^{F}	0.02 ± 0.01^{cF}	0.19 ± 0.01^{dE}	0.33 ± 0.02^{fD}	0.43 ± 0.02^{eCD}	0.51 ± 0.06^{eC}	0.51 ± 0.06^{cC}	0.82 ± 0.01^{cB}	0.94 ± 0.03^{dB}	1.08 ± 0.11^{cA}	1.20 ± 0.12^{cA}	***
	40% CO_2-MAP	0.02 ± 0.01^{I}	0.03 ± 0.02^{dI}	0.22 ± 0.02^{cdH}	0.39 ± 0.01^{eG}	0.52 ± 0.01^{deF}	0.63 ± 0.02^{cdeE}	0.63 ± 0.02^{cE}	0.91 ± 0.03^{cD}	1.02 ± 0.01^{cdC}	1.12 ± 0.01^{cB}	1.25 ± 0.06^{cA}	***
	p	NS	***	***	***	***	***	***	***	***	***	***	
TMA-N (mg/100 g)	Air	0.80 ± 0.05^{H}	1.90 ± 0.12^{aH}	3.00 ± 0.08^{aH}	5.52 ± 0.29^{aG}	7.02 ± 0.58^{aFG}	9.00 ± 0.58^{aEF}	10.02 ± 0.58^{aDE}	12.00 ± 0.29^{aD}	15.04 ± 0.58^{aC}	20.02 ± 0.15^{aB}	23.02 ± 0.73^{aA}	***
	CO-MAP	0.80 ± 0.05^{G}	0.90 ± 0.06^{cG}	1.10 ± 0.16^{eG}	1.50 ± 0.17^{dG}	2.04 ± 0.29^{deFG}	3.00 ± 0.29^{efEF}	3.54 ± 0.17^{eE}	5.00 ± 0.58^{deD}	7.00 ± 0.17^{eC}	8.52 ± 0.58^{dB}	10.00 ± 0.58^{cA}	***
	30% O_2-MAP	0.80 ± 0.05^{H}	1.20 ± 0.12^{bH}	$2.00\pm0.06b^{GH}$	3.50 ± 0.12^{bFG}	4.00 ± 0.29^{bF}	5.04 ± 0.58^{bF}	7.02 ± 0.29^{bE}	9.02 ± 0.16^{bD}	11.00 ± 0.29^{bC}	16.00 ± 0.29^{bB}	18.04 ± 0.15^{bA}	***
	20% O_2-MAP	0.80 ± 0.05^{E}	1.10 ± 0.06^{bE}	1.60 ± 0.06^{cE}	3.24 ± 0.17^{bcD}	3.92 ± 0.17^{bD}	4.52 ± 0.29^{bcD}	6.00 ± 0.58^{bcC}	7.04 ± 0.29^{cC}	10.04 ± 0.29^{bcB}	15.02 ± 0.29^{bcA}	16.00 ± 0.58^{bA}	***
	10% O_2-MAP	0.80 ± 0.05^{H}	1.04 ± 0.06^{cH}	1.40 ± 0.12^{cdGH}	2.92 ± 0.17^{cFG}	3.50 ± 0.29^{bcEF}	4.02 ± 0.29^{bcdEF}	5.00 ± 0.58^{cdDE}	6.00 ± 0.58^{cdD}	9.02 ± 0.58^{cdC}	13.02 ± 0.16^{cB}	15.02 ± 0.15^{bA}	***
	60% CO_2-MAP	0.80 ± 0.05^{H}	0.90 ± 0.12^{cGH}	1.10 ± 0.06^{eGH}	1.42 ± 0.17^{dGH}	1.70 ± 0.12^{eFG}	2.50 ± 0.17^{fEF}	3.00 ± 0.36^{eE}	4.00 ± 0.58^{eD}	5.00 ± 0.58^{fC}	7.50 ± 0.29^{dB}	9.02 ± 0.29^{cA}	***
	40% CO_2-MAP	0.80 ± 0.05^{H}	0.92 ± 0.05^{cGH}	1.22 ± 0.06^{deGH}	1.82 ± 0.12^{dG}	2.82 ± 0.17^{cdF}	3.50 ± 0.12^{defEF}	4.02 ± 0.17^{deE}	6.04 ± 0.12^{cdD}	7.54 ± 0.29^{deC}	9.50 ± 0.29^{dB}	11.00 ± 0.58^{cA}	***
	p	NS	***	***	***	***	***	***	***	***	***	***	
TVB-N (mg N/100 g)	Air	6.32 ± 0.06^{J}	12.60 ± 0.17^{aI}	20.00 ± 0.58^{aH}	23.82 ± 0.35^{aG}	26.60 ± 0.35^{aF}	32.20 ± 0.75^{aE}	37.80 ± 0.58^{aD}	40.60 ± 0.35^{aC}	42.04 ± 0.85^{aC}	45.52 ± 0.54^{aB}	50.40 ± 0.38^{aA}	***
	CO-MAP	6.32 ± 0.06^{I}	6.72 ± 0.01^{cdI}	10.22 ± 0.13^{dH}	15.44 ± 0.23^{eG}	18.20 ± 0.12^{eF}	21.02 ± 0.23^{eE}	23.12 ± 0.06^{dD}	25.20 ± 0.12^{dC}	28.02 ± 0.85^{deB}	32.22 ± 0.24^{cA}	33.62 ± 0.54^{cdA}	***
	30% O_2-MAP	6.32 ± 0.06^{I}	7.84 ± 0.02^{bI}	13.44 ± 0.25^{bH}	19.60 ± 0.35^{bG}	25.24 ± 0.58^{bF}	26.60 ± 0.58^{bF}	29.44 ± 0.23^{bE}	32.20 ± 0.12^{bD}	36.42 ± 0.41^{bC}	39.24 ± 0.66^{bB}	42.00 ± 0.54^{bA}	***
	20% O_2-MAP	6.32 ± 0.06^{I}	7.06 ± 0.12^{cI}	12.60 ± 0.17^{bcH}	18.22 ± 0.12^{cG}	23.80 ± 0.58^{cF}	24.54 ± 0.75^{cF}	26.62 ± 0.58^{cE}	30.12 ± 0.58^{cD}	33.60 ± 0.44^{bcC}	37.80 ± 0.54^{bB}	40.62 ± 0.40^{bA}	***
	10% O_2-MAP	6.32 ± 0.06^{I}	7.06 ± 0.06^{cI}	11.93 ± 0.26^{cH}	16.82 ± 0.58^{dG}	19.62 ± 0.35^{dF}	20.34 ± 0.58^{eF}	22.40 ± 0.23^{dE}	26.60 ± 0.58^{dD}	28.72 ± 0.41^{deC}	32.22 ± 0.37^{cB}	35.72 ± 0.16^{cA}	***
	60% CO_2-MAP	6.32 ± 0.06^{I}	6.58 ± 0.06^{dI}	9.24 ± 0.14^{eH}	13.16 ± 0.09^{fG}	16.82 ± 0.46^{fF}	18.22 ± 0.58^{fF}	21.02 ± 0.58^{eE}	23.82 ± 0.36^{eD}	25.94 ± 0.16^{eC}	28.00 ± 0.20^{dB}	30.84 ± 0.54^{dA}	***
	40% CO_2-MAP	6.32 ± 0.06^{I}	6.86 ± 0.06^{cI}	10.92 ± 0.29^{dH}	16.80 ± 0.35^{dG}	19.60 ± 0.17^{dF}	22.40 ± 0.75^{dE}	23.80 ± 0.58^{dE}	26.60 ± 0.26^{dD}	30.82 ± 0.35^{cdC}	33.62 ± 0.18^{cB}	36.44 ± 0.35^{cA}	***
	p	NS	***	***	***	***	***	***	***	***	***	***	

Composition of gas mixtures used in MAP of different groups of salmon fillets are shown in Table 1. Results are presented as mean ± standard error. Means within a column with different letters (a–e) are significantly different ($p<0.05$). Means within a row with different letters (A–H) are significantly different ($p<0.05$). ***, $p<0.001$; NS, not significant; TBARS, thiobarbituric acid reactive substance; MDA, malondialdehyde; TMA-N, trimethylamine nitrogen; TVB-N, total volatile basic nitrogen; MAP, modified atmosphere packaging.

while increasing CO_2 levels in the package reduced the formation of oxidative compounds.

The TBARS value is an efficient indicator of rancidity and is widely used to determine the degree of fatty acid oxidation of seafood [Bulut *et al*., 2023]. While in some studies TBARS levels of less than 5 mg MDA/kg are considered to be the threshold for good quality, the maximum acceptable limit for chilled fish intended for human consumption is approved at 8 mg MDA/kg [Secci & Parisi, 2016]. In the present study, TBARS value reached 1.17 and 1.20 mg MDA/kg in the salmon samples packaged in the modified atmosphere containing CO and high CO_2, while 2.40 mg MDA/kg was determined in the air-packaged samples at the end of storage (**Table 3**).

The TMA-N values of salmon fillets showed an increase in all packages parallel to the deterioration process throughout the storage time (**Table 3**). This increase was greater in the samples packaged with ambient air than in the modified atmosphere-packaged samples, while a relatively slower rise was observed in the 60% CO_2-MAP ones. The TMA-N value obtained on the last day of storage in the air-packaged samples reached 23.02 mg/100 g and differed significantly compared to MA-packages, whereas salmon samples packaged in CO-MAP and 60% CO_2-MAP did not exceed 10 mg/100 g on the 27th day of storage, while those packaged in high O_2 exceeded 10 mg/100 g after 21 days (p<0.001).

The most widely used chemical parameters for determining the quality of fish and fishery products are TMA-N and TVB-N. The TMA-N value indicates the reduction in trimethylamine oxide due to the activity of spoilage organisms. Besides, this value also includes trimethylamine (formed by spoilage bacteria), dimethylamine (formed by autolytic enzymes), ammonia (formed by deamination of amino acids) and other volatile nitrogenous compounds related to spoilage [Fuentes-Amaya *et al*., 2016]. Although it varies for fish species, TMA-N value of 10–15 mg/100 g is the limit of acceptability and spoilage, while it is below 2 mg/100 g in very fresh fish [Summers *et al*., 2017].

The TVB-N values of salmon fillets increased in all packaging groups throughout the storage time (**Table 3**). A significant (p<0.001) difference was observed in TVB-N values between the air-packaged and modified atmosphere-packaged salmon. Especially the TVB-N levels of salmon fillets packaged with ambient air showed a faster increase compared to the other packages, and also the fillets showed signs of deterioration by exceeding 30 mg N/100 g on the 12th day. TVB-N values of these samples were recorded as 50.40 mg N/100 g on the last day of storage. Salmon packaged with CO and 60% CO_2 exceeded 30 mg N/100 g only after the 24th day of storage.

TVB-N are the total nitrogen compounds including ammonia, amines and other alkaline nitrogenous substances formed as a result of protein degradation during the storage process in seafood [Zhang *et al*., 2022]. Thus, the TVB-N value determines volatile nitrogen formed in the products [Fuentes-Amaya *et al*., 2016]. The increase in the level of nitrogenous compounds with the progression of spoilage in seafood is an important criterion in determining its shelf-life. In the seafood quality classification based on TVB-N values, up to 25 mg N/100 g denotes high quality, up to 30 mg N/100 g indicates good quality, up to 35 mg N/100 g denotes acceptable food and above 35 mg N/100 g is considered as spoilt [Fuentes-Amaya *et al*., 2016]. Maximum limits for TVB-N content depending on the fish species are provided as 25–35 mg N/100 g in the EU Regulation 1022/2008 [Esteves *et al*., 2021].

Fletcher *et al*. [2002] determined that TVB-N values of salmon remaining below 20 mg N/100 g for 90 days in MAP containing various level of CO_2 (10, 20, 30, 40, 60, 80 and 100 cm^3) at 0°C, whereas high CO_2 concentrations caused a decrease in the salmon overall quality. De la Hoz *et al*. [2000] reported that the TVB-N value of salmon fillets remained stable (<5 mg N/100 g) until the 9th day in all packages, while a significant increase in its values was observed especially in air-packaged salmon fillets that reached to 20 mg N/100 g at the end of storage. Moreover, it was noted that the initial TVB-N values could be maintained for 11 days in the salmon fillets packaged with CO_2. Similarly, Kritikos *et al*. [2020] reported that the TVB-N values of salmon slices did not reach the regulatory limit of 30–35 mg N/100 g at the end of 11 days shelf-life. Furthermore, in the present study, salmon fillets packaged with CO and high concentration of CO_2 exceeded 20 mg N/100 g only after the 12th day of storage. In addition, Zhang *et al*. [2022] emphasized that the greater increase in TVB-N values of fish was observed in air-packing compared to MAP. This was mainly due to the higher CO_2 content in MAP, which delayed bacterial activity and chemical reactions [Sivertsvik *et al*., 2003]. The changes observed in TVB-N values of modified atmosphere-packaged salmon under cold storage were consistent with the results obtained from bacterial counts of fish [Qian *et al*., 2022]. Additionally, modified atmosphere packaging has been proved effective in delaying protein degradation regardless of gas composition and can be used to extend the shelf-life of fish that plays an effective role in keeping TVB-N levels below consumable limits (approximately 20 mg N/100 g) [Bulut *et al*., 2023].

Instrumental color evaluation

The color parameters (CIE L^*, a^*, b^*) and total color difference (ΔE) of salmon fillets stored under modified atmospheres and air during the cold storage for 27 days are given in **Table 4**. A significant difference was observed in the lightness values of salmon fillets throughout the storage time between air-packaged and MAP--packaged samples (p<0.001). The L^* values of salmon stored under MAP increased during the first 9 days of storage and then showed a decreasing trend until the end of storage. The L^* value of the air-packaged samples was almost constant during entire storage, while the values recorded for high CO_2 and CO containing packages were lower than those determined for the air-packaged ones. The increase in the L^* values may be explained by denaturation of protein and the difference in reflective properties due to drip loss on fillet surfaces [Chan *et al*., 2021b].

There was a significant decrease in the redness values of air-packaged salmon during storage period (p<0.001), while bright red color was retained in CO-MAP and 40% CO_2-MAP. However, 60% CO_2 in the package atmosphere caused a decrease

Table 4. Instrumental color parameters of salmon fillets packaged in air and modified atmosphere during storage period.

Characteristic	Group	Day 0	Day 1	Day 3	Day 6	Day 9	Day 12	Day 15	Day 18	Day 21	Day 24	Day 27	*p*
*L**	Air	51.87^{F}	52.21^{bEF}	54.31^{aA}	53.33^{cB}	53.16^{cBC}	52.8^{bCD}	52.44^{cDE}	52.91^{bBC}	53.09^{aBC}	52.36^{bDE}	52.06^{bEF}	***
	CO-MAP	51.87^{BC}	51.48^{cCDE}	50.57^{eF}	51.54^{dCDE}	52.4^{dA}	52.08^{cAB}	51.67^{dBCD}	51.27^{cDE}	51.11^{cE}	51.09^{dE}	49.54^{eG}	***
	30% O_2-MAP	51.87^{A}	50.61^{dDE}	49.51^{fF}	51.21^{deB}	51.15^{fBC}	50.44^{eDE}	49.49^{fF}	50.16^{dE}	50.74^{cCD}	51.55^{cAB}	50.23^{dE}	***
	20% O_2-MAP	51.87^{D}	53.29^{aBC}	53.61^{bB}	54.43^{bA}	53.71^{bB}	53.69^{aB}	53.64^{aB}	53.55^{aB}	53.24^{aBC}	53.04^{aC}	52.88^{aC}	***
	10% O_2-MAP	51.87^{E}	52.23^{bDE}	52.89^{cC}	54.66^{abA}	54.62^{aA}	54.13^{aB}	53.31^{abC}	53.03^{bC}	52.94^{aC}	52.37^{bD}	51.92^{bE}	***
	60% CO_2-MAP	51.87^{EF}	51.53^{cFG}	52.29^{dE}	55^{aA}	54.53^{aB}	54.05^{aC}	53.01^{bD}	52.95^{bD}	52.88^{aD}	51.77^{cF}	51.22^{cG}	***
	40% CO_2-MAP	51.87^{A}	50.89^{dCDE}	50.39^{eF}	50.88^{eCDE}	51.77^{eA}	51.11^{dCD}	50.66^{eDEF}	51.32^{cBC}	51.59^{bAB}	51.95^{bcA}	50.51^{dEF}	***
	SE	0.05	0.19	0.38	0.37	0.28	0.31	0.32	0.26	0.22	0.14	0.25	***
	p	NS	***	***	***	***	***	***	***	***	***	***	
*a**	Air	24.11^{BC}	24.54^{bA}	24.25^{cB}	23.99^{cCD}	23.93^{eCDE}	23.84^{dDEF}	23.71^{deF}	23.75^{dEF}	23.42^{dG}	22.71^{dH}	22.02^{cI}	***
	CO-MAP	24.11^{F}	23.99^{cF}	24.85^{bE}	25.05^{bD}	25.54^{bB}	25.66^{bAB}	25.8^{bA}	25.67^{bAB}	25.32^{bC}	25.18^{bCD}	24.17^{bF}	***
	30% O_2-MAP	24.11^{G}	25.61^{aE}	25.86^{aD}	26.01^{aCD}	26.84^{aA}	26.71^{aAB}	26.64^{aB}	26.6^{aB}	26.53^{aB}	26.13^{aC}	25.32^{aF}	***
	20% O_2-MAP	24.11^{A}	23.38^{dD}	23.69^{dC}	24.12^{cA}	24.16^{deA}	24.02^{dAB}	23.84^{dBC}	23.24^{eD}	22.83^{eE}	22.14^{eF}	20.35^{fG}	***
	10% O_2-MAP	24.11^{A}	23.27^{dC}	23.58^{dB}	23.97^{cA}	24.1^{deA}	23.96^{dA}	23.55^{eB}	23.06^{efD}	22.81^{eE}	21.88^{fF}	21.05^{dG}	***
	60% CO_2-MAP	24.11^{A}	23.21^{bE}	23.49^{dD}	23.71^{dC}	24.06^{dAB}	23.89^{dBC}	23.05^{fEF}	22.94^{fFG}	22.84^{eG}	21.78^{fH}	20.81^{eI}	***
	40% CO_2-MAP	24.11^{C}	24.03^{cC}	24.79^{bB}	24.88^{bB}	25.16^{cA}	25.19^{cA}	25.22^{cA}	25.15^{cA}	25.09^{cA}	24.69^{cB}	24.01^{bC}	***
	SE	0.02	0.18	0.18	0.17	0.23	0.23	0.28	0.31	0.31	0.37	0.40	***
	p	NS	***	***	***	***	***	***	***	***	***	***	

Table 4 cont. Instrumental color parameters of salmon fillets packaged in air and modified atmosphere during storage period.

Characteristic	Group	Day 0	Day 1	Day 3	Day 6	Day 9	Day 12	Day 15	Day 18	Day 21	Day 24	Day 27	*p*
*b**	Air	26.93^{A}	26.04^{cdB}	25.81^{cBC}	25.74^{dBC}	25.69^{dBC}	25.54^{dCD}	25.45^{dCD}	25.15^{dDE}	24.97^{cdE}	23.32^{eF}	21.63^{eG}	***
	CO-MAP	26.93^{A}	26.19^{cC}	26.98^{bA}	26.66^{cAB}	26.41^{cBC}	26.33^{cBC}	26.25^{cBC}	25.99^{cC}	25.23^{cD}	24.35^{cE}	23.87^{cF}	***
	30% O_2-MAP	26.93^{D}	26.95^{bD}	27.63^{aC}	28.01^{aBC}	28.76^{aA}	28.79^{aA}	28.88^{aA}	28.18^{aB}	27.93^{aBC}	26.94^{aD}	26.59^{aD}	***
	20% O_2-MAP	26.93^{A}	25.76^{deB}	24.66^{dCD}	24.25^{fDEF}	24.03^{fF}	24.22^{eEF}	24.52^{eCDE}	24.59^{eCDE}	24.69^{deC}	24.28^{cdCDEF}	21.89^{eG}	***
	10% O_2-MAP	26.93^{A}	25.6^{eB}	25.01^{dC}	24.79^{eCD}	24.33^{fEF}	24.3^{eEF}	24.28^{eEF}	24.41^{eDEF}	24.59^{deDE}	24.08^{cdF}	21.69^{eG}	***
	60% CO_2-MAP	26.93^{A}	26.43^{cB}	25.54^{cC}	25.13^{eD}	24.79^{bDE}	24.54^{eEF}	24.23^{eFG}	24.34^{eF}	24.41^{eEF}	23.9^{dG}	23.08^{dH}	***
	40% CO_2-MAP	26.93^{C}	27.54^{aAB}	27.81^{aA}	27.36^{bBC}	27.14^{bBC}	27.31^{bBC}	27.5^{bAB}	27.56^{bAB}	27.26^{bBC}	26.29^{bD}	25.9^{bE}	***
	SE	0.04	0.15	0.27	0.29	0.35	0.36	0.37	0.33	0.30	0.28	0.42	***
	p	NS	***	***	***	***	***	***	***	***	***	***	
Δ*E*	Air	–	1.045^{dG}	2.688^{bC}	1.887^{cEF}	1.798^{bEF}	1.694^{bF}	1.636^{dF}	2.093^{bDE}	2.410^{bCD}	3.903^{aB}	5.700^{cA}	***
	CO-MAP	–	0.845^{eH}	1.497^{eF}	1.032^{eG}	1.611^{bF}	1.675^{bEF}	1.833^{cDE}	1.918^{bcD}	2.221^{bC}	2.900^{dB}	3.840^{eA}	***
	30% O_2-MAP	–	1.959^{aD}	3.02^{aBC}	2.283^{bD}	3.365^{aBC}	3.502^{aAB}	3.983^{aA}	3.269^{aBC}	2.852^{aC}	2.045^{eD}	2.066^{fD}	***
	20% O_2-MAP	–	1.979^{aF}	2.891^{abE}	3.706^{aB}	3.435^{aCD}	3.266^{aD}	3.002^{bE}	3.009^{aE}	2.921^{aE}	3.503^{cC}	6.369^{aA}	***
	10% O_2-MAP	–	1.614^{bF}	2.238^{cEF}	3.519^{aBCD}	3.785^{aB}	3.471^{aBCD}	3.068^{bBCD}	2.966^{aCD}	2.883^{aDE}	3.653^{bcBC}	6.068^{bA}	***
	60% CO_2-MAP	–	1.084^{dG}	1.579^{deF}	3.633^{aBC}	3.414^{aCD}	3.242^{aDE}	3.117^{bDE}	3.04^{aE}	2.997^{aE}	3.824^{abB}	5.112^{dA}	***
	40% CO_2-MAP	–	1.157^{cCD}	1.851^{dA}	1.326^{dBC}	1.075^{cD}	1.374^{bB}	1.738^{cdA}	1.335^{cBC}	1.071^{cD}	0.867^{fE}	1.709^{gA}	***
	SE	–	0.10	0.13	0.24	0.23	0.20	0.19	0.17	0.14	0.23	0.40	***
	p	–	***	***	***	***	***	***	***	***	***	***	

Composition of gas mixtures used in MAP of different groups of salmon fillets are shown in Table 1. Means within a column with different letters (a–f) are significantly different ($p<0.05$). Means within a row with different letters (A–H) are significantly different ($p<0.05$). ***, $p<0.001$; NS, not significant; SE, standard error; *L**, lightness; *a**, redness; *b**, yellowness; Δ*E*, total color difference; MAP, modified atmosphere packaging.

Table 5. Sensorial properties of salmon fillets packaged in air and modified atmosphere during storage period.

Characteristic	Group	Day 1	Day 3	Day 9	Day 15	Day 21	Day 27
Color intensity	Air	8.50^{b}	8.00^{c}	7.50^{c}	6.00^{d}	5.00^{d}	3.50^{e}
	CO-MAP	9.00^{a}	8.98^{a}	8.50^{a}	7.50^{a}	6.00^{b}	5.00^{b}
	30% O_2-MAP	8.50^{b}	8.00^{c}	7.00^{d}	6.00^{d}	5.00^{d}	4.00^{d}
	20% O_2-MAP	8.98^{a}	8.50^{b}	7.00^{d}	6.50^{c}	5.50^{c}	4.50^{c}
	10% O_2-MAP	8.98^{a}	8.50^{b}	7.50^{c}	6.50^{c}	5.50^{c}	5.00^{b}
	60% CO_2-MAP	9.00^{a}	8.98^{a}	8.00^{b}	7.50^{a}	6.50^{a}	5.50^{a}
	40% CO_2-MAP	8.98^{a}	8.98^{a}	8.00^{b}	7.00^{b}	6.00^{b}	5.00^{b}
	SE	0.04	0.07	0.09	0.10	0.09	0.10
	p	***	***	***	***	***	***
Appearance	Air	8.50^{b}	8.00^{c}	7.00^{c}	6.00^{c}	5.00^{c}	4.00^{d}
	CO-MAP	8.98^{a}	8.50^{b}	8.00^{a}	7.00^{a}	6.50^{a}	5.50^{a}
	30% O_2-MAP	8.50^{b}	8.00^{c}	7.00^{c}	6.00^{c}	5.00^{c}	4.50^{c}
	20% O_2-MAP	8.98^{a}	8.50^{b}	7.00^{c}	6.00^{c}	5.00^{c}	4.50^{c}
	10% O_2-MAP	8.98^{a}	8.50^{b}	7.50^{b}	6.50^{b}	5.00^{c}	5.00^{b}
	60% CO_2-MAP	8.98^{a}	8.98^{a}	8.00^{a}	7.00^{a}	6.50^{a}	5.50^{a}
	40% CO_2-MAP	8.98^{a}	8.98^{a}	8.00^{a}	7.00^{a}	6.00^{b}	5.00^{b}
	SE	0.04	0.06	0.08	0.08	0.11	0.08
	p	***	***	***	***	***	***
Tenderness	Air	8.50^{b}	8.00^{b}	6.00^{d}	5.50^{d}	4.48^{d}	3.48^{d}
	CO-MAP	8.98^{a}	8.50^{a}	7.50^{a}	7.00^{a}	6.00^{a}	5.50^{a}
	30% O_2-MAP	8.50^{b}	8.00^{b}	6.50^{c}	6.00^{c}	5.00^{c}	4.48^{c}
	20% O_2-MAP	8.50^{b}	8.00^{b}	7.00^{b}	6.50^{b}	5.00^{c}	4.48^{c}
	10% O_2-MAP	8.98^{a}	8.48^{a}	7.00^{b}	6.50^{b}	5.48^{b}	5.00^{b}
	60% CO_2-MAP	8.98^{a}	8.50^{a}	7.48^{a}	7.00^{a}	6.00^{a}	5.50^{a}
	40% CO_2-MAP	8.98^{a}	8.50^{a}	7.48^{a}	7.00^{a}	5.98^{a}	5.00^{b}
	SE	0.04	0.05	0.09	0.09	0.10	0.10
	p	***	***	***	***	***	***
Off-odor	Air	8.98	8.00^{c}	7.50^{b}	6.00^{d}	5.00^{d}	3.46^{d}
	CO-MAP	8.98	8.98^{a}	8.00^{a}	7.48^{a}	6.50^{a}	5.48^{a}
	30% O_2-MAP	8.98	8.00^{c}	7.00^{c}	6.00^{d}	5.50^{c}	4.46^{c}
	20% O_2-MAP	8.98	8.50^{b}	7.00^{c}	6.50^{c}	5.00^{d}	4.46^{c}
	10% O_2-MAP	8.96	8.98^{a}	7.50^{b}	6.50^{c}	5.46^{c}	5.00^{b}
	60% CO_2-MAP	8.98	8.96^{a}	8.00^{a}	7.48^{a}	6.00^{b}	5.00^{b}
	40% CO_2-MAP	8.98	8.98^{a}	8.00^{a}	7.00^{b}	6.00^{b}	5.00^{b}
	SE	0.01	0.07	0.07	0.10	0.09	0.10
	p	NS	***	***	***	***	***

Composition of gas mixtures used in MAP of different groups of salmon fillets are shown in Table 1. Means within a column with different letters (a–d) are significantly different ($p<0.05$). ***, $p<0.001$; NS, not significant; SE, standard error.

in the stability of red color. The yellowness values of salmon showed a decrease throughout storage time in packages containing air and 10–20% O_2, while the changes in b^* values increased until the 18th day of storage in MA-packages containing 40% CO_2 gas mixture, and then slightly decreased until the end of storage. Also, a constant change was recorded in CO-MAP during the same period. The losing of redness and yellowness value in salmon fillets may also be associated with an increase in protein denaturation and drip loss during storage, independent of the packaging method. Additionally, the higher ΔE in salmon fillets was generally recorded in the O_2-MAP groups during 27-day cold storage. However, the smallest color change was observed in CO-MAP until 21st day of storage, while salmon packaged with 40% CO_2 remained stable in this respect during entire storage.

Chan *et al*. [2021b] reported that the packaging of salmon fillets with 60% CO_2 resulted in a decrease the redness and yellowness values during storage period, which is in line with our findings. The decline in redness and yellowness values of salmon fillets was associated with the increase in protein denaturation and drip loss during storage, regardless of the packaging method.

Sensory evaluation

The sensory evaluation (appearance, color intensity, off-odor, tenderness) scores of salmon fillets during the cold storage for 27 days are given in **Table 5**. The sensorial properties of the air-packaged samples remained within acceptable limits only until the 15th day. However, the changes in their chemical and microbial parameters after this period showed that they were consumable for only one week in cold storage. Furthermore, it was revealed by sensory evaluations that the shelf-life of salmon fillets can exceed 2 weeks when packaged with CO-MAP and 60% CO_2-MAP.

The tenderness scores of cold-stored salmon samples showed similar changes within the groups until the 15th day of storage. As a result of microbial and chemical changes occurring in salmon samples over time, there was a loss in the tenderness of the samples belonging to all groups. At the end of the 27-day storage period, although the tenderness scores of the samples stored in CO-MAP and 60% CO_2-MAP were found to be higher, no significant difference was detected between them and the other groups. Salmon fillets packaged with CO and CO_2/N_2 gas mixtures remained within the consumable limits in terms of odor and color characteristics until the end of the storage period, while their appearance characteristics changed in parallel with structural alteration.

Preservation techniques are industrially utilized ways to ensure both food safety and the sensory appeal of fresh salmon. Thus, the packaging methods for seafood have evolved with the use of modified atmosphere packaging [Merlo *et al*., 2019]. The CO_2 used in MAP suppresses microbial growth by prolonging the lag phase and reducing the accumulation of hypoxanthine and volatile bases, *i.e.*, compounds responsible for spoilage. This minimizes the formation of unpleasant odors in salmon [Chan *et al*., 2021b]. Similar with the present study, salmon fillets packaged with 75% CO_2/25% N_2 gas mixture maintained acceptable sensory properties for 27 days of storage, while total bacterial loads exceeded 10^6 CFU/g after 18 days. Furthermore, increasing the CO_2 concentration to 90% enabled the product to remain acceptable in terms of sensory properties for up to 28 days [Fernandez *et al*., 2009].

Despite the increasing count of *Pseudomonas*, there was minimal organoleptic change in salmon fillets after 30 days with no negative change in structure or odor. The off-odor caused by trimethylamine and sulfhydryl and the bitter taste due to the increase in hypoxanthine are responsible for the microbial spoilage by *Pseudomonas* spp. [Milne & Powell, 2014]. In addition, degradation products formed by spoilage microorganisms, such as *Hafnia alvei*, *Photobacterium phosphoreum* and *Carnobacterium maltaromaticum*, are also responsible for the undesirable odors of salmon under MAP [Macé *et al*., 2013].

CONCLUSIONS

The findings of this study confirmed that MAP with 60% CO_2 and 0.4% CO could be an alternative means for extending cold storage of salmon fillets at 1°C. Selecting appropriate gas combinations in the packaging of fresh salmon under modified atmosphere provides extended shelf-life while maintaining the quality parameters of the product by preventing oxidation, maintaining color stability, retarding microbial growth and improving sensory properties. Consequently, modified atmosphere packaging under high concentrations (60–50%) of CO_2 or low level of CO (0.4%) was determined as an effective treatment in extending the shelf-life of salmon and other fatty fish species by preserving their quality characteristics.

RESEARCH FUNDING

The present work was supported by the Research Fund of İstanbul University-Cerrahpaşa, İstanbul, Turkey, Project no. TYO-2016-20400.

CONFLICT OF INTERESTS

Authors declare no conflict of interests.

ORCID IDs

E. Akkaya https://orcid.org/0000-0002-2665-4788
E.B. Bingol https://orcid.org/0000-0002-6452-4706
A.S. Engin https://orcid.org/0000-0003-0303-9157
H. Colak https://orcid.org/0000-0002-8293-7053
H. Hampikyan https://orcid.org/0000-0002-9032-7861

REFERENCES

1. Amanatidou, A., Schluter, O., Lemkau, K., Gorris, L.G.M., Smid, E.J., Knorr, D. (2000). Effect of combined application of high pressure treatment and modified atmospheres on the shelf life of fresh Atlantic salmon. *Innovative Food Science & Emerging Technologies, 1*(2), 87-98. https://doi.org/10.1016/S1466-8564(00)00007-2
2. AMSA (2012). *Meat Color Measurement Guidelines*. American Meat Science Association, Champaign, Il, USA.
3. AOAC (2000). *Official Method 971.14, Fish and other marine products, Trimethylamine nitrogen in seafood*. Association of Official Analytical Chemists Arlington, VA, USA.
4. AOAC (2005). *Official Methods of Analysis of AOAC International* (17th ed.) Association of Official Analytical Chemists, Washington, DC., USA.

5. Arulkumar, A., Paramithiotis, S., Paramasiva, S. (2023). Biogenic amines in fresh fish and fishery products and emerging control. *Aquaculture and Fisheries, 8*(4), 431-450. **https://doi.org/10.1016/j.aaf.2021.02.001**
6. Bogdanović, T., Petričević, S., Brkljača, M., Listeš, I., Pleadin, J. (2020). Biogenic amines in selected foods of animal origin obtained from the Croatian retail market. *Food Additives & Contaminants: Part A, 37*(5), 815-830. **https://doi.org/10.1080/19440049.2020.1726503**
7. Bulut, M., Okutan, G., Alwazeer, D., Boran, G. (2023). Hydrogen inclusion in modified atmosphere extends the shelf life of chilled rainbow trout fillets. *Turkish Journal of Fisheries and Aquatic Sciences, 23*(6), art. no. TRJFAS22515. **https://doi.org/10.4194/TRJFAS22515**
8. Chan, S.S., Rotabakk, B.T., Løvdal, T., Lerfall, J., Roth, B. (2021a). Skin and vacuum packaging of portioned Atlantic Salmon originating from refrigerated seawater or traditional ice storage. *Food Packaging and Shelf Life, 30*, art. no. 100767. **https://doi.org/10.1016/j.fpsl.2021.100767**
9. Chan, S.S., Skare, M., Rotabakk, B.T., Sivertsvik, M., Lerfall, J., Løvdal, T., Roth, B. (2021b). Evaluation of physical and instrumentally determined sensory attributes of Atlantic Salmon portions packaged in modified atmosphere and vacuum skin. *LWT – Food Science and Technology, 146*, art. no. 111404. **https://doi.org/10.1016/j.lwt.2021.111404**
10. Conway, E.J., Byrne, A. (1933). An absorption apparatus for the micro-determination of certain volatile substances. I. The micro-determination of ammonia. *Biochemical Journal*, *27*, 419-429.
11. Cooksey, K. (2014). Chapter 19 – Modified atmosphere packaging of meat, poultry and fish. In: J.H. Han (Ed.), *Innovations in Food Packaging*, Academic Press, USA, pp. 475-493. **https://doi.org/10.1016/B978-0-12-394601-0.00019-9**
12. Cornforth, D.P., Hunt, M.C. (2008). Low-oxygen packaging of fresh meat with carbon monoxide: Meat quality, microbiology, and safety. In: *The American Meat Science Association (AMSA) White Paper Series Number 2*, USA.
13. Çelebi Sezer, Y., Bulut, M., Boran, G., Alwazeer, D. (2022). The effects of hydrogen incorporation in modified atmosphere packaging on the formation of biogenic amines in cold stored rainbow trout and horse mackerel. *Journal of Food Composition and Analysis, 112*, art. no. 104688. **https://doi.org/10.1016/j.jfca.2022.104688**
14. Dadáková, E., Krízek, M., Pelikánová, T. (2009). Determination of biogenic amines in foods using ultra-performance liquid chromatography (UPLC). *Food Chemistry, 116*(1), 365-370. **https://doi.org/10.1016/j.foodchem.2009.02.018**
15. De la Hoz, L., Lopez-Galvez, D., Fernandez, M., Hierro, E., Ordonez, J. (2000). Use of carbon dioxide enriched atmospheres in the refrigerated storage (2°C) of salmon (*Salmo salar*) steaks. *European Food Research and Technology, 210*, 179-188. **https://doi.org/10.1007/PL00005509**
16. Djenane, D., Roncalés, P. (2018). Carbon monoxide in meat and fish packaging: Advantages and limits. *Foods, 7*(2), art. no. 12. **https://doi.org/10.3390/foods7020012**
17. EFSA (2011). Scientific opinion on risk based control of biogenic amine formation in fermented foods EFSA Panel on Biological Hazards, European Food Safety Authority. *EFSA J*, *9*(10), art. no. 2393. **https://doi.org/10.2903/j.efsa.2011.2393**
18. Esteves, E., Guerra, L., Aníbal, J. (2021). Effects of vacuum and modified atmosphere packaging on the quality and shelf-life of gray triggerfish (*Balistes capriscus)* fillets. *Foods*, *10*(2), art. no. 250. **https://doi.org/10.3390/foods10020250**
19. EU (2013). European Union Commission Regulation (EU) No. 1019/2013 amending Annex I to Regulation (EC) No. 2073/2005 as regards histamine in fishery products.
20. FAO/WHO (2018). Histamine in Salmonids: joint FAO/WHO literature review. Food and Agriculture Organization of the United Nations/World Health Organization. **https://www.who.int/publications/i/item/9789241514439**
21. FDA (2005). Compliance Policy Guide (CPG) Sec. 540.525 Decomposition and histamine raw, frozen tuna and mahi-mahi; canned tuna; and related species. Food and Drug Administration.
22. Fernandez, K., Aspe, E., Roeckel, M. (2009). Shelf-life extension on fillets of Atlantic salmon (*Salmo salar*) using natural additives, superchilling and modified atmosphere packaging. *Food Control, 20*(11), 1036-1042. **https://doi.org/10.1016/j.foodcont.2008.12.010**
23. Fletcher, G.C., Summers, G., Corrigan, V., Cumarasamy, S., Dufour, J.P. (2002). Spoilage of king salmon (*Oncorhynchus tshawytscha*) fillets stored under different atmospheres. *Journal of Food Science, 67*(6), 2362-2374. **https://doi.org/10.1111/j.1365-2621.2002.tb09555.x**
24. Fuentes-Amaya, L.F., Munyard, S., Fernandez-Piquer, J., Howieson, J. (2016). Sensory, microbiological and chemical changes in vacuum-packaged blue spotted emperor (*Lethrinus* sp), saddletail snapper (*Lutjanus malabaricus*), crimson snapper (*Lutjanus erythropterus*), barramundi (*Lates calcarifer*) and Atlantic salmon (*Salmo salar*) fillets stored at 4°C. *Food Science & Nutrition, 4*(3), 479-489. **https://doi.org/10.1002/fsn3.309**
25. Houicher, A., Bensid, A., Regenstein, J.M., Ozogul, F. (2021). Control of biogenic amine production and bacterial growth in fish and seafood products using phytochemicals as biopreservatives: A review. *Food Bioscience, 39*, art. no. 100807. **https://doi.org/10.1016/j.fbio.2020.100807**
26. ISO (1998). Microbiology of food and animal feeding stuffs. *Horizontal method for the enumeration of mesophilic lactic acid bacteria-Colony-count technique at 30 degrees C* (ISO Standard No. 15214:1998).
27. ISO (2007). Sensory analysis. *General guidance for the design of test rooms* (ISO Standard No. 8589:2007).
28. ISO (2008). Microbiology of food and animal feeding stuffs. *Horizontal method for the enumeration of yeasts and moulds-Part 1: Colony count technique in products with water activity greater than 0.95* (ISO Standard No. 21527-1:2008).
29. ISO (2010). Meat and meat products. *Enumeration of presumptive Pseudomonas spp.* (ISO Standard No. 13720:2010).
30. ISO (2012). Sensory analysis. *General guidelines for the selection, training and monitoring of selected assessors and expert sensory assessors* (ISO Standard No. 8586:2012).
31. ISO (2013). Microbiology of the food *chain. Horizontal method for the enumeration of microorganisms-Part 1: Colony count at 30°C by the pour plate technique* (ISO Standard No. 4833-1:2013).
32. ISO (2016). Sensory analysis. *Methodology-General guidance for establishing a sensory profile* (ISO Standard No. 13299:2016).
33. ISO (2017a). Microbiology of the food chain. *Preparation of test samples, initial suspension and decimal dilutions for microbiological examination-Part 1: General rules for the preparation of the initial suspension and decimal dilutions* (ISO Standard No. 6887-1:2017).
34. ISO (2017b). Microbiology of the food chain. *Horizontal method for the detection and enumeration of Enterobacteriaceae-Part 2: Colony-count technique* (ISO Standard No. 21528-2:2017).
35. ISO (2017c). Microbiology of the food chain. *Enumeration of Brochothrix spp.-Colony-count technique* (ISO Standard No. 13722:2017).
36. ISO (2019). Microbiology of the food chain. *Horizontal method for the enumeration of psychrotrophic microorganisms* (ISO Standard No. 17410:2019).
37. Kritikos, A., Aska, I., Ekonomou, S., Mallouchos, A., Parlapani, F.F., Haroutounian, S.A., Boziaris, I.S. (2020). Volatilome of chill-stored European seabass (*Dicentrarchus labrax*) fillets and Atlantic salmon (*Salmo salar*) slices under modified atmosphere packaging. *Molecules, 25*(8), art. no. 1981. **https://doi.org/10.3390/molecules25081981**
38. Macé, S., Joffraud, J-J., Cardinal, M., Malcheva, M., Cornet, J., Lalanne, V., Chevalier, F., Sérot, T., Pilet, M.-F., Dousset, X. (2013). Evaluation of the spoilage potential of bacteria isolated from spoiled raw salmon (*Salmo salar*) fillets stored under modified atmosphere packaging. *International Journal of Food Microbiology, 160*(3), 227-238. **https://doi.org/10.1016/j.ijfoodmicro.2012.10.013**
39. Merlo, T.C., Contreras-Castillo, C.J., Saldaña, E., Barancelli, G.V., Dargelio, M.D.B., Yoshida, C.M.P., Ribeiro Junior, E.E., Massarioli, A., Venturini, A.C. (2019). Incorporation of pink pepper residue extract into chitosan film combined with a modified atmosphere packaging: Effects on the shelf life of salmon fillets. *Food Research International, 125*, art. no. 108633. **https://doi.org/10.1016/j.foodres.2019.108633**
40. Milne, D., Powell, S.M. (2014). Limited microbial growth in Atlantic salmon packed in a modified atmosphere. *Food Control, 42*, 29-33. **https://doi.org/10.1016/j.foodcont.2014.01.035**
41. Ouahioune, L.A., Wrona, M., Nerín, C., Djenane, D. (2022). Novel active biopackaging incorporated with macerate of carob (*Ceratonia siliqua L.*) to extend shelf-life of stored Atlantic salmon fillets (*Salmo salar L.*). *LWT – Food Science and Technology, 156*, art. no. 113015. **https://doi.org/10.1016/j.lwt.2021.113015**
42. Powell, S.M., Tamplin, M.L. (2012). Microbial communities on Australian modified atmosphere packaged Atlantic salmon. *Food Microbiology, 30*(1), 226-232. **https://doi.org/10.1016/j.fm.2011.10.002**
43. Prester, L., Macan, J., Varnai, V.M., Orct, T., Vukušić, J., Kipčić, D. (2009). Endotoxin and biogenic amine levels in Atlantic mackerel (*Scomber scombrus*), sardine (*Sardina pilchardus*) and Mediterranean hake (*Merluccius merluccius*) stored at 22°C. *Food Additives and Contaminants, 26*(3), 355-362. **https://doi.org/10.1080/02652030802520878**
44. Qian, Y.-F., Liu, C.-C., Zhang, J.-J., Ertbjerg, P., Yang, S.-P. (2022). Effects of modified atmosphere packaging with caried CO_2 and O_2 concentrations on the texture, protein, and odor characteristics of salmon during cold storage. *Foods, 11*(22), art. no. 3560. **https://doi.org/10.3390/foods11223560**
45. Saraiva, C., Vasconcelos, H., de Almeida José, M.M.M. (2017). A chemometrics approach applied to Fourier transform infrared spectroscopy (FTIR) for monitoring the spoilage of fresh salmon (*Salmo salar*) stored under modified atmospheres. *International Journal of Food Microbiology, 241*, 331-339. **https://doi.org/10.1016/j.ijfoodmicro.2016.10.038**
46. Secci, G., Parisi, G. (2016). From farm to fork: Lipid oxidation in fish products. A review. *Italian Journal of Animal Science, 15*(1), 124-136. **https://doi.org/10.1080/1828051X.2015.1128687**

47. Shrestha, S., Min, Z. (2006). Effect of lactic acid pretreatment on the quality of fresh pork packed in modified atmosphere. *Journal of Food Engineering, 72*(3), 254-260.
https://doi.org/10.1016/j.jfoodeng.2004.12.004
48. Sivertsvik, M., Rosnes, J.T., Kleiberg, G.H. (2003). Effect of modified atmosphere packaging and superchilled storage on the microbial and sensory quality of Atlantic salmon (*Salmo salar*) fillets. *Journal of Food Science, 68*(4), 1467-1472.
https://doi.org/10.1111/j.1365-2621.2003.tb09668.x
49. Summers, G., Wibisono, R.D., Hedderley, D.I., Fletcher, G.C. (2017). Trimethylamine oxide content and spoilage potential of New Zealand commercial fish species. *New Zealand Journal of Marine and Freshwater Research, 51*(3), 393-405.
https://doi.org/10.1080/00288330.2016.1250785
50. Surówka, K., Rzepka, M., Özoğul, F., Özoğul, Y., Surówka, B., Ligaszewski, M. (2021). Nucleotide degradation, biogenic amine level and microbial contamination as quality indicators of cold-stored rainbow trout (*Oncorhynchus mykiss*) gravid. *Food Chemistry, 346*, art. no. 128904.
https://doi.org/10.1016/j.foodchem.2020.128904
51. Tsironi, T.N., Taoukis, P.S. (2018). Current practice and innovations in fish packaging. *Journal of Aquatic Food Product Technology, 27*(10), 1024-1047.
https://doi.org/10.1080/10498850.2018.1532479
52. Zhang, X., Pan, C., Chen, S., Xue, Y., Wang, Y., Wu, Y. (2022). Effects of modified atmosphere packaging with different gas ratios on the quality changes of golden pompano (*Trachinotus ovatus*) fillets during superchilling storage. *Foods, 11*(13), art. no. 1943.
https://doi.org/10.3390/foods11131943

ORIGINAL ARTICLE
http://journal.pan.olsztyn.pl

Polish Journal of Food and Nutrition Sciences
2024, Vol. 74, No. 4, 340–349
DOI: 10.31883/pjfns/194785
ISSN 1230-0322, e-ISSN 2083-6007

Osmotic Dehydration of Orange Fruits in Sucrose and Prickly Pear Molasses Solutions: Mass Transfer and Quality of Dehydrated Products

Raghda Yazidi[1,2], Walid Yeddes[1], Katarzyna Rybak[3], Dorota Witrowa-Rajchert[3], Wissem Aidi Wannes[3,*], Majdi Hammami[1], Kamel Hessini[4], Moufida Saidani Tounsi[1], Małgorzata Nowacka[3]

[1]Laboratory of Aromatic and Medicinal Plants, Borj Cedria Biotechnology Center, BP901, 2050 Hammam-Lif, Tunisia
[2]Faculty of Science of Tunis, University of Tunis, EL Manar, 2092 Tunis, Tunisia
[3]Department of Food Engineering and Process Management, Institute of Food Sciences, Warsaw University of Life Sciences—SGGW, 02-776 Warsaw, Poland
[4]Department of Biology, College of Sciences, Taif University, 21944 Taif, Saudi Arabia

The osmotic dehydration of orange fruit slices in sucrose and prickly pear molasses was studied in order to examine the changes in total mass loss, water loss, and solid gain as well as physical properties (dry matter content, total soluble solid and color parameters) during this process. The contents of total phenolics, ascorbic acid, and sugars, as well as antioxidant capacity and texture parameters of fresh orange slices and these dehydrated in both solutions were also analyzed. The osmotic dehydration was carried out at a temperature of 30°C for 3 h and after this processing time, the total mass loss of orange slices dehydrated in molasses solution was higher (0.18 kg/kg) compared to that treated in a sugar solution (0.16 kg/kg). Throughout the process, higher ratios of water loss to solid gain were noted for orange slices dehydrated in molasses solution than in the sucrose one. No significant difference was found in water activity between orange slices dehydrated in both solutions. Molasses induced more substantial and perceptible color alterations in orange slices compared to sucrose with total color difference values of 9.12 and 3.28, respectively. Immersion in osmotic solutions reduced hardness of orange slices from 0.63 N for fresh slices to 0.52 N and 0.40 N for these dehydrated in sucrose and molasses solutions, respectively. Compression work values of dehydrated orange slices were 0.38 mJ after the treatment in a sucrose solution and 0.36 mJ in the molasses one. The total phenolic content, antioxidant capacity in ABTS assay and ascorbic acid content increased in dehydrated slices compared to fresh material, particularly in the slices processed in molasses (2,197 mg CA/100 g DM, 6.26 mg Trolox/g DM and 50.14 mg/100 g, respectively). Sugar profiles of dehydrated orange slices varied, with molasses favoring glucose (5.47 mg/100 g DM) and reducing fructose (1.80 mg/100 g DM) compared to sucrose. Prickly pear molasses could be incorporated into the preservation of seasonal fruits as a valuable osmotic solution.

Keywords: antioxidant capacity, antioxidant content, hypertonic solution, osmotic agent, physical properties, sugar profile

INTRODUCTION

Citrus fruits, renowned for their nutritional richness and distinctive flavors, have become a staple food in global consumption patterns. Among these, oranges stand out as a particularly valuable source of essential bioactive compounds, including polyphenols, carotenoids, ascorbic acid, and limonoids, contributing not only to their distinct taste and aroma but also to a myriad of health benefits [Liu *et al.*, 2022; Lv *et al.*, 2015]. Despite

***Corresponding Author:**
e-mail: aidiwissem@yahoo.fr (Dr. W.A. Wannes)

Submitted: 7 August 2024
Accepted: 17 October 2024
Published on-line: 13 November 2024

their appeal, fresh oranges face perishability issues due to a high water content of 87% [Omar & Matjafri, 2013]. In response to this challenge, various processing techniques, such as dehydration, have been explored to extend shelf life, and at the same time reduce packaging, storage, and transportation costs [Sun *et al.*, 2019]. Osmotic dehydration (OD) emerges as a pivotal method in this context, distinguished for its cost-effectiveness and unique mass transfer dynamics [Abrahão & Corrêa, 2023]. This technique involves immersing food in hypertonic solutions, creating counter-current flows that facilitate the removal of water from the tissue to the surrounding solution and the diffusion of osmotic solutes into the tissue, effectively preserving the food product [Ahmad, 2023]. As a non-thermal processing technique, OD has gained favor in recent years due to increasing consumer demand for fresh, nutritious foods and the need for energy--efficient and environmentally friendly technologies [Abrahão & Corrêa, 2023]. OD offers several advantages, including the preservation of flavor and color, suppression of enzyme browning, and reduced energy consumption [Abrahão & Corrêa, 2023]. The effectiveness of OD is influenced by various parameters, such as the type of osmotic agent, concentration of hypertonic solution, agitation, temperature, immersion time, sample-to--solution ratio, and the characteristics of the material undergoing the process [Ahmad, 2023]. The concentration of the osmotic agent solution plays a crucial role in impacting mass transfer kinetics; with higher concentrations resulting in faster osmosis rates. This concentration-dependent effect influences the rate of water loss and solid gain during extended osmotic treatment [Salehi *et al.*, 2023].

The most commonly used osmotic agents for OD of fruits and vegetables are sucrose, invert sugar, sodium chloride, corn syrup, and combinations thereof [Yadav & Singh, 2014]. Recently, natural sweeteners and by-products of the sugar industry have also been increasingly studied in this aspect, including honey, jaggery, sugar beet molasses and cane molasses [Kaur *et al.*, 2022]. Other unconventional osmotic agents successfully used in fruit dehydration were concentrated fruit juices and fruit syrups [González-Pérez *et al.*, 2021; Kowalska *et al*, 2023]. Because these osmotic agents contain many nutritional and bioactive compounds in addition to sugars, they positively influence the nutritional, health-promoting and sensory quality of dried fruits.

The edible fruit of prickly pear cactus is popular in Mexico and in the Mediterranean region. It contains sugar (15 g/100 g) and other nutrients and bioactive compounds including protein, minerals, amino acids, vitamins, flavonoids, and betalains [Cota-Sánchez, 2016; Jimenez-Aguilar *et al.*, 2014]. In our previous study, the molasses (sugar syrup) from prickly pear by-products with a superior sugar level (39.93°Brix) and antioxidant capacity was obtained [Yazidi *et al.*, 2024]. Its formulation was optimized by using statistical modeling, and the optimal cooking conditions were established at 78.35°C for 79.70 min, with the following proportion of ingredients: 0.265 g of pulp, 0.710 g of peel, and 0.025 g of seed. In this study, we proposed the pioneering use of prickly pear molasses as an osmotic agent.

Against this backdrop, the aim of this study was to characterize the osmotic dehydration of orange fruit slices in prickly pear molasses and sucrose solutions. The research not only explored the changes in total mass loss, water loss and solid gain during the process, but also entailed an in-depth analysis of the chemical and physical properties of the obtained material, comparing it with fresh orange slices.

MATERIAL AND METHODS

Preparation of raw material and osmotic solution

Fresh Navelina oranges (*Citrus sinensis* var. *Navelina*) were taken from Polish company which imported them from Spain. Oranges were washed and cut into 3-mm slices for OD. Two osmotic agents, sucrose and prickly pear molasses, were employed. To obtain molasses, prickly pear (*Opuntia ficus-indica*) fruits were harvested in August 2022 from naturalized plantations in Sbikha, Kairouan, Tunisia. Fruits were selected at the 50% color-break stage to ensure uniform ripeness and optimal sugar content. Prickly pear fruit underwent a cleaning process to remove spines, cut two sides, and the remaining fruit was divided into four parts. Equal parts of fruit and water were heated for about 1 h, filtered through a 2-mm sieve, and the filtrate was concentrated to a soluble solid content of 70°Brix.

Osmotic dehydration

The OD treatment was conducted according to procedure described by Nowacka *et al.* [2014]. The orange slices were submerged in a 70°Brix osmotic agent solution (sucrose or molasses) with a mass ratio of 1:4. The process was carried out at 30°C for 3 h in a glass vessel placed in a shaking water bath. After 0.5, 1, 2, and 3 h, the samples were removed from the solution using a metal sieve and then dried for 10 s on both sides on filter paper. The mass transfer dynamic during OD was assessed by determining total mass loss (TML), water loss (WL), and solid gain (SG). TML of the sample underwent a reduction due to water loss and at same time weight increased due to a solute gain. Thus, TML represents the difference between water loss and solid gain. WL (kg/kg) was defined as the water loss of the sample during OD on fresh sample weight basis and was calculated using Equation (1):

$$WL = \frac{M_0 - M_i}{W_0} \quad (1)$$

SG (kg/kg) was the total gain of sugar and other solids by the sample on fresh sample weight basis, and was calculated using Equation (2):

$$SG = \frac{S_i - S_0}{W_0} \quad (2)$$

where: M_0 is the water content of a fresh sample (kg), M_i is the water content of an osmotically dehydrated sample (kg), S_0 is the solid content of a fresh sample (kg), S_i is the solid content of an osmotically dehydrated sample (kg), and W_0 is the total weight of a fresh sample (kg).

The moisture content was determined using AOAC International method by drying the fresh and osmotically dehydrated orange slices in a Binder FP115 oven (Binder, Tuttlingen, Germany) at 105°C until constant weight [AOAC, 2002]. The entire OD process was conducted in duplicate.

Determination of physical properties

Dry matter content determination involved both fresh and osmotically dehydrated orange slices after 0.5, 1, 2, and 3 h, employing the gravimetric method with drying at 70°C [da Silva *et al.*, 2014]. Water activity measurements were conducted at room temperature in triplicate for each sample using the AquaLab Series 3TE water activity meter (Decagon Devices, Inc., Pullman, WA, USA). Color on the sample surface was quantified using a colorimeter (Model CR-300, Minolta, Osaka, Japan), examining parameters such as L^* (lightness), a^* (redness/greenness), b^* (yellowness/blueness), hue angle (H) in ten replications. The total color difference (ΔE) was calculated using Equation (3):

$$\Delta E = \sqrt{(\Delta L^*)^2+(\Delta a^*)^2+(\Delta b^*)^2} \quad (3)$$

where: ΔL^*, Δa^* and Δb^* are the differences between the individual color parameters of dehydrated orange slices and the corresponding color parameters of fresh orange slices.

Texture properties were assessed through a penetration test using a TA-HDi500 texture analyzer (Stable Micro Systems, Surrey, UK), performing at least 10 replicates for each sample. The maximum force (hardness, N) needed to penetrate the orange slices, and compression work (mJ) were recorded.

Total soluble solids, expressed in °Brix, were measured directly using a refractometer (PAL-3, Atago Co., Ltd., Tokyo, Japan).

Microstructure imaging

The microstructure of fresh and osmotically dehydrated for 3 h orange slices was imaged as described by Kowalska *et al.* [2023]. Samples were affixed to a metallic table and coated with a 5-mm layer of gold using the Leica EM ACE200 system (Leica Microsystems GmbH, Vienna, Austria). Cross-sectional examinations were conducted employing a Phenom XL scanning electron microscope (Thermo Fisher Scientific, Waltham, MA, USA), operating at an accelerating voltage of 10 kV and a chamber pressure of 60 Pa. A minimum of four images were captured for each cross-section, and at least six images were obtained for the surface of each sample at a magnification of 500×.

Total phenolic content and antioxidant capacity determinations

The analyses encompassed extraction, total phenolic content (TPC) determination, and assessment of antioxidant capacity. The extraction procedure, adapted from Nowacka *et al.* [2019], involved crushing each orange slice sample, followed by combining 300 mg of the sample with 10 mL of an 80% (*v/v*) ethanol solution and 0.1 M HCl (85:15, *v/v*). After 12 h of extraction with continuous shaking and subsequent centrifugation, the supernatant was collected for analysis. TPC in extracts and hypertonic solutions was evaluated using the Folin–Ciocalteu reagent and a chlorogenic acid (CA) standard curve. Results were expressed as mg CA/100 g dry matter (DM) of the sample [Chun & Kim, 2004].

Antioxidant capacity was measured as $ABTS^{\bullet+}$ scavenging activity and reducing power. The assay with 2,2′-azino-bis-(3-ethylbenzothiazoline-6-sulfonic acid) (ABTS) was performed using the method developed by Re *et al.* [1999]. The absorbance of the reaction mixture with samples and generated $ABTS^{\bullet+}$ was measured at a wavelength of 734 nm. The results were expressed as mg Trolox /g DM based on a calibration curve determined from this standard (100–1,000 µM). The reducing power of the samples was determined according to the procedure with potassium ferricyanide and $FeCl_3$ described by Oyaizu [1986]. The absorbance was measured at a wavelength of 700 nm. The results were expressed as mg Trolox /g DM. All analyses were conducted in triplicate.

Ascorbic acid content determination

Ascorbic acid content of fresh and osmotically dehydrated for 3 h orange slices was determined using the H-Class ultra-performance liquid chromatography (UPLC) system with a photodiode array detector (Waters, Milford, MA, USA) [Kowalska *et al.*, 2023]. Crushed material (0.05 g) was extracted with 10 mL of a solution of 3% meta-phosphoric acid, 8% acetic acid, and 1 mM EDTA (*v/v/v*) for 10 min, followed by centrifugation (6,000×*g*, 5°C, 5 min). The filtered supernatant was analyzed after a 2-fold dilution with a 0.1% formic acid solution in Milli-Q water. Separation was conducted on a Waters HSS T3 column (100×2.1 mm, 1.8 µm). The flow rate of the mobile phase (0.1% formic acid) was 0.25 mL/min, the injection volume was 5 µL, and the temperatures of the column thermostat and samples were 25 and 4°C, respectively. The absorbance recorded at 245 nm was used to quantify ascorbic acid in orange slices. Results were expressed as mg/100 g DM of the sample based on the calibration curve plotted for the ascorbic acid standard.

Sugar content determination

The high-performance liquid chromatography (HPLC) Spectra-SYSTEM with a P100 pump, a refractive index detector and a Rheodyne injection valve with a 20 µL-sample loop (Waters, Milford, MA, USA) was employed for sugar content determination in fresh and dehydrated orange slices. Separation occurred on a Sugar-Pak I column (300×6.5 mm; Waters) at 90°C, with a mobile phase (Milli-Q water) flow rate of 0.6 mL/min [Yang *et al.*, 2021]. The homogenized material (approximately 0.3 g in triplicate) was suspended with 10 mL of water at 80°C, extracted at 25°C for 4 h, and after filtration, analyzed by HPLC. Standard solutions containing the reference compounds (fructose, glucose and sucrose) were prepared in milli-Q water. Retention time of standards was used to identify individual sugars in the samples. Quantification was based on the calibration curves plotted for standards. Results were expressed as mg/100 g DM of orange slices.

Total carotenoid content determination

The spectrophotometric method was employed to determine the total carotenoid content in the orange samples.

The extraction process involved two stages: initially, with 100% acetone, followed by the addition of petroleum ether (100%), a more specific solvent for carotenoid extraction, into the mixture, while the acetone fraction was discarded [Rodriguez-Amaya, 2001]. The absorbance of the collected petroleum ether fraction was measured at 450 nm. The total carotenoid content was quantified and expressed as mg of β-carotene equivalent *per* kg of sample DM.

Statistical analysis

Results reported in this work are presented as mean of three independent values accompanied by standard deviation. Experimental data were analyzed using JMP 14 software (SAS Institute Inc., Cary, NC, USA). Analysis of variance (ANOVA) was performed and Tukey-Kramer comparison test was used to estimate significant differences through osmotic dehydration time ($p<0.05$). Student's *t*-test was used to show significant difference ($p<0.05$) between osmotically dehydrated orange slices and fresh orange slices.

RESULTS AND DISCUSSION

Osmotic dehydration of orange fruit slices in sucrose and molasses solutions

In the process of OD, water migrates from the food matrix into the hypertonic solution, while solutes from the solution permeate into the food matrix. This phenomenon is driven by the variance in osmotic pressure between the food tissue and the osmotic solution [Abrahão & Corrêa, 2023]. The changes in total mass loss, water loss, solid gain, and the ratio of water loss to solid gain for slices of orange fruits during OD in sucrose and molasses solutions demonstrated distinctive patterns (**Table 1**). In sucrose, total mass loss steadily increased from 0.07 to 0.16 kg/kg between 0.5 and 3 h of processing. Immersion in molasses escalated total mass loss from 0.07 to 0.18 kg/kg during the same processing period, significantly ($p<0.05$) exceeding the values recorded for the samples dehydrated in the sucrose solution at each time point after 0.5 h of the dehydration, suggesting a faster process possibly due to higher osmotic potential. The orange slice water loss increased gradually from 0.13 kg H_2O/kg at 0.5 h to 0.26 kg H_2O/kg at 3 h in the sucrose solution, suggesting an effective dehydration process. Similarly, immersion in the molasses solution demonstrated an escalating water loss from 0.08 kg H_2O/kg at 0.5 h to 0.25 kg H_2O/kg at 3 h. Solid gain of orange slices dehydrated in the sucrose solution increased progressively from 0.06 kg/kg to 0.11 kg/kg, while that recorded for samples dehydrated in molasses, although following a similar trend, consistently displayed lower values, implying that the sucrose solution induced a more significant solid gain. The water loss to solid gain ratio during the OD of orange fruits in sucrose and molasses solutions provided insights into the efficiency of the dehydration process. In sucrose, the ratio ranged from 2.12 to 2.36 without significant ($p\geq0.05$) differences between dehydration time points, indicating that for each unit of solid gained, approximately 2.12 to 2.36 units of water were lost. On the other hand, in molasses, the ratio decreased from 4.01 at 0.5 h to 3.12 at 3 h, suggesting a higher water loss for each unit of solid gained compared to immersion in the sucrose solution.

Molasses notable osmotic potential has made it a preferred choice for enhancing the dehydration process in food applications [Filipović *et al.*, 2022; Nićetin *et al.*, 2022; Šuput *et al.*, 2020]. El Hosry *et al.* [2023] reported that fruit molasses has the complex composition. This complex composition of molasses solutions

Table 1. Mass loss, water loss, solid gain and physicochemical characteristics of orange fruits during their osmotic dehydration in sucrose and prickly pear molasses solutions.

Parameter	Treatment	Osmotic dehydration time (h)			
		0.5	1	2	3
Total mass loss (kg/kg)	Sucrose-treated	0.07 ± 0.01^{Ac}	0.08 ± 0.02^{Bc}	0.11 ± 0.05^{Bb}	0.16 ± 0.07^{Ba}
	Molasses-treated	0.07 ± 0.02^{Ad}	0.12 ± 0.04^{Ac}	0.15 ± 0.07^{Ab}	0.18 ± 0.02^{Aa}
Water loss (kg H_2O/kg)	Sucrose-treated	0.13 ± 0.01^{Ad}	0.15 ± 0.05^{Ac}	0.17 ± 0.07^{Bb}	0.26 ± 0.12^{Aa}
	Molasses-treated	0.08 ± 0.03^{Bd}	0.14 ± 0.05^{Ac}	0.21 ± 0.12^{Ab}	0.25 ± 0.11^{Aa}
Solid gain (kg/kg)	Sucrose-treated	0.06 ± 0.02^{Ab}	0.07 ± 0.01^{Ab}	0.08 ± 0.05^{Ab}	0.11 ± 0.03^{Aa}
	Molasses-treated	0.02 ± 0.00^{Bc}	0.04 ± 0.00^{Bb}	0.07 ± 0.02^{Ba}	0.08 ± 0.01^{Ba}
Water loss/solid gain	Sucrose-treated	2.16 ± 0.12^{Ba}	2.14 ± 0.33^{Ba}	2.12 ± 0.11^{Ba}	2.36 ± 0.09^{Ba}
	Molasses-treated	4.01 ± 0.27^{Aa}	3.51 ± 0.33^{Ab}	3.01 ± 0.22^{Ad}	3.12 ± 0.12^{Ac}
Total soluble solids (°Brix)	Sucrose-treated	17.53 ± 1.02^{Ad}	21.12 ± 0.89^{Ac}	24.33 ± 0.99^{Bb}	25.83 ± 0.77^{Ba}
	Molasses-treated	18.18 ± 1.35^{Ad}	20.55 ± 1.03^{Ac}	25.71 ± 0.99^{Ab}	28.06 ± 1.33^{Aa}
Dry matter (g/100 g)	Sucrose-treated	22.55 ± 0.75^{Ad}	24.25 ± 0.55^{Ac}	25.75 ± 0.36^{Ab}	31.21 ± 0.88^{Aa}
	Molasses-treated	22.49 ± 1.20^{Ad}	24.23 ± 0.72^{Ac}	25.77 ± 0.93^{Ab}	31.25 ± 0.99^{Aa}

Results are shown as mean ± standard deviation ($n=3$). Different letters a–d in rows indicate significant differences between the samples at different dehydration times ($p<0.05$). Different A and B letters indicate significant differences between treatments separately for each dehydration time and parameter ($p<0.05$).

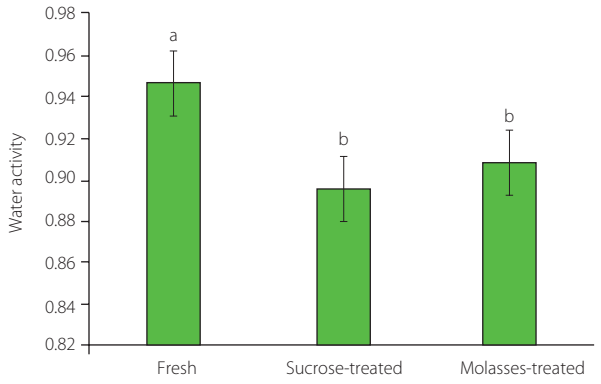

Figure 1. Water activity of fresh orange slices and these dehydrated in sucrose and prickly pear molasses solutions. Different letters above bars indicate statistical differences ($p<0.05$).

may be the reason for a higher rate of total mass loss of the dehydrated material compared to dehydration in a sugar solution, which was observed in our study during OD of orange fruit. Molasses was produced from prickly pear fruit that contains not only sucrose but also other solutes, such as organic acids, minerals, and non-sugar organic compounds [Belviranlı *et al.*, 2019; Tsegay, 2020]. This diverse composition contributes to a higher osmotic potential in molasses compared to a simple sugar solution.

Impact of osmotic dehydration on the water activity of orange slices

Fresh orange fruit exhibited a water activity of 0.947 (**Figure 1**), indicating high water availability for biological and chemical reactions. No statistically significant ($p\geq0.05$) difference existed between a water activity of orange slices dehydrated for 3 h in the sucrose solution (0.895) and prickly pear molasses (0.909), indicating comparably reduced water availability in these solutions *vs*. fresh fruit. Kowalska *et al.* [2023] noted that fruit juice concentrates (from chokeberry, strawberry and cherry) as osmotic agents significantly reduced water activity, with the most substantial decrease observed in strawberries dehydrated in cherry concentrate (0.873). Sucrose and molasses solutions, with lower water activity, contributed to food preservation by inhibiting microbial growth and enzymatic reactions [Gomez *et al.*, 2021]. Understanding these values is crucial for assessing the impact of different solutions on food system stability and shelf life [Tapia *et al.*, 2020].

Impact of hypertonic solution type on total soluble solid and dry matter contents of orange slices during osmotic dehydration

The trends in changes in the total soluble solid content of orange slices during fruit OD in sucrose and molasses solutions are shown in **Table 1**. During OD in the sucrose solution, the content of total soluble solids increased continuously from 17.53°Brix at 0.5 h to 25.83°Brix at 3 h, indicating ongoing solute accumulation in orange slices. The total soluble solids of fruits dehydrated in molasses showed a similar trend, with values increasing from 18.18°Brix at 0.5 h to 28.06°Brix at 3 h, suggesting that prickly pear molasses was a more concentrated solute environment than sucrose. Compared to the total soluble solids of fresh orange fruit (10.00°Brix), OD resulted in a notable increase in solute content. As the total soluble solid content of orange slices increased over dehydration time in both sucrose and molasses solutions, a corresponding increase in dry matter content was found, showcasing the absorption of substances dissolved in hypertonic solutions by the orange fruit. Rubio-Arraez *et al.* [2015] also studied the effect of isomaltulose, oligofructose and aqueous extract of stevia solutions on total soluble solid contents of orange slices during osmotic dehydration and they found that the content of soluble solids in orange slices augmented in conjunction with the elongation of the dehydration time.

Impact of osmotic dehydration on orange fruit color

Results of color analysis of fresh orange slices and these osmotically dehydrated in the sucrose solution and prickly pear molasses for 3 h, depicted by L^*, a^*, b^*, ΔE and H° values, are shown in **Table 2**. Fresh orange slices were characterized by L^*, a^*, and b^* color parameters at the levels of 44.69, −1.64, and 22.15, respectively. The L^* increased gradually from 44.80 at 0.5 h to 47.50 at 3 h for orange slices dehydrated in the sucrose solution, while immersion in the molasses solution caused a decrease of L^* from 39.50 at 0.5 h to 31.20 at 3 h. Similarly, the b^* increased gradually from 22.40 at 0.5 h to 23.50 at 3 h for orange slices dehydrated in the sucrose solution, while decreased from 26.40 at 0.5 h to 23.02 at 3 h upon slices immersion in the molasses solution. For a^*, there was an increase from −3.50 at 0.5 h to −2.50 at 3 h in the sucrose solution and from 3.10 at 0.5 h to 11.90 at 3 h in the molasses solution. According to Kowalska *et al.* [2023], the type of osmotic agent had a significant impact on the absolute color difference. Orange slices dehydrated in a molasses solution had a darker color compared with those dehydrated in a sucrose solution. This was related to the penetration of colored substances contained in the molasses solution into the fruit. Immersion in the sucrose solution resulted in minimally perceptible color changes of orange slices compared to fresh fruits, indicated by low ΔE values (3.28) and consistent hue values (**Table 2**), suggesting stable color tone. In contrast, orange slices dehydrated in molasses showed more pronounced color transformations with higher ΔE values (19.12) and a significant shift in hue from 94.23° (fresh fruits) to 62.75° (dehydrated fruits). These results suggested that molasses induced more substantial and perceptible color alterations in the orange fruit compared to sucrose, possibly due to the complex composition of molasses, including non-sugar components [Samborska *et al.*, 2019]. These findings highlight the importance of considering color changes as part of the quality assessment for orange fruits osmotically dehydrated in different solutions.

Impact of osmotic dehydration on orange slice texture parameters and microstructure

Texture, a key quality parameter, was assessed in osmotically dehydrated orange fruits after 3 h in various solutions (**Figure 2**).

Table 2. Color parameters of orange fruits during their osmotic dehydration in sucrose and prickly pear molasses solutions.

Parameter	Treatment	Osmotic dehydration time (h)			
		0.5	1	2	3
L*	Sucrose-treated	44.80 ± 0.80^{Ac}	45.60 ± 0.80^{Ab}	46.30 ± 1.10^{Aa}	47.50 ± 1.10^{Aa}
	Molasses-treated	39.50 ± 1.40^{Ba}	39.10 ± 1.80^{Ba}	36.00 ± 3.20^{Bb}	31.20 ± 1.90^{Bc}
*a**	Sucrose-treated	-3.50 ± 0.50^{Bb}	-2.30 ± 0.20^{Ba}	-3.20 ± 0.30^{Bb}	-2.50 ± 0.40^{Ba}
	Molasses-treated	3.10 ± 1.20^{Ac}	4.10 ± 2.10^{Ac}	6.20 ± 2.40^{Ab}	11.90 ± 2.80^{Aa}
*b**	Sucrose-treated	22.40 ± 1.00^{Ba}	22.60 ± 1.80^{Ba}	22.10 ± 2.40^{Ba}	23.50 ± 2.50^{Aa}
	Molasses-treated	26.40 ± 2.60^{Aa}	27.00 ± 2.70^{Aa}	25.90 ± 2.30^{Aa}	23.02 ± 2.20^{Ab}
Δ*E*	Sucrose-treated	1.90 ± 0.10^{Bd}	1.27 ± 0.06^{Bc}	2.20 ± 0.11^{Bb}	3.28 ± 0.16^{Ba}
	Molasses-treated	8.21 ± 0.41^{Ad}	9.34 ± 0.47^{Ac}	12.30 ± 0.62^{Ab}	19.12 ± 0.96^{Aa}
H°	Sucrose-treated	98.95 ± 1.95^{Aa}	95.85 ± 1.79^{Ab}	98.10 ± 1.91^{Aa}	96.03 ± 1.80^{Ab}
	Molasses-treated	83.38 ± 1.17^{Ba}	81.41 ± 1.07^{Ba}	76.51 ± 1.83^{Bb}	62.75 ± 1.14^{Bc}

Results are shown as mean ± standard deviation (n=3). Different letters a–d in rows indicate significant differences between the samples at different dehydration times (p<0.05). Different A and B letters indicate significant differences between treatments separately for each dehydration time and parameter (p<0.05). L^*, lightness; a^*, redness/greenness; b^*, yellowness/blueness; H°, hue angle; Δ*E*, total color difference compared to fresh orange slices.

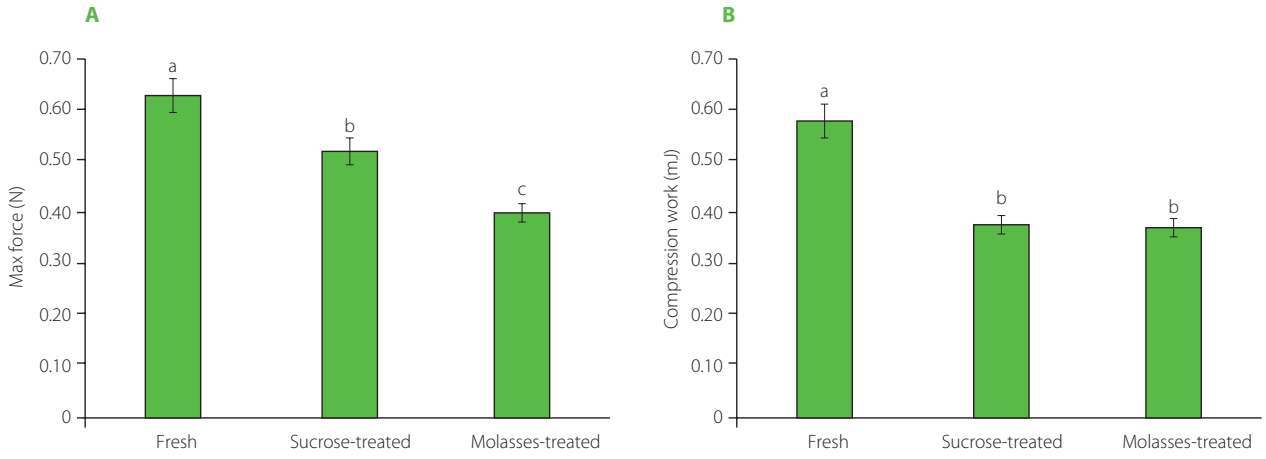

Figure 2. Texture parameters of fresh orange slices and these dehydrated in sucrose and prickly pear molasses solutions; maximum force (**A**) and compression work (**B**). Different letters above bars indicate statistical differences (p<0.05).

Immersion in both sucrose and molasses solutions reduced hardness of orange slices to 0.52 N and 0.40 N, respectively, compared to the fresh state (0.63 N). Compression work of dehydrated orange slices was also lower (in sucrose solution – 0.38 mJ and in molasses solution – 0.36 mJ) compared to that of the fresh orange slices (0.58 mJ), reflecting a softer texture. These findings were consistent with the results reported by Kowalska *et al.* [2023] for strawberries osmo-dehydrated in fruit juice concentrates as hypertonic solutions. Additionally, Gamboa-Santos *et al.* [2021] revealed that OD of strawberries resulted in reduced elasticity and increased hardness due to the concentration and penetration of osmotic substances.

Microstructural analysis highlighted regular cellular arrangements in fresh slices, while dehydration in molasses induced significant tissue alterations, forming new crystals (**Figure 3**). This phenomenon was attributed to the substantial difference in osmotic pressure between the hypertonic solution and the rich composition of molasses, including non-sugar constituents. The distinctive microstructural changes emphasized the profound impact of solution choice on the physical characteristics of osmotically dehydrated orange fruits.

■ Effect of osmotic dehydration on total phenolic content and antioxidant capacity of orange slices.

The total phenolic content and antioxidant capacity of fresh and dehydrated orange slices are shown in **Table 3**. Immersion in both sucrose and molasses solutions caused that the total phenolic content significantly (p<0.05) decreased compared to fresh slices, for which TPC was 2,536 mg CA/100 g. In fact, the sucrose-treated slices had 1,512 mg CA/100 g DM, while

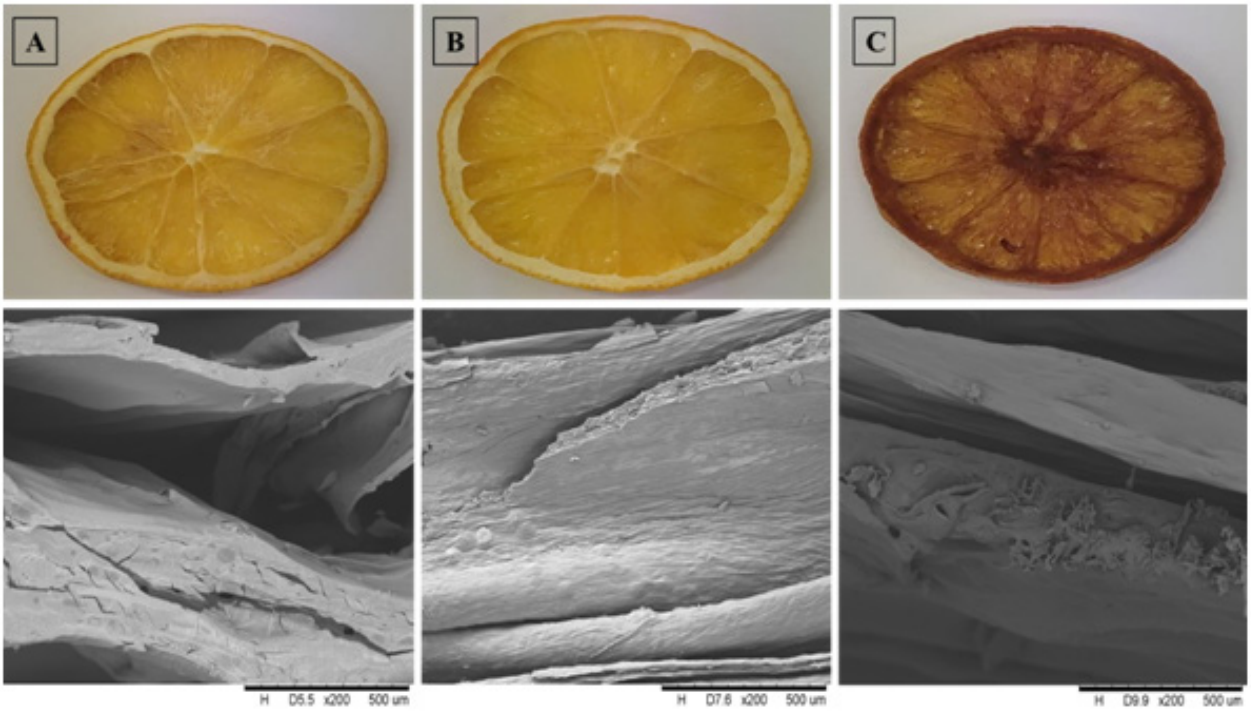

Figure 3. Appearance photos and microstructure images by scanning electron microscopy (500× magnification) of fresh orange slices (**A**) and after their 3-h osmotic dehydration in a sucrose solution (**B**) and pearly pear molasses (**C**).

Table 3. Total phenolic content and antioxidant capacity of fresh orange slices, orange slices after 3-h osmotic dehydration in a sucrose solution and pearly pear molasses, and hypertonic solutions.

Sample	Total phenolic content (mg CA/100 g DM)	$ABTS^{\bullet+}$ scavenging activity (mg Trolox/g DM)	Reducing power (mg Trolox/g DM)
Orange slice			
Fresh	2,536±47^{a}	7.73±0.13^{a}	4.04±0.06^{a}
Sucrose-treated	1,512±29^{c}	2.68±0.31^{c}	2.32±0.33^{b}
Molasses-treated	2,197±78^{b}	6.26±0.06^{b}	1.74±0.16^{c}
Hypertonic solution			
Sucrose	5±20^{B}	0^{B}	0^{B}
Molasses	1,587±62^{A}	3.50±0.06^{A}	12.17±0.62^{A}

Results are shown as mean ± standard deviation (n=3). Different letters in columns indicate significant differences (p<0.05). CA, chlorogenic acid equivalent; DM, dry matter.

the molasses-treated ones had 2,197 mg CA/100 g DM. Devic *et al.* [2010] stated that the main mechanism responsible for decreasing phenolic compound content in fruits during OD is water diffusion, because water-soluble phenolics can be leached out together with the water flowing from the dehydrated plant material to the hypertonic solution. Another phenomenon that may occur during OD and cause the loss of some individual phenolics is their degradation by hydrolysis resulting in lower molecular weight molecules that can more easily pass through the cell membrane into the hypertonic solution [Almeida *et al*., 2015].

Antioxidant capacity, evaluated through ABTS and reducing power assays, showcased the molasses-treated slices with higher $ABTS^{\bullet+}$ scavenging activity (6.26 mg Trolox/g DM) than the sucrose-treated ones (2.68 mg Trolox/g DM). However, the sucrose-treated slices displayed greater reducing power (2.32 mg Trolox/g DM) than these immersed in molasses (1.74 mg Trolox/g DM). Similar results were obtained by Nićetin *et al.* [2022], who reported that the antioxidant capacity determined by ABTS and reducing power assays were increased after OD treatment of celery root in sugar beet molasses (1.10–1.13 mM Trolox/L and 1.54–1.58 mM Fe^{2}/L, respectively) compared to the fresh samples (1.01 mM Trolox/L and 1.52 mM Fe^{2}/L, respectively). They also found a strong positive correlation between the total phenolic content and antioxidant capacity in the ABTS assay (0.86, $p \leq 0.01$) and reducing power (0.79, $p \leq 0.01$). The composition of the osmotic solution has a direct effect on the retention of bioactive compounds in the dehydrated material during OD and, consequently, on its antioxidant capacity [Giovanelli

Table 4. Contents of ascorbic acid, total carotenoids and sugars in fresh orange slices and after their 3-h osmotic dehydration in a sucrose solution and pearly pear molasses.

Orange slice	Ascorbic acid (mg /100 g DM)	Total carotenoids (mg/kg DM)	Sucrose (mg/100 g DM)	Glucose (mg/100 g DM)	Fructose (mg/100 g DM)
Fresh	42.77±0.15^{b}	31.44±0.19^{a}	2.41±0.02^{c}	1.54±0.02^{b}	4.22±0.08^{a}
Sucrose-treated	27.20±2.15^{c}	20.54±1.39^{b}	41.41±0.12^{a}	0.77±0.06^{c}	3.30±0.09^{b}
Molasses-treated	50.14±1.59^{a}	21.53±0.99^{b}	38.10±0.05^{b}	5.47±0.03^{a}	1.80±0.20^{c}

Results are shown as mean ± standard deviation (n=3). Different letters in columns indicate significant differences between the samples (p<0.05). DM, dry matter.

et al., 2012]. Moreover, Almeida *et al.* [2015] who osmotically dehydrated banana slices in sucrose solutions, found that high concentrations of the osmotic solution resulted in a protective effect on phenolics, mainly tannins, and higher retention of antioxidant capacity. The authors concluded that the incorporation of solute into the banana tissue created a barrier to leaching of soluble solids, including phenolic compounds.

Impact of osmotic dehydration on content of ascorbic acid, total carotenoids, and sugars

The contents of ascorbic acid, total carotenoids and sugars in fresh orange slices and following 3 h of OD in various solutions are displayed in **Table 4**. Statistical analysis uncovered significant (p<0.05) differences in ascorbic acid content among dehydrated orange slices. Specifically, the molasses-treated slices exhibited significantly higher ascorbic acid content, at 50.14 mg/100 g DM, in contrast to the fresh slices (42.77 mg/100 g DM) and the sucrose-treated slices (27.20 mg/100 g DM). This indicates that molasses played a protective role in preserving ascorbic acid during dehydration, possibly due to its significant antioxidant capacity. Kowalska *et al.* [2023] used different fruit juice concentrates as osmotic agents and found the highest vitamin C content in fruits dehydrated in the strawberry juice concentrate (220.48 mg/100 g DM), and the lowest one in strawberries dehydrated in a sucrose solution (65.60 mg/100 g DM). However, the vitamin C content was equal to 235.80 mg/100 g DM in the fresh strawberries. These authors noticed that the low content of vitamin C in the strawberries dehydrated in the sucrose solution and juice concentrates could be due to the low content or lack of vitamin C in these osmotic agents.

There was no significant difference in the total carotenoid content of osmotically dehydrated orange slices between sucrose (20.54 mg/kg DM) and molasses (21.53 mg/kg) treatments, while fresh slices boasted a total carotenoid content of 31.44 mg/kg DM (**Table 4**). Azoubel *et al.* [2008] found that the total carotenoid content of mango slightly decreased (around 3% of loss) after osmotic dehydration in a sucrose solution for 80 min, and it could be partially associated with pigment diffusion from the fruit to the solution.

In osmotically dehydrated orange slices after 3 h, sugar composition displayed notable differences between treatments in sucrose and molasses solutions (**Table 4**). A higher content of sucrose was determined in the sucrose-treated slices (41.41 mg/100 g DM) and the molasses-treated slices (38.10 mg/100 g DM) as compared to the fresh slices (2.41 mg/100 g DM). The molasses-treated slices demonstrated higher glucose (5.47 mg/100 g DM) and lower fructose (1.80 mg/100 g DM) contents compared to the sucrose-treated slices (0.77 mg/100 g DM and 3.30 mg/100 g DM, respectively). Kowalska *et al.* [2023] also reported that the sucrose content increased in strawberry dehydrated in a sucrose solution, while it was reduced after immersion in fruit juice concentrates as compared to fresh strawberry. They explained that the second observations could be due to the sucrose leak from the strawberry tissue to fruit juice concentrates. These authors also found an increase in glucose and fructose contents in strawberries immersed in strawberry and cherry juice concentrates and a decrease in these sugars content in strawberries dehydrated in sucrose and chokeberry juice concentrates. Furthermore, the fructose content was higher in the fruits treated in the strawberry juice concentrate. They deduced that these differences can be result of the different molar masses of the osmotic solutions used. Those with lower molar masses allow for an increased diffusion of the substance into the tissue of the raw material.

CONCLUSIONS

This study showcased the effective OD of orange fruit using both sucrose and prickly pear molasses solutions, each influencing dehydrated fruits quality differently. While both treatments demonstrated distinctive patterns in total mass loss, water loss, solid gain, and the ratio of water loss to solid gain, color, texture and microstructure. Notably, no significant difference was found in water activity between orange slices dehydrated in the sucrose solution and prickly pear molasses. Dehydration in molasses resulted in higher antioxidant capacity of orange slices and preservation of ascorbic acid as compared to the sucrose solution. According to the sugar profiles, orange slices dehydrated in molasses had favored glucose content and reduced fructose content compared to the product obtained by immersion in the sucrose solution.

The choice between sucrose solution and prickly pear molasses hinges on desired characteristics, with molasses offering faster dehydration, enhanced antioxidant activity, and a softer texture, offset by deeper color changes and higher sugar absorption. Conversely, dehydration in a sucrose solution yields a lighter, firmer product with a more balanced sugar profile, albeit with

slower dehydration and reduced antioxidant properties. This study paves the way for faster, healthier orange dehydration. By optimizing molasses use or finding new natural agents, we can create products with diverse colors, textures, and nutrient profiles to suit different consumer tastes.

ACKNOWLEDGEMENTS

The authors extend their appreciation to Taif University, Saudi Arabia, for supporting this work through project number (TU-DSPP-2024-115).

RESEARCH FUNDING

This research was funded by Taif University, Saudi Arabia, Project No. (TU-DSPP-2024-115).

CONFLICT OF INTERESTS

The authors declare that they have no conflict of interest.

ADDITIONAL INFORMATION

The data presented in this study are available on request from the corresponding author.

ORCID IDs

M. Hammami https://orcid.org/0000-0002-4376-0638
K. Hessini https://orcid.org/0000-0002-8929-9234
M. Nowacka https://orcid.org/0000-0003-4689-6909
K. Rybak https://orcid.org/0000-0003-3595-0818
M. Saidani Tounsi https://orcid.org/0000-0003-0669-8414
W. Aidi Wannes https://orcid.org/0000-0003-3134-0457
D. Witrowa-Rajchert https://orcid.org/0000-0002-0937-3204
R. Yazidi https://orcid.org/0009-0006-8861-8754
W. Yeddes https://orcid.org/0000-0002-1439-7956

REFERENCES

1. Abrahão, F.R., Corrêa, J.L.G. (2023). Osmotic dehydration: More than water loss and solid gain. *Critical Reviews in Food Science and Nutrition*, *63*(17), 2970-2989. https://doi.org/10.1080/10408398.2021.1983764
2. Almeida, J., Mussi, L., Oliveira, D., Pereira, N. (2015). Effect of temperature and sucrose concentration on the retention of polyphenol compounds and antioxidant activity of osmotically dehydrated bananas. *Journal of Food Processing and Preservation*, *39*(6), 1061-1069. https://doi.org/10.1111/jfpp.12321
3. AOAC (2002). *Official Methods of Analysis, Official Method 934.06* The Association of Official Analytical Chemists International, Gaithersburg, MD, USA.
4. Azoubel, P., Balem de Oliveira, S., de Brito Araujo, A.J., Alves Silva, I.R., Park, K.J. (2008). Influence of osmotic preatreatment on the total carotenoids content of drid mango. *CIGR - International Conference of Agricultural Engineering XXXVII Congresso Brasileiro de Engenharia Agrícola*. CONBEA 2008, Brazil, *Artigo em anais de congresso*, 37, 1-3. http://www.alice.cnptia.embrapa.br/alice/handle/doc/160469
5. Belviranlı, B., Al-Juhaimi, F., Özcan, M.M., Ghafoor, K., Babiker, E.E., Alsawmahi, O.N. (2019). Effect of location on some physico-chemical properties of prickly pear (*Opuntia ficus-indica* L.) fruit and seeds. *Journal of Food Processing and Preservation*, *43*(3), art. no. e13896. https://doi.org/10.1111/jfpp.13896
6. Chun, O.K., Kim, D.O. (2004). Consideration on equivalent chemicals in total phenolic assay of chlorogenic acid-rich plums. *Food Research International*, *37(4)*, 337-342. https://doi.org/10.1016/j.foodres.2004.02.001
7. Cota-Sánchez, J.H. (2016). Chapter 28 – Nutritional composition of the prickly pear (*Opuntia ficus-indica*) fruit. In M.S.J. Simmonds, V. Preedy (Eds.), *Nutritional Composition of Fruit Cultivars,* Academic Press, pp. 691-712). https://doi.org/10.1016/B978-0-12-408117-8.00028-3
8. da Silva, W.P., da Silva e Silva, C.M.D.P., de Farias Aires, J.E., da Silva Jr, A.S. (2014). Osmotic dehydration and convective drying of coconut slices: Experimental determination and description using one-dimensional diffusion model. *Journal of the Saudy Society of Agricultural Sciences, 13*(2), 162-168. https://doi.org/10.1016/j.jssas.2013.05.002
9. Devic, E., Guyot, S., Daudin, J.D., Bonazzi, C. (2010). Effect of temperature and cultivar on polyphenol retention and mass transfer during osmotic dehydration of apples. *Journal of Agricultural and Food Chemistry*, *58*(1), 606-614. https://doi.org/10.1021/jf903006g
10. El Hosry, L., Bou-Mitri, C., Bou Dargham, M., Abou Jaoudeh, M., Farhat, A., El Hayek, J., Bou Mosleh, J.M., Bou-Maroun, E. (2023). Phytochemical composition, biological activities and antioxidant potential of pomegranate fruit, juice and molasses: A review. *Food Bioscience, 55,* art. no. 103034. https://doi.org/10.1016/j.fbio.2023.103034
11. Filipović, V., Filipović, J., Lončar, B., Knežević, V., Nićetin, M., Filipović, I. (2022). Synergetic dehydration method of osmotic treatment in molasses and successive lyophilization of peaches. *Journal of Food Processing and Preservation*, *46*(5), art. no. e16512. https://doi.org/10.1111/jfpp.16512
12. Gamboa-Santos, J., Vasco, M.F., Campañone, L. (2021). Diffusional analysis and textural properties of coated strawberries during osmotic dehydration treatment. *Journal of Berry Research*, *11*(1), 151-169. https://doi.org/10.3233/JBR-200554
13. Giovanelli, G., Brambilla, A., Rizzolo, A., Sinelli, N. (2012). Effects of blanching pre-treatment and sugar composition of the osmotic solution on physico-chemical, morphological and antioxidant characteristics of osmodehydrated blueberries (*Vaccinium corymbosum* L.). *Food Research International*, *49*(1), 263-271. https://doi.org/10.1016/j.foodres.2012.08.015
14. Gomez, E.J., Delgado, J.A., Gonzalez, J.M. (2021). Influence of water availability and temperature on estimates of microbial extracellular enzyme activity. *PeerJ*, *9*, art. no. e10994. https://doi.org/10.7717/peerj.10994
15. González-Pérez, J.E., Ramírez-Corona, N., López-Malo, A. (2021). Mass transfer during osmotic dehydration of fruits and vegetables: Process factors and non-thermal methods. *Food Engineering Reviews*, *13*, 344–374. https://doi.org/10.1007/s12393-020-09276-3
16. Jimenez-Aguilar, D.M., Mujica-Paz, H., Welti-Chanes, J. (2014). Phytochemical characterization of prickly pear (*Opuntia* spp.) and of its nutritional and functional properties: A review. *Current Nutrition & Food Science*, *10*(1), 57-69. https://www.eurekaselect.com/article/59830
17. Kaur, D., Singh, M., Zalpouri, R., Singh, I. (2022). Osmotic dehydration of fruits using unconventional natural *sweete*ners and non-thermal-assisted technologies: A review. *Journal of Food Processing and Preservation, 46*(12), art. no. e16890. https://doi.org/10.1111/jfpp.16890
18. Kowalska, H., Trusinska, M., Rybak, K., Wiktor, A., Witrowa-Rajchert, D., Nowacka, M. (2023). Shaping the properties of osmo-dehydrated strawberries in fruit juice concentrates. *Applied Sciences*, *13*(4), art. no. 2728. https://doi.org/10.3390/app13042728
19. Liu, N., Yang, W., Li, X., Zhao, P., Liu, Y., Guo, L., Huang, L., Gao, W. (2022). Comparison of characterization and antioxidant activity of different citrus peel pectins. *Food Chemistry*, *386*, art. no. 132683. https://doi.org/10.1016/j.foodchem.2022.132683
20. Lv, X., Zhao, S., Ning, Z., Zeng, H., Shu, Y., Tao, O., Xiao, C., Lu, C., Liu, Y. (2015). Citrus fruits as a treasure trove of active natural metabolites that potentially provide benefits for human health. *Chemistry Central Journal, 9*, art. no. 68. https://doi.org/10.1186/s13065-015-0145-9
21. Manzoor, A., Jan, B., Rizvi, Q.U.E.H., Junaid, P.M., Pandith, J.A., Dar, I.H., Bhat, S.A., Ahmad, S. (2023). Chapter 7 – Osmotic dehydration technology for preservation of fruits and vegetables. In M.R. Goyal, F. Ahmad (Eds). *Quality Control in Fruit and Vegetable Processing*. 1st edition, Apple Academic Press. https://doi.org/10.1201/9781003304999
22. Nićetin, M., Pezo, L., Pergal, M., Lončar, B., Filipović, V., Knežević, V., Demir, H., Filipović, J., Manojlović, D. (2022). Celery root phenols content, antioxidant capacities and their correlations after osmotic dehydration in molasses. *Foods*, *11*(13), art. no. 1945. https://doi.org/10.3390/foods11131945
23. Nowacka, M., Tylewicz, U., Laghi, L., Dalla Rosa, M., Witrowa-Rajchert, D. (2014). Effect of ultrasound treatment on the water state in kiwifruit during osmotic dehydration. *Food Chemistry*, *144*, 18-25. https://doi.org/10.1016/j.foodchem.2013.05.129
24. Nowacka, M., Wiktor, A., Anuszewska, A., Dadan, M., Rybak, K., Witrowa-Rajchert, D. (2019). The application of unconventional technologies as pulsed electric field, ultrasound and microwave-vacuum drying in the production of dried cranberry snacks. *Ultrasonics Sonochemistry*, *56*, 1-13. https://doi.org/10.1016/j.ultsonch.2019.03.023
25. Omar, A.F., Matjafri, M.Z. (2013). Principles, methodologies and technologies of fresh fruit quality assurance. *Quality Assurance and Safety of Crops & Foods, 5*(3), 257-271. https://doi.org/10.3920/QAS2012.0175
26. Oyaizu, M. (1986). Studies on products of browning reaction prepared from glucoseamine. *Japanese Journal of Nutrition, 44*(6), 307-314. (in Japanese, English abstract). https://doi.org/10.5264/eiyogakuzashi.44.307

27. Re, R., Pellegrini, N., Proteggente, A., Pannala, A., Yang, M., Rice-Evans, C. (1999). Antioxidant activity applying an improved ABTS radical cation decolorization assay. *Free Radical Biology & Medicine*, *26*(9-10), 1231-1237. **https://doi.org/10.1016/S0891-5849(98)00315-3**
28. Rodriguez-Amaya, D.B. (2001). *A Guide to Carotenoid Analysis in Foods*. Washington DC: ILSI Press, pp. 23-51.
29. Rubio-Arraez, S., Capella, J.V., Ortolá, M.D., Castelló, M.L. (2015). Kinetics of osmotic dehydration of orange slices using healthy sweeteners. *International Food Research Journal, 22*(5), 2162-2166.
30. Salehi, F., Cheraghi, R., Rasouli, M. (2023). Mass transfer analysis and kinetic modeling of ultrasound-assisted osmotic dehydration of kiwifruit slices. *Scientific Reports*, *13*(1), art. no. 11859. **https://doi.org/10.1038/s41598-023-39146-x**
31. Samborska, K., Eliasson, L., Marzec, A., Kowalska, J., Piotrowski, D., Lenart, A., Kowalska, H. (2019). The effect of adding berry fruit juice concentrates and by-product extract to sugar solution on osmotic dehydration and sensory properties of apples. *Journal of Food Science and Technology*, *56*(4), 1927-1938. **https://doi.org/10.1007/s13197-019-03658-0**
32. Sun, Q., Zhang, M., Mujumdar, A.S. (2019). Recent developments of artificial intelligence in drying of fresh food : A review. *Critical Reviews in Food Science and Nutrition*, *59*(14), 2258-2275. **https://doi.org/10.1080/10408398.2018.1446900**
33. Šuput, D., Filipović, V., Lončar, B., Nićetin, M., Knežević, V., Lazarević, J., Plavšić, D. (2020). Modeling of mushrooms (*Agaricus bisporus*) osmotic dehydration process in sugar beet molasses. *Food and Feed Research*, *47*(2), 175-187. **https://doi.org/10.5937/ffr47-28436**
34. Tapia, M.S., Alzamora, S.M., Chirife, J. (2020). Chapter 14 – Effects of water activity (a_w) on microbial stability as a hurdle in food preservation. In G.V. Barbosa-Canovas, A.J. Fontana Jr, S.J. Schmidt, T.P. Labuza (Eds.), *Water Activity in Foods*, 1st edition, John Wiley & Sons, Ltd., pp. 323-355. **https://doi.org/10.1002/9781118765982.ch14**
35. Tsegay, Z.T. (2020). Total titratable acidity and organic acids of wines produced from cactus pear (*Opuntia-ficus-indica*) fruit and Lantana camara (*L. Camara*) fruit blended fermentation process employed response surface optimization. *Food Science & Nutrition*, *8*(8), 4449-4462. **https://doi.org/10.1002/fsn3.1745**
36. Yadav, A.K., Singh, S.V. (2014). Osmotic dehydration of fruits and vegetables : A review. *Journal of Food Science and Technology*, *51*(9), 1654-1673. **https://doi.org/10.1007/s13197-012-0659-2**
37. Yang, S., Meng, Z., Li, Y., Chen, R., Yang, Y., Zhao, Z. (2021). Evaluation of physiological characteristics, soluble sugars, organic acids and volatile compounds in 'Orin' apples (*Malus domestica*) at different ripening stages. *Molecules*, *26*(4), art. no. 807. **https://doi.org/10.3390/molecules26040807**
38. Yazidi, R., Yeddes, W., Djebali, K., Hammami, M., Aidi-Wannes, W., Ben Farhat, M., Msaada, K., Saidani Tounsi, M. (2024). Optimizing prickly pear by-product valorization: formulating molasses with enhanced antioxidant capacities and sugar contents. *International Journal of Environmental Health Research*, 1-12. **https://doi.org/10.1080/09603123.2024.2337831**

ORIGINAL ARTICLE
http://journal.pan.olsztyn.pl

Polish Journal of Food and Nutrition Sciences
2024, Vol. 74, No. 4, 350–362
DOI: 10.31883/pjfns/194251
ISSN 1230-0322, e-ISSN 2083-6007

Gomphrenin-Based Decarboxylated and Acylated Pigments from *Basella alba* L. Fruit Extracts Impair Survival of Colorectal Cancer Cells but Not Normal Cells – *In Vitro* Study

Katarzyna Sutor-Świeży[1], Łukasz Kozioł[1], Mateusz Knap[1], Ewa Dziedzic[2], Monika Bieniasz[2], Przemysław Mielczarek[3,4], Monika Baj-Krzyworzeka[5], Rafał Szatanek[5], Sylwia Bobis-Wozowicz[6], Łukasz Popenda[7], Sławomir Wybraniec[1,*#], Małgorzata Tyszka-Czochara[8#]

[1]Department C-1, Faculty of Chemical Engineering and Technology, Cracow University of Technology, ul. Warszawska 24, 31-155 Krakow, Poland
[2]Faculty of Biotechnology and Horticulture, University of Agriculture in Krakow, al. 29 Listopada 54, 31-425 Krakow, Poland
[3]Department of Analytical Chemistry and Biochemistry, Faculty of Materials Science and Ceramics, AGH University of Krakow, al. Adama Mickiewicza 30, 30-059 Krakow, Poland
[4]Laboratory of Proteomics and Mass Spectrometry, Maj Institute of Pharmacology, Polish Academy of Sciences, ul. Smętna 12, 31-343 Krakow, Poland
[5]Department of Clinical Immunology, Faculty of Medicine, Institute of Pediatrics, Jagiellonian University Medical College, ul. Wielicka 265, 30-688 Kraków, Poland
[6]Department of Cell Biology, Faculty of Biochemistry, Biophysics and Biotechnology, Jagiellonian University, ul. Gronostajowa 7, 30-387 Kraków, Poland
[7]NanoBioMedical Centre, Adam Mickiewicz University, ul. Wszechnicy Piastowskiej 3, 61-614 Poznan, Poland
[8]Faculty of Pharmacy, Jagiellonian University Medical College, ul. Medyczna 9, 30-688 Krakow, Poland

The fast-growing, soft-stemmed vine, *Basella alba* L., yields high quantities of gomphrenin pigments in its dark-violet fruits which can be converted to their decarboxylated derivatives while still possessing coloring properties. These pigments are much less investigated in terms of the health-promoting properties than their source counterparts. Hence, decarboxylated derivatives with potential health-promoting properties were generated by controlled thermal modifications of gomphrenin structure. Bioactivity experiments were performed on gomphrenin acylated (malabarin and globosin) and decarboxylated derivatives (17-decarboxy-gomphrenin, 2-decarboxy-gomphrenin, and 2,17-bidecarboxy-gomphrenin) derived from the fruit extracts using preparative HPLC. High-resolution mass spectrometric analyses of decarboxylated gomphrenins brought deep fragmentation patterns in the positive ionization mode. The combination of elimination pathways specific to 17-decarboxy-gomphrenin and 2-decarboxy-gomphrenin contributed to the generation of pyridinium, dihydroindolic, as well as indolic and dehydrated indolic derivative ions characteristic of the fragmentation spectra of 2,17-bidecarboxy-gomphrenin. First studies on two Duke's type C colorectal adenocarcinoma cell lines were performed on the isolated pigments. HT-29 cell line was obtained from a primary ("*in situ*") colon tumor, SW620 cancer cells was derived from a metastatic site, whereas non-cancerous CHO-K1 cell line served for comparative purposes. Gomphrenin, 2-decarboxy-gomphrenin and malabarin revealed the highest cytotoxic properties towards cancer cells, affecting cell proliferation and aggravating cancer cell survival due to programmed cell death. The obtained results show specific, beneficial health properties of decarboxylated and acylated gomphrenins.

Keywords: acylated betacyanins, betalains, colorectal adenocarcinoma, decarboxylated gomphrenins, dehydrogenated gomphrenins, plant pigments

***Corresponding Author:**
e-mail: slawomir.wybraniec@pk.edu.pl (Prof. S. Wybraniec)
#These Authors (S. Wybraniec and M. Tyszka-Czochara, e-mail: malgorzata.tyszka-czochara@uj.edu.pl) contributed equally to this work.

Submitted: 20 July2024
Accepted: 8 October 2024
Published on-line: 13 November 2024

INTRODUCTION

Betacyanins (a subgroup of betalain plant pigments) are imine derivatives of betalamic acid which forms betanidin by condensation with (2*S*)-5,6-dihydroxy-2,3-dihydro-1*H*-indole-2-carboxylic acid (*cyclo*-DOPA). The above condensation results in the formation of the basic structural unit of betacyanins [Strack *et al*., 2003; Tanaka *et al*., 2008]. Other betacyanins, namely betacyanin glycosides as well as their acylated derivatives, can be regarded formally as formed upon the condensation of betalamic acid with glycosylated (as well as subsequently acylated) derivatives of *cyclo*-DOPA, however, the order of condensation, glycosylation and acylation is still a subject of debate [Miguel, 2018; Slimen *et al*., 2017]. A characteristic attribute of all betacyanin structures is the presence of nitrogen atoms derived from the dihydroindole moiety and betalamic acid [Mabry & Dreiding, 1968]. As indicated by recent literature reports, betacyanins can currently be divided into 7 subtypes based on the following primary structures: betanin, melocactin, amaranthin, oleracin, apiocactin, gomphrenin and glabranin, which differ in substituents [Kumorkiewicz-Jamro *et al*., 2021].

The most known betacyanin is betanin (betanidin 5-*O*-*β*--glucoside). It has a glucosyl moiety attached to the carbon atom at the position C-5 [Gandía-Herrero *et al*., 2010] and is sourced mainly from *Beta vulgaris* L. (beetroot, red beet). Betanin is a compound with the most thoroughly studied physicochemical, antioxidant and bioactivity properties [Amjadi *et al*., 2018; da Silva *et al*., 2019; Esatbeyoglu *et al*., 2015; Knorr *et al*., 2015; Kumorkiewicz-Jamro *et al*., 2020; Wendel *et al*., 2016; Wybraniec *et al*., 2013; Wybraniec & Michalowski, 2011]. Compounds from the gomphrenin group can be found mainly in plants of the *Basellaceae* family, particularly in *Basella alba* L. and its variety *Basella alba* L. var. "Rubra" (Malabar spinach) [Arokoyo *et al*., 2018; Cai *et al*., 2003; Khan & Giridhar, 2015].

B. alba is native to the Indian subcontinent, Southeast Asia and New Guinea where it is widely used as a leaf vegetable [Adhikari *et al*., 2012]. It is a fast-growing, soft-stemmed vine, reaching 10 m in length with thick, semi-succulent, heart-shaped leaves. It has small, dark blue stone fruits and distinctive branched climbing stems [Chaurasiya *et al*., 2021].

The total betacyanin content in the mature fruits of *B. alba* plants is 42.0 mg/100 g and in those of *B. alba* "Rubra" is 86.6 mg/100 g. Gomphrenin is the major compound in these plants – *ca*. 40% of all betacyanins in both varieties, whereas other compounds found are derivatives the properties of which are still not fully explored [Sutor-Świeży *et al*., 2022a].

The stability of betalains in solutions is curbed by environmental factors such as: pH, water activity, light, presence of oxygen, temperature, presence of enzymes, compounds with antioxidant activity or metal cations [Herbach *et al*., 2006; Stintzing & Carle, 2004]. Betalains are stable in the pH range from 3 to 7, with environment pH 4–6 found optimal for their stability, which has been reported to increase in anaerobic conditions [Azeredo, 2009]. In the optimal pH range, temperature is a key determinant of their degradation [Kapadia *et al*., 2003].

However, by appropriately selecting the reaction conditions, it is possible to generate decarboxylated derivatives with potentially different antioxidant and bioactive properties [Kumorkiewicz *et al*., 2020; Wybraniec & Mizrahi, 2005]. The use of stabilizing agents, such as ethylenediaminetetraacetic acid (EDTA) or citrates, enables even more precise control of the resulting thermal decarboxylation products [Herbach *et al*., 2006; Pasch & von Elbe, 1979; Sutor-Świeży *et al*., 2022b]. Recently, we have conducted controlled thermal modifications of gomphrenin structure in order to obtain decarboxylated derivatives, and then, isolated the purified compounds [Sutor-Świeży *et al*., 2024].

Due to the potential health-promoting properties of the betacyanin compounds as well as still insufficient study on this topic, the important approach of the present study was also to find out if the obtained gomphrenin derivatives express health--promoting activities. Growing body of literature report anticancer [Kumar *et al*., 2015a, b] and inflammatory [Lin *et al*., 2010] potential of gomphrenin. However, the studies conducted so far have mainly focused on extracts, but not isolated compounds, while the activity of decarboxylated gomphrenin derivatives has not been studied yet. Therefore, in this contribution, we aimed at verifying if decarboxylated and acylated gomphrenin derivatives may affect cell proliferation and aggravate cancer cell survival due to programmed cell death.

To achieve this goal, two Duke's type C colorectal adenocarcinoma cell lines were employed. The HT-29 cell line was obtained from a primary (*"in situ"*) colon tumor, and SW620 cancer cells was derived from a metastatic site. Non-cancerous CHO-K1 cell line was used for comparative purposes.

MATERIAL AND METHODS

Reagents

Formic acid, acetone, methanol (mass spectrometric grade), and water were obtained from Sigma Chemical Co. (St. Louis, MO, USA).

Plant material

The plants of *B. alba* were cultivated in a greenhouse of the University of Agriculture (Faculty of Biotechnology and Horticulture) in Cracow, Poland, according to the recently presented procedure [Sutor-Świeży *et al*., 2024]. The plants were grown at controlled temperature and moisture for proper flowering and fruiting (photo of the plants is shown in Figure S1 in Supplementary Materials). Matured *B. alba* fruits were collected and used for analyses.

Preparation of *B. alba* fruit extract

B. alba fruit extract was prepared according to a recently published procedure [Sutor-Świeży *et al*., 2024]. Typically, 1 kg of the fruits was extracted 3 times with water (1 L) for 30 min at room temperature, and the combined extracts were centrifuged as well as filtered through a 0.2 mm i.d. pore size filter and a bed of 0.063/0.200 mm silica (J.T. Baker, Deventer, Holland). Purification of 0.03 M HCl acidified extract was performed by means of open column chromatography (150 mm height

Table 1. Chromatographic, spectrophotometric and low-resolution mass spectrometric data of the gomphrenin-based pigments obtained from *Basella alba* L. fruits.

No.	Compound	Abbreviation	R_t (min)	λ_{max} (nm)	*m/z* $[M+H]^+$	*m/z* MS/MS of $[M+H]^+$
1	Gomphrenin	Gp	7.9	539	551	389; 343; 297; 269; 253; 150
2	17-Decarboxy-gomphrenin	17-dGp	8.1	509	507	345; 299; 255; 214; 164; 152
3	2-Decarboxy-gomphrenin	2-dGp	9.6	534	507	345; 299; 255; 178; 162; 150
4	2,17-Bidecarboxy-gomphrenin	2,17-dGp	10.2	510	463	301; 255; 214; 164; 152; 150
5	Malabarin	Mb	12.8	545	713	669; 551; 389; 343; 297; 253
6	Globosin	Gb	14.4	544	697	653; 551; 389; 343; 297; 253

R_t, retention time; λ_{max}, the wavelength at the light absorption maximum; *m/z*, mass-to-charge ratio.

× 50 mm i.d.) on strongly acidic cation exchange resin (Strata X-C, Phenomenex, Torrance, CA, USA) acidified with 0.03 M HCl before adsorption of the pigments. The betacyanin fraction was eluted with water after prior purification with 1% formic acid, and the eluates were pooled before concentration using a rotary evaporator under reduced pressure at 25°C. The extracts were stored at -20°C for preservation over several weeks before exact experiments.

Generation of decarboxylated gomphrenins in semi--preparative scale for bioactivity assays

Decarboxylated gomphrenins at specific positions were obtained according to recently published procedures [Sutor-Świeży *et al*., 2024] in a diluted 2-L purified fruit extract solution (total betacyanin concentration of 30–60 µM). Pigment 17-decarboxy--gomphrenin was generated in a fruit extract aqueous solution (60 µM total betacyanins) containing 100 mM citric acid, following 3-h heating at 65°C. Similarly, the pigments 2-decarboxy- and 2,17-bidecarboxy-gomphrenin were generated in a fruit extract aqueous solution (30 µM total betacyanins) with 100 mM citric acid, subjected to 2–3 h of heating at 70°C. The resulting solutions were adsorbed onto a Chromabond silica C18 (Macherey & Nagel Co. Düren, Germany) column, and the pigments were subsequently eluted with a formic acid/acetone/water (1/50/49, *v/v/v*) solution and concentrated before preparative high-performance liquid chromatographic (HPLC) separation.

Isolation and purification of gomphrenin pigment from extracts

Gomphrenin and acylated gomphrenins were separated from *B. alba* purified fruit extract, and decarboxylated gomphrenins were isolated from the reaction mixtures obtained from the purified extract by heating (described in the previous section) on a HPLC semipreparative column Synergy Hydro-RP 250 mm × 30 mm i.d., 10 µm (Phenomenex), along with a 20 mm × 25 mm i.d. guard column of the same material (Phenomenex), according to a previously described procedure [Sutor-Świeży *et al*., 2024]. A typical gradient system consisting of 1% aqueous formic acid (solvent A) and acetone (solvent B) was used as follows: 0 min, 14% B; increasing to 10 min, 20% B; increasing to 15 min, 24% B; increasing to 28 min, 28% B; increasing to 36 min; 75% B. The injection volume was 25 mL, and a flow rate was 45 mL/min. Detection was performed using a UV-Vis detector at two selected wavelengths from the range of 510–540 nm, depending on the separated pigments, at column temperature of 22°C. The fraction obtained after concentration in a rotary evaporator at 25°C under reduced pressure were stored at –20°C for further analyses.

Chromatographic analysis with detection by low- and high-resolution mass spectrometric systems

A low-resolution mass spectrometric system LCMS-8030 (Shimadzu, Kyoto, Japan) controlled by LabSolutions software (v. 5.60 SP1, Shimadzu) equipped with HPLC pumps (LC-20ADXR), a SIL-20ACXR injector and an SPD-M20A detector was applied for the identification and determination of the obtained analytes. The same conditions as recently reported [Sutor-Świeży *et al*., 2024] were applied for the analytical separation of the pigments with the eluent gradient composed of aqueous 2% formic acid (solvent A) and methanol (solvent B): (t (min), % A), (0, 90), (12, 60), (15, 20), (19, 20). Detected pigments were readily assigned according to their chromatographic, optical and mass spectrometric properties presented in **Table 1** based on our previous study [Sutor-Świeży *et al*., 2024].

The LC-MS analyses with high-resolution mass spectrometric detection were performed using an Orbitrap Exploris™ 240 Mass Spectrometer (Thermo Fisher Scientific, Brema, Germany) according to the conditions provided in our recent report [Sutor-Świeży *et al*., 2024]. The detector was coupled to an HPLC Dionex UltiMate 3000 chromatographic separation system operating under Xcalibur software (Thermo Fisher Scientific) version 4.5.445.18.

Cell cultures

The following certified cell lines were derived from the American Type Cell Culture (ATCC) collection (LGC Standards-ATCC, Teddington, Great Britain): HT-29, Duke's type C colorectal adenocarcinoma (HTB-23); SW 620, Duke's type C colorectal adenocarcinoma (CCL-227), and CHO-K1 normal ovary cells (CCL-61). The HT-29 and SW 620 cells were grown in Dulbecco's Modified Eagle's Medium, DMEM (Gibco Laboratories, Grand Island, NY, USA), and the CHO-K1 cells were cultured in DMEM/F12 medium (Gibco Laboratories). All the media were supplemented with

10% (*v/v*) fetal bovine serum (FBS, Eurx, Gdańsk, Poland) and with an antibiotic solution (100 IU/mL penicillin, 0.1 mg/mL streptomycin; Sigma-Aldrich, Seelze, Germany). Prior to experiments, the cells were cultured for 24 h to obtain monolayers and were kept under standard culture conditions (humidified atmosphere, 37°C, 5% CO_2 in air), as described elsewhere [Adach *et al*., 2016; Tyszka-Czochara *et al*., 2021]. The tested compounds (listed in **Table 1**) were dissolved in an appropriate medium before cell culture experiments. Each experiment was repeated three times.

Cytotoxicity assays

For experiments, 100 µL of a suspension of exponentially dividing HT-29 or SW 620 cells at density of 1.0×10^5 cells/mL (CHO-K1 at density of 1.5×10^5 cells/mL) were inserted onto 96-well cell culture plates (BD Biosciences, San Jose, CA, USA) and incubated for 24 h. The 3-[4,5-dimethylthiazol-2yl]-2,5-diphenyl tetrazolium bromide (MTT) colorimetric assay was performed for the detection of cell proliferation, as described previously [Adach *et al*., 2015]. The cells were exposed to the tested compounds (listed in **Table 1**), each at concentrations of 0.01, 0.1, 1 and 10 mg/mL, for 24 h. The cells cultured in the medium with no additives served as positive controls (100% of growth). The cytotoxic effect of anti-cancer drug, Doxorubicin (DOX), at a concentration of 10 µg/mL was also determined.

The medium was removed after incubation, and the MTT reagent (Sigma-Aldrich) was added to each well, and incubation was continued for 1 h. During incubation, generated MTT formazan was dissolved in dimethyl sulfoxide (DMSO, Sigma-Aldrich), and the absorbance was recorded at 570 nm (with reference λ at 630 nm) in a microplate reader (Infinite M200 Pro, Tecan, Grödig, Austria). The amount of reduced MTT salt was proportional to the number of metabolically active (living) cells in the population exposed to gomphrenins. The results were expressed as cell proliferation (% of control cells).

Apoptosis and necrosis detection

HT-29 and SW 620 cells were seeded at density of 1.0×10^5 cells/mL (CHO-K1 at density of 1.5×10^5 cells/mL) into 6-well cell culture plates (Sarstedt AG&Co. KG, Nümbrecht, Germany) and incubated for 24 h to establish cell monolayer. Then, they were treated for 24 h with the tested pigments at concentrations of 0.01, 0.1, 1 and 10 mg/mL. Control cells were exposed for 24 h to the medium only. DOX at a concentration of 10 µg/mL was used in experiments as cytotoxicity control. For cell death detection, the cells were detached with a trypsin/EDTA solution (Gibco Laboratories), washed with Dulbecco's Phosphate Buffered Saline (DPBS, Gibco Laboratories) and centrifuged at 350×*g* for 5 min. Then, cell suspensions were exposed for 30 min in the dark to appropriate fluorescent dyes in a binding solution according to the recommended protocol (Biotium, Inc., Fremont, CA, USA). Fluorescent dyes used in the measurement were 488-AnnexinV (Biotium, excitation maximum at 490 nm/emission maximum at 515 nm), Ethidium homodimer (Biotium, EthD-III; excitation maximum at 528 nm/emission maximum at 617 nm) and SYTO 41 Blue Fluorescent Nucleic Acid Stain (Thermo Fisher Scientific Inc., Waltham, MA, USA, excitation maximum at 483 nm/emission maximum at 503 nm, used for proper discrimination between cells and debris). The assessment of apoptotic and necrotic cells was performed with a flow cytometer (FACSCanto10C) operated under software BD FACSCanto (BD Biosciences). The cells were gated according to forward (FSC), side scatter (SSC) and appropriate fluorescence parameters as described elsewhere [Tyszka-Czochara *et al*., 2017]. The results were given as the percentage of apoptotic/necrotic cells of total counted cells.

Statistical analysis

All experiments were conducted in triplicate. For the biological studies, data were analyzed using a one-way analysis of variance (ANOVA) followed by Tukey's test, and differences were considered to be significant at $p<0.05$. All results were expressed as mean and standard deviation (SD) of the mean. Calculations were carried out using the commercially available package, Statistica PL v.10 (StatSoft, Tulsa, OK, USA).

RESULTS AND DISCUSSION

Gomphrenin pigments isolated from *B. alba* fruits and their decarboxylated derivatives

Antioxidant and anti-inflammatory properties of decarboxylated and acylated gomphrenins compared to gomphrenin, a potent bioactive betacyanin, were reported in our recent work [Sutor-Świeży *et al*., 2024]. *In vitro* screening experiments revealed also that these pigments demonstrated strong anti-inflammatory properties in lipopolysaccharide (LPS)-activated human macrophages. Therefore, in this contribution, further characterization of gomphrenin decarboxylation mechanism as well as first results on the fragmentation pathways of the novel decarboxylated gomphrenins are presented. Sufficient quantities of decarboxylated and acylated gomphrenins (**Figure 1**) obtained in the study enabled further bioactivity experiments. The structures of *B. alba* endogenous gomphrenin and acylated gomphrenins (malabarin and globosin) were analyzed previously by nuclear magnetic resonance (NMR) techniques [Sutor-Świeży *et al*., 2022a]. Decarboxylated gomphrenins (2-decarboxy-gomphrenin, 17-decarboxy-gomphrenin and 2,17-bidecarboxy-gomphrenin) were structurally elucidated by NMR very recently [Sutor-Świeży *et al*., 2024].

Mechanism of gomphrenin 17-decarboxylation

In this study, 17-decarboxy-gomphrenin and 2,17-bidecarboxy-gomphrenin were generated in controlled thermal conditions in the purified *B. alba* extract at 65-75°C, which was elaborated previously [Sutor-Świeży *et al*., 2024]. Based on the previous mechanism reported for betanidin [Dunkelblum *et al*., 1972], the mechanism of 17-decarboxy-gomphrenin formation is presented in **Figure 2**. The monodecarboxylation of gomphrenin which involves the loss of the C-19 carboxyl with concomitant migration of the double bond C-17=C-18 to C-14=C-15 is proposed, which was proved previously by deuteration and NMR study on betanidin [Dunkelblum *et al*., 1972].

It became clear that carbons C-15 and C-17 of betanidin had interchanged to become C-17 and C-15, respectively,

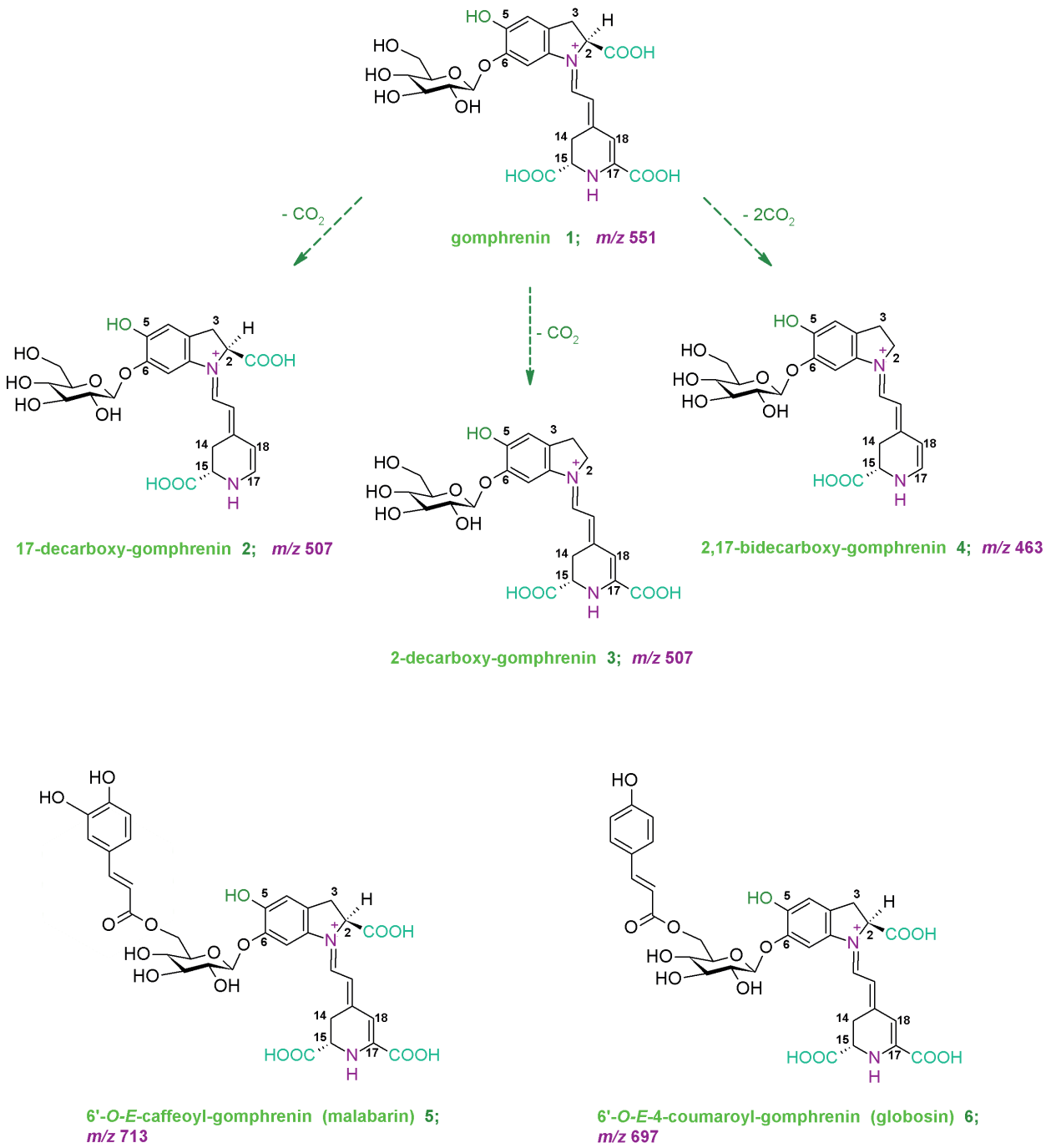

Figure 1. Chemical structures of novel decarboxylated gomphrenins and endogenous gomphrenin pigments obtained from *Basella alba* fruits.

in decarboxybetanidin and that the decarboxylation removed C-19 of betanidin [Dunkelblum *et al*., 1972]. Therefore, in the current reaction scheme (**Figure 2**), the rotation of the dihydropyridinic moiety in the last step of the pathway resulted in establishing the final 17-decarboxylated system. The structures of the generated decarboxylated gomphrenins were confirmed by NMR analyses [Sutor-Świeży *et al*., 2024].

The matrix effect on the pigment generation in the extract as well as the extract purification using a cation exchanger under various conditions were decisive in obtaining the required quantities of the selected decarboxylated gomphrenins. The removal of a substantial portion of the unfavorable matrix from the extract enabled efficient protection of the pigments from degradation presumably due to the removal of unknown reactive species.

A tremendous influence on the decarboxylation pathways was observed for the addition of citrates whose high concentration played a significant role in enhancing the formation of 2-decarboxy-gomphrenin [Sutor-Świeży *et al*., 2024], thus highly inhibiting the Dunkelblum *et al.* [1972] pathway of 17-decarboxylation. The above-elaborated methods were applied for the selective generation of 2-decarboxy-gomphrenin,

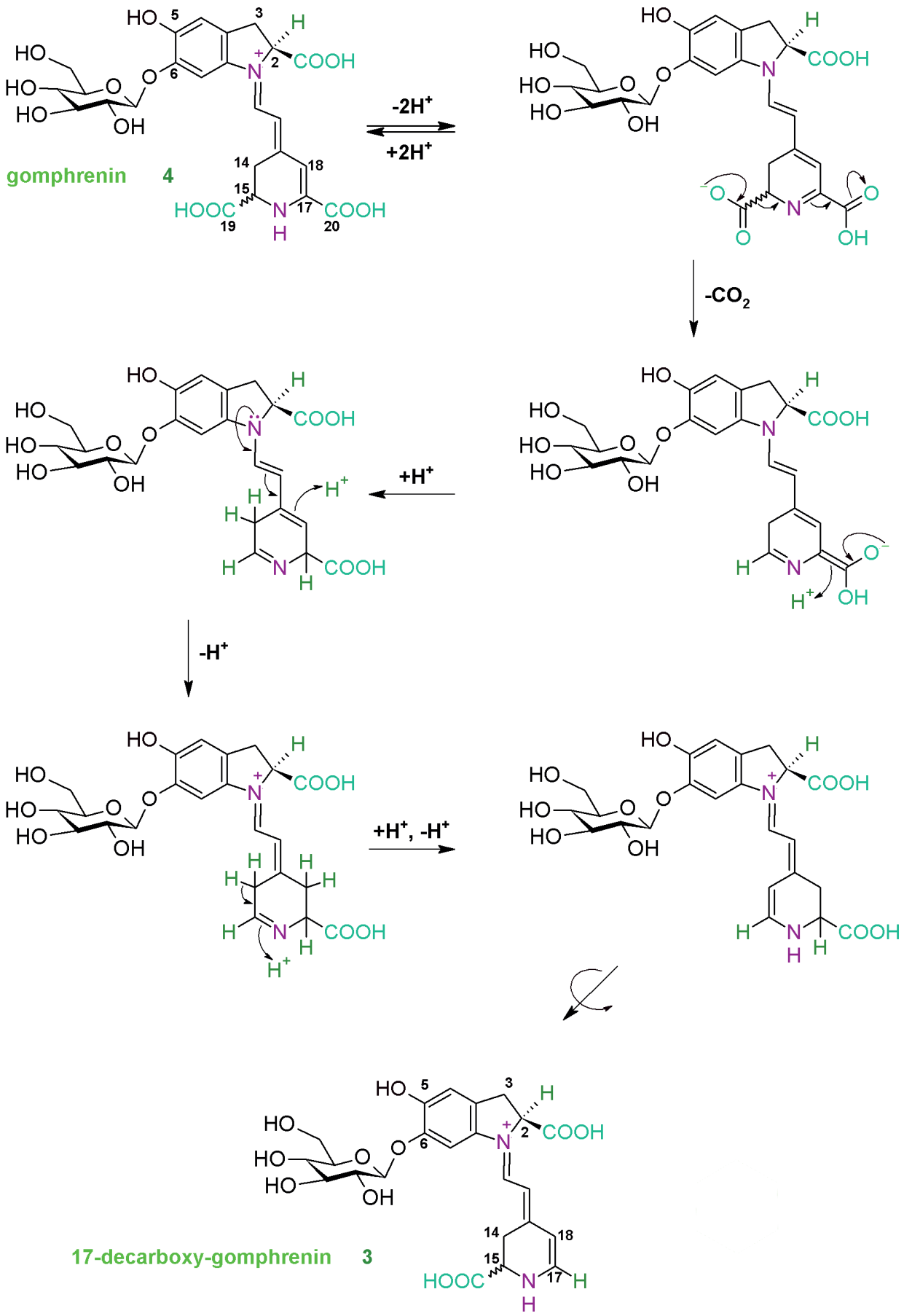

Figure 2. Formation of 17-decarboxy-gomphrenin based on the previous mechanism reported for betanidin by Dunkelblum *et al.* [1972].

17-decarboxy-gomphrenin and 2,17-bidecarboxy-gomphrenin for the following studies.

- **Fragmentation results on novel decarboxylated gomphrenins in the high-resolution mass spectrometric Orbitrap system**

Except for confirmation of the chemical formulas [Sutor-Świeży *et al.*, 2024], $C_{23}H_{27}N_2O_{11}$ for 17-decarboxy-gomphrenin (**2**) and 2-decarboxy-gomphrenin (**3**) as well as $C_{22}H_{27}N_2O_9$ for 2,17-bidecarboxy-gomphrenin (**4**), based on exact *m/z* values (**Table S1** in Supplementary Materials), first detailed results on the pigment fragmentation experiments were obtained in this study by high-resolution mass spectrometric experiments in the Orbitrap system (**Table S1**). The list of the *m/z* values obtained and calculated for most abundant ions formed during the fragmentation is presented in **Table S1**. The elimination profiles (**Figure 3**) as well as chemical structures of the generated ions (**Figures S2** and **S3** in Supplementary Materials) are also depicted.

In the case of 2-decarboxy-gomphrenin (**3**), fragmentation experiments (**Tables 1** and **S1**, **Figure 3**) of the protonated molecular ion (*m/z* 507) resulted in its deglucosylation (*m/z* 345; – Glc) and subsequent neutral loss of formic acid (*m/z* 299; – HCOOH), presumably from carbons C-14,15 because it leads

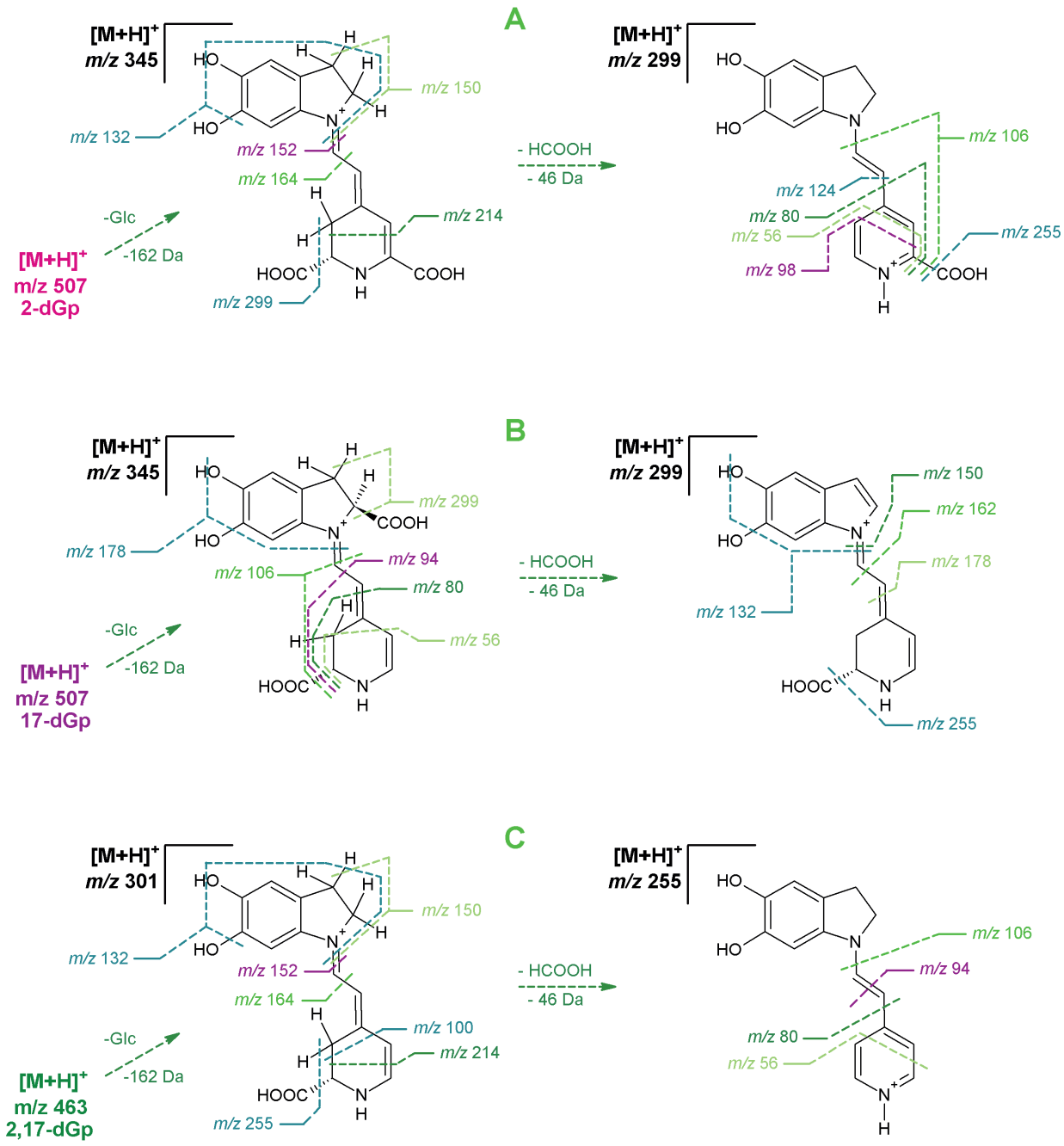

Figure 3. MS^n fragmentation pathways of 2-decarboxy-gomphrenin, 2-dGp (**A**), 17-decarboxy-gomphrenin, 17-dGp (**B**), and 2,17-bidecarboxy-gomphrenin, 2,17-dGp (**C**). Mass spectrometric data are shown in Table S1 in Supplementary Materials.

to the dehydrogenation of C-14,15 and formation of derivatives of the pyridinium cation. The loss of formic acid can also be regarded as the concurrent elimination of H_2O and CO [O'Hair *et al*., 2000]. Both scissions lead to the oxidation/dehydrogenation of the dihydropyridinic ring. Therefore, further fragmentation steps resulted in the formation of pyridinium-based ions (*m/z* 106, 80, and 56), either coupled with the elimination of the last carboxyl at C-17 (*m/z* 255; – CO_2) or with no decarboxylation (*m/z* 124 and 98).

The elimination of betalamic acid and its derivatives from the starting deglucosylated precursor (**3**) (*m/z* 345) resulted mainly in the generation of ions comprising the dihydroindolic system (*m/z* 214, 164, and 152) as well as the indolic (*m/z* 150) and dehydrated indolic (*m/z* 132) structures.

In contrast to **3**, for 17-decarboxy-gomphrenin (**2**), except of deglucosylation (*m/z* 345; – Glc), a neutral loss of formic acid (*m/z* 299; – HCOOH) is predicted at carbons C-2,3 instead of C-14,15, based on the previously indicated prevailing tendency of concurrent dehydrogenation and decarboxylation at carbons C-2,3 in betacyanins [Wybraniec & Michalowski, 2011] during their oxidation. These observations are supported in the current fragmentation study by the formation of the indolic (*m/z* 178 and 162) instead of the dihydroindolic (*m/z* 214, 164, and 152) derivatives, demonstrating the dehydrogentation position in the product of HCOOH neutral loss (*m/z* 299) at C-2,3 (**Figure 3**).

Further fragmentation of the precursor ion at *m/z* 299 enabled detecting the indolic (*m/z* 150) and dehydrated indolic (*m/z* 132) structures, as in the case of **3**. The decarboxylation of the precursor (*m/z* 299) at carbon C-15 enabled confirming the formation of an ion at *m/z* 255. In turn, the fragments detected at *m/z* 94 indicate the presence of a mono-decarboxylated betalamic acid derivative with the carboxyl present at carbon C-15.

Detection of pyridinium-based ions (*m/z* 106, 80, and 56) from both the precursors (*m/z* 345 and 299) confirms that their formation is feasible, as in the case of **3**; however, with accompanying deformyloxylation (– HCOOH).

The fragmentation of 2,17-bidecarboxy-gomphrenin (**4**) resulted in the generation of a spectral pattern similar to the patterns of **2** and **3**; however, with key differences. The formation of dihydroindolic (*m/z* 214, 164, and 152) as well as indolic (*m/z* 150) and dehydrated indolic (*m/z* 132) derivatives indicates similarities between the structure of the deglucosylated precursor **4** and deglucosylated **3**. The same can be stated for the detected pyridinium-based ions (*m/z* 106, 94, 80, and 56) which can be generated from both the fragments of **4** (*m/z* 301 and 255) and were confirmed for both the deglucosylated precursors from **2** and **3**. The main difference in the fragmentation patterns is the presence of an ion at *m/z* 100 (instead of *m/z* 98 detected after fragmentation of **3**), indicating the presence of a carboxylated fragment generated from the mono-decarboxy-betalamyl moiety in **4** (**Figure 3**).

The presented in-depth interpretation of high-resolution mass spectrometric (HRMS) fragmentation coupled with NMR results obtained previously [Sutor-Świeży *et al*., 2024] confirmed the decarboxylated pigment structures (**2**-**4**).

Antiproliferative and proapoptotic activity of gomphrenin and its decarboxylated derivatives

Biological activity of decarboxylated and acylated gomphrenin derivatives has been poorly investigated so far. It was reported that gomphrenin-type betalains may modulate cellular function *via* several mechanisms in the human body [Farabegoli *et al*., 2017]. A potential chemopreventive effect exerted by betalains was proposed, including a systemic action in the intestine, liver and peripheral tissues [Rahimi *et al*., 2019]. Therefore, in the present experiments, the MTT assay was employed to determine the effect of the pigment **1**-**6** treatment on the survival of cancer as well as non-cancerous cells.

The isolated individual gomphrenin as well as decarboxylated (2-dGp, 17-dGp and 2,17-dGp) and acylated (Mb and Gb) gomphrenin derivatives (**1**-**6**) from *B. alba* fruits expressed toxicity against cancer cell lines, HT-29 and SW620, in particular at concentrations 1 and 10 mg/mL. The comparative plots are presented in **Figure 4**. Our study demonstrated that tested betacyanins exert antiproliferative effect on both cancer cell lines at concentrations of 1 mg/mL and 10 mg/mL. The individual gomphrenin derivatives inhibited colorectal cancer cell growth to different extent. At concentration of 1 mg/mL, all the compounds (**1**-**6)** were toxic to cancer cells, but among the derivatives, 2-dGp and Mb were the most active. It should be noted that Gp, among others, at 1 mg/mL did not express any harmful effect on non-cancerous cells while it was still toxic towards tumor cells.

The biological action of acylated gomphrenins remains unknown; therefore, the finding that both acylated Gp derivatives can significantly restrain tumor cell growth compared to untreated cells, is of interest.

Extracts obtained from *Hylocereus polyrhizus* contributed to the chemopreventive effect against the formation of DNA breaks in the pUC19 plasmid under the influence of hydrogen peroxide/UV radiation and even stimulated the formation of native DNA forms [Tsai *et al*., 2019]. It was reported that gomphrenins had cytotoxic effects on cancer cells (SiHa) without negative effects on normal cells [Herb & Schramm, 2021; Kumar et al., 2015a]. The extract containing gomphrenin reduced the rate of T24 bladder cancer cells proliferation also without harming normal cells [Scarpa et al., 2016]. It should be emphasized that the biological action of acylated gomphrenins is not yet known, therefore, the finding that both acylated Gp derivatives can significantly restrain tumor cell growth, is of interest.

So far, only the cellular effects of some acylated polyphenol derivatives have been tested, and it was found that aromatic acyls, *i.e.*, galloyl derivatives, appeared to improve anti-cancer efficacy of compounds through enhancement of their binding affinities to molecular targets [Essa *et al*., 2023]. In this report, we found that both acylated Gp (5 and 6) had great ability to hamper cell proliferation (**Figure 4**) and both were able to induce cell death due to apoptosis (**Figure 5**).

As reported before, betalains can contribute to the inhibition of proliferation of tumors, such as melanoma cancer cells,

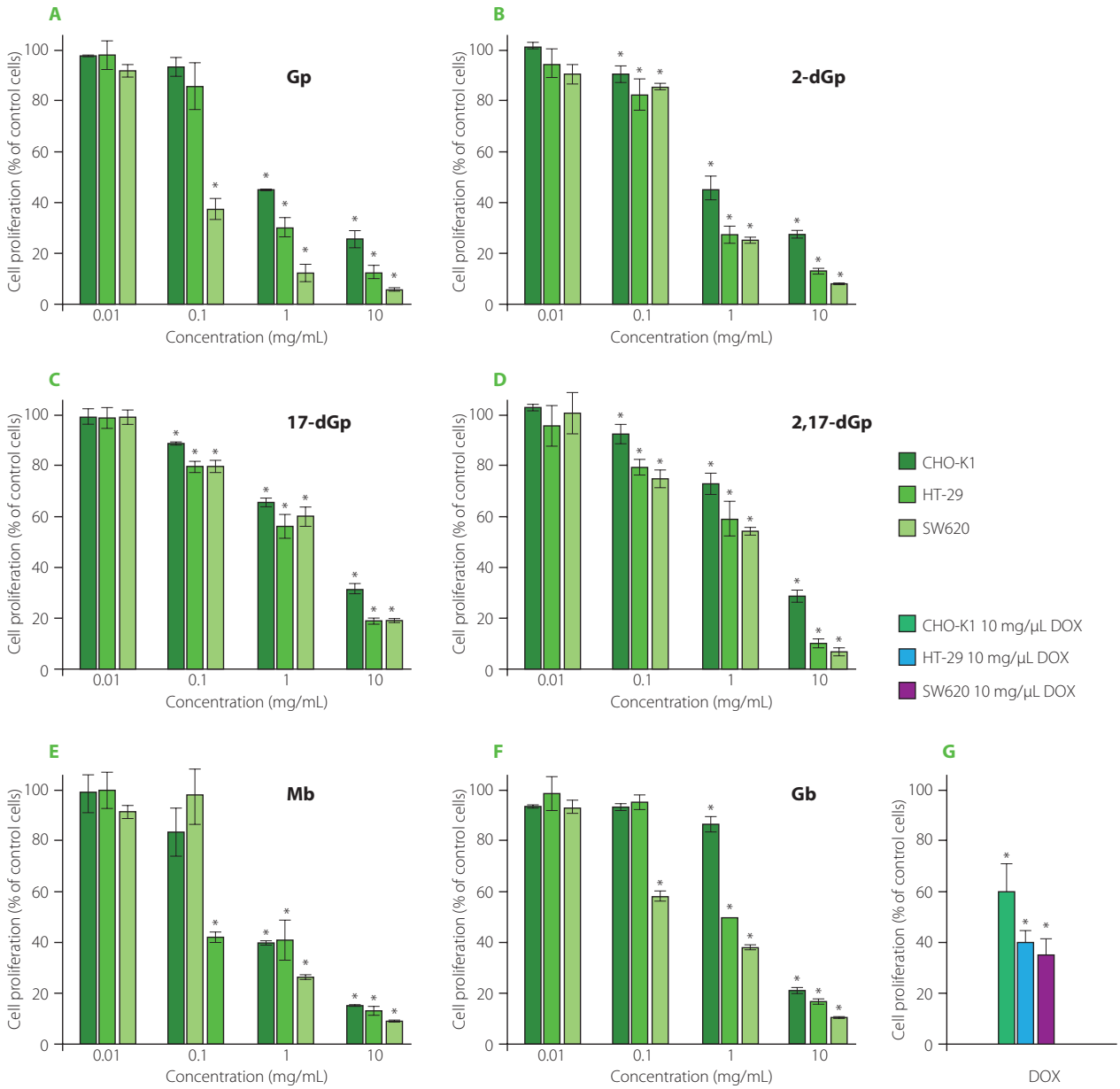

Figure 4. The effect of gomphrenin, Gp (**A**), 2-decarboxy-gomphrenin, 2-dGp (**B**), 17-decarboxy-gomphrenin, 17-dGp (**C**), 2,17-bidecarboxy-gomphrenin, 2,17-dGp (**D**), malabarin, Mb (**E**), and globosin, Gb (**F**) on cell proliferation as measured with MTT assay. The cells were exposed to specific concentrations of compounds for 24 h. Control cells were grown in medium only and they were treated as maximal (100%) cell viability. Doxorubicin (DOX) at a concentration of 10 µg/mL was used for comparative reasons (**G**). The results were expressed as the percentage of viable and metabolically active cells relative to the total counted cells. Means and standard deviations are shown (n=3). *Denotes significant difference *vs*. control (p<0.05).

suppress the development of prostate and breast cancer [Khan, 2016] and delay chemically-induced lung tumorigenesis due to the progressive elimination of cancer cells *via* apoptosis [Zhang *et al*., 2013]. A programmed cell death, apoptosis, is a critical biological process that protects an organism against the development of cancer. A study performed by Tesoriere *et al.* [2013] on the human intestinal carcinoma cell line Caco2 showed that betalains triggered the mitochondrial-dependent apoptotic pathway, which resulted in cancer cell death.

The data presented in **Figure 5**, indicate that all individual acylated as well as decarboxylated gomphrenins induced cell death due to apoptosis and necrosis in human colorectal carcinoma HT-29 and SW620 cell lines. The finding that acylated and decarboxylated gomphrenins are capable of inducing cell death *via* apoptosis may be of interest when designing modifications of Gp derivatives with targeted biological activity. Therefore, the proapoptotic activity of gomphrenin derivatives towards cancer cells can potentially foster a very beneficial effect.

A positive control used in the study, DOX, caused massive cell death at 1 µg/mL due to both mechanisms, apoptosis and necrosis. However, the results obtained for gomphrenins should be compared to the effect of DOX with caution. Taking into account the inhibitory activity of gomphrenins, it should be noted that the reference drug showed similar effects as Gp derivatives at a concentration approximately one thousand times lower than

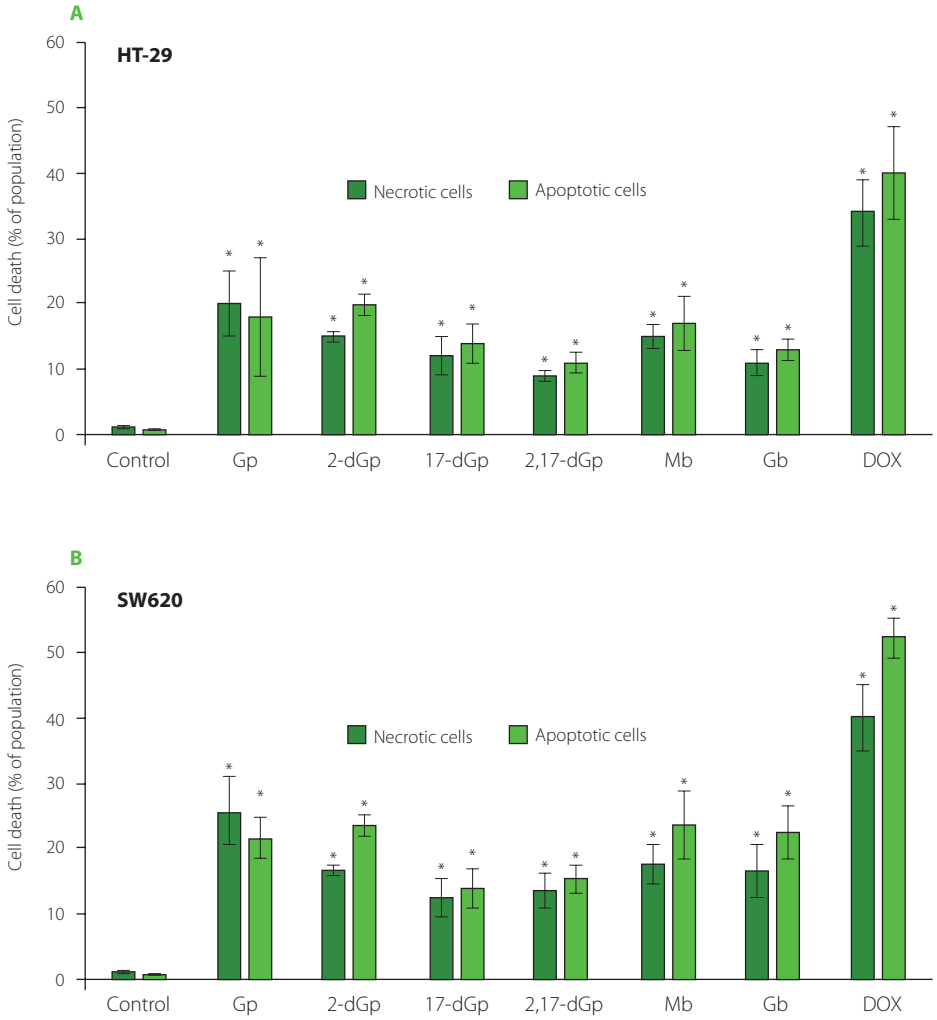

Figure 5. The effect of gomphrenin (Gp), 17-decarboxy-gomphrenin (17-dGp), 2-decarboxy-gomphrenin (2-dGp), 2,17-bidecarboxy-gomphrenin (2,17-dGp), globosin (Gb), and malabarin (Mb) on induction of cell death as measured using flow cytometry (apoptosis/necrosis assay). HT-29 cells (**A**) and SW620 cells (**B**) were exposed to 1 mg/mL concentration of compounds for 24 h. Control cells were grown in medium only and they were treated as maximal (100%) cell viability. Doxorubicin (DOX) at a concentration of 10 µg/mL was used for comparative reasons. The results were expressed as the percentage of apoptotic or necrotic cells relative to the total cells. Means and standard deviations are shown (n=3). *Denotes significant difference *vs*. control (p<0.05).

that of the tested compounds. However, it is known that DOX effectively inhibits the proliferation of colon cancer cells by restraining cellular divisions and that it is clinically used in cancer treatment regimens.

Both human cell lines employed in this study express morphological features of adenocarcinoma, the most common form of colon cancer which constitute up to 98% of all cases of colorectal cancer in humans. Moreover, both cell lines represent cells derived from tumor *in situ* at an advanced stage, which invade colon tissue (HT-29) and which pervaded the intestinal wall to the nearest lymph node (SW620) [ATCC, 2024]. Accordingly, both cell lines differ in their gene profile related to carcinogenesis and are commonly used in research models of colon cancer prevention by food compounds [van Erk *et al*., 2005]. In particular, all gomphrenins were toxic towards SW620 cells, which is of interest considering SW620 colorectal cancer cells characteristics, including their high proliferative capacity and chemotherapy resistance [Kawamoto *et al*., 2010]. We previously showed that among the tested gomphrenins, 2-dGp and Gp expressed the highest antioxidant activity in the 2,2'-azino-bis(3-ethylbenzothiazoline)-6-sulfonic acid (ABTS), ferric reducing antioxidant power (FRAP) and oxygen radical absorbance capacity (ORAC) assays, and this activity was even higher than that of a reference compound, caffeic acid [Sutor-Świeży *et al*., 2024]. It was shown by Zielińska-Przyjemska *et al.* [2012] and comprehensively reviewed by Sadowska-Bartosz & Bartosz [2021] and Bastos & Schliemann [2021] that betalains expressing high antioxidant capacity may play an important role in chemoprevention in humans. The data obtained here may be another promising prerequisite for further experiments on decarboxylated and acylated Gp derivatives' role in the prevention of gastrointestinal tract cancer.

As reported by many authors, chronic inflammation can promote carcinogenesis at the stage of initiation and progression of cancer [Landskron *et al*., 2014]. Emerging data indicate that betacyanins may express regulatory action towards immune

cells [Tyszka-Czochara *et al*., 2016]. Moreover, gomphrenins may act as potential anti-inflammatory agents *via* inhibition of inflammatory mediators, especially endotoxin-induced secretion of interleukin-1β (IL-1*β*), prostaglandin E2 (PGE2) and nitric oxide (NO) as well as the main pro-inflammatory cytokines with systemic effects [Ghonime *et al*., 2015], tumor necrosis factor α (TNF-*α*), cyclooxygenase-2 (COX-2), inducible nitric oxide synthase (iNOS) and interleukin-6 (IL-6). Our recent study demonstrated anti-inflammatory properties of several betalainic pigments, including decarboxylated and acylated gomphrenins [Sutor-Świeży *et al*., 2024]. It was found that 2-dGp and 17-dGp specifically targeted IL-6 production in LPS-activated human macrophages. In the previous work, we also demonstrated that acylated gomphrenins, Gb and Mb, were able to significantly reduce IL-8 secretion from human macrophages during inflammation. Since IL-8 is involved in the inflammatory process underlying the development of colon cancer [Lee *et al*., 2012], the ability of acylated gomphrenins to modulate inflammation *via* the principal regulatory cytokine, IL-8, is of interest. In line with the published results, our present study data confirm that both acylated Gp derivatives tested, Gb and Mb, are effective in restraining adenocarcinoma cells survival.

In the present experiments, gomphrenins revealed cytotoxic properties towards cancer cells at microgram and milligram concentrations. In fact, poor bioavailability of betacyanins was previously reported by a number of studies and was also attributed to gomphrenin [Khan, 2016]. Several *in vivo* experiments on betalain activity confirmed their limited absorption after oral intake, probably because of their degradation in the gastrointestinal tract [Khan, 2016]. At the same time, betalains as cationic compounds have high affinity for negatively-charged cell membranes, thus improving their influence on cells and their efficacy as antioxidants [Kanner *et al.*, 2001]. It can be presumed that following the intake of a large dose of betacyanins, *e.g.*, in the form of supplements or food enriched in particular compounds, they can still affect intestinal cells.

Considering the likely modifications of betacyanin molecules, our former experiments suggested that amaranthin-type betacyanin oxidation products were the most stable among all the tested pigments, especially during the preparative purification and isolation [Kumorkiewicz-Jamro *et al*., 2023]. In particular, betanin glycosylated in the C-5 position was oxidized more slowly than gomphrenin glycosylated in the C-6 position [Kumorkiewicz *et al*., 2018]. It is of interest whether gomphrenin oxidation products retain their intracellular action and biological activity in the body.

CONCLUSIONS

Sufficient quantities of decarboxylated gomphrenins, mostly 17-decarboxy-gomphrenin and 2,17-bidecarboxy-gomphrenin, were obtained in controlled thermal decarboxylation in the purified *B. alba* extract at 65–75°C, presumably according to the previously reported decarboxylation mechanism of betanidin [Dunkelblum *et al*., 1972]. The addition of citrates promotes the generation of 2-decarboxy-gomphrenin due to the inhibition of the Dunkelblum *et al*. [1972] pathway of 17-decarboxylation.

The presented in-depth interpretation of HRMS fragmentation supports the confirmation of decarboxylated pigment structures. Fragmentation pattern of 2,17-bidecarboxy-gomphrenin (**4**) is a combination of both the fragmentation pathways specific for 17-decarboxy-gomphrenin (**2**) and 2-decarboxy-gomphrenin (**3**). Especially, the formation of dihydroindolic as well as indolic and dehydrated indolic derivatives indicated similarities between the structures of 2-decarboxy-gomphrenin (**3**) and 2,17-bidecarboxy-gomphrenin (**4**), whereas the generation of pyridinium-based ions confirmed the presence of 17-decarboxylated and non-decarboxylated betalamic acid components specific for **2** as well as **3**, respectively.

Inhibitory action of isolated gomphrenin derivatives on cancer cell lines has not been demonstrated before. We performed preliminary studies with promising findings suggesting that decarboxylated and acylated gomphrenins can exert beneficial effects and positively influence human health. All these pigments have potential for the application in the food industry.

SUPPLEMENTARY MATERIALS

The following are available online at **https://journal.pan.olsztyn.pl/Gomphrenin-Based-Decarboxylated-and-Acylated-Pigments-from-Basella-alba-L-Fruit-Extracts,194251,0,2.html**; **Table S1**. High-resolution mass spectrometric data obtained by the Orbitrap system for the novel decarboxylated gomphrenins and their fragmentation ions. **Figure S1**. Image of cultivated B. alba plant in a greenhouse with ripening fruits containing gomphrenin-based pigments. **Figure S2**. Detected primary MS^n fragmentation ions of 17-decarboxy-gomphrenin (2), 2-decarboxy-gomphrenin (3) and 2,17-bidecarboxy-gomphrenin (4) (**Table S1**). **Figure S3**. Detected secondary MS^n fragmentation ions of 17-decarboxy-gomphrenin (2), 2-decarboxy-gomphrenin (3) and 2,17-bidecarboxy-gomphrenin (4) (**Table S1**).

RESEARCH FUNDING

This research was financed by Polish National Science Centre for years 2018-2021 (Project No. UMO-2017/27/B/NZ9/02831) except of the apoptosis/necrosis assay financed by Jagiellonian University Medical College (Project No. N/42/DBS/000284).

CONFLICT OF INTERESTS

The authors declare that they have no conflicts of interest.

ORCID IDs

M. Baj-Krzyworzeka https://orcid.org/0000-0002-5227-3006
M. Bieniasz https://orcid.org/0000-0002-3275-6262
S. Bobis-Wozowicz https://orcid.org/0000-0002-2200-6767
E. Dziedzic https://orcid.org/0000-0002-0570-6163
M. Knap https://orcid.org/0009-0000-2398-5250
Ł. Kozioł https://orcid.org/0009-0000-1059-2263
P. Mielczarek https://orcid.org/0000-0002-3275-6262
Ł. Popenda https://orcid.org/0000-0003-1117-3081
K. Sutor-Świeży https://orcid.org/0000-0001-7354-5376
R. Szatanek https://orcid.org/0000-0003-1327-6092
M. Tyszka-Czochara https://orcid.org/0000-0001-7945-1039
S. Wybraniec https://orcid.org/0000-0002-1263-4188

REFERENCES

1. Adach, A., Daszkiewicz, M., Tyszka-Czochara, M. (2016). A family of complexes with: N-scorpionate-type and other N-donor ligands obtained *in situ* from pyrazole derivative and zerovalent cobalt. Physicochemical and cytotoxicity studies. *RSC Advances*, *6*(50), 44070–44079. **https://doi.org/10.1039/c6ra06439f**
2. Adach, A., Daszkiewicz, M., Tyszka-Czochara, M., Barszcz, B. (2015). New oxovanadium(IV) complexes with pincer ligand obtained *in situ*: experimental and theoretical studies on the structure, spectroscopic properties and antitumour activity. *RSC Advances*, *5*(104), 85470–85479. **https://doi.org/10.1039/c5ra12561h**
3. Adhikari, R., Naveen Kumar, H.N., Shruthi, S.D. (2012). A review on medicinal importance of *Basella alba* L. *International Journal of Pharmaceutical Sciences and Drug Research*, *4*(2), 110–114.
4. Amjadi, S., Ghorbani, M., Hamishehkar, H., Roufegarinejad, L. (2018). Improvement in the stability of betanin by liposomal nanocarriers: its application in gummy candy as a food model. *Food Chemistry*, *256*, 156–162. **https://doi.org/10.1016/j.foodchem.2018.02.114**
5. Arokoyo, D.S., Oyeyipo, I.P., DuPlessis, S.S., Aboua, Y.G. (2018). Antioxidant activities of *Basella alba* aqueous leave extract in blood, pancreas, and gonadal tissues of diabetic male Wistar rats. *Pharmacognosy Research*, *10*(1), 31–36. **https://doi.org/10.4103/pr.pr_84_17**
6. ATCC. (n.d.). *ATCC cell products*. **https://www.atcc.org/cell-products#t=productTab&numberOfResults=24**
7. Azeredo, H.M.C. (2009). Betalains: properties, sources, applications, and stability - a review. *International Journal of Food Science and Technology*, *44*(12), 2365–2376. **https://doi.org/10.1111/j.1365-2621.2007.01668.x**
8. Bastos, E.L., Schliemann, W. (2021). Betalains as antioxidants. In H.M. Ekiert, K.G. Ramawat, J. Arora (Eds.), *Plant Antioxidants and Health. Reference Series in Phytochemistry*, Springer, Cham, Switzerland, pp. 1–44. **https://doi.org/10.1007/978-3-030-45299-5_9-2**
9. Cai, Y., Sun, M., Corke, H. (2003). Antioxidant activity of betalains from plants of the *Amaranthaceae*. *Journal of Agricultural and Food Chemistry*, *51*(8), 2288–2294. **https://doi.org/10.1021/jf030045u**
10. Chaurasiya, A., Pal, R.K., Verma, P.K., Katiyar, A., Kumar, R., Kumar, N. (2021). An updated review on Malabar spinach (*Basella alba* and *Basella rubra*) and their importance. *Journal of Pharmacognosy and Phytochemistry*, *10*(2), 1201–1207. **https://doi.org/10.22271/phyto.2021.v10.i2p.13974**
11. da Silva, D.V.T., dos Santos Baião, D., de Oliveira Silva, F., Alves, G., Perrone, D., Del Aguila, E.M., Flosi Paschoalin, V.M. (2019). Betanin, a natural food additive: stability, bioavailability, antioxidant and preservative ability assessments. *Molecules*, *24*(3), art. no. 458. **https://doi.org/10.3390/molecules24030458**
12. Dunkelblum, E., Miller, H.E., Dreiding, A.S. (1972). On the mechanism of decarboxylation of betanidine. A contribution to the interpretation of the biosynthesis of betalaines. *Helvetica Chimica Acta*, *55*(2), 642–648. https://doi.org/10.1002/hlca.19720550239
13. Esatbeyoglu, T., Wagner, A.E., Schini-Kerth, V.B., Rimbach, G. (2015). Betanin - a food colorant with biological activity. *Molecular Nutrition and Food Research*, *59*(1), 36–47. **https://doi.org/10.1002/mnfr.201400484**
14. Essa, A.F., Teleb, M., El-Kersh, D.M., El Gendy, A.E.N.G., Elshamy, A.I., Farag, M.A. (2023). Natural acylated flavonoids: their chemistry and biological merits in context to molecular docking studies. *Phytochemistry Reviews*, *22*(6), 1469–1508. **https://doi.org/10.1007/s11101-022-09840-1**
15. Farabegoli, F., Scarpa, E.S., Frati, A., Serafini, G., Papi, A., Spisni, E., Antonini, E., Benedetti, S., Ninfali, P. (2017). Betalains increase vitexin-2-O-xyloside cytotoxicity in CaCo-2 cancer cells. *Food Chemistry*, *218*, 356–364. **https://doi.org/10.1016/j.foodchem.2016.09.112**
16. Gandía-Herrero, F., Escribano, J., García-Carmona, F. (2010). Structural implications on color, fluorescence, and antiradical activity in betalains. *Planta*, *232*(2), 449–460. **https://doi.org/10.1007/s00425-010-1191-0**
17. Ghonime, M., Emara, M., Shawky, R., Soliman, H., El-Domany, R., Abdelaziz, A. (2015). Immunomodulation of RAW 264.7 murine macrophage functions and antioxidant activities of 11 plant extracts. *Immunological Investigations*, *44*(3), 237–252. **https://doi.org/10.3109/08820139.2014.988720**
18. Herb, M., Schramm, M. (2021). Functions of ROS in macrophages and antimicrobial immunity. *Antioxidants*, *10*(2), art. no. 313. **https://doi.org/10.3390/antiox10020313**
19. Herbach, K.M., Stintzing, F.C., Carle, R. (2006). Betalain stability and degradation - structural and chromatic aspects. *Journal of Food Science*, *71*(4), R41–R50. **https://doi.org/10.1111/j.1750-3841.2006.00022.x**
20. Kanner, J., Harel, S., Granit, R. (2001). Betalains - a new class of dietary cationized antioxidants. *Journal of Agricultural and Food Chemistry*, *49*(11), 5178–5185. **https://doi.org/10.1021/jf010456f**
21. Kapadia, G.J., Azuine, M.A., Sridhar, R., Okuda, Y., Tsuruta, A., Ichiishi, E., Mukainake, T., Takasaki, M., Konoshima, T., Nishino, H., Tokuda, H. (2003). Chemoprevention of DMBA-induced UV-B promoted, NOR-1-induced TPA promoted skin carcinogenesis, and DEN-induced phenobarbital promoted liver tumors in mice by extract of beetroot. *Pharmacological Research*, *47*(2), 141–148. **https://doi.org/10.1016/S1043-6618(02)00285-2**
22. Kawamoto, H., Yuasa, T., Kubota, Y., Seita, M., Sasamoto, H., Shahid, J.M., Hayashi, T., Nakahara, H., Hassan, R., Iwamuro, M., Kondo, E., Nakaji, S., Tanaka, N., Kobayashi, N. (2010). Characteristics of CD133+ human colon cancer SW620 cells. *Cell Transplantation*, *19*(6–7), 857–864. **https://doi.org/10.3727/096368910X508988**
23. Khan, M.I. (2016). Plant betalains: safety, antioxidant activity, clinical efficacy, and bioavailability. *Comprehensive Reviews in Food Science and Food Safety*, *15*(2), 316–330. **https://doi.org/10.1111/1541-4337.12185**
24. Khan, M.I., Giridhar, P. (2015). Plant betalains: Chemistry and biochemistry. *Phytochemistry*, *117*, 267–295. **https://doi.org/10.1016/j.phytochem.2015.06.008**
25. Knorr, F.J., McHale, J.L., Clark, A.E., Marchioro, A., Moser, J.E. (2015). Dynamics of interfacial electron transfer from betanin to nanocrystalline TiO_2: The pursuit of two-electron injection. *Journal of Physical Chemistry C*, *119*(33), 19030–19041. **https://doi.org/10.1021/acs.jpcc.5b05896**
26. Kumar, S.S., Manoj, P., Giridhar, P., Shrivastava, R., Bharadwaj, M. (2015a). Fruit extracts of *Basella rubra* that are rich in bioactives and betalains exhibit antioxidant activity and cytotoxicity against human cervical carcinoma cells. *Journal of Functional Foods*, *15*, 509–515. **https://doi.org/10.1016/j.jff.2015.03.052**
27. Kumar, S.S., Manoj, P., Shetty, N.P., Prakash, M., Giridhar, P. (2015b). Characterization of major betalain pigments - gomphrenin, betanin and isobetanin from *Basella rubra* L. fruit and evaluation of efficacy as a natural colourant in product (ice cream) development. *Journal of Food Science and Technology*, *52*(8), 4994–5002. **https://doi.org/10.1007/s13197-014-1527-z**
28. Kumorkiewicz-Jamro, A., Górska, R., Krok-Borkowicz, M., Mielczarek, P., Popenda, Ł., Lystvan, K., Pamuła, E., Wybraniec, S. (2023). Unveiling alternative oxidation pathways and antioxidant and cardioprotective potential of amaranthin-type betacyanins from spinach-like *Atriplex hortensis* var.'*Rubra*'. *Journal of Agricultural and Food Chemistry*, *71*(41), 15017–15034. **https://doi.org/10.1021/acs.jafc.3c03044**
29. Kumorkiewicz-Jamro, A., Starzak, K., Sutor, K., Nemzer, B., Pietrzkowski, Z., Popenda, Ł., Wybraniec, S. (2020). Structural study on hypochlorous acid-mediated chlorination of betanin and its decarboxylated derivatives from an anti-inflammatory *Beta vulgaris* L. extract. *Molecules*, *25*(2), art. no. 378. **https://doi.org/10.3390/molecules25020378**
30. Kumorkiewicz-Jamro, A., Świergosz, T., Sutor, K., Spórna-Kucab, A., Wybraniec, S. (2021). Multi-colored shades of betalains: recent advances in betacyanin chemistry. *Natural Product Reports*, *38*, 2315–2346. **https://doi.org/10.1039/d1np00018g**
31. Kumorkiewicz, A., Sutor, K., Nemzer, B., Pietrzkowski, Z., Wybraniec, S. (2020). Thermal decarboxylation of betacyanins in red beet betalain-rich extract. *Polish Journal of Food and Nutrition Sciences*, *70*(1), 7–14. **https://doi.org/10.31883/pjfns/114897**
32. Kumorkiewicz, A., Szneler, E., Wybraniec, S. (2018). Conjugation of oxidized betanidin and gomphrenin pigments from *Basella alba* L. fruits with glutathione. *Journal of Agricultural and Food Chemistry*, *66*(48), 12815–12826. **https://doi.org/10.1021/acs.jafc.8b04941**
33. Landskron, G., De la Fuente, M., Thuwajit, P., Thuwajit, C., Hermoso, M.A. (2014). Chronic inflammation and cytokines in the tumor microenvironment. *Journal of Immunology Research*, *2014*, art. no. 149185. **https://doi.org/10.1155/2014/149185**
34. Lee, Y.S., Choi, I., Ning, Y., Kim, N.Y., Khatchadourian, V., Yang, D., Chung, H.K., Choi, D., LaBonte, M.J., Ladner, R.D., Nagulapalli Venkata, K.C., Rosenberg, D.O., Petasis, N.A., Lenz, H.-J., Hong, Y.-K. (2012). Interleukin-8 and its receptor CXCR2 in the tumour microenvironment promote colon cancer growth, progression and metastasis. *British Journal of Cancer*, *106*(11), 1833–1841. **https://doi.org/10.1038/bjc.2012.177**
35. Lin, S.-M., Lin, B.-H., Hsieh, W.-M., Ko, H.-J., Liu, C.-D., Chen, L.-G., Chiou, R.Y.-Y. (2010). Structural identification and bioactivities of red-violet pigments present in *Basella alba* fruits. *Journal of Agricultural and Food Chemistry*, *58*(19), 10364–10372. **https://doi.org/10.1021/jf1017719**

36. Mabry, T., Dreiding, A.S. (1968). The betalains. In T.J. Mabry, R.E. Alston, V.C. Runecles (Eds.), *Recent Aadvances in Phytochemistry*, Vol. 1, Appleton-Century-Crofts, New York, pp. 145–160.
37. Miguel, M.G. (2018). Betalains in some species of the *Amaranthaceae* family: A review. *Antioxidants*, *7*(4), art. no. 53. **https://doi.org/10.3390/antiox7040053**
38. O'Hair, R.A.J., Broughton, P.S., Styles, M.L., Frink, B.T., Hadad, C.M. (2000). The fragmentation pathways of protonated glycine: A computational study. *Journal of the American Society for Mass Spectrometry*, *11*(8), 687–696. **https://doi.org/10.1016/S1044-0305(00)00143-4**
39. Pasch, J.H., von Elbe, J.H. (1979). Betanine stability in buffered solutions containing organic acids, metal cations, antioxidants, or sequestrants. *Journal of Food Science*, *44*(1), 72–75. **https://doi.org/10.1111/j.1365-2621.1979.tb10007.x**
40. Rahimi, P., Abedimanesh, S., Mesbah-Namin, S.A., Ostadrahimi, A. (2019). Betalains, the nature-inspired pigments, in health and diseases. *Critical Reviews in Food Science and Nutrition*, *59*(18), 2949–2978. **https://doi.org/10.1080/10408398.2018.1479830**
41. Sadowska-Bartosz, I., Bartosz, G. (2021). Biological properties and applications of betalains. *Molecules*, *26*(9), art. no. 2520. **https://doi.org/10.3390/molecules26092520**
42. Scarpa, E.S., Emanuelli, M., Frati, A., Pozzi, V., Antonini, E., Diamantini, G., Di Ruscio, G., Sartini, D., Armeni, T., Palma, F., Ninfali, P. (2016). Betacyanins enhance vitexin-2-O-xyloside mediated inhibition of proliferation of T24 bladder cancer cells. *Food and Function*, *7*(12), 4772–4780. **https://doi.org/10.1039/c6fo01130f**
43. Slimen, I.B., Najar, T., Abderrabba, M. (2017). Chemical and antioxidant properties of betalains. *Journal of Agricultural and Food Chemistry*, *65*(4), 675–689. **https://doi.org/10.1021/acs.jafc.6b04208**
44. Stintzing, F.C., Carle, R. (2004). Functional properties of anthocyanins and betalains in plants, food, and in human nutrition. *Trends in Food Science and Technology*, *15*(1), 19–38. **https://doi.org/10.1016/j.tifs.2003.07.004**
45. Strack, D., Vogt, T., Schliemann, W. (2003). Recent advances in betalain research. *Phytochemistry*, *62*(3), 247–269. **https://doi.org/10.1016/S0031-9422(02)00564-2**
46. Sutor-Świeży, K., Antonik, M., Dziedzic, E., Bieniasz, M., Mielczarek, P., Popenda, Ł., Pasternak, K., Tyszka-Czochara, M., Wybraniec, S. (2022a). Structural studies on diverse betacyanin classes in matured pigment-rich fruits of *Basella alba* L. and *Basella alba* L. var. 'Rubra' (Malabar spinach). *International Journal of Molecular Sciences*, *23*(19), art. no. 11243. **https://doi.org/10.3390/ijms231911243**
47. Sutor-Świeży, K., Górska, R., Kumorkiewicz-Jamro, A., Dziedzic, E., Bieniasz, M., Mielczarek, P., Popenda, Ł., Pasternak, K., Tyszka-Czochara, M., Baj-Krzyworzeka, M., Stefańska, M., Błyszczuk, P., Wybraniec, S. (2024). *Basella alba* L. (Malabar spinach) as an abundant source of betacyanins: identification, stability, and bioactivity studies on natural and processed fruit pigments. *Journal of Agricultural and Food Chemistry*, *72*(6), 2943–2962. **https://doi.org/10.1021/acs.jafc.3c06225**
48. Sutor-Świeży, K., Proszek, J., Popenda, Ł., Wybraniec, S. (2022b). Influence of citrates and EDTA on oxidation and decarboxylation of betacyanins in red beet (*Beta vulgaris* L.) betalain-rich extract. *Molecules*, *27*(24), art. no. 9054. **https://doi.org/10.3390/molecules27249054**
49. Tanaka, Y., Sasaki, N., Ohmiya, A. (2008). Biosynthesis of plant pigments: Anthocyanins, betalains and carotenoids. *Plant Journal*, *54*(4), 733–749. **https://doi.org/10.1111/j.1365-313X.2008.03447.x**
50. Tesoriere, L., Gentile, C., Angileri, F., Attanzio, A., Tutone, M., Allegra, M., Livrea, M.A. (2013). Trans-epithelial transport of the betalain pigments indicaxanthin and betanin across Caco-2 cell monolayers and influence of food matrix. *European Journal of Nutrition*, *52*(3), 1077–1087. **https://doi.org/10.1007/s00394-012-0414-5**
51. Tsai, Y., Lin, C.G., Chen, W.L., Huang, Y.C., Chen, C.Y., Huang, K.F., Yang, C.H. (2019). Evaluation of the antioxidant and wound-healing properties of extracts from different parts of *Hylocereus polyrhizus*. *Agronomy*, *9*(1), art. no. 27. **https://doi.org/10.3390/agronomy9010027**
52. Tyszka-Czochara, M., Adach, A., Grabowski, T., Konieczny, P., Pasko, P., Ortyl, J., Świergosz, T., Majka, M. (2021). Selective cytotoxicity of complexes with N,N,N-donor dipodal ligand in tumor cells. *International Journal of Molecular Sciences*, *22*(4), art. no. 1802. **https://doi.org/10.3390/ijms22041802**
53. Tyszka-Czochara, M., Bukowska-Strakova, K., Majka, M. (2017). Metformin and caffeic acid regulate metabolic reprogramming in human cervical carcinoma SiHa/HTB-35 cells and augment anticancer activity of Cisplatin *via* cell cycle regulation. *Food and Chemical Toxicology*, *106*(Part A), 260–272. **https://doi.org/10.1016/j.fct.2017.05.065**
54. Tyszka-Czochara, M., Pasko, P., Zagrodzki, P., Gajdzik, E., Wietecha-Posluszny, R., Gorinstein, S. (2016). Selenium supplementation of amaranth sprouts influences betacyanin content and improves anti-inflammatory properties via NFκB in murine RAW 264.7 macrophages. *Biological Trace Element Research*, *169*(2), 320–330. **https://doi.org/10.1007/s12011-015-0429-x**
55. van Erk, M.J., Krul, C.A.M., Caldenhoven, E., Stierum, R.H., Peters, W.H., Woutersen, R.A., van Ommen, B. (2005). Expression profiling of colon cancer cell lines and colon biopsies: towards a screening system for potential cancer-preventive compounds. *European Journal of Cancer Prevention*, *14*(5), 439–457. **https://doi.org/10.1097/01.cej.0000174781.51883.21**
56. Wendel, M., Nizinski, S., Gierszewski, M., Prukala, D., Sikorski, M., Starzak, K., Wybraniec, S., Burdzinski, G. (2016). Chemical quenching of singlet oxygen by betanin. *Photochemical and Photobiological Sciences*, *15*(7), 872–878. **https://doi.org/10.1039/c6pp00037a**
57. Wybraniec, S., Michalowski, T. (2011). New pathways of betanidin and betanin enzymatic oxidation. *Journal of Agricultural and Food Chemistry*, *59*(17), 9612–9622. **https://doi.org/10.1021/jf2020107**
58. Wybraniec, S., Mizrahi, Y. (2005). Generation of decarboxylated and dehydrogenated betacyanins in thermally treated purified fruit extract from purple pitaya (*Hylocereus polyrhizus*) monitored by LC-MS/MS. *Journal of Agricultural and Food Chemistry*, *53*(17), 6704–6712. **https://doi.org/10.1021/jf050700t**
59. Wybraniec, S., Starzak, K., Skopińska, A., Nemzer, B., Pietrzkowski, Z., Michałowski, T. (2013). Studies on nonenzymatic oxidation mechanisms in neobetanin, betanin, and decarboxylated betanins. *Journal of Agricultural and Food Chemistry*, *61*(26), 6465–6476. **https://doi.org/10.1021/jf400818s**
60. Zhang, Q., Pan, J., Wang, Y., Lubet, R., You, M. (2013). Beetroot red (betanin) inhibits vinyl carbamate- and benzo(a)pyrene-induced lung tumorigenesis through apoptosis. *Molecular Carcinogenesis*, *52*(9), 686–691. **https://doi.org/10.1002/mc.21907**
61. Zielińska-Przyjemska, M., Olejnik, A., Kostrzewa, A., Łuczak, M., Jagodziński, P.P., Baer-Dubowska, W. (2012). The beetroot component betanin modulates ROS production, DNA damage and apoptosis in human polymorphonuclear neutrophils. *Phytotherapy Research*, *26*(6), 845–852. **https://doi.org/10.1002/ptr.3649**

ORIGINAL ARTICLE
http://journal.pan.olsztyn.pl

Polish Journal of Food and Nutrition Sciences
2024, Vol. 74, No. 4, 363–375
DOI: 10.31883/pjfns/194694
ISSN 1230-0322, e-ISSN 2083-6007

Dietary Fiber with Functional Properties Counteracts the Thwarting Effects of Copper Nanoparticles on the Microbial Enzymatic Activity and Short-Chain Fatty Acid Production in the Feces of Rats

Jerzy Juśkiewicz[1,*], Bartosz Fotschki[1], Anna Stępniowska[2], Ewelina Cholewińska[2], Dorota Napiórkowska[1], Aleksandra Marzec[2], Łucja Brzuzan[1], Joanna Fotschki[1], Ewa Żary-Sikorska[3], Katarzyna Ognik[2]

[1]Department of Biological Function of Food, Division of Food Science, Institute of Animal Reproduction and Food Research of the Polish Academy of Sciences, 10 Tuwima Street, 10-748 Olsztyn, Poland
[2]Department of Biochemistry and Toxicology, Faculty of Animal Sciences and Bioeconomy, University of Life Sciences, 13 Akademicka Street, 20-950 Lublin, Poland
[3]Department of Microbiology and Food Technology, Faculty of Agriculture and Biotechnology, Bydgoszcz University of Science and Technology, 7 Kaliskiego Ave., 85-796 Bydgoszcz, Poland

The present study aimed to scrutinize the hypothesis that the dietary addition of fiber with functional properties would prevent the thwarting effects of copper nanoparticles (Cu-NP) on fecal microbial metabolic activity. The Wistar rats were fed for 6 weeks with diets with two different contents of Cu-NP (a recommended dose of 6.5 mg/kg or doubled) and four sources of dietary fiber: control – cellulose; and experimental – pectin, inulin, and psyllium. The activity of bacterial enzymes and short-chain fatty acids (SCFA) production were analyzed in the excreted feces collected on subsequent days of feeding. The inclusion of Cu-NP to the diet, especially in the higher dose tested, resulted in a rapid reduction in the fecal microbial enzymatic activity after only the first day of feeding. The addition of functional fiber to diets containing Cu-NP enhanced bacterial α-glucosidase, β-glucosidase, β-glucuronidase, α-arabinofuranosidase activity and SCFA production *vs*. diets with control cellulose. That effect was most rapidly evident with pectin, while the effect of inulin or psyllium addition exceeded that of pectin only in some cases, *i.e.*, α-glucosidase activity as well as content of propionic and butyric acids. In conclusion, the high potential of dietary functional fiber in reducing the suppressive effect of Cu-NP on the intestinal microbiota activity should be recognized.

Keywords: fecal microbial activity, inulin, nanominerals, pectin, psyllium, rats

INTRODUCTION

Copper is one of the most important trace elements, essential for both humans and animals to ensure that life processes occur harmoniously, maintaining a state of homeostasis [Malavolta *et al*., 2015]. The main sources of Cu include food, drinking water, and Cu-containing supplements [Herman *et al*., 2022; Olivares & Uauy, 1996]. Sources of copper in food can be both inorganic and organic, with the latter being considered more bioavailable and having higher retention in the body [Jankowski *et al*., 2020]. However, comparative results of organic *vs*. inorganic Cu sources are inconsistent. In recent years, researchers have focused on copper nanoparticles (Cu-NP) as an alternative to the aforementioned sources, due to the unique physical and biological properties of nanometals, including bioavailability, which may limit excessive copper excretion in feces and urine. Some authors suggest that Cu-NP in the body may

***Corresponding Author:**
e-mail: j.juskiewicz@pan.olsztyn.pl (Prof. J. Juśkiewicz)

Submitted: 26 August 2024
Accepted: 16 October 2024
Published on-line: 19 November 2024

play the same role as copper from conventional sources, while still allowing for reduced supplementation options [Kiyani *et al*., 2022]. But, in our opinion, the truth about the dietary Cu-NP should be rediscovered. In the first years of the current century, the results regarding Cu-NP application as an alternative feed component were rather rare. Gonzales-Eguia *et al*. [2009] demonstrated enhanced production parameters of piglets fed a diet with Cu-NP supplementation. On the other hand, Pineda *et al*. [2013] showed disrupted development of internal organs in chicken embryos. The Cu-NP has more and more applications in daily life these days. They are utilized in the manufacturing of chips, power sources, gas detectors, photovoltaic generators, electronic devices, and heating systems [Zhang *et al*., 2023]. Cu-NP have been used at a growing rate in the manufacturing of medications and beauty products because of their strong bactericidal characteristics [Anreddy, 2018; Ermini & Voliani, 2021]. Cu-NP are also proposed by some researchers as a potential dietary supplement for consumers struggling with mineral deficiencies in the body [Baravkar *et al*., 2021; Kargin *et al*., 2021; Lee *et al*., 2016].

There is no doubt that adjusting the dietary fiber content and fiber type may, directly and indirectly, affect copper bioavailability by modifying its absorption and modulating the bioavailability of mineral antagonists. Studies indicate that soluble fiber is beneficial, which, in addition to increasing the bioavailability of copper, favorably modulates the passage of digestive contents in the gut [Baye *et al*., 2017]. Different dietary fibers substantially affect the large intestinal pH values, dry matter content, buffering capacity of digesta, and finally the microbial community actions in the large gut lumen [Perler *et al*., 2023]. The impact of consumed nanoparticles in the body, including on bacteria colonizing the large intestine, is usually described as a double-edged sword effect that both benefits and harms. This rule appears to apply to the interaction between gut microbes and Cu-NP. Our previous studies have shown that the addition of Cu-NP to the cellulose-containing diet of rats resulted in reduced proliferation of the cecal microbiota and lower bacterial enzymatic activity, leading to a diminished amount of short-chain fatty acids (SCFAs) produced [Cholewińska *et al*., 2018]. Strychalski *et al*. [2021] showed the modulatory effect of dietary fiber type on the enzyme release rate from bacterial cells, thus creating a large intestinal environment with higher or lower extracellular enzyme activity.

Considering that fiber is an essential dietary component and that its type would be critical to the absorption and subsequent physiological action of Cu-NP, the present study aimed to verify the hypothesis that the effect of Cu-NP on the metabolic status of the fecal microbial community is strongly reliant on the physiological function of different dietary fiber types. In the present study, it has been proposed that a dietary concomitant presence of Cu-NP with either a control inert (cellulose) or a prebiotic (inulin) or a viscous (pectin) or a bulking (psyllium) fiber would significantly and in a different way alter the enzymatic activity of the bacteria and the synthesis of short-chain fatty acids in the rat feces.

MATERIAL AND METHODS

Nanoparticles and fiber source

Copper nanoparticles (Cu-NP) were purchased at Sky Spring Nanomaterials Incorporation (Houston, TX, USA). The characteristics of the Cu-NP preparation were as follows: spherical morphology, powder with 99.9% purity, particle size of 40–60 nm, specific surface area of 12 m^2/g, bulk density of 0.19 g/mL, and true density of 8.9 g/mL. In the diets prepared in our laboratory (Institute of Animal Reproduction and Food Research of the Polish Academy of Sciences, Olsztyn, Poland), α-cellulose (Sigma, Poznań, Poland) was used as control fiber, whereas inulin (FrutafitTex, Sensus, the Netherlands), pectin (PectinE 440(I), Brouwland, Beverlo, Belgium), and psyllium (Psyllium husk powder, NaturaleBio, Rome, Italy) were used as fibers with different functional properties.

The *in vivo* protocol

The animal study was conducted on 100 nine-week-old outbred male Wistar rats (Cmdb:Wi) fed diets with two Cu-NP contents (recommended 6.5 mg/kg (L) and two-times higher (H)) along with different dietary fibers (cellulose, inulin, psyllium, pectin; see **Figure S1** in Supplementary Materials). The rats were randomly assigned to ten study groups, with 10 animals in each group. The experimental group schema was as follows: Control C and CH groups, fed a control diet containing $CuCO_3$ of 6.5 and 13 mg/kg and 8% of cellulose (n=10 per group); groups CN and CNH, fed diets with L and H content of Cu-NP, respectively, and 8% of cellulose; groups PN and PNH, fed diets with L and H content of Cu-NP, respectively, 2% of cellulose and 6% of pectin; groups JN and JNH, fed diets with L and H content of Cu-NP, respectively, 2% of cellulose and 6% of inulin; groups SN and SNH, fed diets with L and H content of Cu-NP, respectively, 2% of cellulose and 6% of psyllium. The Local Ethics Committee for Animal Experiments in Olsztyn (Poland) approved the experimental protocol (No. 19/2021). The environment in the animal room was characterized by a stable temperature (22±1°C), relative humidity of 60±5%, a 12-h light-dark cycle, and a ventilation rate of 15 air changes *per* hour. The experiment lasted 6 weeks, and the animals had unlimited access to diet and water. The nutritional acclimation period on diet C was 5 days for all rats (see **Table 1** for diet compositions).

Sample collection and analyses

The fecal samples were collected on days 0, 1, 2, 7, 14, 21, and 42. The fecal pH was measured just after sample collection (pH meter, Model 301, Hanna Instruments, Vila do Conde, Portugal). The details of detreminations of the fecal ammonia, SCFA content and bacterial enzyme (α- and β-glucosidase, β-glucuronidase, α-arabinofuranosidase) activity were provided elsewhere [Gugołek *et al*., 2021]. In brief, ammonia released from fresh feces was difuded to boric acid solution in Conway's dishes and detremined by titration with sulfuric acid. Results were expressed in mg/g.

Gas chromatography method was used to determine the SCFA content in fecal digesta. The separation of SCFA was

Table 1. The composition (%) of control diets with $CuCO_3$ at two levels (C and CH) and experimental diets with Cu nanoparticles (Cu-NP) at two levels (CN and CNH), and with Cu-NPs and replacing part of celulose with pectin (PN and PNH), inulin (JN and JNH) and psyllium (SN and SNH).

Component	C/CH	CN/CNH	PN/PNH	JN/JNH	SN/SNH
Casein[1]	14.8	14.8	14.8	14.8	14.8
DL-methionine	0.2	0.2	0.2	0.2	0.2
Cellulose	8.0	8.0	2.0	2.0	2.0
Pectin	–	–	6	–	–
Inulin	–	–	–	6	–
Psyllium	–	–	–	–	6
Choline chloride	0.2	0.2	0.2	0.2	0.2
Rapeseed oil	8.0	8.0	8.0	8.0	8.0
Cholesterol	0.3	0.3	0.3	0.3	0.3
Vitamin mix[2]	1.0	1.0	1.0	1.0	1.0
Mineral mix[3]	3.5	3.5	3.5	3.5	3.5
Maize starch[4]	64.0	64.0	64.0	64.0	64.0
Cu source					
$CuCO_3$ (mg/kg diet)	6.5/13	0	0	0	0
Cu-NP (mg/kg diet)	0	6.5/13	6.5/13	6.5/13	6.5/13

[1]Casein preparation: crude protein 89.7%, crude fat 0.3%, ash 2.0%, and water 8.0%. [2]AIN-93G-VM, g/kg mix: 3.0 nicotinic acid, 1.6 Ca pantothenate, 0.7 pyridoxine-HCl, 0.6 thiamin-HCl, 0.6 riboflavin, 0.2 folic acid, 0.02 biotin, 2.5 vitamin B_{12} (cyanocobalamin, 0.1% in mannitol), 15.0 vitamin E (all-*rac*-α-tocopheryl acetate, 500 IU/g), 0.8 vitamin A (all-*trans*-retinyl palmitate, 500,000 IU/g), 0.25 vitamin D_3 (cholecalciferol, 400,000 IU/g), 0.075 vitamin K_1 (phylloquinone), 974.655 powdered sucrose. [3]In the experimental diets with Cu-NPs the MX was deprived of $CuCO_3$ and the CuNPs preparation was added as an emulsion along with dietary rapeseed oil. [4]Maize starch preparation: crude protein 0.6%, crude fat 0.9%, ash 0.2%, total dietary fiber 0%, and water 8.8%.

carried out on a SGE BP21capillary column (30 m × 0.53 mm, Cole-Parmer, Vernon Hills, IL, USA) connected to the Shimadzu GC-2010 chromatograph with a flame ionization detector (Kyoto, Japan). Initial column temperature was 85°C and it was finally raised to 180°C at the rate of 8°C/min. Temperatures of the detector and the injector were maintained at 180°C and 85°C, respectively. Identification of individual SCFA in the samples was performed comparing the retention times of their peaks with those of standards, including acetic, propionic, butyric, *iso*-butyric, *iso*-valeric, and valeric acids, which were purchased from Sigma-Aldrich (St. Louis, MO, USA). Quantitative evaluation was performed based on the generated standard curves. Content of SCFA in fecal digesta was expressed in μmol/g.

The appropriate *p*-nitrophenol glycosides were used as substrates to determine the α-glucosidase, β-glucosidase, β-glucuronidase, and α-arabinofuranosidase activities in fecal digesta. These were *p*-nitrophenyl-α-D-glucopyranoside, *p*-nitrophenyl-β-D-glucopyranoside, *p*-nitrophenyl-β-D-glucuronide, and *p*-nitrophenyl-α-L-arabinofuranoside, respectively. *p*-Nitrophenol released from the substrates was quantified by measuring the absorbance of the reaction mixture at 400 nm. The enzymatic activity was expressed as μmol *p*-nitrophenol released *per* h *per* g of feces. The total enzymatic activity was assessed after bacterial cell lysis of fecal contents by homogenization with glass beads (diameter of 212–300 μm) in ice using the FastPrep®-24 system (MP Biomedicals, St. Ana, CA, US). Fecal digesta samples were not homogenized for extracellular enzymatic activity determination. Values of the intracellular enzyme activity were calculated based on the difference.

Statistical analysis

The data were subjected to two-way analysis of variance (ANOVA) and Student's *t*-test. A single experimental group (CN, PN, JN, SN) was compared with the control C group using the *t*-test. Similarly, the CNH, PNH, JNH, SNH groups were compared with the aid of the *t*-test with the control CH group. Two-way ANOVA (all groups treated with copper nanoparticles: CN, CNH, PN, PNH, JN, JNH, SN, SNH) was applied to assess the effects of two main factors: D – the dose of added Cu-NP (L, 6.5 mg/kg and H, 13 mg/kg) and F – dietary fiber type (cellulose, pectin, inulin and psyllium) as well as the D×F interaction. The Duncan's multiple range test was used to assess means when ANOVA revealed significant treatment effects. Before performing any statistical analysis, the data were examined for normality of distribution. Differences with $p<0.05$ were considered significant (Statistica 12.0; StatSoft Corp., Kraków, Poland).

RESULTS AND DISCUSSION

A number of *in vivo* studies have demonstrated an important role of the content of standard dietary sources of copper in modulating the large gut microbiota profile [Cheng *et al*., 2020; Zhang *et al*., 2019], and even a stronger effect of the dietary inclusion

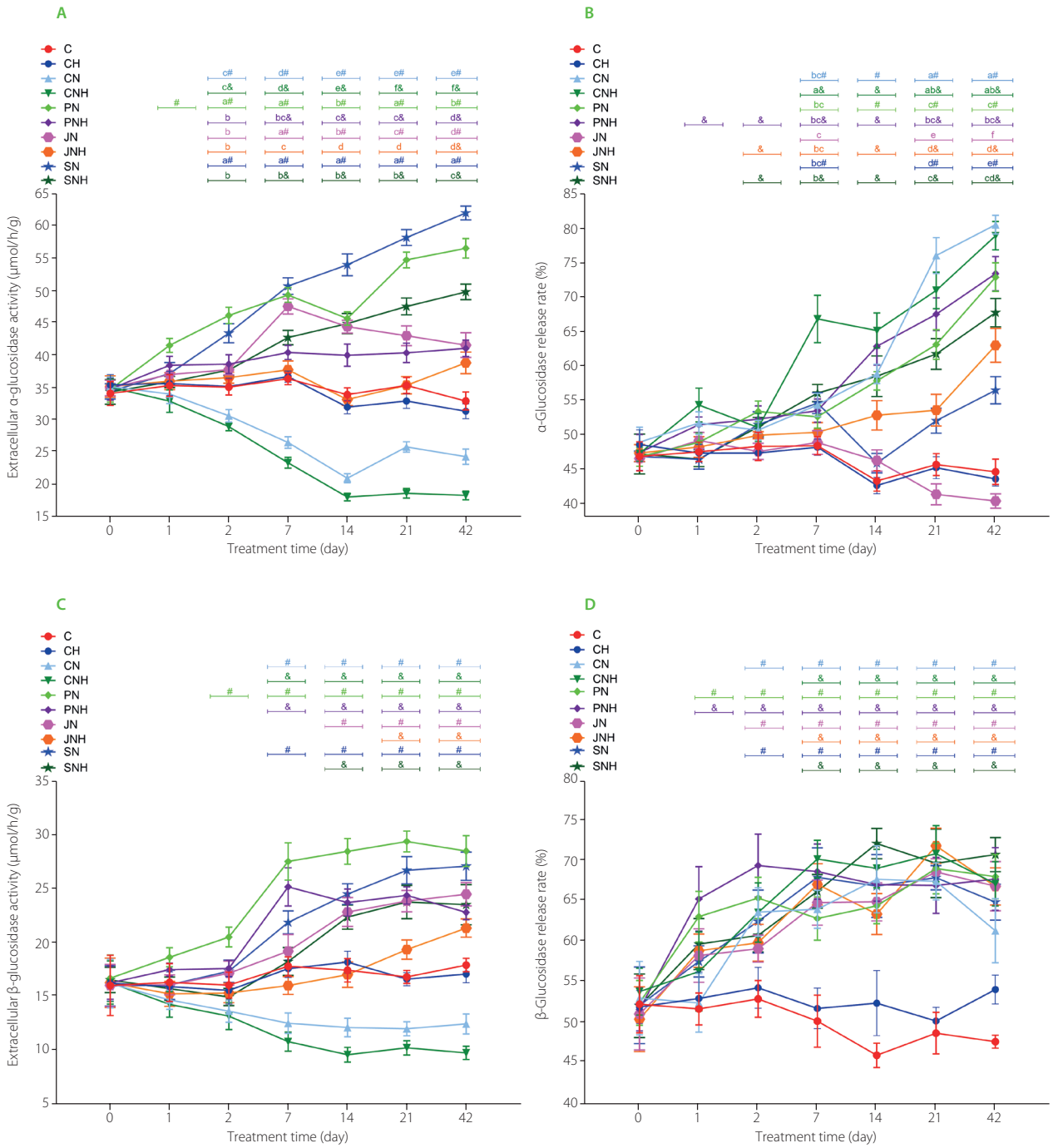

Figure 1. Extracellular microbial activity of α-glucosidase (**A**) and β-glucosidase (**C**) in the feces of rats during the feeding period as well as the release rate of α-glucosidase (**B**) and β-glucosidase (**D**).

The dietary treatments: groups C and CH, fed a control diet with standard and enhanced Cu content from $CuCO_3$ (6.5 and 13 mg/kg, respectively) and 8% cellulose; groups CN and CNH, fed diets with Cu-nanoparticles (Cu-NP) content of 6.5 and 13 mg/kg, respectively, and 8% cellulose; groups PN and PNH, fed diets with Cu-NP content of 6.5 and 13 mg/kg, respectively, 2% cellulose and 6% pectin; groups JN and JNH, fed diets with Cu-NP content of 6.5 and 13 mg/kg, respectively, 2% cellulose and 6% inulin; groups SN and SNH, fed diets with Cu-NP content of 6.5 and 13 mg/kg, respectively, 2% cellulose and 6% psyllium. Significant differences ($p<0.05$) between groups for an individual treatment time are marked with different letters (a–e) shown above the graph (the color of the points on the curve corresponds to the color of the letters). They are indicated only in the case of a significant interaction D×F ($p<0.05$). Significant differences between each group fed diet with Cu-NP content of 6.5 mg/kg (CN, PN, JN, SN) and the control C are indicated by # (*t*-test, $p<0.05$). Significant differences between each group fed diet with Cu-NP content of 13 mg/kg (CNH, PNH, JNH, SNH) and the control CH are indicated by & (*t*-test, $p<0.05$).

of copper nanoparticles on the composition and activity of the intestinal microbial community [Cholewińska *et al*., 2018; Lai *et al*., 2022]. Bacteriological screenings (for example, identifying specific bacterial taxa) are important for defining the gut environment, but they are restricted in their usefulness to studies of organism metabolism, nutrition, and health condition [Bankier *et al*., 2018; Utembe *et al*., 2022]. An alternative approach is to use biochemical assays to assess the functional activity of the entire microbiome. Their findings could help understand the contribution of the community of microbes in gut metabolism.

Previous research conducted by our team endeavored to assess the amount and composition of the microbial digestion end products (ammonia, SCFAs) along with the activity of particular bacterial enzymes in the large intestine digesta, in the latter case, instead of the bacterial count [Gugołek *et al*., 2021].

The two-way ANOVA showed that, irrespective of Cu-NP dietary application, the functional fiber (pectin, inulin, psyllium) addition to a diet enhanced the extracellular activity of fecal bacterial α-glucosidase on day 1 as compared to the cellulose treatment (main fiber effect in the two-way ANOVA; **Figure 1A**). The D×F interaction indicated the highest extracellular activity of that enzyme on day 2 in groups PN and SN while on day 7 – in groups PN, JN, and SN. On the next subsequent days 14, 21, 42, the highest extracellular activity of fecal α-glucosidase was determined in the rats fed a diet with psyllium and a lower one when feeding animal a diet with Cu nanoparticles at 6.5 mg/kg diet. During all days analyzed between day 2 and 42, the lowest extracellular activity was found in the CN and CNH groups, with the reduction in activity on days 21 and 42 being most pronounced in the latter group ($p<0.05$ *vs*. all other groups). In the aforementioned time interval (days 2–42), the addition of the higher dose of nanoparticles to the diet resulted in suppressed activity in the functional fibre-fed groups. The exception were the groups fed with inulin (JN and JNH) where extracellular activities of α-glucosidase in the feces were similar on day 2 and day 42. On days 2, 7, 14, 21, and 42, the *t*-test showed significantly lower activity of fecal extracellular α-glucosidase in the Cu-NP groups fed diets containing cellulose as compared to their $CuCO_3$ control counterparts (CN *vs*. C and CNH *vs*. CH). In the case of diets containing functional fibers, the *t*-test showed an increase in this activity regardless of nanoparticle dose compared to control cellulose diets without copper nanoparticles. The exception was the JNH group, whose feces showed higher extracellular α-glucosidase activity compared to the CH group only in the last measurement, *i.e.*, on day 42. Regardless of fiber type, the dietary addition of the higher Cu-NP dose significantly diminished the intracellular activity of bacterial α-glucosidase in the rat feces on days 1, 2, and 7 (**Table S1** in Supplementary Materials). Two-way ANOVA showed that all three functional fibers enhanced that activity on those days as compared to cellulose, irrespective of Cu-NP dose. The significant D×F interaction noted on days 14, 21, and 42 revealed the highest intracellular activity in the JN and SN groups ($p<0.05$), and the lowest one – in the CN and CNH groups. During all measurement days (period 1–42), the CN and CNH groups showed lower intracellular activity of bacterial fecal α-glucosidase compared to the C and CH groups, respectively (*t*-test). On days 14, 21, and 42, all the fiber-fed groups showed significantly suppressed intracellular activity of bacterial α-glucosidase in the feces as compared to the respective control groups C or CH. The significant effects ($p<0.05$) of both fiber type and Cu-NP content in diets on the total fecal α-glucosidase activity on days 1 and 2 were shown by two-way ANOVA (**Table S2** in Supplementary Materials). Irrespective of fiber type, a lower total α-glucosidase activity was found in the treatments with the higher dietary dose of Cu-NP. A significant D×F interaction revealed the highest total α-glucosidase activity in the feces of PN, JN, and SN rats on day 7 ($p<0.05$). On the next subsequent days 14, 21, 42, the aforementioned activity was the highest in groups JN and SN. The CN and CNH feces were characterized by significantly lower total activity of bacterial α-glucosidase on days from 2 to 42 as compared to their respective controls (C and CH, respectively; *t*-test). On those days (2, 7, 14, 21, 42), the feces of rats fed diets with pectin, inulin, psyllium and with the low Cu-NP dose were characterized by significantly enhanced total activity of bacterial α-glucosidase in comparison to the C control (*t*-test). The two-way ANOVA showed that, irrespective of Cu-NP dose, the treatments with inulin and psyllium caused a significant decrease in the percentage of fecal microbial α-glucosidase release rate on day 1 ($p<0.05$ *vs*. cellulose treatment; **Figure 1B**). On day 14, the release rate of α-glucosidase was significantly lower in the inulin and psyllium treatments than in the cellulose and pectin ones. Regardless of the fiber type, the high Cu-NP dose enhanced the α-glucosidase release rate on day 14 *vs*. the low nanoparticle dose ($p<0.05$). A significant D×F interaction noted on days 21 and 42 indicated the highest release rate of that enzyme into the fecal environment in the CN group and the lowest one in the JN animals. On day 7, there was a comparable situation, with the highest release rate being noted in the CNH rat feces.

The two-way ANOVA indicated that, regardless the Cu-NP addition, the highest activity of bacterial extracellular β-glucosidase was recorded since day 1 till 42 in feces of the rats fed the diet with pectin (**Figure 1C**). Irrespective of the fiber type, the effect of Cu-NP content in diet on extracellular β-glucosidase activity on days 2-42 was significant ($p<0.05$); the high Cu-NP content caused a lower enzyme activity. As compared *via* the *t*-test with their respective control groups, the CN and CHN feces were characterized by significantly diminished extracellular β-glucosidase activity on days 7, 14, 21, and 42. All pectin, inulin and psyllium groups showed higher extracellular β-glucosidase activity on days 21 and 42 as compared to their respective controls (*t*-test). Regardless of the Cu-NP addition, the "functional fiber" treatments enhanced the intracellular activity of fecal bacterial β-glucosidase compared to the cellulose treatment from the second measuring day ($p<0.05$) except day 2 for the pectin treatment (**Table S3** in Supplementary Materials). This enzyme activity was decreased by the high Cu-NP dose *vs*. the low dose on days 7, 14, 21, and 42, irrespective of dietary fiber type. On day 2, the *t*-test showed suppressed intracellular activity of fecal bacterial β-glucosidase in the CN, CNH, and PNH groups ($p<0.05$ *vs*. respective controls C and CH). On the subsequent days, that activity in all groups fed diets with Cu-NP was diminished *vs*. respective controls fed diets with $CuCO_3$ (*t*-test). From day 2, all "functional fiber" treatments significantly increased ($p<0.05$) the total activity of fecal β-glucosidase compared to cellulose treatment, irrespective of Cu-NP addition (**Table S4** in Supplementary Materials). Regardless of the fiber type, the higher Cu-NP content in diet caused a significantly lower total β-glucosidase activity in the rat feces on all measuring days, except day 0 and 1 ($p<0.05$). The two-way ANOVA showed that, regardless

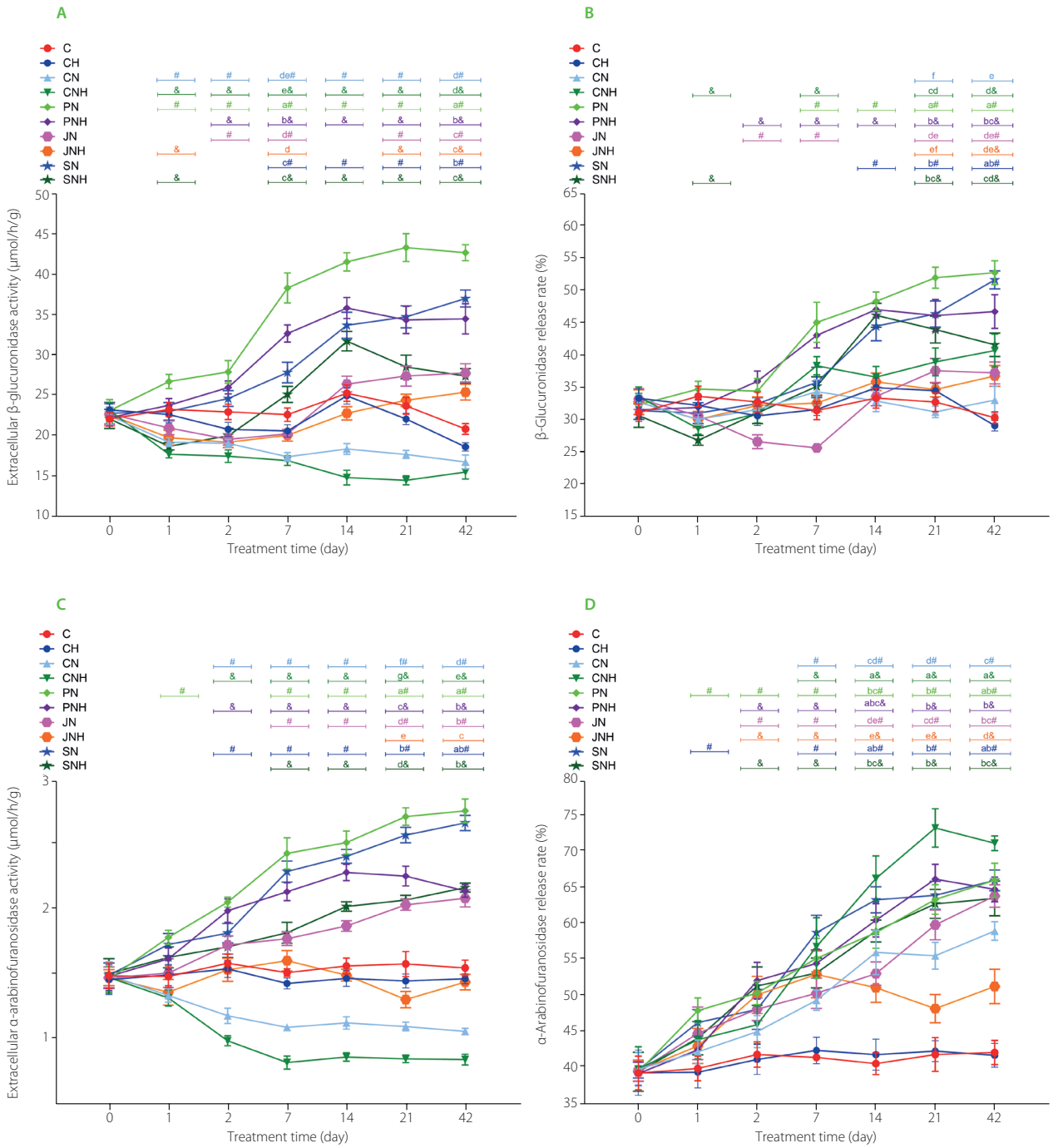

Figure 2. Extracellular microbial activity of β-glucuronidase (**A**) and α-arabinofuranosidase (**C**) in the feces of rats during the feeding period as well as the release rate of β-glucuronidase (**B**) and α-arabinofuranosidase (**D**).
The dietary treatments: groups C and CH, fed a control diet with standard and enhanced Cu content from $CuCO_3$ (6.5 and 13 mg/kg, respectively) and 8% cellulose; groups CN and CNH, fed diets with Cu-nanoparticles (Cu-NP) contnet of 6.5 and 13 mg/kg, respectively, and 8% cellulose; groups PN and PNH, fed diets with Cu-NP content of 6.5 and 13 mg/kg, respectively, 2% cellulose and 6% pectin; groups JN and JNH, fed diets with Cu-NP content of 6.5 and 13 mg/kg, respectively, 2% cellulose and 6% inulin; groups SN and SNH, fed diets with Cu-NP content of 6.5 and 13 mg/kg, respectively, 2% cellulose and 6% psyllium. Significant differences ($p<0.05$) between groups for an individual treatment time are marked with different letters (a–e) shown above the graph (the color of the points on the curve corresponds to the color of the letters). They are indicated only in the case of a significant interaction D×F ($p<0.05$). Significant differences between each group fed diet with Cu-NP content of 6.5 mg/kg (CN, PN, JN, SN) and the control C are indicated by # (*t*-test, $p<0.05$). Significant differences between each group fed diet with Cu-NP content of 13 mg/kg (CNH, PNH, JNH, SNH) and the control CH are indicated by & (*t*-test, $p<0.05$).

of the dietary Cu-NP dose, the addition of pectin to a diet containing copper nanoparticles caused a significant increase in the fecal microbial β-glucosidase release rate on day 1 ($p<0.05$ vs. cellulose; **Figure 1D**). The *t*-test showed that from day 7 all feces of the rats from groups fed diets with Cu-NP showed an increased percentage of β-glucosidase release rate in comparison to the respective controls C or CH ($p<0.05$).

Regardless the fiber type, the higher content of Cu-NP in diets resulted in diminished extracellular activity of bacterial β-glucuronidase on days 1, 2, 14, and 21 (**Figure 2A**). On those

days, the pectin dietary addition caused the highest enzyme activity, irrespective of Cu-NP dose ($p<0.05$). A significant D×F interaction was noted on days 7 and 42, and the nature of that interaction revealed the highest extracellular β-glucuronidase in the PN feces ($p<0.05$ vs. all other groups). The *t*-test showed that from day 1 till the end of experiment the CN and CNH feces were characterized with a significantly lower extracellular activity of bacterial β-glucuronidase in comparison to their respective controls C and CH ($p<0.05$). The dietary treatments with pectin, inulin and psyllium caused a significant increase in intracellular fecal activity of β-glucuronidase *vs*. cellulose on day 1, regardless of the Cu-NPs dose (**Table S5** in Supplementary Materials). On the subsequent measuring days, a significant D×F interaction was noted and its nature indicated the highest intracellular β-glucuronidase activity upon rat feeding a diet with inulin and the lower dose of copper nanoparticles. The *t*-test showed that CN and CNH groups had significantly lowered activity of intracellular β-glucuronidase from day 2 till the end of experiment ($p<0.05$ *vs*. C and CH, respectively). On days 14, 21, 42, such a situation was also observed in the pectin and psyllium groups (except PNH *vs*. CH on day 21). All treatments with "functional fiber" enhanced the total activity of fecal bacterial β-glucuronidase on day 1 *vs*. cellulose, irrespective of Cu-NP dose (**Table S6** in Supplementary Materials). Regardless of the fiber type, the high Cu-NP dose in a diet decreased that activity *vs*. L dose ($p<0.05$). A significant D×F interaction noted on measuring days 2, 7, 14, 21, 42 revealed the highest and the lowest total activity of fecal bacterial β-glucuronidase in the PN and CNH groups, respectively. Generally, the *t*-test showed that total β-glucuronidase activity in the feces of both pectin groups (PN and PNH) was significantly higher than in C and CH controls on all measuring days. The percentage of β-glucuronidase release rate was significantly decreased by the higher Cu-NP dose, irrespective of the fiber type ($p<0.05$ *vs*. low dose; **Figure 2B**). The two-way ANOVA showed that, regardless of Cu-NP dose, the fiber pectin treatment caused the highest fecal β-glucuronidase release rate on days 1, 2, and 7 ($p<0.05$ other fibers). On day 14, the pectin and psyllium treatments increased the β-glucuronidase release rate in comparison to the cellulose and inulin treatments. A significant D×F interaction recorded on days 21 and 42 showed the highest and the lowest β-glucuronidase release rate in the PN and CN groups, respectively. The *t*-test showed that on day 42 all groups, except the CN, showed an increased percentage of β-glucuronidase release rate concerning their controls without Cu-NP. The two-way ANOVA showed that, regardless of the Cu-NP dose, the treatments with pectin and psyllium significantly enhanced the extracellular activity of fecal bacterial α-arabinofuranosidase on day 1 as compared to the cellulose and inulin treatments ($p<0.05$; **Figure 2C**). On the subsequent measuring days, *i.e.*, days 2, 7, and 14, the highest and the lowest activity of this enzyme were noted in the pectin and cellulose treatments, respectively. On those days, the higher Cu-NP dose increased extracellular activity of α-arabinofuranosidase in the feces *vs*. the low nanoparticle dose, irrespective of dietary fiber type. On days 21 and 42, a significant D×F interaction revealed that the PN feces showed the highest extracellular activity of bacterial α-arabinofuranosidase and that the CNH feces showed the lowest ones. The *t*-test showed that on day 7 and subsequent measuring days, the CN and CNH diets caused a decrease, while remaining dietary treatments (except JN) caused an increase in fecal bacterial α-arabinofuranosidase activity in comparison to the respective controls without nanoparticle application, *i.e.*, C and CH ($p<0.05$). The two-way ANOVA showed that, regardless of the Cu-NP dose, the pectin and psyllium dietary addition increased intracellular α-arabinofuranosidase activity on day 1 as compared to the cellulose treatments ($p<0.05$; **Table S7** in Supplementary Materials). On days 2, 7, and 14, the pectin, inulin and psyllium treatments excelled the control cellulose one in this respect. A significant D×F interaction revealed the lowest activity of fecal intracellular α-arabinofuranosidase in the CNH rats on days 21 and 42 ($p<0.05$ *vs*. all remaining groups). As indicated **Table S8** in Supplementary Materials, regardless of the Cu-NP dose, the total activity of fecal bacterial α-arabinofuranosidase was significantly enhanced by pectin and psyllium treatments on day 1 ($p<0.05$ *vs*. cellulose and inulin), while on days 2, 7, 14, 21 all three functional fiber treatments excelled the cellulose one in this respect ($p<0.05$). A D×F interaction noted on day 42 showed the lowest and the highest total α-arabinofuranosidase activity in the CNH and PN, SN groups, respectively (in both cases $p<0.05$ *vs*. all other groups). The *t*-test revealed that on all measuring days, the CN, CNH, and JNH groups showed suppressed total α-arabinofuranosidase activity as compared to respective C and CH controls. A significant D×F interaction noted on days 14, 21, 42 showed the highest and the lowest release rate of bacterial fecal α-arabinofuranosidase in the CNH and JNH groups, respectively (**Figure 2D**). Interestingly, on those days, the CN group showed significantly lower release rate of that enzyme as compared to the CNH one. In the "functional" fiber counterparts, such a situation was noted on days 21 and 42 between groups JN and JNH ($p<0.05$). The *t*-test revealed that from day 7 till the end of the experiment all groups fed diets with copper nanoparticles were characterized with significantly enhanced fecal α-arabinofuranosidase release rate *vs*. respective controls, i.*e.*, C and CH ($p<0.05$).

The fecal acetic acid content on day 1 was significantly diminished by the higher Cu-NP dose as compared to the low Cu-NP dose, regardless of the fiber type (**Figure 3A**). On the subsequent measuring days, a significant D×F interaction was noted with regard to fecal acetic acid. On days 2, 7, 14, and 42, the lowest acetic acid content was determined in the CNH rat feces, while on Day 21 – in the CN and CNH rat feces ($p<0.05$ *vs*. all remaining groups). The highest acetic acid content in the feces was noted on day 2 in the feces of the PN and JN rats, on day 7 – in those of JN rats, on day 14 – in those of PN, JN and JNH rats, and on days 21 and 42 – in those of the PN animals (in all cases $p<0.05$ *vs*. other groups). The *t*-test revealed decreased acetic acid content on days 1 and 2 in all experimental groups, except JN as compared to respective C and CH controls ($p<0.05$). On the subsequent measuring days, such a decrease was noted in the CN, CNH, PNH, SN, and SNH groups ($p<0.05$ *vs*. respective

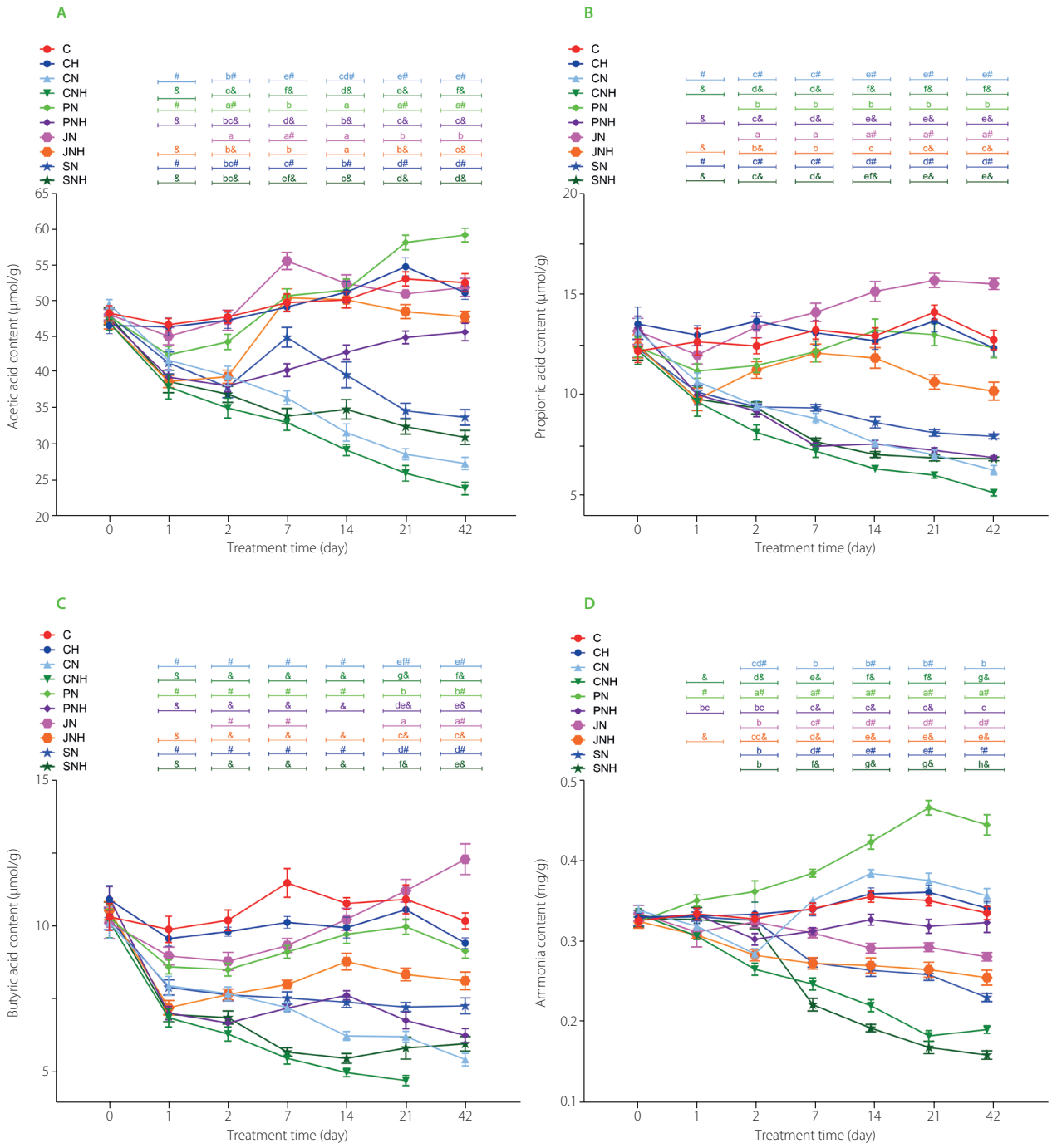

Figure 3. The content of acetic acid (**A**), propionic acid (**B**), butyric acid (**C**) and ammonia (**D**) in the feces of rats during the feeding period.
The dietary treatments: groups C and CH, fed a control diet with standard and enhanced Cu content from $CuCO_3$ (6.5 and 13 mg/kg, respectively) and 8% cellulose; groups CN and CNH, fed diets with Cu-nanoparticles (Cu-NP) content of 6.5 and 13 mg/kg, respectively, and 8% cellulose; groups PN and PNH, fed diets with Cu-NP content of 6.5 and 13 mg/kg, respectively, 2% cellulose and 6% pectin; groups JN and JNH, fed diets with Cu-NP content of 6.5 and 13 mg/kg, respectively, 2% cellulose and 6% inulin; groups SN and SNH, fed diets with Cu-NP content of 6.5 and 13 mg/kg from, respectively, 2% cellulose and 6% psyllium. Significant differences ($p<0.05$) between groups for an individual treatment time are marked with different letters (a–e) shown above the graph (the color of the points on the curve corresponds to the color of the letters). They are indicated only in the case of a significant interaction D×F ($p<0.05$). Significant differences between each group fed diet with Cu-NP content of 6.5 mg/kg (CN, PN, JN, SN) and the control C are indicated by # (*t*-test, $p<0.05$). Significant differences between each group fed diet with Cu-NP content of 13 mg/kg (CNH, PNH, JNH, SNH) and the control CH are indicated by & (*t*-test, $p<0.05$).

C or CH). On day 1, the fecal concentration of propionic acid was diminished by the higher Cu-NP dose, irrespective of fiber type ($p<0.05$ *vs.* L dose; **Figure 3B**). A D×F interaction showed that from day 2 till the end of the experiment the highest and the lowest propionic acid fecal content followed the dietary treatments with JN and CNH diets, respectively (in both cases $p<0.05$ *vs.* all other groups). The *t*-test revealed that the JN feces were the only ones attributed with significantly enhanced propionic acid fecal content *vs.* C group on days 14, 21, and 42 ($p<0.05$). The decreased fecal butyric acid content followed the higher Cu-NP dietary dose treatment *vs.* the low dose on days 1, 2, 7, and 14, regardless of the fiber type ($p<0.05$; **Figure 3C**). On day 2,

the inulin treatment excelled the other fiber treatments with regard to butyric acid content, irrespective of Cu-NP dose. On day 7, such an increase in butyric acid content was noted in the pectin and inulin treatments as compared to the cellulose and psyllium ones. On day 14, the lowest and the highest butyric acid fecal content were determined in the cellulose and inulin treatments, respectively (in both cases $p<0.05$ *vs*. remaining fiber treatments). A significant D×F interaction noted on days 21 and 42 showed the lowest and the highest butyric acid content in the feces in the CNH and JN groups, respectively. The *t*-test revealed that all groups with dietary addition of copper nanoparticles had lowered butyric acid content in the feces *vs*. respective C and CH controls, except group JN on days 1, 14, 21, and 42. Additionally, on day 42, the JN feces were characterized with enhanced butyric acid content *vs*. group C (*t*-test).

An enhanced fecal content of putrefactive SCFA followed the pectin dietary addition on days 2 and 7, irrespective of Cu-NP dose ($p<0.05$ *vs*. remaining fiber treatments; **Table S9** in Supplementary Materials). On days 21 and 42, the CNH and PN rats had the lowest and the highest putrefactive SCFA content in the feces, respectively. The *t*-test showed that all experimental Cu-NP groups had lowered fecal putrefactive SCFA as compared to their respective C or CH controls from day 2, except the PN group. The two-way ANOVA showed that on day 1, the higher Cu-NP dose caused a decrease in the total fecal SCFA content, regardless of the fiber type ($p<0.05$ *vs*. L dose; **Table S10** in Supplementary Materials). From day 2, a significant D×F interaction was noted for fecal total SCFA in all subsequent measuring days. The nature of that interaction indicated the lowest total SCFA level in the CNH group on all measuring days (on day 7 in the SNH group as well) and the highest total SCFA content on days 2 and 7 in the JN feces, on day 14 – in the JN and PN feces, and on days 21 and 42 – in the PN feces (in all cases $p<0.05$ *vs*. other groups).

As in our previous experiments with the addition of various nanoparticles to the diet [Cholewińska *et al*., 2018], dietary Cu-NP used in the present experiment suppressed the activity of most of the analyzed bacterial enzymes in the feces and diminished the amounts of SCFAs produced by the microbiota. As for the effect of the doubled Cu-NP dose, lower levels of enzyme activity and amounts of bacterial metabolites were indeed found, although this was not a doubly suppressive effect. One of the most important results observed was the limiting effect of Cu-NP on extracellular enzymatic activity and greater release of bacterial enzymes into the environment from within the bacterial cells upon the influence of nanoparticles. The extracellular activity of bacterial enzymes has direct implications for the rate at which nutrients and non-nutrients undergo microbial digestion in the large intestine. Extracellular enzyme activity is influenced by the type and counts of bacterial species present in the digesta and by the rate of enzyme secretion by bacterial cells. With regard to the presented hypothesis, a higher release rate of glycoside hydrolases could be an important adaptive mechanism of intestinal bacteria which enables them to acquire additional energy from the large intestine through fermentation in the situation when Cu-NP seem to reduce bacterial activity and probably bacterial count. Doubling the dose of copper nanoparticles added to the diet increased the percentage of enzymes released, although in some cases the increase was not statistically significant, such as for α-glucosidase and β-glucosidase in the last two measurements on days 21 and 42. According to some reports, nanoparticles may reduce the amount of microorganisms by entering bacteria through nanometric holes and disrupting internal organellas [Azam *et al*., 2012]. Mahapatra *et al*. [2008] showed diminished effect of nano-CuO on *Klebsiella, Salmonella* and *Shigealla* count *via* damaging intracellular enzymes. Lai *et al*. [2022] concluded their research that among a broad range of Cu-NP's properties, their capability for microbial growth inhibition, membrane disruption, DNA damage, and enhancement in oxidative stress in bacteria are of paramount importance when intestinal environment is considered. In the present experiment, the release rate of intracellular enzymes into fecal milieu was not totally enhanced under the higher tested copper nanoparticle dose, indicating selective inhibition of enzymatic activity rather than disruption of the bacterial cell membrane. Copper attached to nanoparticles made from chitosan removed gastrointestinal pathogens such as *Salmonella* species, but left *Lactobacilli* and other beneficial commensals unharmed, according to Han *et al*. [2010] study.

In the present experiment, it was hypothesized that the dietary inclusion of fiber with prebiotic (inulin), viscous (pectin) or bulking (psyllium) properties would alleviate adverse effects of copper nanoparticles on intestinal microbial activity, the latter effect observed in our previous experiments with diets containing cellulose [Cholewińska *et al*., 2018]. The scientific literature demonstrates that viscous dietary fiber effectively delays and reduces the absorption of nutrients in the intestine [Deehan *et al*., 2022]. This, of course, causes these nutrients to be transported to the large intestine in greater quantities, and therein used by the microbiota for growth and metabolite production. Żary-Sikorska and co-authors [2016] confirmed in their *in vivo* study that, compared to prebiotic fructans and less processed fiber-polyphenol preparations, pectin had the greatest viscosity-enhancing properties in the small intestine and was fermented most rapidly, sometimes too vigorously, in the large intestine. At this point, there is little need to elaborate on the well-studied theme of the prebiotic positive effect of inulin-type fibers on the gut microbiota in both a taxa-dependent manner and its metabolic activity [Juśkiewicz *et al*., 2007]. An interesting case, and therefore not missed in this experiment, is the intestinal behavior of psyllium. Psyllium is a viscous, gel-forming fiber, claimed to ferment at a slow rate at the entire length of large gut, contributing more fecal mass due to the bulking ability [Harris et al., 2023; McRorie Jr., 2015]. This raises the question of whether these effects of various fiber on the viscosity of the intestinal contents, the rate of passage and the formation of SCFAs has, and what, implications for the consequences of the presence of nanoparticles in the diet. The recent work of our team [Cholewińska *et al*., 2023] showed that dietary pectin, inulin and psyllium diminished the absorption of copper nanoparticles and protected the small intestine by strengthening the intestinal barrier *via* DNA repair

mechanisms and inflammatory processes inhibition. Thus, it must be assumed that, in our experiment, a significant amount of copper nanoparticles had reached the large intestine of the rat together with the fiber and then appeared in the feces, modifying the enzymatic and metabolic activity of the microbiota.

It is interesting to observe whether the rapid fermentation of pectin in the rat cecum followed by its passage through the colon would leave "fiber fuel" for the fecal bacteria to produce enzymes and metabolites in the form of SCFAs. Our study results and literature data indicate that fructans, such as inulin, fructooligosaccharide or oligofructose, are well utilized by the large intestinal microbiota [Makki *et al*., 2018]; hence, we were intrigued before performing the analyses as to whether the enzymatic activity in the feces would be significant or meagre. In contrast, it was almost certain that psyllium residues would appear in the feces, with the reservation that this type of fiber is poorly fermented by bacteria. The results indicated that the enzymatic activity of the fecal microbiota increased after the addition of each of the three types of functional fiber. The fastest and strongest increase in enzyme activity was found as early as on the first measurement day for pectin. Interestingly, the increase in extracellular activity of the analyzed enzymes was also evident with the other fibers. Even more surprising was that, in some cases, the addition of psyllium was not inferior to the effects of pectin; this was the case, *e.g.*, on day 1 for extracellular and total α-arabinofuranosidase, total α-glucosidase, and total β-glucuronidase activities. Such a result may indicate that the fermentation processes of psyllium already proceeding in the cecum and colon have compromised the chemical structure of this fiber or that the gel structure produced by psyllium effectively "arrested" copper nanoparticles within it. But, this was not fully confirmed by the results obtained for SCFA, as the amounts of acids produced, including acetic, butyric and propionic acids, were significantly lower than in the pectin and inulin treatments. On the other hand, the amount of SCFA produced by fecal microbiota from the psyllium groups excelled the SCFA analyzed in the CN and CNH feces. Therefore, it can be concluded that psyllium is not as inert for fermentation processes in the gut as the control fiber cellulose is. For instance, the final effect of psyllium noted on day 42 on the total activity of a marker enzyme β-glucuronidase specific to the adverse microbiota was more similar to that of inulin than pectin. High activity of β-glucuronidase is associated with pathogenic bacterial species rather than the beneficial ones [Lee *et al*., 2022]. The activity of β-glucuronidase is not specific only for *E. coli*, and it is also found in *Shigella* and *Yersinia* strains, as well as to some extent in *Flavobacterium* spp., *Bacteroides* spp., *Staphylococcus* spp., *Streptococcus* spp., and *Clostridium* spp. [Gao *et al*., 2022; Fiksdal & Tryland, 2008]. However, β-glucuronidase activity is intrinsic to more than 90% of *E. coli* strains, while almost all other coliform bacteria lack this activity [Poulouxi & Prodromidis, 2020]. In our previous *in vivo* experiments, we have shown some correlations between dietary fiber supplementation and the intensity of fermentation processes in the large intestine. In a study with rats administered a dietary grapefruit extract, inulin did not counteract clearly detrimental effects of the extract in the hindgut due to a high dose of grapefruit preparation containing not only flavonoids but also silicon dioxide and glycerol [Jurgoński *et al*., 2012]. This can, in some respects, be related to the effect of the high Cu-NP dose in the experiment presented here, *i.e.*, a strong reduction in enzymatic activity and the amount of SCFAs produced despite the dietary content of functional fiber, albeit not as drastic as in the CNH group (cellulose fiber, high dose of nanoparticles). In another experiment [Juśkiewicz *et al*., 2007], it has been shown that the typical effect of inulin in the rat cecum is only observed when fiber level in the diet was relatively high. Furthermore, the acquired data demonstrated rapid reversibility of cecal fermentation intensity to that of the control cellulose group by removing inulin from the diet or lowering supplementation. Thus, it is reasonable to assume that, in the present experiment, the adverse effects of copper nanoparticles on the activity of the fecal microbiota would have been evident within a short time after the withdrawal of pectin, inulin and psyllium from the diet.

On day 1, the fecal ammonia content was significantly enhanced by the pectin treatment *vs*. cellulose and inulin treatment, regardless of Cu-NP dose (**Figure 3D**). A significant D×F interaction showed the highest fecal ammonia content in the PN group on all measuring days from day 2 ($p<0.05$ *vs*. all other groups). The lowest ammonia level on day 2 was determined in the CNH rat feces, while on the remaining subsequent days – in the SNH group. The *t*-test showed a significant increase in fecal ammonia in the PN rats on all measuring days *vs*. control C. The two-way ANOVA revealed that, irrespective of dietary Cu-NP dose, the inulin treatment decreased significantly fecal pH on day 1 as compared to the cellulose and psyllium treatments (**Table S11** in Supplementary Materials). On the subsequent measuring days, such a decrease in fecal pH *vs*. cellulose treatment was noted on day 2 in pectin and inulin, on days 7 and 14 – in pectin, inulin, and psyllium, and on days 21 and 42 – in pectin and psyllium treatments. The *t*-test revealed that on day 2, fecal pH was decreased in the JN *vs*. C and in JNH *vs*. CH, while on day 7 – in JN, JNH, and PN groups vs. respective controls. On day 14, such a decrease was observed on fecal pH in the SN rats ($p<0.05$ *vs*. C; *t*-test).

A very interesting result was the content of ammonia in the feces of rats fed psyllium diets. The group of rats receiving the higher tested dose of nanoparticles along with the cellulose diet had very low levels of ammonia in the feces, and the addition of psyllium further exacerbated this decrease. It is clear that the copper nanoparticles interfered with the normal processes of digestion and absorption of proteins in the small intestine; hence, their large amount ended up in the large intestine, then in the feces, where protein fermentation is a putrefactive process. The abundance of protein available to microbial communities is one of the causes of excessive cecal ammonia generation [Griffin & Bradshaw, 2019]. But fermentation processes involve the gut microbiota, and its activity in this regard was also reduced by the addition of Cu-NP. As a result, the lower level of nanoparticles affected the observed levels of ammonia and putrefactive SCFA

to a much lesser extent than the higher dose of Cu-NP. And at this point, the effect of psyllium on ammonia and putrefactive SCFA levels should be regarded as positive, since psyllium proactively reduced the levels of putrefactive substances without significantly inhibiting the enzymatic activity of the microbiota. It has been found that excessive intestinal ammonia release can damage epithelial cells by altering their morphology and disrupting their metabolism [Bell *et al*., 2023]. Undigested in the upper intestine amino acids, such as valine, leucine and isoleucine, may undergo the anaerobic microbial breakdown and be converted into compounds with not only strong odor but unhealthy properties as well, such as iso-butyric, iso-valeric and valeric acids, as well as cadaverine, putrescine, other amines, and hydrogen sulfide and methyl mercaptan [Markowiak-Kopeć & Śliżewska, 2020]. Excessive accumulation of isobutyric, valeric and isovaleric acids, *i.e.*, putrefactive SCFA, indicates malfunctioning fermentation and digestion processes [Badri *et al*., 2021].

CONCLUSIONS

The addition of copper nanoparticles to the diet resulted in a drastic and rapid reduction in the enzymatic activity of the microbiota in the rat feces after only the first day of feeding. This was related to both extracellular and intracellular activity. The percentage of enzyme release from the bacterial cell to the external environment in the feces was higher when nanoparticles were used in the diets, compared to control diets containing respective doses of calcium carbonate. Analyses showed that the double dose of Cu-NP had a stronger suppressive effect on bacterial enzyme activity compared to the lower dose. This was already evident after the first or second day of feeding, and this condition persisted until the end of the 42-day experiment. The addition of functional fiber to diets containing copper nanoparticles significantly increased bacterial enzyme activity compared to the diets with nanoparticles and control cellulose. The aforementioned effect was the strongest and most rapidly evident with pectin, while the effect of the addition of inulin or psyllium exceeded that of pectin only in some cases, *i.e.*, α-glucosidase activity. Inulin, a typical and established prebiotic, most favorably reduced the suppressive effect of nanoparticles in relation to the fecal content of butyric acid and propionic acid in rats. However, it should be noted that this beneficial effect of inulin on the content of individual SCFAs was only apparent at the lower Cu-NP dose. In the final phase of the experimental feeding, the positive effects of the addition of inulin to the diet with nanoparticles in relation to propionic and butyric acids were also evident compared to the control group fed a diet with cellulose but lacking Cu-NP. In the case of psyllium, its addition to the diet most strongly reduced fecal ammonia formation, high concentrations of which in the intestine can be detrimental to the health status of the colonic epithelium. To summarize in one sentence, the high potential of dietary fiber in the form of pectin, inulin or psyllium in mitigating the suppressive effect of copper nanoparticles on the enzymatic and metabolic activity of the intestinal microbiota should be recognized.

SUPPLEMENTARY MATERIALS

The following are available online at **https://journal.pan.olsztyn.pl/Dietary-Fiber-with-Functional-Properties-Counteracts-the-Thwarting-Effects-of-Copper,194694,0,2.html**; **Table S1.** Fecal microbial intracellular α-glucosidase activity (μmol/h/g) during the experimental feeding period in rats. **Table S2.** Fecal microbial total α-glucosidase activity (μmol/h/g) during the experimental feeding period in rats. **Table S3.** Fecal microbial intracellular β-glucosidase activity (μmol/h/g) during the experimental feeding period in rats. **Table S4.** Fecal microbial total β-glucosidase activity (μmol/h/g) during the experimental feeding period in rats. **Table S5.** Fecal microbial intracellular β-glucuronidase activity (μmol/h/g) during the experimental feeding period in rats. **Table S6.** Fecal microbial total β-glucuronidase activity (μmol/h/g) during the experimental feeding period in rats. **Table S7.** Fecal microbial intracellular α-arabinofuranosidase activity (μmol/h/g) during the experimental feeding period in rats. **Table S8**. Fecal microbial total α-arabinofuranosidase activity (μmol/h/g) during the experimental feeding period in rats. **Table S9.** Fecal content (μmol/g) of putrefactive short-chain fatty acids (*iso*-butyric+*iso*-valeric+valeric acids) during the experimental feeding period in rats. **Table S10.** Fecal content (μmol/g) of total short-chain fatty acids during the experimental feeding period in rats. **Table S11.** Fecal pH values during the experimental feeding period in rats. **Figure S1.** Experimental schema.

RESEARCH FUNDING

This work was financed from the National Science Centre, Grant No. 2021/41/B/NZ9/01104.

CONFLICT OF INTERESTS

Authors declare no conflict of interests.

ADDITIONAL INFORMATION

The experimental protocol was approved by the Local Ethics Committee for Animal Experiments (Approval No. 19/2021; Olsztyn, Poland).

ORCID IDs

Ł. Brzuzan **https://orcid.org/0000-0001-6877-4633**
E. Cholewińska **https://orcid.org/0000-0003-0437-4766**
B. Fotschki **https://orcid.org/0000-0002-9727-7481**
J. Fotschki **https://orcid.org/0000-0002-0116-0909**
J. Juśkiewicz **https://orcid.org/0000-0003-0068-5970**
A. Marzec **https://orcid.org/0000-0002-4074-1570**
K. Ognik **https://orcid.org/0000-0003-4393-4092**
A. Stępniowska **https://orcid.org/0000-0003-2424-8935**
E. Żary-Sikorska **https://orcid.org/0000-0001-8140-3861**

REFERENCES

1. Anreddy, R.N.R. (2018). Copper oxide nanoparticles induces oxidative stress and liver toxicity in rats following oral exposure. *Toxicology Reports*, *5*, 903-904. **https://doi.org/10.1016/j.toxrep.2018.08.022**
2. Azam, A., Ahmed, A.S., Oves, M., Khan M.S., Memic, A. (2012). Size-dependent antimicrobial properties of CuO nanoparticles against Gram-positive and -negative bacterial strains. *International Journal of Nanomedicine*, *7*, 3527-3535. **https://doi.org/10.2147/IJN.S29020**

3. Badri, D.V., Jackson, M.I., Jewell, D.E. (2021). Dietary protein and carbohydrate levels affect the gut microbiota and clinical assessment in healthy adult cats. *Journal of Nutrition*, *151*(12), 3637-3650. **https://doi.org/10.1093/jn/nxab308**
4. Bankier, C., Cheong, Y., Mahalingam, S., Edirisinghe, M., Ren, G., Cloutman-Green, E., Ciric, L. (2018). A comparison of methods to assess the antimicrobial activity of nanoparticle combinations on bacterial cells. *PLoS One*, *13*(2), art. no. e0192093. **https://doi.org/10.1371/journal.pone.0192093**
5. Baravkar, P.N., Sayyed, A.A., Rahane, C.S., Chate, G.P., Wavhale, R.D., Pratinidhi, S.A., Banerjee, S.S. (2021). Nanoparticle properties podulate their pffect on the puman plood punctions. *BioNanoScience*, *11*, 816-824. **https://doi.org/10.1007/s12668-021-00874-x**
6. Baye, K., Guyot, J.P., Mouquet-Rivier, C. (2017). The unresolved role of dietary fibers on mineral absorption. *Critical Reviews in Food Science and Nutrition*, *57*(5), 949-957, **https://doi.org/10.1080/10408398.2014.953030**
7. Bell, H.N., Huber, A.K., Singhal, R., Korimerla, N., Rebernick, R.J., Kumar, R., El-Derany, M.O., Sajjakulnukit, P., Das, N.K., Kerk, S.A., Solanki, S., James, J.G., Kim, D., Zhang, L., Chen, B., Mehra, R., Frankel, T.L., Győrffy, B., Fearon, E.R., Pasca di Magliano, M., Gonzalez, F.J., Banerjee, R., Wahl, D.R., Lyssiotis, C.A., Green, M., Shah, Y.M. (2023). Microenvironmental ammonia enhances T cell exhaustion in colorectal cancer. *Cell Metabolism*, *35*(1), 134-149.e6. **https://doi.org/10.1016/j.cmet.2022.11.013**
8. Cheng, S., Mao, H., Ruan, Y., Wu, C., Xu, Z., Hu, G., Guo, X., Zhang, C., Cao, H., Liu, P. (2020). Copper changes intestinal microbiota of the cecum and rectum in female mice by 16S rRNA gene sequencing. *Biological Trace Element Research*, *193*, 445-455. **https://doi.org/10.1007/s12011-019-01718-2**
9. Cholewińska, E., Marzec, A., Sołek, P., Fotschki, B., Listos, P., Ognik, K., Juśkiewicz, J. (2023). The effect of copper nanoparticles and a different source of dietary fibre in the diet on the integrity of the small intestine in the rat. *Nutrients*, *15*(7), art. no. 1588. **https://doi.org/10.3390/nu15071588**
10. Cholewińska, E., Ognik, K., Fotschki, B., Zduńczyk, Z., Juśkiewicz, J. (2018). Comparison of the effect of dietary copper nanoparticles and one copper(II) salt on the copper biodistribution and gastrointestinal and hepatic morphology and function in a rat model. *PLoS One*, *13*(5), art. no. e0197083. **https://doi.org/10.1371/journal.pone.0197083**
11. Deehan, E.C., Zhang, Z., Riva, A., Armet, A.M., Perez-Muñoz, M.E., Nguyen, N.K., Krysa, J.A., Seethaler, B., Zhao, Y.Y., Cole, J., Li, F., Hausmann, B., Spittler, A., Nazare, J.A., Delzenne, N.M., Curtis, J.M., Wismer, W.V., Proctor, S.D., Bakal, J.A., Bischoff, S.C., Knights, D., Field, C.J., Berry, D., Prado, C.M., Walter, J. (2022). Elucidating the role of the gut microbiota in the physiological effects of dietary fiber. *Microbiome*, *10*, art. no. 77. **https://doi.org/10.1186/s40168-022-01248-5**
12. Ermini, M.L., Voliani, V. (2021). Antimicrobial nano-agents: The copper age. *ACS Nano*, *15*(4), 6008-6029. **https://doi.org/10.1021/acsnano.0c10756**
13. Fiksdal, L., Tryland, I. (2008). Application of rapid enzyme assay techniques for monitoring of microbial water quality. *Current Opinion in Biotechnolology*, *19*(3), 289-294. **https://doi.org/10.1016/j.copbio.2008.03.004**
14. Gao, S., Sun, R., Singh, R., Yu So, S., Chan, C.T.Y., Savidge, T., Hu, M. (2022). The role of gut microbial β-glucuronidase in drug disposition and development. *Drug Discovery Today*, *27*(10), art. no. 103316. **https://doi.org/10.1016/j.drudis.2022.07.001**
15. Gonzales-Eguia, A., Fu, C.-M., Lu, F.-Y., Lien, T.-F. (2009). Effects of nanocopper on copper availability and nutrients digestibility, growth performance and serum traits of piglets. *Livestock Science*, *126*(1-3), 122-129. **https://doi.org/10.1016/j.livsci.2009.06.009**
16. Griffin, J.W.D., Bradshaw, P.C. (2019). Effects of a high protein diet and liver disease in an *in silico* model of human ammonia metabolism. *Theoretical Biology and Medical Modelling*, *16*, art. no. 11. **https://doi.org/10.1186/s12976-019-0109-1**
17. Gugołek, A., Kowalska, D., Strychalski, J., Ognik, K., Juśkiewicz, J. (2021). The effect of dietary supplementation with silkworm pupae meal on gastrointestinal function, nitrogen retention and blood biochemical parameters in rabbits. *BMC Veterinary Research*, *17*, art. no. 204. **https://doi.org/10.1186/s12917-021-02906-w**
18. Han, X.Y., Du, W.L., Fan, C.L., Xu, Z.R. (2010). Changes in composition a metabolism of caecal microbiota in rats fed diets supplemented with copper-loaded chitosan nanoparticles. *Journal of Animal Physiology and Animal Nutrition*, *94*(5), 138-144. **https://doi.org/10.1111/j.1439-0396.2010.00995.x**
19. Harris, H.C., Pereira, N., Koev, T., Khimyak, Y.Z., Yakubov, G.E., Warren, F.J. (2023). The impact of psyllium gelation behaviour on *in vitro* colonic fermentation properties. *Food Hydrocolloids*, *139*, art. no. 108543. **https://doi.org/10.1016/j.foodhyd.2023.108543**
20. Herman, M., Janiak, M.A., Sadlik, J.K., Piekoszewski, W., Amarowicz, R. (2022). Iron, zinc, copper, manganese and chromium in green teas, their transfer to extracts and correlations between contents of elements and bioactive compounds. *Polish Journal of Food and Nutrition Sciences*, *72*(4), 421-429. **https://doi.org/10.31883/pjfns/156394**
21. Jankowski, J., Otowski, K., Kozłowski, K., Pietrzak, P., Ferenc, K., Ognik, K., Juśkiewicz, J., Sawosz, E., Zduńczyk, Z. (2020). Effect of different levels of copper nanoparticles and copper sulfate on morphometric indices, antioxidant status and mineral digestibility in the small intestine of turkeys. *Annals of Animal Science*, *20*(3), 975-990. **https://doi.org/10.2478/aoas-2020-0013**
22. Jurgoński, A., Juśkiewicz, J., Kowalska, K., Zduńczyk, Z. (2012). Does dietary inulin affect biological activity of a grapefruit flavonoid-rich extract? *Nutrition & Metabolism*, *9*, art. no. 31. **https://doi.org/10.1186/1743-7075-9-31**
23. Juśkiewicz, J., Zduńczyk, Z., Frejnagel, S. (2007). Caecal parameters of rats fed diets supplemented with inulin in exchange for sucrose. *Archives of Animal Nutrition*, *61*(3), 201-210. **https://doi.org/10.1080/17450390701297735**
24. Kargin, D. (2021). Changes in serum physiological and biochemical parameters of male Swiss Albino mice after oral administration of metal oxide nanoparticles (ZnO, CuO, and ZnO+CuO). *Biological Trace Element Research*, *199*, 4218-4224. **https://doi.org/10.1007/s12011-020-02560-7**
25. Kiyani, M.M., Butt, M.A., Rehman, H., Mustafa, M., Sajjad, A.G., Shah, S.S.H., Mahmood, T., Bokhari, S.A.I. (2022). Evaluation of antioxidant activity and histopathological changes occurred by the oral ingestion of CuO nanoparticles in monosodium urate crystal-induced hyperuricemic BALB/c mice. *Biological Trace Element Research*, *200*, 217-227. **https://doi.org/10.1007/s12011-021-02615-3**
26. Lai, M.-J., Huang, Y.-W., Chen, H.-C., Tsao, L.-I., Chang Chien, C.-F., Singh, B., Liu, B.R. (2022). Effect of size and concentration of copper nanoparticles on the antimicrobial activity in *Escherichia coli* through multiple mechanisms. *Nanomaterials*, *12*(21), art. no. 3715. **https://doi.org/10.3390/nano12213715**
27. Lee, I.C., Ko, J.W., Park, S.H., Lim, J.O., Shin, I.S., Moon, C., Kim, S.H., Heo, J.D., Kim, J.C. (2016). Comparative toxicity and biodistribution of copper nanoparticles and cupric ions in rats. *International Journal of Nanomedicine*, *2016*(11*)*, 2883-2900. **https://doi.org/10.2147/IJN.S106346**
28. Lee, S.Y., Lee, D.Y., Kang, J.H., Kim, J.H., Jeong, J.W., Kim, H.W., Kim, J.H., Kim, H.C., Kim, J.C. (2022). Relationship between gut microbiota and colorectal cancer: Probiotics as a potential strategy for prevention. *Food Research International*, *156*, art. no. 111327. **https://doi.org/10.1016/j.foodres.2022.111327**
29. Mahapatra, O., Bhagat, M., Gopalakrishnan, C., Arunachalam, K.D. (2008). Ultrafine dispersed CuO nanoparticles and their antibacterial activity. *Journal of Experimental Nanoscience*, *3*(3), 185-193. **https://doi.org/10.1080/17458080802395460**
30. Makki, K., Deehan, E.C., Walter, J., Bäckhed, F. (2018). The impact of dietary fiber on gut microbiota in host health and disease. *Cell Host & Microbe*, *23*(6), 705-715. **https://doi.org/10.1016/j.chom.2018.05.012**
31. Malavolta, M., Piacenza, F., Basso, A., Giacconi, R., Costarelli, L., Mocchegiani, E. (2015). Serum copper to zinc ratio: Relationship with aging and health status. *Mechanisms of Ageing and Development*, *151*, 93-100. **https://doi.org/10.1016/j.mad.2015.01.004**
32. Markowiak-Kopeć, P., Śliżewska, K. (2020). The effect of probiotics on the production of short-chain fatty acids by human intestinal microbiome. *Nutrients*, *12*(4), art. no. 1107. **https://doi.org/10.3390/nu12041107**
33. McRorie, Jr J.W. (2015). Psyllium is not fermented in the human gut. *Neurogastroenterology & Motility*, *27*, 1681-1682. **https://doi.org/10.1111/nmo.12649**
34. Olivares, M., Uauy, R. (1996). Copper as an essential nutrient. *American Journal of Clinical Nutrition*, *63*(5), 791S-796S. **https://doi.org/10.1093/ajcn/63.5.791**
35. Perler, B.K., Friedman, ES., Wu, G.D. (2023). The role of the gut microbiota in the relationship between diet and human health. *Annual Review of Physiology*, *85*, 449-468. **https://doi.org/10.1146/annurev-physiol-031522-092054**
36. Pineda, L., Sawosz, E., Vadalasetty, K.P., Chwalibog, A. (2013). Effect of copper nanoparticles on metabolic rate and development of chicken embryos. *Animal Feed Science and Technology*, *186*(1-2), 125-129. **https://doi.org/10.1016/j.anifeedsci.2013.08.012**
37. Poulouxi, S., Prodromidis, M.I. (2020). Indirect determination of *Escherichia coli* based on β-D-glucuronidase activity and the voltammetric oxidation of phenolphthalein at graphite screen-printed electrodes. *Journal of Electroanalytical Chemistry*, *879*, art. no. 114752. **https://doi.org/10.1016/j.jelechem.2020.114752**

38. Strychalski, J., Juskiewicz, J., Kowalska, D., Gugołek, A. (2021). Performance indicators and gastrointestinal response of rabbits to dietary soybean meal replacement with silkworm pupae and mealworm larvae meals. *Archives of Animal Nutrition*, *75*(4), 294-310. **https://doi.org/10.1080/1745039X.2021.1962171**
39. Utembe, W., Tlotleng, N., Kamng'ona, A.W. (2022). A systematic review on the effects of nanomaterials on gut microbiota. *Current Research in Microbial Sciences*, *3*, art. no. 100118. **https://doi.org/10.1016/j.crmicr.2022.100118**
40. Żary-Sikorska, E., Juśkiewicz, J., Jundziłł, A., Rybka, J. (2016). Effects of diets varying in the type of dietary fibre and its combination with polyphenols on gut function, microbial activity and antioxidant status in rats. *Journal of Animal and Feed Sciences*, *25*(3), 250-258. **https://doi.org/10.22358/jafs/65560/2016**
41. Zhang, W., Roy, S., Rhim, J.W. (2023). Copper-based nanoparticles for biopolymer-based functional films in food packaging applications. *Comprehensive Reviews in Food Science and Food Safety*, *22*(3), 1933-1952. **https://doi.org/10.1111/1541-4337.13136**
42. Zhang, Y., Zhou, J., Dong, Z., Li, G., Wang, J., Li, Y., Wan, D., Yang, H., Yin, Y. (2019). Effect of dietary copper on intestinal microbiota and antimicrobial resistance profiles of *Escherichia coli* in weaned piglets. *Frontiers in Microbiology*, *10*, art. no. 2808. **https://doi.org/10.3389/fmicb.2019.02808**

ORIGINAL ARTICLE
http://journal.pan.olsztyn.pl

Polish Journal of Food and Nutrition Sciences
2024, Vol. 74, No. 4, 376–386
DOI: 10.31883/pjfns/195146
ISSN 1230-0322, e-ISSN 2083-6007

Nutritional Value and Antioxidant Capacity of Mexican Varieties of Sweet Potato (*Ipomoea batatas* L.) and Physicochemical and Sensory Properties of Extrudates

Rosa M. García-Martínez, José O. Rodiles-López*, Héctor E. Martínez-Flores

Faculty of Chemical Pharmacobiology, Michoacana University of San Nicolás of Hidalgo, Tzintzuntzan 173, Colonia Matamoros, CP. 58240, Michoacán, México

The objective of the study was to perform a nutritional analysis and antioxidant capacity of three varieties of sweet potatoes, *Ipomoea batatas* L., from Mexico, classified by color as: purple, yellow and white. In addition, sweet potato extrudates were produced and evaluated for their nutritional, antioxidant, sensory and texture properties. The average content of macronutrients for the three varieties was 77.92 g of carbohydrate, 10.51 g of dietary fiber, 8.25 g of protein, and 0.53 g of lipid *per* 100 g tuber on a dry matter (DM) basis. The purple variety exhibited the highest content of fiber as well as zinc and sodium, and the white one displayed the highest content of protein. In turn, contents of calcium, iron, and magnesium were the highest in yellow potatoes. Ascorbic acid content ranged from 60.6 to 106.0 mg/100 g DM, being higher in the yellow potatoes, and the total phenolic content ranged from 216 to 581 mg GAE/100 g DM, being higher in the purple potatoes. The average antioxidant capacity was 40.7 and 23.4 µmol TE/g DM in DPPH and ABTS assays. A lower total phenolic content and antioxidant capacity of extruded sweet potatoes were found with respect to the fresh ones. Among the extrudates, the purple ones had the highest total phenolic content (307 mg GAE/100 g DM) and exhibited the highest antiradical activity in the ABTS assay (15.5 µmol TE/g DM). They were also scored the highest in the sensory analysis, although the instrumental texture analysis showed their greater hardness (64.4 N) compared to the yellow and white extrudates (46.9 and 30.5 N, respectively). Extrudates of the three potato varieties exhibited a sweet taste and, thus, can be considered as sweetener substitutes in snacks with increased nutritional and bioactive potential.

Keywords: colored potatoes, extrusion, potato tuber, proximate analysis, texture parameters

ABBREVIATIONS

SP, sweet potato, *Ipomoea batatas*; RH, relative humidity; DM, dry matter; WM, wet matter; %DRI, percentages of the dietary reference intakes; GAE, gallic acid equivalent; TE, Trolox equivalent.

INTRODUCTION

The sweet potato (SP), *Ipomoea batatas* L., is the second most important tuber crop globally and is harvested in over 110 countries. It is native to and domesticated in tropical America, between Mexico and Peru. Sweet potato is a globally important vegetable, ranking among the six most important food crops after rice, wheat, potato, corn and manioc [Grüneberg *et al*., 2017; Leonel *et al*., 2023]. As reported by the Food and Agriculture Organization of the United Nations (FAO), its global production in 2022 reached 86.4 million tons, with Mexico contributing 81,095 tons [Ritchie *et al*., 2023]. According to this report, China accounted for most of the global production at 53.9%, followed by Malawi (9.3%), Tanzania (4.9%), and Nigeria (4.6%). A diversity

*Corresponding Author:
Cell phone: (+52) 443-433-5401; e-mail: jose.rodiles@umich.mx (J.O. Rodiles-López)

Submitted: 26 February 2024
Accepted: 23 October 2024
Published on-line: 20 November 2024

of varieties is observed, displaying a range of colors, including orange, red, purple, yellow, brown, cream and white, and each variety possesses a distinct chemical and nutritional composition [Oloniyo *et al*., 2021]. Sweet potato composition includes carbohydrates, dietary fibers, vitamins, minerals, and several bioactive metabolites. The purple variety is characterized by its significant content of anthocyanins, while the yellow and orange varieties contain carotenoids and are dense in provitamin A [Tang *et al*., 2015]. In addition to their high water-soluble dietary fiber content, sweet potato tips are also a rich source of protein when compared to other vegetables, as well as iron, potassium, vitamins B_2, C, and E [Hong *et al*., 2022]. The main carbohydrate of sweet potato is starch; however, the tubers contain also significant amount of sucrose, glucose and fructose, which are responsible for their sweet taste [Leonel *et al*., 2023]. Also, during storage and cooking, the presence of maltose is observed due to the hydrolysis of starch by α- and β-amylases.

Several biological activities of sweet potatoes have been reported, both in leaves and root tubers, including antioxidant, anti-inflammatory, antimicrobial, antifungal, antiviral, antidiabetic, antimutagenic, hepatoprotective, anticoagulant, and anticarcinogenic ones [Murnihati *et al*., 2020; Vergun *et al*., 2020]. These activities vary depending on the part of the tuber and the color. Bioactive compounds of sweet potatoes, including phenolic acids, flavonoids, anthocyanins, ascorbic acid, and carotenoids enable these effects to occur [Hossain *et al*., 2022; Makori *et al*., 2020].

The root pulp of sweet potatoes can be cooked, fried, roasted, or used as an ingredient in stews. It is widely used in the food industry, including in baby food, cakes, pastries, frozen vegetables, ice cream, ready-to-eat meals, chips, syrups, starches, snacks, as well as beverages such as juices and teas, and in confectionery products due to the distinctive colors offered by its different varieties. On an industrial level, starch, sugar, alcohol and natural dyes are also extracted. In addition, public awareness of the health risks associated with wheat gluten is opening a new market niche [Escobar-Puentes *et al*., 2022; Hong *et al*., 2022].

The objective of this study was to compare the nutritional composition and antioxidant capacity of three varieties of sweet potatoes native to Mexico, namely purple, yellow, and white, as well as extruded products obtained from these potatoes. The sensory and texture properties of extruded sweet potatoes were also analyzed in the study.

MATERIALS AND METHODS

Raw material

Tubers of three types of sweet potato (SP), *Ipomoea batatas* L., were used in this study based on their color: purple, yellow, and white (**Figure 1**). The SP are indigenous to the Mexican state of Michoacán and were procured from a market in the city of Morelia. For analysis, they were washed with distilled water and sliced into approximately 5-cm thick pieces, including the peel, and dehydrated at 50°C for 48 h in an oven (model 9023A, Ecoshel, Pharr, TX, USA). Subsequently, the samples were ground and passed through a 60-mesh sieve, resulting in a flour with a particle size of less than 260 µm. The dry matter (DM) content of the samples was calculated by the difference in weight before and after drying.

Preparation of extrudates

The fresh SP were blanched for 10 min at boiling temperature, the peel was removed, and they were cut into 5-cm thick pieces. Subsequently, they were dehydrated in a gas oven at 55±5°C for up to 2 h at separate intervals to obtain varying levels of humidity. The final humidity levels achieved were 15–20% in 30 min, 10–15% in 60 min, and 5–10% in 120 min. The extruder equipment was assembled in a laboratory within the Universidad Michoacana de San Nicolás de Hidalgo, México. The screw-type extruder used had a helical worm of circular panel with a 1-cm diameter, and a blade and a die made of stainless steel which allowed to produce 1-cm diameter filament. It was powered by a 1 HP Marver model 10012 series 1009 motor (Crompton, Mumbai, India). The extrusion of SP was conducted without any additives. After extrusion, the products were placed in a gas oven set to 90±5°C for 1 h to remove excess moisture and achieve the desired texture.

Analysis of proximate composition, dietary fiber content and mineral contents

The proximate composition analysis of potatoes and extrudates was conducted according to AOAC International methods [AOAC, 2000]; moisture (method no. 934.01), protein (method no. 960.52), lipids (method no. 920.85), ash (method no. 942.05), and crude fiber (962.09) were determined. The content of dietary fiber (total, soluble and insoluble fractions) was assessed using the method of Prosky *et al*. [1988], with a total dietary fiber assay kit (Sigma-Aldrich, Saint Louis, MO, USA). The analyses were conducted in triplicate. The content of carbohydrates was calculated by difference from the data on moisture, protein, lipid, ash, and dietary fiber. The roots' metabolizable energy was estimated using conversion factors of 4 kcal/g for proteins and carbohydrates, 9 kcal/g for lipids, and a value of 2 kcal/g for dietary fiber, as indicated in the data provided by the FAO [2003].

The determination of SP starch was conducted in accordance with the stipulations of the Mexican standard NOM-F321-S1978 [1978], which represents a modified iteration of the Lane-Eynon procedure. A quantity of 5 g of the sweet potato powder was placed in a container with 150 mL of water and 25 mL of concentrated HCl, and the contents were mixed thoroughly. The solution was heated for 75 min, cooled and neutralized with $NaOH/H_2O$ (1:1, *w/v*) solution. Subsequently, the hydrolysate, after filling the volume to 250 mL was filtered. Then, the 10-fold diluted filtrate was transferred to a burette and was added dropwise to the flask containing a mixture of $CuSO_4{\times}5H_2O$ solution and $NaKC_4H_4O_6{\times}4H_2O$ solution. Just prior to the complete reduction of the copper, 1 mL of the 0.2% aqueous solution of methylene blue was added. The titration was completed until the indicator lost its coloration. Starch content in the sample (g/100 g DM) was calculated utilizing a glucose-to-starch conversion factor of 0.9.

Certain minerals including calcium, copper, iron, potassium, magnesium, sodium, and zinc of SP were quantified using atomic absorption spectrometry. Digestion was performed using nitric acid, according to the procedure described by Uddin *et al*. [2016]. A quantity of 0.5 g of the sample was weighed, and 5 mL of 65% HNO_3 was added. The resulting mixture was then boiled gently over a water bath maintained at 90°C for a period of 1–2 h until a clear, fully digested solution was obtained. The solution was then filtered using Whatman 42 filter paper (2.5 µm). Enough deionized water was then added to the final sample's volume to 50 mL. The analysis was conducted in triplicate using an atomic absorption spectrometer model AAnalyst 200 (Perkin Elmer, Waltham, MA, USA). The results were reported as mg/100 g DM.

Determination of ascorbic acid and total xanthophyll contents

Ascorbic acid in potatoes was quantified using the titrimetric method with 2,6-dichloroindophenol according to the AOAC International procedure (967.21) [AOAC, 2000] and its content was expressed as mg/100 g DM.

The total xanthophyll content was determined in accordance with the AOAC International method no. 970.64 [AOAC, 2000]. A sample weighing 50 mg was mixed with 3 mL of a solution composed of hexane, ethanol, acetone and toluene (10:6:7:7, *v/v/v/v*), and then 2 mL of 40% KOH in 80% methanol was added. The mixture was then incubated at 20°C for 16 h, brought to a volume of 10 mL with 10% $NaSO_4$ and shaken for 2 min in a vortex mixer. It was then allowed to stand for 1 h until the epiphase had clarified in the dark. Subsequently, the solution was transferred to a centrifuge tube and centrifuged at 3,000×g for 5 min. The absorbance was determined at a wavelength of 474 nm using a spectrophotometer, with hexane used as the blank. The total xanthophyll content was calculated using extinction coefficient for *trans*-lutein (236 L/(g×cm)) and expressed in µg/g potato sample.

Determination of total phenolic content, total flavonoid content, and antioxidant capacity

An extraction of each of the three SPs and three extrudates was conducted in order to determine the content of total phenolics, total flavonoids (only extrudates), and antioxidant capacity *via* assays with 2,2-diphenyl-1-picrylhydrazyl (DPPH) radicals and with 2,2'-azino-bis (3-ethylbenzothiazoline-6-sulfonic acid) (ABTS) radical cations. The powdered samples were treated as follows: 10 mL of ethanol (75%) was added to 1 g of each sample and stirred for 24 h in the dark. The samples were then centrifuged at 3,910×g for 10 min, after which the supernatants were collected and kept at 4°C until used for analyses.

The total phenolic content was determined using the colorimetric method with the Folin-Ciocalteau reagent, following the procedure established by Singleton *et al*. [1999] with minor modifications suggested by Treviño-Gómez *et al*. [2017]. A 250 µL aliquot of the extract was combined with 250 µL of 2 N Folin-Ciocalteu reagent and 250 µL of 20% Na_2CO_3, agitated, and incubated at 40°C for 30 min. Subsequently, 2 mL of distilled water were added to the mixture, which was then vortexed. The samples were subjected to absorbance measurement at 750 nm using a spectrophotometer (Genesys 20, Thermo Fisher Scientific Inc.). Gallic acid was used as a standard and the results were reported as mg gallic acid equivalent (GAE)/100 g DM.

The total flavonoid content of the extrudates was evaluated in accordance with the methodology described by Zhishen *et al*. [1999]. A 150 µL aliquot of each extract was combined with 150 µL of 5% $NaNO_2$, 150 µL of 10% $AlCl_3$, and 1 mL of 0.1 M NaOH. Subsequently, the samples were analyzed using a spectrophotometer (Genesys 20, Thermo Fisher Scientific Inc.) at an absorbance of 510 nm. The standard used was quercetin, and the results were expressed as mg quercetin equivalent (QE)/100 g DM.

The determination of DPPH radical scavenging activity was conducted according to the method developed by Brand-Williams *et al*. [1995] with modifications proposed by Ru *et al*. [2019]. In summary, 200 µL of each extract was added to 3 mL of the DPPH radical solution in methanol (100 µM). The samples were homogenized for 10 s, then the reaction mixture was incubated in the dark at room temperature for 30 min, after which its absorbance was measured at 517 nm using a spectrophotometer (Genesys 20, Thermo Fisher Scientific Inc.). The results were expressed as µmol Trolox equivalent (TE)/g DM using a standard curve of Trolox.

The ABTS assay was conducted in accordance with the methodology outlined by Re *et al*. [1999]. Firstly, a solution consisting of ABTS (7 mM) and potassium persulfate (2.45 mM) was mixed at room temperature in the dark for 20 h to generate $ABTS^{\bullet+}$. Then, methanol was used to dilute the $ABTS^{\bullet+}$ mixture to an absorbance around 0.70 at 734 nm. Subsequently, 0.1 mL of each extract was combined with 3.9 mL of the aforementioned $ABTS^{\bullet+}$ solution. The reaction mixture was kept at room temperature for 6 min, then the absorbance was recorded at 734 nm. The results were calculated based on the calibration curve plotted with Trolox and were expressed as µmol Trolox equivalent (TE)/g DM.

Texture analysis

A texture analysis by compression was conducted on the three extrudates using a Brookfield CT3 texture analyzer with TexturePro CT v1.7 Build 28 software (Brookfield Engineering Lab. Inc, Middleboro, MA, USA). The apparatus was operated with a TA11/1000 probe TA-SB element. The analysis was conducted on a single cycle with the target at 6.0 mm and an activation load of 0.07 N at a speed of 0.5 mm/s and 0.5 mm/s lap speed with a sampling rate of 50 points *per* s. The sample was 16.0 mm in length and 6.0 mm in height. The analysis was performed at room temperature (25±2°C) with 10 samples *per* extrudate.

Sensory analysis

Forty untrained participants were used to perform a sensory analysis of the extruded products using a hedonic test. The acceptability of the extrudates was determined using a 5-point hedonic scale, where 5 corresponded to "I like very much"; 4 to "I like"; 3 to "I neither like nor dislike"; 2 to "I dislike"; and 1 to

Table 1. Proximate composition and metabolized energy value of Mexican sweet potatoes with different tuber colors.

Constituent/Parameter	Purple	Yellow	White
Moisture (g/100 g)	60.80±1.52^{b}	72.44±2.17^{a}	68.54±1.37^{a}
Carbohydrate (g/100 g DM)	75.64±1.72^{b}	80.79±1.16^{a}	77.35±1.38^{ab}
Starch (g/100 g DM)	59.67±3.12^{a}	43.87±2.94^{b}	43.77±3.04^{b}
Dietary fiber (g/100 g DM)	13.56±1.20^{a}	8.33±0.61^{b}	9.65±0.73^{b}
Soluble fiber (g/100 g DM)	1.20±0.10^{b}	1.18±0.09^{b}	1.88±0.13^{a}
Insoluble fiber (g/100 g DM)	12.36±1.10^{a}	7.15±0.52^{b}	7.77±0.60^{b}
Protein (g/100 g DM)	7.97±0.42^{b}	7.03±0.33 ^{b}	9.73±0.48^{a}
Lipid (g/100 g DM)	0.15±0.02^{b}	1.20±0.10^{a}	0.25±0.03^{b}
Ash (g/100 g DM)	2.68±0.09^{b}	2.65±0.12^{b}	3.02± 0.13^{a}
Energy value (kcal/100 g)	363±3^{c}	379±1^{a}	370±2^{b}

Results are shown as mean ± standard deviation. Different letters in the same row indicate the significant differences (p<0.05). DM, dry matter.

"I dislike very much". Color, odor, texture, and taste of the samples were evaluated.

Color parameter analysis

The color was evaluated in fresh, blanched, and extruded sweet potatoes from the three varieties. A Spectro-guide 45/0 colorimeter was employed for this purpose (BYK-Gardner GmbH, Geretsried, Germany). Values were obtained based on the CIELab scale with a brightness of D65, viewing angle of 10° and aperture diameter of 8 mm. The instrument provided darkness/brightness (L*), green/red intensity (a*), and blue/yellow intensity (b*). Three replicates of measurements were conducted for each sample, and the instrument was calibrated with a white ceramic plate standard prior to each procedure.

Statistical analysis

Analyses of nutritional composition, mineral content, bioactive compound content, antioxidant capacity, and color parameters were performed in triplicate. For texture parameters and sensory scores, the number of repetitions were 10 and 40, respectively. Results were subjected to a one-way analysis of variance (ANOVA) using JMP software version 8.0 (JMP Statistical Discovery LLC, Cary, NC, USA). Means were compared using Tukey's test, and differences were considered significant when p<0.05.

RESULTS AND DISCUSSION

Macronutrients of sweet potatoes

The results of proximate analysis of SP are presented in **Table 1**. Moisture content was 60.80 g/100 g in purple, 72.44 g/100 g in yellow, and 68.54 g/100 g in white potatoes, with an average of 67.26 g/100 g. The moisture content of yellow and white varieties did not differ significantly (p≥0.05).

The three varieties under examination had an average dry matter content of 32.74 g/100 g. Grüneberg *et al*. [2017] conducted a comprehensive study of SP with 1,174 clones analyzed in various environments and determined an average dry matter content of 34.9 g/100 g. They also noted that genotypic factors had a greater impact on variability than environmental factors. Rowena *et al*. [2009] reported a dry matter content of 32.46 g/100 g after analyzing five varieties from the Philippines, while Teow *et al*. [2007] found a value of 30.2 g/100 g after studying nineteen clones from the USA.

Carbohydrates were found to be the most abundant nutrient of SP (**Table 1**), with an average content of 77.92 g/100 g DM. The highest content was found in the yellow variety, while the lowest content was in the purple variety. These findings were statistically significant (p<0.05). Additionally, the white variety did not differ statistically (p≥0.05) from the yellow and purple varieties. Armijos *et al*. [2020] reported an average of 81.66 g/100 g DM in carbohydrate content for seven varieties native to Ecuador with yellow, orange, and purple colors. Nascimento *et al*. [2015] studied three Brazilian SP varieties (white and orange) from organic cultivation and reported that their carbohydrate content was 57.21 g/100 g DM, being higher in the white variety, which is consistent with the results of our study. The content of starch, the main carbohydrate fraction of SP, ranged from 43.87 to 59.67 g/100 g DM (**Table 1**), and a significantly (p<0.05) higher value was noted for the purple variety compared to the other varieties. Armijos *et al*. [2020] reported an average of 60.56 g/100 g DM in starch content of SP with yellow, orange, and purple colors. Grüneberg *et al*. [2017] found that starch content of different clones of *I. batatas* was 66.0 g/100 g DM, while the content of sucrose, glucose, and fructose in DM was 10.3 g/100 g, 2.2 g/100 g, and 1.7 g/100 g, respectively. Nascimento *et al*. [2015] reported a starch content of 29.3 g/100 g DM in Brazilian SP. In turn, Hossain *et al*. [2022] who analyzed eight SP varieties from Bangladesh, reported an average starch content of 52.72 g/100 g in powdered dry roots. It is also noteworthy that the purple varieties exhibit the highest starch content, which is comparable to that determined in the present study.

The lipid content of SP was minimal with an average of 0.53/100 g DM, and the yellow variety had a significantly (p<0.05) higher lipid content (1.20 g/100 g DM) than the other varieties (**Table 1**). Armijos *et al*. [2020] and Hossain *et al*. [2022] reported lipid contents of 1.35 and 1.51 g/100 g DM, respectively. The latter author noted that the highest content of lipids was

Table 2. Mineral content of Mexican sweet potatoes with different tuber colors (mg/100 g dry matter).

Mineral	Purple	Yellow	White	%DRI	
				Men	Women
Calcium	44.4±1.8^{c}	139.8±5.7^{a}	72.8±2.4^{b}	2.6	2.6
Iron	10.5±0.4^{b}	12.8±0.5^{a}	11.4±0.4^{b}	46.8	20.8
Potassium	2,439±119^{b}	2,948±133^{a}	2,948±105^{a}	26.4	34.6
Magnesium	75.3±3.2^{c}	117.4±4.4^{a}	104.0±4.2^{b}	7.7	10.0
Sodium	106.9±4.3^{a}	87.8±3.5^{b}	54.0±2.3^{c}	1.8	1.8
Zinc	1.17±0.04^{a}	0.40±0.01^{b}	0.00±0.0	2.6	3.6

Results are shown as mean ± standard deviation. Different letters in the same row indicate the significant differences (p<0.05). %DRI, percentage of the dietary reference intakes of the minerals by consuming 100 g of fresh sweet potato calculated according to recommendations of the National Institutes of Health in USA [NIH, 2022].

found in the yellow variety, a finding that aligns with the results of our research.

The average protein content was 8.25 g/100 g DM, with the white variety having the highest content (9.73 g/100 g) and differing significantly (p<0.05) in this respect from the other varieties (**Table 1**). Armijos *et al*. [2020] reported a protein content of 6.50 g/100 g DM, while Grüneberg *et al*. [2017] reported a range from 2.7 to 8.9 g/100 g DM for different clones of *I. batatas*. Leonel *et al*. [2023] analyzed data from multiple authors and reported values between 1.3 and 9.5 g/100 g DM.

The dietary fiber content was observed to be an average of 10.51 g/100 g DM, with 9.09 g/100 g DM being insoluble fiber and 1.42 g/100 g DM being soluble fiber. The white variety had the highest amount of soluble fiber, while the purple one had the highest amount of insoluble fiber (**Table 1**). Armijos *et al*. [2020] reported a soluble fiber content of 2.82 g/100 g DM and an insoluble fiber content of 10.17 g/100 g DM in differently colored Ecuadorian SP. Additionally, Leonel *et al*. [2023] reported a dietary fiber content of 19.36 g/100 g DM.

The average metabolized energy value of the three types of sweet potato was 371 kcal/100 g DM, according to theoretical data (**Table 1**). However, there were statistically significant (p<0.05) differences between the three varieties, being higher in the yellow variety and lower in the purple one. Vergun *et al*. [2020] found that the energy values of SP from Ukraine, when determined using calorimetric equipment, ranged from 342 to 362 kcal/100 g

To sum up, the macronutrient composition of sweet potatoes varied depending on their variety. Yellow potatoes had a higher content of carbohydrates and lipids, purple ones – dietary fiber, and white ones – proteins and ash.

Micronutrients of sweet potatoes

The mineral analysis results displaying the content of calcium, iron, potassium, magnesium, sodium, and zinc in dry matter of sweet potatoes are presented in **Table 2**. The copper was also analyzed but not detected. The level of calcium ranged from 44.4 to 139.8 mg/100 g DM, with the yellow variety having almost twice as much of this element as the other varieties. Our results were lower than those obtained by Armijos *et al*. [2020], who reported an average calcium content of 229 mg/100 g DM in Ecuadorian potatoes. Musilová *et al*. [2017] also determined a higher calcium content in the pulps of SP from the Slovak Republic (average of 468 mg/100 g DM). The average potassium content in Mexican potatoes in our study was found to be 2,778 mg/100 g DM, which was lower than the values reported by Armijos *et al*. [2020] (average of 3,501 mg/100 g DM) and higher than those reported by Musilová *et al*. [2017] (1,204 mg/100 g DM in pulp). The sodium levels varied significantly (p<0.05) among the three samples in the range of 54.0–106.9 mg/100 g DM, (**Table 2**). The average value found in this study was higher than those reported by other authors in the field; with Armijos *et al*. [2020] reporting 75.7 mg/100 g DM, while Musilová *et al*. [2017] reporting 63.4 mg/100 g DM in flesh.

Iron was determined in this study within a range from 10.5 to 12.8 mg/100 g DM (**Table 2**). Armijos *et al*. [2020] and Grüneberg *et al*. [2017] reported the iron content of 13.7 and 15.6 mg/100 g DM, respectively. Magnesium was recorded within a range from 75.3 to 117.4 mg/100 g DM with an average of 98.9 mg/100 g DM (**Table 2**). Lower magnesium levels were found in yellow, orange, and purple varieties from Ecuador with an average of 50.0 mg/100 g DM [Armijos *et al*., 2020] and in pulps of Slovak sweet potatoes with an average of 75.2 mg/100 g DM [Musilová *et al*., 2017]. Zinc was not detected in the white variety and its content in the yellow and purple SPs was 0.40 and 1.17 mg/100 g DM, respectively. Armijos *et al*. [2020] reported an average zinc content of 1.57 mg/100 g DM; Grüneberg *et al*. [2017] reported 0.93 mg/100 g DM, and Musilová *et al*. [2017] determined it at 0.92 mg/100 g DM.

This study found that, among the analyzed SP varieties, the yellow variety was the rich source of calcium, iron, and magnesium. On the other hand, the purple variety had the highest content of sodium and zinc but a lower potassium content.

Table 2 also shows the percentages of the dietary reference intakes (DRI) of the analyzed minerals by consuming 100 g of fresh sweet potato, which were calculated based on the recommendations of the National Institutes of Health (NIH) in USA, [NIH, 2022] (the average content of each mineral for the three

Table 3. Content of antioxidants and antioxidant capacity of Mexican sweet potatoes and extrudates obtained therefrom.

Content/Activity	Purple	Yellow	White
Sweet potatoes			
Ascorbic acid content (mg/100 g DM)	64.8±4.2^{b}	106.0±6.4^{a}	60.6±3.8^{b}
Total xanthophyll content (µg/g DM)	175±12^{b}	395±25^{a}	185±13^{b}
Total phenolic content (mg GAE/100 g DM)	581±36^{a}	388±25^{b}	216±14^{c}
DPPH$^{\bullet}$ radical scavenging activity (µmol TE/g DM)	39.8±2.1^{a}	41.7±2.8^{a}	40.5±2.4^{a}
ABTS$^{\bullet+}$ scavenging activity (µmol TE/g DM)	28.2±1.7^{a}	22.1±1.8^{b}	19.9±1.3^{b}
Extruded sweet potatoes			
Total flavonoid content (mg QE/100 g DM)	60.6±1.2^{a}	29.6±0.4^{b}	11.4±0.3^{c}
Total phenolic content (mg GAE/100 g DM)	307±14^{a}	115±3^{b}	45±4^{c}
DPPH$^{\bullet}$ radical scavenging activity (µmol TE/g DM)	10.9±0.4^{b}	16.9±1.5^{a}	9.2±1.0^{b}
ABTS$^{\bullet+}$ radical scavenging activity (µmol TE/g DM)	15.5±0.2^{a}	13.8±0.5^{b}	13.3±0.4^{b}

Results are shown as mean ± standard deviation. Different letters in the same row indicate the significant differences (p<0.05). QE, quercetin equivalents; GAE, gallic acid equivalents; TE, Trolox equivalents; DM, dry matter.

varieties was used). The reference values are for people aged 19 to 50 years. It is noted that sweet potatoes were a micronutrient--rich food, providing high levels of potassium and iron, as well as magnesium. In addition, the sodium content was very low, providing only 1.8% of the recommended daily intake.

Contents of ascorbic acid, total xanthophylls and total phenolics in sweet potatoes

The contents of ascorbic acid, total xanthophylls, and total phenolics in different varieties of SP are shown in **Table 3**. The ascorbic acid content ranged from 60.6 to 106.0 mg/100 g DM. The yellow variety had the highest content, being 1.7 times higher than that of the other varieties. According to literature data, ascorbic acid content of Ecuadorian yellow, orange, and purple varieties of sweet potatoes was on average 67.2 mg/100 g DM [Armijos *et al*., 2020], while Ukrainian SP contained approximately 41.5 mg of this compound in 100 g of pulp [Vergun *et al*., 2020]. Vidal *et al*. [2018] compiling information from various authors, reported an ascorbic acid content ranging from 2.4 to 25.0 mg/100 g wet matter (WM), and Gichuhi *et al*. [2014] reported a value ranging from 6.4 to 15.5 mg/100 g WM for organic sweet potatoes from the USA. Considering the average content of ascorbic acid in the samples in our study and DRI of vitamin C recommended by NIH regulations [NIH, 2022], women and men over 19 years would receive 32.8% and 27.3% of DRI, respectively, by consuming 100 g of fresh sweet potato.

Total xanthophyll content of three SP varieties ranged from 175 to 395 µg/g DM with an average of 252 (**Table 3**). The yellow variety showed its highest quantity, followed by white and purple varieties. Escobar-Puentes *et al*. [2022] analyzing studies of several authors, reported that the carotenoid content of sweet potatoes was 509 µg/g DM, with the highest content found in orange, followed by yellow, white, and purple potatoes. The authors also noted that these contents could be higher than those found in carrots and mangoes, which are typically recognized as reliable sources of carotenoids.

The average total phenolic content of SP was 395 GAE mg/100 g DM with a range from 216 to 581 mg GAE/100 g DM. Sweet potatoes cultivated in the Philippines had an average total phenolic content of 567 mg GAE/100 g DM, with a higher content found in the purple varieties, followed by yellow and white ones [Rowena *et al*., 2009]. Escobar-Puentes *et al*. [2022] in a review publication reported values ranging from 140 to 1,230 mg GAE/100 g DM, with the highest noted for purple potatoes, followed by orange, yellow, and white ones. The findings of this study indicated that the purple variety exhibited the highest total phenolic content, followed by the yellow and then the white variety, which was consistent with the above-mentioned literature data. Musilová *et al*. [2017] reported that the content of total phenolics in the peel of SP was higher than in the pulp. On the other hand, Murnihati *et al*. [2020] found that the main antioxidant compounds in purple sweet potatoes were anthocyanins and other polyphenols, while orange and yellow sweet potatoes mainly contained carotenoids. Our research findings are consistent with these conclusions.

Antioxidant capacity of sweet potatoes

The results of the antioxidant capacity of potatoes measured as the antiradical activity against DPPH$^{\bullet}$ and ABTS$^{\bullet+}$ and reported as µmol TE/g DM are shown in **Table 3**. The DPPH assay results showed homogeneity of values with no statistical difference (p≥0.05) between differently colored potatoes. However, the ABTS assay indicated that the purple potatoes had significantly (p<0.05) higher antioxidant capacity compared to the other samples.

Table 4. Proximate composition, metabolized energy value and texture parameters of extruded sweet potatoes.

Constituent/Parameter	Purple	Yellow	White
Moisture (g/100 g)	6.41±0.51^{a}	6.86±0.58^{a}	5.97±0.54^{a}
Carbohydrate (g/100 g DM)	88.57±0.77^{a}	89.76±0.73^{a}	88.43±0.83^{a}
Crude fiber (g/100 g DM)	2.30±0.20^{a}	0.99±0.12^{c}	1.46±0.15^{b}
Protein (g/100 g DM)	6.76±0.42^{a}	6.60±0.44^{a}	7.63±0.53^{a}
Lipid (g/100 g DM)	0.13±0.02^{b}	0.50±0.04^{a}	0.14±0.02^{b}
Ash (g/100 g DM)	2.24±0.14^{a}	2.15±0.12^{a}	2.35±0.13^{a}
Energy value (kcal/ 100 g)	387±1^{b}	392±1^{a}	388±1^{b}
Hardness (N)	64.4±4.0^{a}	46.9±5.7^{b}	30.5±4.4^{c}
Adhesiveness (N)	0.251±0.056^{a}	0.237±0.054^{ab}	0.183±0.069^{b}
Fracturability strength (N)	28.1±3.2^{a}	23.7±2.4^{b}	17.7±1.6^{c}
Number of fractures	11.1±2.3^{b}	14.3±3.6^{ab}	16.9±4.4^{a}

Results are shown as mean ± standard deviation. Different letters in the same row indicate the significant differences (p<0.05). DM, dry matter.

The average DPPH• radical scavenging activity of Mexican sweet potatoes was 40.7 µmol TE/g. This value was consistent with that reported by Zhang *et al*. [2022] for Chinese pigmented sweet potatoes (average of 39.3 µmol TE/g) and was slightly higher compared to that noted by Tang *et al*. [2015] (average of 25.1 µmol TE/g). In the second mentioned study, unlike in our study, higher DPPH• radical scavenging activity was observed in the purple and orange sweet potatoes than in the white and yellow ones. Makori *et al*. [2020] found that antiradical activity against DPPH• was dependent on the part of the potato tuber and reported higher values for the skin than for the flesh.

The mean value in the ABTS assay obtained in our study was 23.4 µmol TE/g. Armijos *et al*. [2020] and Zhang *et al*. [2022] reported the averages of 33.6 and 28.2 µmol TE/g for Ecuadorian and Chinese sweet potato varieties, respectively.

Proximate composition of sweet potato extrudates

In preliminary studies on obtaining extruded sweet potatoes, the fresh potatoes were dried at 50–60°C for various times to achieve different moisture contents of 5–10% (120 min), 10–15% (60 min), and 15–20% (30 min), and subsequently extruded. The dried products with a 5–10% moisture content had good color and flavor; however, they became excessively stiff over time. On the other hand, the extruded products with a moisture content of 10–15% exhibited favorable organoleptic properties and a crunchy consistency. Furthermore, these products demonstrated a seamless and uniform flow within the equipment. In contrast, the extruded products with a moisture content of 15–20% exhibited a pasty consistency and an indeterminate shape, which resulted in equipment blockages. Based on these findings, SP with a humidity range of 10–15% were selected for further production. According to the preliminary sensory evaluation, the products had a sweet taste, pleasing color and odor, high hardness, medium breaking, and high dryness, without being adhesive to the palate.

The results of a proximate analysis conducted on extrudates of each sweet potato variety are shown in **Table 4**. The moisture contents of the extruded purple, yellow, and white potatoes were 6.41 g/100 g, 6.86 g/100 g, and 5.97 g/100 g, respectively, and no significant (p≥0.05) differences were found between them. The extrudates had a protein content with an average of 7.00 g/100 g DM, with no significant (p≥0.05) difference between the three products. Extruded potatoes were also rich in carbohydrates (88.43–89.76 g/100 g DM), while the constituent which was devoid of any significant content was lipid (0.13–0.50 g/100 g DM). The average energy value was 389 kcal/100 g DM, theoretical data, being significantly (p<0.05) higher for the extruded yellow potatoes compared to the other varieties. The macronutrient content and energy value of the extrudates were consistent with the literature data, *e.g.*, the carbohydrate, protein and lipid contents of extruded purple sweet potatoes reported by Palupi *et al*. [2024] were 85.57, 5.51 and 0.56 g/100 g DM, respectively, and provided 369.28 kcal/100 g.

Total phenolic content, total flavonoid content, and antioxidant capacity of sweet potato extrudates

The contents of total phenolics and total flavonoids, as well as the antioxidant capacity of extruded Mexican sweet potatoes are shown in **Table 3**. A significant difference was observed in the total flavonoid content among the extrudates obtained from the three sweet potato varieties, with the product from purple variety exhibiting the highest total flavonoid content and the extruded potatoes of white variety exhibiting the lowest. Simultaneously, the purple extrudate exhibited the highest total phenolic content, followed by yellow, and finally white one, with a notable distinction (p<0.05). Regarding the results

of the DPPH assay, the yellow extrudate exhibited the highest value, demonstrating a statistically significant difference ($p<0.05$) compared to the other varieties; conversely, the purple and white extrudates did not differ statistically significantly ($p\geq0.05$) from one another. The extruded potatoes of the purple variety exhibited the highest values in the ABTS assay, while no statistically significant difference ($p\geq0.05$) was observed between the yellow and white varieties.

A decrease was observed in all extruded SP with respect to fresh SP when total phenolic content was subjected to analysis. A similar trend was observed in antioxidant activity, as determined by both the DPPH and ABTS assays. The blanching and extrusion process has a direct impact on the content of bioactive compounds and antioxidant capacity. Tang *et al*. [2015] reported that thermal treatment can reduce the quality of SP due to chemical degradation and the reduction of bioactive compounds such as phenolics and carotenoids. Boiling is a better heating method for keeping carotenoids, while steaming preserves more phenolic substances (excluding anthocyanin), and roasting keeps more anthocyanins.

Texture parameters of sweet potato extrudates

The texture properties of the three extrudates (purple, yellow, and white) were determined by evaluating several physical parameters, including hardness, adhesiveness, fracturability strength, as well as the number of fractures according to fracturability strength, and respective results are presented in **Table 4**. The proximate chemical composition of the three types of sweet potatoes was found to affect the texture properties of the extrudates obtained therefrom, resulting in observable differences among them.

Hardness is defined as the force required to compress or penetrate a food item with teeth; according to results (**Table 4**), the extruded purple sweet potato exhibited the highest hardness, followed by the yellow and finally the white extruded products, showing a significant ($p<0.05$) difference between the three samples. The proximate composition indicated that the purple variety had the highest dietary fiber content (**Table 1**). In contrast, the white sweet potato, the least hard extrudate of the three varieties, exhibited the highest protein content and a lower content of dietary fiber than the purple sample. The yellow sweet potato exhibited an intermediate value. Considering these findings, it can be posited that the high fiber content in potatoes was associated with enhanced hardness of the extruded products, whereas the high protein content was linked to a reduction in hardness.

The same trend was observed for adhesiveness as for hardness, with the extruded potatoes of the purple variety exhibiting the highest values and these of the white variety demonstrating the lowest values (**Table 4**). Adhesiveness is the force required to separate a food substance from another surface, such as the palate, lips, or teeth.

The requisite force to fracture the extrudates and the number of fractures generated by this force were also determined. In terms of fracturability, the extrudates from the purple variety required a greater degree of force to break them, whereas these made of the white variety necessitated less force. This finding aligns with the hardness data, as extruded white sweet potato was the least hard, and therefore required less force to fracture. Similarly, the white potato extrudate generated a greater number of fractures *per* unit of piece, with a statistically significant difference ($p<0.05$) compared to the purple potato extrudate, and yellow extrudates exhibited an intermediate value between the purple and white ones.

Sensory analysis of sweet potato extrudates

A sensory analysis was conducted by 40 untrained panelists for the three SP extrudates. A 5-point hedonic scale was used, and scores of color, odor, texture, and taste are shown in **Table 5**. The purple extruded product was the one with the best sensory characteristics, presenting an average score of 4.45, followed by the yellow product with a value of 4.25 and finally the white extruded product with a value of 3.89. The purple and yellow extrudates exhibited no significant difference ($p\geq0.05$), and comparable white and yellow were not different significantly ($p\geq0.05$) from one another. However, the white extrudate was found to differ from the purple extrudate ($p<0.05$), demonstrating a lower level of acceptance. The main difference was in the color, since the purple color was more pleasant and accepted and white was less acceptable. No differences were observed between the extrudates in terms of odor and texture. On the other hand, the purple extrudate was rated more favorably in terms of taste, followed by the yellow and white extrudates. In general, the panelists commented that the taste was pleasant and sweet, although no sugar or other sweetener was utilized. Overall acceptance of the three extruded products was 84%.

Color parameters of fresh, blanched and extruded sweet potatoes

The color of fresh, blanched, and extruded products from the three types of sweet potatoes were evaluated, and the values of parameters L^*, a^* and b^* according to the CIELab scale are shown in **Table 6**. **Figure 1** depicts the images of fresh sweet potatoes. At the L^* parameter level, the purple variety exhibited a value of 29.13, while the yellow variety demonstrated a value of 71.38 and the white variety exhibited a value of 84.58. Armijos *et al*. [2020] reported L^* values ranging from 13.89 to 71.61 for a variety of pigmented sweet potatoes. In turn, Tang *et al*. [2015] reported a value of 49.25 for the purple variety, 85.53 for the orange, 87.39 for the yellow, and 86.74 for the white one. The findings align with the values recorded in our research. The parameter a^*, in which positive values correlate with red pigments and negative values with green pigments, showed 26.38 for the purple sample, 28.78 for the yellow sample, and 1.58 for the white one (**Table 6**). Armijos *et al*. [2020] referred to values from 13.07 to 34.30, which were reported for different Ecuadorian varieties. Conversely, Tang *et al*. [2015] reported 23.83 for purple, 9.05 for orange, 5.72 for yellow, and 0.08 for white potatoes; with the data for the purple and white varieties aligning with our findings, whereas the orange and yellow varieties exhibiting lower values, suggesting that our varieties possess a greater degree

Table 5. Results of sensory evaluation of extruded sweet potatoes.

Attribute	Purple	Yellow	White
Color	4.60±0.24^{a}	4.35±0.14^{a}	3.55±0.20^{b}
Odor	4.55±0.15^{a}	4.20±0.25^{a}	4.05±0.28^{a}
Texture	4.20±0.27^{a}	4.35±0.26^{a}	4.05±0.27^{a}
Taste	4.45±0.16^{a}	4.10±0.27^{ab}	3.90±0.13^{b}
Average score	4.45±0.20^{a}	4.25±0.23^{ab}	3.89±0.22^{b}

The values correspond to the scores on the five-point hedonic scale. Results are shown as mean ± standard deviation. Different letters in the same row indicate represent the significant differences ($p<0.05$).

Table 6. Color parameters of fresh, blanched and extruded sweet potatoes.

Parameter	Variety	Fresh	Blanched	Extruded
*L**	Purple	29.13±0.57^{c}	30.99±1.01^{b}	40.40±0.48^{a}
	Yellow	71.38±1.19^{a}	55.31±2.51^{b}	38.36±1.57^{c}
	White	84.58±0.40^{a}	78.45±2.31^{b}	60.70±3.46^{c}
*a**	Purple	26.38±1.31^{a}	15.93±0.97^{b}	8.71±0.25^{c}
	Yellow	28.74±1.77^{a}	30.18±1.26^{a}	14.49±0.60^{b}
	White	1.58±0.08^{b}	0.32±0.03^{c}	2.29±0.03^{a}
*b**	Purple	−5.82±0.35^{b}	12.89±0.78^{a}	12.25±0.35^{a}
	Yellow	37.13±1.28^{b}	40.93±1.81^{a}	17.05±0.48^{c}
	White	18.20±1.15^{a}	16.98±0.18^{a}	12.00±0.32^{b}

Results are shown as mean ± standard deviation. Different letters in the same row show significant differences ($p<0.05$). *L**, darkness/brightness; *a**, intensity green/red; *b**, intensity blue/yellow.

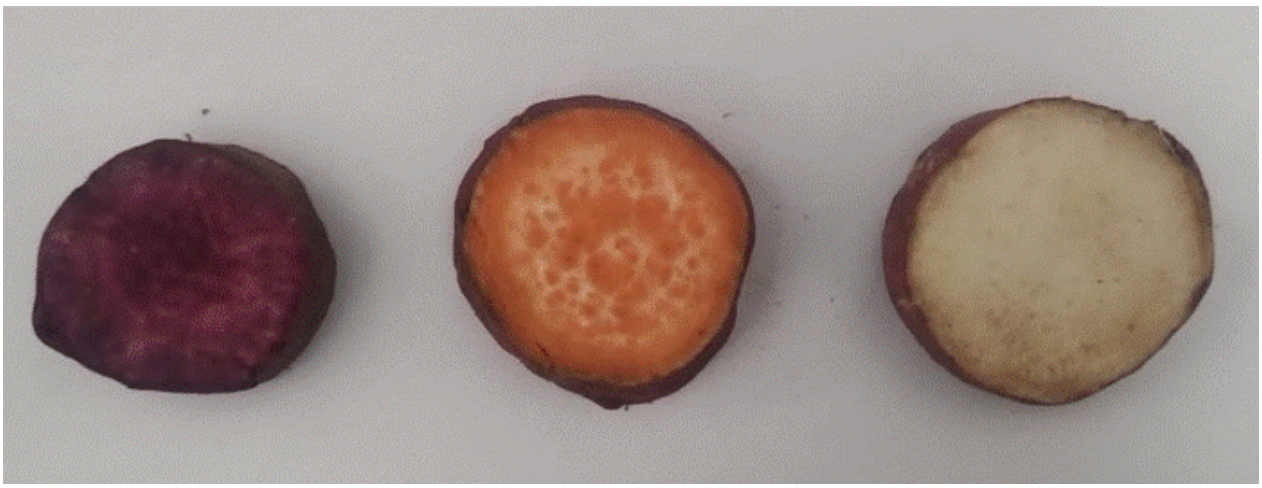

Figure 1. Appearance of fresh purple (left), yellow (center) and white (right) sweet potatoes.

of red pigmentation than those reported by the aforementioned author. Regarding the *b** parameter, where positive values are associated with yellow tones and negative values with blue, a significant difference was observed among the three sweet potato varieties (**Table 6**). The values of 37.13 and 18.20 were measured for yellow and white varieties, respectively. The color of the purple variety was characterized by a negative value of *a** parameter, −5.82, indicating a tendency towards blue. Armijos *et al.* [2020] referred to values from −8.89 to 57.81, whereas Tang *et al.* [2015] reported −9.56 for purple, 23.21 for orange, 25.83 for yellow, and 15.41 for white potatoes. These values are in accordance with those measured in this study.

It is noteworthy that the purple pigmentation of sweet potatoes is attributed to anthocyanins, which impart a dark hue and correspond with the lowest value of the *L** parameter [Tang *et al.*, 2015]. The presence of anthocyanins in purple sweet

potatoes could also be the reason for differences in the *L** value among the three sweet potato varieties included in our study. Additionally, purple pigmentation coincided with the highest content of phenolic compounds (**Table 3**). In contrast, the highest value of the *L** parameter (whiteness) was observed in the white sweet potato. This may be attributed to the absence of colored pigments in the sample, which exhibited the lowest total phenolic content. Similarly, the color of the yellow sweet potato was characterized by the highest *b** value and the highest total xanthophyll content.

A color analysis was also conducted on blanched and extruded sweet potatoes, noting that blanching represents a preliminary step preceding the preparation of the extrudates. Results are shown in **Table 6**. In the purple sweet potatoes, it was observed that the blanching process caused a lightening of the color of fresh sweet potatoes, significantly ($p<0.05$) increasing the *L** value, and this phenomenon was more pronounced in the extruded samples. Regarding parameter *a**, which concerns green/red, the fresh-blanched-extruded sample displayed a significant decrease ($p<0.05$) in purple color in accordance with the prevailing tendency to transition from red to green. With respect to parameter *b**, which refers to blue/yellow, no perceptible differences were observed between the blanched and extruded samples ($p\geq0.05$). However, these samples differed from the fresh sample, exhibiting a tendency towards yellow and a loss of purple color.

In yellow products, the *L** values demonstrated a proclivity towards darkening, fresh sweet potatoes exhibited a higher *L** value than blanched ones, with this effect being further accentuated in extruded sweet potatoes. On the *a** parameter, no distinction was observed between the fresh and blanched samples; however, the extruded samples exhibited a loss of red coloration. Conversely, in the case of the *b** parameter, the blanched product exhibited a greater yellow than the fresh sample, whereas the extruded product displayed a diminished yellow pigmentation in comparison to the fresh and blanched sweet potatoes.

In the white sweet potatoes, it was observed that the brightness tended to decrease with blanching, with a more pronounced decrease evident in the extruded sample. Furthermore, both samples exhibited statistically significant differences ($p<0.05$) with respect to fresh sweet potatoes. The *a** parameter revealed that blanching caused the red color to shift towards green in comparison to fresh sweet potatoes, but extrusion resulted in the opposite effect, with extruded sweet potatoes exhibiting a reddish hue. Additionally, on the *b** parameter, a tendency from yellow to blue was observed, with a more pronounced one in the extruded product. There was no statistically significant difference ($p\geq0.05$) between the fresh and blanched SP samples, but a notable discrepancy was observed when comparing them to the extruded products.

CONCLUSIONS

The assessment of the nutritional value of the three varieties of sweet potatoes native to Mexico: purple, yellow, and white, showed that the purple variety exhibited the highest content of dietary fiber and starch, the yellow demonstrated the highest levels of carbohydrates and lipids, and the white exhibited the highest content of proteins and minerals. Conversely, yellow potatoes exhibited the mayor content of calcium, iron, and magnesium, whereas purple had the highest content of zinc and sodium. With respect to antioxidant content and antioxidant capacity, the yellow variety was characterized by the mayor levels of ascorbic acid and total xanthophylls, while the purple one demonstrated the highest total phenolic content. All varieties demonstrated antioxidant capacity in both the DPPH and ABTS assays. The extrudates prepared from the three varieties were well accepted in sensory analysis, especially the product from purple potatoes, and the panelists noted a sweet taste of the extrudates. Color parameter analysis indicated alterations in the hue of fresh sweet potatoes regarding blanching and extrusion processes. The extrusion process resulted in a reduction in the total phenolic content and antioxidant capacity, as determined by DPPH and ABTS assays, in comparison to the fresh sweet potatoes; however, the extrudates still showed antioxidant potential.

Mexican sweet potatoes can be considered a valuable raw material with nutritional and bioactive properties, suitable for the production of extrudates with good consumer acceptability. Their sweet taste can be used as an advantage in the composition of snacks, replacing sweeteners and preserving the natural character of the product.

RESEARCH FUNDING

There was no funding for this research. All research equipment was provided by the Faculty of Pharmacobiology Chemistry of the Universidad Michoacana de San Nicolás de Hidalgo, Mexico.

CONFLICT OF INTERESTS

The authors declare that they have no competing interests.

ORCID IDs

R.M. García-Martínez https://orcid.org/0009-0002-8552-8383
H.E. Martínez-Flores https://orcid.org/0000-0002-0044-9399
J.O. Rodiles-López https://orcid.org/0000-0002-0953-9980

REFERENCES

1. AOAC. (2000). *Official Methods of Analysis* (14th ed.). The Association of Official Analytical Chemists International, Gaithersburg, MD, USA.
2. Armijos, G., Villacrés, E., Quelal, M., Cobeña, G., Álvarez, J. (2020). Physicochemical and functional evaluation of seven sweet potato varieties from Manabí-Ecuador. *Revista Iberoamericana de Tecnología Postcosecha, 21*(2), 244-255 (in Spanish, English abstract).
3. Brand-Williams, W., Cuvelier, M., Berset, C. (1995). Use of a free radical method to evaluate antioxidant activity. *Food Science and Technology*, *28*(1), 25–30. https://doi.org/10.1016/S0023-6438(95)80008-5
4. Escobar-Puentes, A., Palomo, I., Rodríguez, L., Fuentes, E., Villegas-Ochoa, M., González-Aguilar, G., Olivas-Aguirre, F., Wall-Medrano, A. (2022). Sweet potato (*Ipomoea batatas* L.) phenotypes: From agroindustry to health effects. *Foods, 11*(7), art. no. 1058. https://doi.org/10.3390/foods11071058
5. FAO (2003). *Food Energy–Methods of Analysis and Conversion Factors*. FAO Food and Nutrition Paper 77. Food and Agriculture Organization of the United Nations, Rome.
6. Gichuhi, P., Kpomblekou-A, K., Bovell-Benjamin, A. (2014). Nutritional and physical properties of organic Beauregard sweet potato (*Ipomoea batatas* (L.)) as influenced by broiler litter application rate. *Food Science & Nutrition*, *2*(4), 332-340. https://doi.org/10.1002/fsn3.108

7. Grüneberg, W., Ma, D., Mwanga, E., Carey, E., Huamani, K., Diaz, F., Eyzaguirre, R., Guaf, E., Jusuf, M., Karuniawan, A., Tjintokohadi, Y., Song, S., Anil, S., Hossain, M., Rahaman, E., Attalluri, S., Somé, K., Afuape, S., Adofo, K., Lukonge, E., Karanja, L., Ndirigwe, J., Ssemakula, G., Agili, S., Randrianaivoarivony, J., Chiona, M., Chiungu, F., Laurie, S., Ricardo, J., Andrade, M., Rausch, F., Mello, A., Khan, M., Yencho, C. (2017). Advances in sweet potato breeding from 1992 to 2012. In J. Low, M. Nyongesa, S. Quinn, M. Parker (Eds.), *Genetic Improvement of Tropical Crops*.CAB International, pp. 181-218. **https://doi.org/10.1079/9781780644202.0003**
8. Hong, C., Jo, Y., Kim, M., Chung, M., Choi, E., Kim, Y., Lee, J, Jeong, H. (2022). Biological activities of sweet potato (*Ipomoea batatas* L.) tips and tubers. *Food Science & Nutrition*, *10*(11), 4041-4048. **https://doi.org/10.1002/fsn3.2999**
9. Hossain, M., Rahim, A., Moutosi, H., Das, L. (2022). Evaluation of the growth, storage root yield, proximate composition, and mineral content of colored sweet potato genotypes. *Journal of Agriculture and Food Research, 8,* art. no. 100289. **https://doi.org/10.1016/j.jafr.2022.100289**
10. Leonel, M., Ouros, L., Lossolli, N., Leonel, S. (2023). Chapter 46 – Sweet potato: nutritional aspects of roots and leaves. *In book: Global Health Trends and Perspectives in Health Sciences.* Seven Editora, Brazil. **https://doi.org/10.56238/globalhealthprespesc-046**
11. Makori, S., Mu, T., Sun, H. (2020). Total polyphenol content, antioxidant activity, and individual phenolic composition of different edible parts of 4 sweet potato cultivars. *Natural Product Communications*, *15*(7), 1-12. **https://doi.org/10.1177/1934578X20936931**
12. Murnihati, N., Karuniawan, A., Suganda, T., Andriani, Y., Concibido, V., Levita, J. (2020). Sweet potato (*Ipomoea batatas* (L.) Lam). A review on its bioprospecting. *Journal of Pharmacy and Biological Sciences*, *15*(3), 1-7.
13. Musilová, J., Bystrická, J., Árvay, J., Harangózo, L. (2017). Polyphenols and phenolic acids in sweet potato (*Ipomoea batatas* L.) roots. *Slovak Journal of Food Sciences*, *11*(1), 82-87. **https://doi.org/10.5219/705**
14. Nascimento, K., Lopes, D., Takeiti C., Jr, J., Barbosa, M. (2015). Physicochemical characteristics of tubers from organic sweet potato roots. *Revista Caatinga, 28*(2), 225-234.
15. NIH (2022). *Dietary Reference Intakes (DRI)*. National Institutes of Health. Health Information. Food and Nutrition Board, National Academies. USA. **https://www.ncbi.nlm.nih.gov/books/NBK545442/table/appJ_tab3/?report=objectonly.**
16. NOM-F321-S-1978. (1978). Norma Oficial Mexicana. Determinación de Fécula por Hidrólisis Ácida en Embutidos. Mexico. "Starch Determination by Acid Hydrolysis in Sausages".
17. Oloniyo, R., Omoba, O., Awolu, O. (2021). Biochemical and antioxidant properties of cream and orange-fleshed sweet potato. *Heliyon*, *7*(3), art. no. e06533. **https://doi.org/10.1016/j.heliyon.2021.e06533**
18. Palupi, E., Nurdin, N., Mufida, G., Valentine, F., Pangestika, R., Rimbawan, R., Sulaeman, A., Briawan, D., Filianty, F. (2024). High-fiber extruded purple sweet potato (*Ipomoea batatas*) and kidney bean (*Phaseolus vulgaris*) extends the feeling of fullness. *Polish Journal of Food and Nutrition Sciences*, *74*(1), 82-91. **https://doi.org/10.31883/pjfns/183995**
19. Prosky, L., Asp, N., Schweizer, T., DeVries, J., Furda, I. (1988). Determination of insoluble, soluble, and total dietary fiber in foods and food products: Interlaboratory study. *Journal of AOAC International*, *71*(5), 1017-1023. **https://doi.org/10.1093/jaoac/71.5.1017**
20. Re, R., Pellegrini, N., Proteggente, A., Pannala, A., Yang, M., Rice-Evans, C. (1999). Antioxidant activity applying an improved ABTS radical cation decolorization assay. *Free Radical Biology & Medicine*, *26*(9-10), 1231-1237. **https://doi.org/10.1016/S0891-5849(98)00315-3**
21. Ritchie, H., Rosado, P., Roser, M (2023). Sweet potato production – FAO. Agricultural Production. Food and Agriculture Organization of the United Nations. **https://ourworldindata.org/grapher/sweet-potato-production**
22. Rowena, G., Djanna, F., Inacrist, M. (2009). Phenolic content and antioxidant capacity of Philippine sweet potato (*Ipomoea batatas*) varieties. *Food Chemistry, 113*(4), 1133-1138. **https://doi.org/10.1016/j.foodchem.2008.08.088**
23. Ru, W., Pang, Y., Gan, Y., Liu, Q., Bao, J. (2019). Phenolic compounds and antioxidant activities of potato cultivars with white, yellow, red and purple flesh. *Antioxidants, 8*(10), art. no. 419. **https://doi.org/10.3390/antiox8100419**
24. Singleton, V.L., Orthofer, R., Lamuela-Raventós, R.M. (1999). Analysis of total phenols and other oxidation substrates and antioxidants by means of Folin-Ciocalteu reagent. *Methods in Enzymology, 299,* 152–178. **https://doi.org/10.1016/S0076-6879(99)99017-1**
25. Tang, Y., Cai, W., Xu, B. Yayuan, T., Weixi, C., Baojun, X. (2015). Profiles of phenolics, carotenoids and antioxidative capacities of thermal processed white, yellow, orange, and purple sweet potatoes grown in Guilin, China. *Food Science and Human Wellness*, *4*(3), 123-132. **https://doi.org/10.1016/j.fshw.2015.07.003**
26. Teow, C., Truong, V., McFeeters, R., Thompson, R., Pecota, K., Yencho, G. (2007). Antioxidant activities, phenolic and β-carotene contents of sweet potato genotypes with varying flesh colors. *Food Chemistry*, *103*(3), 829–838. **https://doi.org/10.1016/j.foodchem.2006.09.033**
27. Treviño-Gómez, D., Sánchez-Alejo, E., Gontes-Pérez, I., Wong-Paz, J., Rojas, R., Martínez-Ávila, G. (2017). Antioxidant profile of diverse types of herbal infusions and teas commercially available in Mexico. *American Scientific Research Journal for Engineering, Technology, and Sciences, 31*(1), 67-77.
28. Uddin, A., Khalid, R., Alaama, M., Abdualkader, A., Kasmuri, A., Abbas, S. (2016). Comparative study of three digestion methods for elemental analysis in traditional medicine products using atomic absorption spectrometry. *Journal of Analytical Science and Technology*, *7*, art. no. 6. **https://doi.org/10.1186/s40543-016-0085-6**
29. Vergun, O., Dzhamal, R., Rakhmetova, S., Fishchenko, V., Oksana, S. (2020). Content of nutrients in different parts of *Ipomoea batatas* L. (Lam.). *Agrobiodiversity for Improving Nutrition, Health, and Life Quality, 4*, 101-111. **https://doi.org/10.15414/agrobiodiversity.2020.2585-8246.101-111**
30. Vidal, A., Zaucedo-Zuñiga, A., Ramos-García, M. (2018). Nutritional properties of sweet potato (*Ipomoea batatas* L.) and its benefits on human health. *Revista Iberoamericana de Tecnología Postcosecha*, *19*(2), 1665-1679 (in Spanish, English abstract).
31. Zhang, L., Gao, Y., Deng, B., Ru, W., Tong, Ch., Bao, J. (2022). Physicochemical, nutritional, and antioxidant properties in seven sweet potato flours. *Frontiers in Nutrition*, *9*, art. no. 923257. **https://doi.org/10.3389/fnut.2022.923257**
32. Zhishen, J., Mengcheng, T., Jianming, W. (1999). The determination of flavonoid contents in mulberry and their scavenging effects on superoxide radicals. *Food Chemistry*, *64*(4), 555–559. **https://doi.org/10.1016/S0308-8146(98)00102-2**

ORIGINAL ARTICLE
http://journal.pan.olsztyn.pl

Polish Journal of Food and Nutrition Sciences
2024, Vol. 74, No. 4, 387–398
DOI: 10.31883/pjfns/195435
ISSN 1230-0322, e-ISSN 2083-6007

Seasonal Changes in Fatty Acid Composition of *Chondrostoma regium* Lipids

Semra Kaçar[1]*, Hacer Kayhan Kaya[2], Mehmet Başhan[3]

[1]Department of Nutrition and Dietetics, Faculty of Health Sciences, Mardin Artuklu University, 47100 Mardin, Turkey
[2]Department of Physiology, Faculty of Medicine, Dicle University, 21280 Diyarbakır, Turkey
[3]Department of Biology, Faculty of Science, Dicle University, 21280 Diyarbakır, Turkey

This study examined seasonal variations in fatty acid composition of the phospholipid (PL) fraction, triacylglycerol (TAG) fraction, and phospholipid subclass (phosphatidylcholine, PC; phosphatidylinositol, PI; phosphatidylserine, PS; and phosphatidylethanolamine, PE) of muscle tissue of *Chondrostoma regium*, a freshwater fish inhabiting the Munzur River (Turkey). It was found that the percentages of total monounsaturated fatty acids, myristic acid (C14:0), palmitoleic acid (C16:1*n*7), oleic acid (C18:1*n*9), linoleic acid (C18:2*n*6), and linolenic acid (C18:3*n*3) were higher in TAG fraction than in the PL fraction. The ratio of total polyunsaturated fatty acids to total saturated fatty acids was 1.44–1.85, the atherogenicity index ranged from 0.36 to 0.46, while the thrombogenicity index was determined to be between 0.17 and 0.21 in total lipids. The *n*3/*n*6 ratio ranged from 6.55 to 10.49. The fatty acid levels of the PL and PL subclasses, TAG, and total lipid were influenced by the season. Throughout the year, palmitic acid (C16:0), C18:1*n*9, eicosapentaenoic acid (C20:5*n*3, EPA), and docosahexaenoic acid (C22:6*n*3, DHA) were the most abundant in PC. In PE, the share of *n*3 fatty acids decreased from November to April, and percentages of EPA, DHA and docosapentaenoic acid (C22:5*n*3) were high among the *n*3 fatty acids. The predominant fatty acids in PI were stearic acid (C18:0) and arachidonic acid (C20:4*n*6), and throughout the year, the share of C18:0 was the highest in November. In the PS fraction, the percentages of C16:1*n*7 and C18:1*n*9 were high. In summary, *C. regium* can be deemed an excellent source of nutritionally valuable lipids and recommended for wider use in the human diet.

Keywords: fish lipids, lipid fractions, Munzur River, phospholipids, triacylglycerols

INTRODUCTION

Chondrostoma regium (Heckel, 1843), known as "kababurun" in Turkey, is a member of the Cyprinidae family and is distributed in large river systems such as Tigris, Fırat, Seyhan, Ceyhan and Göksu. It is a planktivorous fish that feeds mainly on Bacillariophyta [Tellioğlu *et al.,* 2004]. It is a species of economic importance and is consumed as food by the local people where it is found.

In addition to being an excellent source of protein, this fish is also rich in lipids with polyunsaturated fatty acids (PUFA), especially *n*3 PUFAs, such as docosahexaenoic acid (DHA) and eicosapentaenoic acid (EPA) [Ackman, 2002; Biandolino *et al.,* 2023; Uysal & Aksoylar, 2005]. These acids are not synthesized in the human body and must be provided with diet. Fish are recommended as an excellent source of dietary *n*3 fatty acids, which are high-energy nutrients, but also their consumption protects against chronic diseases such as cardiovascular diseases [Caffrey *et al.,* 2023], arthritis [Kostoglou-Athanassiou *et al.,* 2020], respiratory disorders [Lemoine *et al.,* 2019], Alzheimer's disease [Canhada *et al.,* 2018] and cancers [D'Eliseo & Velotti, 2016]. In addition, a balanced ratio of *n*3 to *n*6 fatty acids in diet is important for health, *e.g.*, an increase in the *n*6/*n*3 ratio increases the risk for obesity [Simopoulos, 2016].

***Corresponding Author:**
Tel: +90-482-2134002-7202; Fax: +90-482-2134004; e-mail: **semrakacar21@gmail.com** (S. Kaçar)

Submitted: 8 June 2024
Accepted: 30 October 2024
Published on-line: 21 November 2024

Fatty acids are components of triacylglycerols and phospholipids. The first of them are storage lipids, the content of which in the fish muscle is significantly correlated with total lipid content [Shirai *et al*., 2002]. In turn, phospholipids, such as phosphatidylcholine (PC), phosphatidylethanolamine (PE), phosphatidylserine (PS) and phosphatidylinositol (PI) are important structural lipids of the cell membranes [Tocher *et al*., 2008]. Moreover, PC is a substrate in the synthesis of the neurotransmitter, acetylcholine, and has the function of nourishing the brain and improving intelligence [Li *et al.,* 2015]. In turn, PE plays an important role in membrane fusion, whereas PS improves nerve cell function, regulates nerve impulse transmission, and enhances the brain memory. The main acidic phospholipids are found in platelet membranes and are responsible for the coagulation process.

Knowing the FA composition of fish lipids is important when investigating fish biology, such as nutrition, reproduction, adaptation, growth, and development. In addition, it is thought that it would be useful to know the FA composition of *C. regium*, which is consumed by both local community and also populations from the surrounding provinces. Studies have been conducted on the total fatty acid content of *C. regium* [Cengiz *et al*., 2010; Kaçar *et al*., 2018]. However, there are no studies on lipid subclasses. Therefore, the aim of this study was to determine the seasonal changes in the fatty acid composition of phospholipids, triacylglycerols, and phospholipid subclasses of *C. regium* and to estimate the nutritional indices of these lipid fractions.

MATERIAL AND METHODS

Fish collection

Fish (*C. regium*) were collected from Munzur River at a site located in a deep and rocky valley on the Tunceli-Ovacık road (Turkey), approximately 20 km from the city center. The coordinates of this place were 39°10′44.68″N, 39°27′43.08″E. Fish caught in July, November, January, and April were brought to the Dicle University laboratory (Diyarbakır, Turkey) in a cold environment to prevent them from spoiling. Three sexually mature female fish collected in each season were taken for analysis. Their weights and fork lengths were measured, and results are shown in **Table 1**.

Lipid extraction and fractionation

Five grams of muscle were taken from the region between the lateral line and the dorsal fins of each fish collected in each month. Total lipids were extracted from the tissue with the method of Folch *et al*. [1957] using a mixture of chloroform and methanol (2:1, *v/v*), and crude extracts were stored at –80°C until analysis. Fractionation of total lipids was performed using thin layer chromatography (TLC). A mixture of petroleum ether, diethyl ether, and acetic acid (80:20:1, *v/v/v*) was used to run the crude extracts on the plates. The bands corresponding to phospholipid (PL) and triacylglycerol (TAG) fractions established by the standards, were scraped and transferred to tubes. The PL fraction was plated, and the separation of phosphatidylcholine (PC), phosphatidylethanolamine (PE), phosphatidylserine (PS), phosphatidylinositol (PI) was performed using a mixture of chloroform, ethanol, water, and triethylamine (30:35:7:35, *v/v/v*) [Vaden *et al*., 2005]. The bands were scraped and individual PL subclasses were washed out with *n*-hexane.

Fatty acid analysis

Crude extracts and fractions separated by TLC were heated with methanol (4 mL) and sulfuric acid (4 drops) at 85°C under reflux for 2 h to produce methyl esters of fatty acids. Then, the mixtures were extracted three times with 5 mL of *n*-hexane, and analysis of fatty acid methyl esters was performed using a GC 2010 Plus gas chromatograph with a flame ionization detector (Shimadzu, Kyoto, Japan) and a DB-23 capillary column with (50% cyanopropyl)-methylpolysiloxane (30 m × 0.25 mm i.d. × 0.25 µm film thickness) (J & W Scientific, Folsom, CA, USA). The compressed air and hydrogen were used with the flow rates of 400 mL/min and 30 mL/min, respectively. The flow rate of a carrier gas (helium) was 0.5 mL/min. Temperature of the injection port and the detector were constant at 250°C. The split ratio was 1:20. The oven temperature was set at an initial value of 170°C and held constant for 2 min, and then increased from 170°C to 210°C at a rate of 2°C/min. Total analysis time was 42 min. A mixture of methyl esters of fatty acids (Sigma-Aldrich, Saint Louis, MO, USA) was utilized as a standard in the identification of fatty acids. The GC Solution (version 2.4, Shimadzu) software was utilized to obtain chromatograms of methyl esters of fatty acids and total quantities of fatty acids. Peaks in the chromatogram were identified by comparing the retention times of methyl esters of all fatty acids in the standard. The quantitative values were calculated as percentage of total fatty acids. The samples were examined in triplicate.

Nutritional indices calculation

The atherogenic index (AI) and thrombogenic index were (TI) calculated using fish lipid fatty acid data [Biandolino *et al.,* 2023], according to Equations (1) and (2), respectively:

Table 1. Weight and length of *Chondrostoma regium* collected in different seasons, and total lipid content of its muscle.

Parameter	July	November	January	April
Length (cm)	25±10^{b}	31±125^{a}	23±10^{b}	24±13^{b}
Weight (g)	162±8.4^{b}	382±14^{a}	146±4.3^{b}	130±6.5^{c}
Total lipid content (g/100 g)	1.51±0.06^{a}	1.46±0.04^{a}	1.26±0.04^{b}	1.15±0.05^{c}

Values reported are means ± standard deviation (n=3). Means followed by different letters in the same line are significantly different (p<0.05).

$$AI = \frac{4 \times C14:0 + C16:0 + C18:0}{\sum PUFA + \sum MUFA} \quad (1)$$

$$TI = \frac{C14:0 + C16:0 + C18:0}{0.5 \times \sum MUFA + 0.5 \times \sum n6 + 3 \times \sum n3 + \frac{\sum n3}{\sum n6}} \quad (2)$$

where: ∑PUFA, total polyunsaturated fatty acids; and ∑MUFA, total monounsaturated fatty acids.

Statistical analysis

The samples were examined in triplicate. The data were analyzed using one-way analysis of variance (ANOVA), and comparison of means for fish colledted in different seasons was performed using Tukey's test. Differences were determined to be significant at $p<0.05$. The statistical analyses were carried out using SPSS Statistics 22.0 computer program (IBM, Armonk, NY, USA).

RESULTS AND DISCUSSION

Total lipid content

The total lipid content of *C. regium* muscle varied between 1.15 g/100 g (fish caught in April) and 1.51 g/100 g (fish colleted in July) (**Table 1**). These values allow us to consider *C. regium* as a lean fish based on the classification of Ackman [1990], according to which lean fish are those with lipid content less than 2%. In our previous study, we found even a lower total lipid content (0.92%) in female *C. regium* from Atatürk Dam Lake [Kaçar *et al*., 2018].

The total lipid content of *C. regium* muscle was determined to be significantly ($p<0.05$) higher in the pre-reproductive period (January) than in the reproductive period (April) (**Table 1**). According to research [Rasoarahona *et al.,* 2008], muscle tissue's lipid content decreases during the reproductive stage, which is consistent with our study findings. The content of storage lipids changes throughout the breeding and feeding periods, as the total lipids have been reported to increase in the winter but decrease in the summer months [Di Lena *et al*., 2016; Guerra *et al*., 2022]. In the present study, the highest total lipid content was found in the fish from summer (**Table 1**). Later, it was determined that the total lipid content of *C. regium* decreased towards April, which is the breeding season.

Fatty acid composition of total lipids

Fatty acid composition of total lipids of *C. regium* collected in different months is shown in **Table 2**. Total saturated fatty acids (∑SFA) and palmitic acid (main SFA), were found at the lowest levels (26.03% and 18.16% of total FAs, respectively) in April, *i.e.*, in the middle of *C. regium* breeding period. These values started to increase and reached the highest level (32.36% and 24.25% of total FAs for ∑SFA and C16:0, respectively) in January, which was the pre-breeding period. The contribution of total monounsaturated fatty acids (∑MUFA) and C16:1*n*7 in total FAs of *C. regium* lipids was low before fish breeding (January) and increased during the breeding period.

The fatty acid with the highest percentage among SFAs was C16:0 (**Table 2**). C18:0 and C14:0 acids were found in smaller amounts. In turn, C18:1*n*9 and C16:1*n*7 acids were found to be dominant among MUFAs, while EPA and DHA were found to be dominant among polyunsaturated fatty acids. The C18:2*n*6, C18:3*n*3, C20:2*n*6, C20:3*n*6, C20:4*n*6 and C22:5*n*3 acids were also identified, but their share in MUFAs of total lipids was lower. The *n*3/*n*6 ratio of total lipids, which is a significant indicator in determining the nutritional value of fish lipids for humans, was found to be between 6.55 to 10.49.

The share of total polyunsaturated fatty acids in FAs of *C. regium* lipids was higher than that reported in literature for other freshwater fish species [Bušová *et al*., 2020; Emre *et al*., 2020; Łuczyńska *et al*., 2012; Tommonaro *et al*., 2023]. This could be primarily due to water sources. It was expected that fish in cold waters, such as Munzur River, would have greater PUFA levels. Freshwater fish in temperate and warm climates contain less *n*6 fatty acids, because plankton, which fish feed on, inhibits the synthesis of unsaturated fatty acids with a low melting point at a higher temperature, whereas cold and deep-sea fish contain more fatty acids, which melt at a lower temperature [Sushchic *et al*., 2018].

Previous studies have reported that the content of C16:0 was high in total lipids of *C. regium* caught in Atatürk Dam Lake [Kaçar *et al*., 2018] and Tigris River [Cengiz *et al*., 2010]. A similar result was obtained in the present study. Our finding regarding the percentage of C16:1*n*7 in total lipids of *C. regium* was also consistent with literature data [Cengiz *et al*., 2010; Kaçar *et al*., 2018].

Fish obtain fatty acids, such as C18:2*n*6 and C18:3*n*3, which they cannot synthesize, from their food and use these fatty acids as precursors for the production of other PUFAs. Moreover, fish that generally feed on zooplankton are rich in C18:2*n*6 and C20:4*n*6 [Parzanini *et al*., 2020]. However, in this study, these fatty acids were determined to be present in total lipids of *C. regium,* feeding on plankton-based diet, in low percentages. This seems to be specific to this species because previous studies have also shown that *C. regium* lipids contained low levels of C18:2*n*6 and C18:3*n*3 [Cengiz *et al*., 2010; Kaçar *et al*., 2018]. In the total lipid fraction of *C. regium* muscle, the percentage of DHA and particularly EPA was found to be higher than those in many other freshwater fish [Bušová *et al.,* 2020; Emre *et al.,* 2020; Haliloğlu *et al.,* 2004; Tommonaro *et al.,* 2023] and in the same species from other fishing locations [Cengiz *et al*., 2010; Kaçar *et al*., 2018]. Similarly, the *n*3/*n*6 ratio of fatty acids of *C. regium* total lipids was substantially higher than in many freshwater fish (*Sander lucioperca, Pseudophoxinus fahrettini, Capoeta mauricii*) [Emre *et al.,* 2020; Uysal & Aksoylar, 2005], and in *C. regium* from other rivers [Cengiz *et al*., 2010; Kaçar *et al*., 2018]. The quality of fish lipids is usually assessed using several indices including, apart from *n*3/*n*6 ratio, also ∑PUFA/∑SFA ratio, AI and TI based on fatty acid composition [Biandolino *et al.,* 2023].

The ∑PUFA/∑SFA ratio in a human diet is recommended to be above 0.45, whereas AI and TI of foods are recommended to be less than 1.0 and 0.5, respectively [Woloszyn *et al*., 2020].

Table 2. Fatty acid composition (% of total fatty acids) and nutritional indices of total lipids of muscle of *Chondrostoma regium* collected in different seasons.

Fatty acid/Nutritional index	July	November	January	April
C14:0	2.96±0.20^{a}	2.11±0.16^{b}	1.75±0.10^{b}	2.16±0.13^{b}
C15:0	0.32±0.02^{b}	0.48±0.02^{ab}	0.41±0.03^{ab}	0.64±0.03^{a}
C16:0	18.93±0.85^{b}	20.94±1.02^{b}	24.25±1.25^{a}	18.16±0.74^{b}
C17:0	0.47±0.02^{b}	0.39±0.02^{b}	0.22±0.01^{c}	0.58±0.03^{a}
C18:0	6.53±0.35^{a}	5.90±0.25^{ab}	5.73±0.28^{ab}	4.49±0.25^{b}
∑SFA	29.21±1.42^{b}	29.82±1.40^{b}	32.36±1.67^{a}	26.03±1.18^{c}
C16:1*n*7	12.33±0.72^{b}	8.93±0.48^{c}	8.9±0.34^{c}	14.19±0.60^{a}
C18:1*n*9	12.79±0.58^{a}	13.12±0.70^{a}	11.52±0.53^{a}	11.11±0.56^{a}
C20:1*n*9	0.41±0.03^{a}	0.28±0.01^{b}	0.49±0.02^{a}	0.35±0.01^{ab}
∑MUFA	25.53±1.36^{a}	22.33±1.22^{ab}	20.91±1.05^{b}	25.65±1.19^{a}
C18:2*n*6	1.71±0.06^{b}	1.01±0.04^{c}	0.73±0.03^{c}	2.02±0.11^{a}
C18:3*n*3	1.02±0.04^{a}	1.03±0.06^{a}	0.61±0.02^{b}	0.80±0.04^{ab}
C20:2*n*6	0.38±0.02^{b}	0.20±0.^{01ab}	0.27±0.01^{ab}	0.51±0.02^{a}
C20:3*n*6	0.51±0.03^{b}	0.92±0.04^{a}	0.39±0.02^{b}	0.53±0.02^{b}
C20:4*n*6	3.38±0.12^{a}	2.45±0.10^{a}	2.67±0.15^{a}	2.93±0.16^{a}
C20:5*n*3	20.33±1.02^{b}	23.63±1.28^{a}	20.1±0.92^{b}	20.22±0.87^{b}
C22:5*n*3	5.52±0.23^{a}	5.61±0.18^{a}	6.04±0.26^{a}	4.38±0.20^{a}
C22:6*n*3	12.33±0.62^{b}	12.93±0.55^{b}	15.84±0.70^{a}	16.88±0.88^{a}
∑PUFA	45.18±2.10^{a}	47.78±2.18^{a}	46.65±2.34^{a}	48.27±2.32^{a}
∑*n*3	39.2±1.76^{b}	43.2±2.16^{a}	42.59±2.18^{a}	42.28±1.89^{a}
∑*n*6	5.98±0.32^{a}	4.58±0.35^{b}	4.06±0.20^{b}	5.99±0.30^{a}
*n*3/*n*6	6.55±0.08^{b}	9.43±0.12^{a}	10.49±0.23^{a}	7.05±0.11^{b}
∑PUFA/∑SFA	1.55±0.45^{b}	1.60±0.88^{b}	1.44±0.39^{b}	1.85±0.56^{a}
AI	0.43±0.23^{a}	0.42±0.16^{a}	0.46±0.67^{a}	0.36±0.90^{b}
TI	0.20±0.09^{a}	0.19±0.08^{a}	0.21±0.01^{a}	0.17±0.22^{b}

Values reported are means ± standard deviation (n=3). Means followed by different letters in the same line are significantly different (p<0.05). SFA, saturated fatty acids; MUFA, monounsaturated fatty acids; PUFA, polyunsaturated fatty acids; AI; atherogenicity index; TI, thrombogenicity index.

The values of these indices determined for *C. regium* (**Table 2**) met the above criteria and, therefore, this species of fish can be considered as food eliciting health benefits.

Fatty acid composition of the triacylglycerol fraction

The triacylglycerol (TAG) fraction separated from *C. regium* muscle was characterized by the share of the ΣSFA in the total fatty acids in the range of 22.75–27.21%, with the lowest level recorded in the fish caught in January (**Table 3**), which was the pre-breeding season, and when water temperature was low. The percentage of C16:0 was determined as 16.80% of total FAs (January) to 19.73% of total FAs (November). Other predominant SFAs were C14:0 and C18:0. The ∑MUFA ranged from 22.86% to 36.85% of total FAs through the year. The highest contribution of MUFAs to FAs of the TAG fraction was found in the fish collected in April and November, and PUFAs were dominant in the fish from July and January. EPA and DHA among PUFAs, and C16:1*n*7 and C18:1*n*9 among MUFAs, were the most prevalent fatty acids in the TAG fraction of *C. regium*. Previous studies showed that the percentage of the main fatty acid of the fish muscle TAG fraction, C16:0, varied significantly within the species [Kaçar *et al.,* 2018; Kayhan *et al*., 2015; Satar *et al*., 2012]. In turn, Shirai *et al*. [2002] reported that C16:0, C16:1*n*7 and C18:1*n*9 were the major fatty acids of TAG of wild and cultured catfish, and concluded that these fatty acids were primarily used for energy production.

Table 3. Fatty acid composition (% of total fatty acids) and nutritional indices of the triacylglycerol fraction of muscle of *Chondrostoma regium* collected in different seasons.

Fatty acid/Nutritional index	July	November	January	April
C14:0	1.36±0.07^{b}	3.04±0.12^{a}	1.19±0.08^{b}	4.15±0.20^{a}
C15:0	0.37±0.02^{b}	0.53±0.03^{ab}	0.32±0.02^{b}	0.94±0.03^{a}
C16:0	18.16±0.62^{a}	19.73±0.85^{a}	16.8±0.64^{a}	17.82±0.70^{a}
C17:0	0.91±0.03^{a}	0.34±0.02^{b}	0.12±0.01^{c}	0.38±0.02^{b}
C18:0	3.14±0.10^{b}	3.57±0.13^{b}	4.32±0.15^{a}	2.31±0.09^{c}
∑SFA	23.94±1.28^{b}	27.21±1.52^{a}	22.75±1.08^{b}	25.6±1.20^{ab}
C16:1*n*7	10.73±0.52^{c}	17.38±0.70^{b}	13.45±0.62^{c}	20.64±1.01^{a}
C18:1*n*9	11.74±0.58^{b}	15.26±0.61^{a}	14.65±0.64^{a}	15.77±0.72^{a}
C20:1*n*9	0.39±0.02^{b}	0.54±0.03^{b}	1.34±0.10^{a}	0.44±0.02^{b}
∑MUFA	22.86±1.02^{b}	33.18±1.82^{a}	29.44±1.33^{ab}	36.85±1.80^{a}
C18:2*n*6	2.05±0.06^{b}	2.57±0.09^{a}	1.98±0.06^{b}	2.33±0.11^{a}
C18:3*n*3	0.97±0.04^{b}	1.23±0.05^{a}	0.71±0.03^{c}	1.17±0.04^{ab}
C20:2*n*6	0.50±0.02^{a}	0.16±0.01^{b}	0.43±0.02^{a}	0.29±0.01^{b}
C20:3*n*6	0.57±0.02^{a}	0.55±0.02^{a}	0.65±0.03^{a}	0.49±0.02^{a}
C20:4*n*6	4.72±0.20^{a}	1.31±0.10^{b}	3.84±0.15^{a}	1.11±0.09^{b}
C20:5*n*3	24.04±1.11^{a}	20.64±0.97^{b}	22.75±1.13^{ab}	20.48±1.03^{b}
C22:5*n*3	7.34±0.32^{a}	4.70±0.20^{ab}	5.50±0.27^{ab}	3.31±0.19^{b}
C22:6*n*3	12.93±0.58^{a}	8.39±0.47^{b}	11.86±0.63^{a}	8.29±0.38^{b}
∑PUFA	53.12±2.78^{a}	39.55±1.80^{b}	47.72±2.31^{ab}	37.47±1.89^{b}
∑*n*3	45.28±2.19^{a}	34.96±1.72^{b}	40.82±2.12^{ab}	33.25±1.82^{b}
∑*n*6	7.84±0.34^{a}	4.59±0.21^{b}	6.90±0.32^{a}	4.22±0.20^{b}
*n*3/*n*6	5.77±0.05^{b}	7.61±0.04^{a}	5.91±0.34^{b}	7.87±0.89^{a}
∑PUFA/∑SFA	2.22±0.32^{a}	1.45±0.48^{b}	2.10±0.09^{a}	1.46±0.98^{b}
AI	0.31±0.50^{b}	0.44±0.06^{a}	0.28±0.05^{c}	0.46±0.33^{a}
TI	0.14±0.40^{b}	0.20±0.23^{a}	0.15±0.47^{b}	0.19±0.08^{a}

Values reported are means ± standard deviation (n=3). Means followed by different letters in the same line are significantly different (p<0.05). SFA, saturated fatty acids; MUFA, monounsaturated fatty acids; PUFA, polyunsaturated fatty acids; AI, atherogenicity index; TI, thrombogenicity index.

Among the nutritional indices of the TAG fraction, the ∑PUFA/∑SFA ratio ranged from 1.45 (November) to 2.22 (July), AI was from 0.28 (January) to 0.46 (April) and TI varied between 0.14 (July) and 0.20 (November) (**Table 3**). In turn, the *n*3/*n*6 ratio was found to be in the range of 5.77–7.87. Previous research with freshwater fish (*Vimba vimba, Capoeta sieboldu, C. regium*) showed lower values [Görgün *et al.,* 2013, 2014; Kaçar *et al*., 2018]. This was mainly because the two main *n*3 fatty acids, EPA and DHA, were highly abundant in the TAG fraction of *C. regium* in our study, compared to the fish analyzed in other studies, whereas the share of *n*6 fatty acids, C18:2*n*6, C20:4*n*6 and C20:3*n*6, was low.

Fatty acid composition of the phospholipid fraction and its subclasses

The fatty acid composition of the phospholipid (PL) fraction separated from of *C. regium* muscle is shown in **Table 4**. The share of C16:0 and ∑SFA was the highest in PL fatty acids of the fish

Table 4. Fatty acid composition (% of total fatty acids) and nutritional indices of the phospholipid fraction of muscle of *Chondrostoma regium* collected in different seasons.

Fatty acid/Nutritional index	July	November	January	April
C14:0	0.72±0.04^{a}	0.40±0.02^{b}	0.59±0.02^{ab}	0.51±0.03^{ab}
C15:0	0.26±0.01^{b}	0.30±0.02^{a}	0.21±0.02^{b}	0.36±0.02^{a}
C16:0	20.99±1.06^{b}	26.44±1.26^{a}	23.45±1.11^{b}	20.73±1.12^{b}
C17:0	0.04±0.01^{b}	0.55±0.03^{a}	0.55±0.02^{a}	0.68±0.05^{a}
C18:0	8.09±0.30^{a}	8.79±0.39^{a}	7.23±0.27^{a}	7.57±0.35^{a}
∑SFA	30.1±1.58^{b}	36.48±1.63^{a}	32.03±1.69^{b}	29.85±1.51^{b}
C16:1*n*7	4.90±0.22^{a}	3.37±0.20^{a}	4.66±0.21^{a}	3.93±0.17^{a}
C18:1*n*9	12.15±0.60^{a}	12.16±0.54^{a}	13.35±0.68^{a}	9.78±0.87^{b}
C20:1*n*9	0.30±0.02^{b}	0.59±0.03^{a}	0.64±0.03^{a}	0.31±0.02^{b}
∑MUFA	17.35±0.63^{a}	16.12±0.55^{a}	18.65±0.85^{a}	14.02±0.77^{a}
C18:2*n*6	1.82±0.11^{a}	0.65±0.04^{b}	1.47±0.05^{a}	1.57±0.07^{a}
C18:3*n*3	0.62±0.03^{a}	0.45±0.02^{b}	0.53±0.03^{ab}	0.27±0.01^{c}
C20:2*n*6	0.47±0.02^{b}	0.21±0.01^{c}	0.44±0.02^{b}	0.69±0.04^{a}
C20:3*n*6	0.34±0.01^{b}	0.40±0.02^{a}	0.47±0.02^{a}	0.43±0.01^{a}
C20:4*n*6	3.15±0.17^{a}	3.62±0.30^{a}	2.92±0.10^{a}	3.92±0.34^{a}
C20:5*n*3	20.54±1.06^{a}	20.12±1.17^{a}	19.54±0.90^{a}	20.19±1.03^{a}
C22:5*n*3	4.92±0.22^{a}	5.68±0.30^{a}	4.41±0.17^{a}	4.86±0.29^{a}
C22:6*n*3	20.62±1.12^{b}	16.19±0.82^{c}	19.46±0.98^{b}	24.12±1.68^{a}
∑PUFA	52.48±2.60^{b}	47.32±2.23^{c}	49.24±2.41^{c}	56.05±2.76^{a}
∑*n*3	46.7±2.26^{a}	42.44±2.10^{b}	43.94±2.14^{b}	49.44±2.42^{a}
∑*n*6	5.78±0.28^{a}	4.88±0.23^{a}	5.30±0.24^{a}	6.61±0.33^{a}
*n*3/*n*6	8.07±0.67^{a}	8.69±0.45^{a}	8.29±0.30^{a}	7.47±0.40^{a}
∑PUFA/∑SFA	1.74±0.34^{a}	1.30±0.32^{c}	1.54±0.42^{b}	1.88±0.58^{a}
AI	0.34±0.30^{b}	0.44±0.09^{a}	0.38±0.06^{b}	0.32±0.38^{b}
TI	0.19±0.40^{b}	0.24±0.20^{a}	0.21±0.11^{a}	0.17±0.07^{b}

Values reported are means ± standard deviation (n=3). Means followed by different letters in the same line are significantly different (p<0.05). SFA, saturated fatty acids; MUFA, monounsaturated fatty acids; PUFA, polyunsaturated fatty acids; AI, atherogenicity index, TI, thrombogenicity index.

caught in November, but there were no significant (p≥0.05) differences in C18:0 content throughout the year (7.23–8.79% of total FAs). The percentage of C18:1*n*9 was significantly (p<0.05) lower in the sample from April, although the ∑MUFA did not differ significantly (p≥0.05) depending on the month of fishing. The contribution of ∑PUFA to PL fatty acids was the higest in the fish caught in April. Throughout all seasons, the percentage of ∑PUFA was higher than ∑MUFA, and EPA and DHA have been determined as the major PUFAs of PLs. During the reproductive season in April, DHA was found at the highest level. In trun, C20:4*n*6 was detected in low amounts throughout the year. The main fatty acids found in PLs of *C. regium* muscle were consistent with those found in other freshwater fish [Görgün *et al*., 2014, Kayhan *et al.,* 2015; Shirai *et al*., 2002].

The C18:0 was detected at a higher share in PSs than in total lipids (**Table 2** and **4**). Although C18:0 is a saturated fatty acid, it tended to accumulate in the PL fraction. There were no significant (p≥0.05) differences in EPA content throughout the year (**Table 4**). It is expected that phospholipids, which are structural lipids, are rich in PUFAs.

Henderson & Tocher [1987] reported that the *n*3/*n*6 ratio of the PLs of freshwater fish was between 1.6 and 2.0, whereas

Table 5. Fatty acid composition (% of total fatty acids) and nutritional indices of phosphatidylcholine of muscle of *Chondrostoma regium* collected in different seasons.

Fatty acid/Nutritional index	July	November	January	April
C14:0	0.40±0.02^{b}	0.42±0.02^{b}	0.72±0.03^{a}	0.68±0.04^{a}
C15:0	0.23±0.01^{b}	0.31±0.02^{ab}	0.39±0.02^{a}	0.40±0.02^{a}
C16:0	21.95±1.04^{b}	30.53±1.55^{a}	28.83±1.32^{a}	25.8±1.34^{ab}
C17:0	0.83±0.04^{a}	0.51±0.02^{b}	0.51±0.02^{b}	0.46±0.03^{b}
C18:0	6.90±0.31^{a}	2.79±0.12^{b}	2.99±0.27^{b}	5.29±0.55^{a}
∑SFA	30.31±1.58^{a}	34.56±1.60^{a}	33.44±1.55^{a}	32.63±1.74^{a}
C16:1*n*7	4.73±0.20^{b}	4.71±0.28^{b}	7.40±0.44^{a}	4.16±0.18^{b}
C18:1*n*9	12.68±0.64^{a}	13.19±0.55^{a}	14.1±0.63^{a}	12.81±0.57^{a}
C20:1*n*9	0.34±0.02^{b}	0.25±0.01^{b}	0.27±0.02^{b}	0.88±0.05^{a}
∑MUFA	17.75±0.70^{b}	18.15±0.78^{b}	21.77±1.12^{a}	17.85±0.83^{b}
C18:2*n*6	1.15±0.07^{b}	1.81±0.06^{ab}	1.72±0.10^{ab}	2.57±0.10^{a}
C18:3*n*3	0.34±0.03^{b}	0.55±0.03^{a}	0.43±0.02^{ab}	0.36±0.02^{b}
C20:2*n*6	0.54±0.02^{a}	0.14±0.01^{b}	0.13±0.01^{b}	0.31±0.03^{a}
C20:3*n*6	0.40±0.04^{a}	0.26±0.02^{b}	0.46±0.02^{a}	0.44±0.03^{a}
C20:4*n*6	4.88±0.23^{a}	2.20±0.16^{b}	2.79±0.14^{b}	2.74±0.17^{b}
C20:5*n*3	17.63±0.69^{b}	22.32±1.17^{a}	20.54±1.03^{a}	17.15±0.77^{b}
C22:5*n*3	6.05±0.32^{a}	4.35±0.24^{b}	3.15±0.30^{b}	4.21±0.21^{b}
C22:6*n*3	20.88±1.13^{a}	15.58±0.81^{b}	15.48±0.68^{b}	21.66±1.10^{a}
∑PUFA	51.87±2.81^{a}	47.21±2.30^{ab}	44.70±2.42^{b}	49.44±2.49^{ab}
∑*n*3	44.9±2.21^{a}	42.8±2.15^{a}	39.6±2.10^{b}	43.38±2.13^{a}
∑*n*6	6.97±0.28^{a}	4.41±0.23^{b}	5.10±0.34^{b}	6.06±0.28^{a}
*n*3/*n*6	6.44±0.39^{c}	9.70±0.56^{a}	7.76±0.35^{b}	7.15±0.22^{b}
∑PUFA/∑SFA	1.71±0.11^{a}	1.37±0.15^{c}	1.34±0.36^{c}	1.52±0.78^{b}
AI	0.34±1.22^{b}	0.49±1.09^{a}	0.48±1.05^{a}	0.42±0.35^{a}
TI	0.19±0.05^{a}	0.23±0.34^{a}	0.23±0.25^{a}	0.21±0.22^{a}

Values reported are means ± standard deviation (n=3). Means followed by different letters in the same line are significantly different (p<0.05). SFA, saturated fatty acids; MUFA, monounsaturated fatty acids; PUFA, polyunsaturated fatty acids; AI, atherogenicity index; TI, thrombogenicity index.

in in our study it was in the range of 7.47–8.69 (**Table 4**). The main cause for the high *n*3/n6 ratio of the PLs from *C. regium* muscle was the relatively high levels of EPA, one of the essential *n*3 fatty acids, and the very low levels of n*6* fatty acids. Other nutritional indices of PLs from *C. regium* muscle ranged from 1.30 to 1.88 for the ∑PUFA/∑SFA ratio, from 0.32 to 0.44 for AI and from 0.17 to 0.24 for TI.

Considering the fatty acid composition of the phospholipid subclasses, it was observed that the seasonal fatty acid distribution in the phosphatidylcholine (PC) of *C. regium* muscle (**Table 5**) was similar to the fatty acid distribution in the PL fraction (**Table 4**). C16:0, C18:1*n9*, EPA and DHA were found to be characteristic of the PC (**Table 5**). The fatty acid composition allowed to determine quality indices of PC at the levels of 1.34–1.71 for the ∑PUFA/∑SFA ratio, 0.34–0.49 for AI and 0.19–0.23 for TI.

The predominant contribution of C16:0, C18:1*n*9, EPA, and DHA in the fatty acids of PC found in our study was consistent with literature data; these fatty acids have been determined to be prevalent in *Alburnus mossulensis* [Kızmaz, 2021], *Myoxocephalus jaok* [Kostetsky *et al*., 2018], and *Cololabis saira* [Tao *et al.,* 2024]. It has been shown that season, temperature and environment of fish growth, and dietary fatty acids have an effect on the composition of PC fatty acid in fish muscle [Lie *et al*., 1992a]. For example, it was emphasized that the share of C16:0

Table 6. Fatty acid composition (% of total fatty acids) and nutritional indices of phosphatidylethanolamine of muscle of *Chondrostoma regium* collected in different seasons.

Fatty acid/Nutritional index	July	November	January	April
C14:0	0.93±0.03^{a}	0.13±0.01^{b}	0.48±0.02^{ab}	0.70±0.03^{b}
C15:0	0.09±0.01^{a}	0.05±0.01^{b}	0.10±0.02^{a}	0.09±0.01^{a}
C16:0	8.92±0.37^{b}	13.08±0.60^{a}	14.51±0.63^{a}	12.71±0.57^{a}
C17:0	1.16±0.05^{a}	0.79±0.03^{b}	0.91±0.03^{b}	0.77±0.02^{b}
C18:0	11.09±0.51^{a}	11.61±0.42^{a}	7.63±0.37^{b}	10.58±0.58^{a}
∑SFA	22.19±1.06^{a}	25.66±1.13^{a}	23.63±1.09^{a}	24.85±1.15^{a}
C16:1*n*7	3.43±0.18^{a}	1.33±0.06^{b}	2.90±0.14^{ab}	2.40±0.11^{ab}
C18:1*n*9	8.53±0.33^{a}	7.82±0.36^{a}	9.11±0.44^{a}	10.47±0.55^{a}
C20:1*n*9	0.41±0.02^{a}	0.35±0.02^{a}	0.58±0.03^{a}	0.34±0.02^{a}
∑MUFA	12.37±0.58^{a}	9.50±0.49^{b}	12.59±0.63^{a}	13.21±0.54^{a}
C18:2*n*6	1.04±0.04^{a}	0.54±0.02^{b}	0.80±0.03^{b}	1.16±0.07^{a}
C18:3*n*3	0.35±0.02^{a}	0.26±0.01^{a}	0.35±0.03^{a}	0.35±0.03^{a}
C20:2*n*6	0.52±0.03^{a}	0.20±0.01^{b}	0.34±0.01^{ab}	0.57±0.03^{a}
C20:3*n*6	0.56±0.03^{b}	0.53±0.02^{b}	1.13±0.05^{a}	0.76±0.03^{ab}
C20:4*n*6	6.02±0.27^{a}	3.68±0.15^{b}	4.64±0.17^{b}	5.58±0.25^{a}
C20:5*n*3	17.85±0.88^{b}	22.71±1.10^{a}	19.12±0.92^{b}	17.32±0.80^{b}
C22:5*n*3	9.18±0.43^{b}	11.27±0.58^{a}	7.01±0.38^{b}	7.65±0.33^{b}
C22:6*n*3	29.84±1.39^{a}	25.59±1.23^{b}	30.31±1.53^{a}	28.47±1.37^{a}
∑PUFA	65.36±3.24^{a}	64.78±3.19^{a}	63.7±3.22^{a}	61.86±3.02^{a}
∑*n*3	57.22±2.21^{a}	59.83±2.90^{a}	56.79±2.73^{a}	53.79±2.55^{b}
∑*n*6	7.45±0.45^{a}	4.95±0.20^{b}	6.91±0.29^{ab}	8.07±0.37^{a}
*n*3/*n*6	7.68±0.56^{c}	12.08±0.30^{a}	8.21±0.40^{b}	6.66±0.32^{d}
∑PUFA/∑SFA	2.95±0.11^{a}	2.52±0.13^{a}	2.70±0.09^{a}	2.49±0.65^{a}
AI	0.16±0.08^{b}	0.18±0.04^{b}	0.22±0.02^{a}	0.21±0.18^{a}
TI	0.11±0.22^{a}	0.12±0.34^{a}	0.12±0.45^{a}	0.13±0.29^{a}

Values reported are means ± standard deviation (n=3). Means followed by different letters in the same line are significantly different (p<0.05). SFA, saturated fatty acids; MUFA, monounsaturated fatty acids; PUFA, polyunsaturated fatty acids; AI, atherogenicity index; TI, thrombogenicity index.

and C18:1*n*9 increased in PC fatty acids of *A. mossulensis* in November, while the share of EPA and DHA decreased in the same period [Kızmaz, 2021]. In the present study, it was determined that the percentage of EPA in PC fatty acids was significantly higher in the fish caught in November and January than in those from April and July.

Similar to the PC, C16:0, C18:1*n*9, EPA and DHA were shown to be predominant in the fatty acid composition of phosphatidylethanolamine (PE) of *C. regium* muscle (**Table 6**). However, the nutritional indices of PE differed from those of PC; the ∑PUFA/∑SFA ratio of PE was found in the range of 2.49 (April) to 2.95 (July); AI was between 0.16 (July) and 0.22 (January) and TI varied from 0.11 (July) to 0.13 (April). The contribution of ∑MUFA to fatty acids of PE of *C. regium* decreased slightly in November. In addition, the *n*3/*n*6 ratio of PE was found to be higher in lipids of the fish caught in November compared to those caught in other periods. Compared to the results obtained for the PL fraction, the fatty acid composition of PE was richer in C18:0, C20:4*n*6, EPA, C22:5*n*3 and DHA. However, the contribution of C16:0 and C18:1*n*9 to PE was found to be lower than to the PL fraction. Compared to *A. mossulensis* [Kızmaz, 2021], *C. regium*, in our analysis, had a higher EPA and a lower C20:4*n*6 contribution to fatty acids of PE. The high proportions of DHA and EPA in the PE of *C. regium* lipids were consistent with results of studies conducted with halibut

Table 7. Fatty acid composition (% of total fatty acids) and nutritional indices of phosphatidylinositol of muscle of *Chondrostoma regium* collected in different seasons.

Fatty acid/Nutritional index	July	November	January	April
C14:0	1.90±0.06^{a}	0.15±0.01^{c}	1.05±0.04^{b}	1.90±0.05^{a}
C15:0	0.17±0.01^{b}	0.06±0.01^{c}	0.19±0.02^{b}	0.24±0.01^{a}
C16:0	22.54±1.08^{a}	8.03±0.32^{c}	15.37±0.68^{b}	15.11±0.73^{b}
C17:0	1.34±0.07^{a}	0.65±0.03^{b}	0.79±0.04^{b}	1.08±0.04^{a}
C18:0	31.62±1.31^{b}	42.53±2.12^{a}	27.07±1.27^{c}	39.65±1.94^{a}
∑SFA	57.57±2.77^{a}	51.41±2.25^{ab}	44.47±2.19^{b}	57.98±2.80^{a}
C16:1*n*7	4.40±0.22^{a}	1.0±0.05^{c}	2.30±0.09^{b}	4.48±0.15^{a}
C18:1*n*9	6.85±0.31^{b}	8.51±0.45^{a}	6.83±0.28^{b}	9.97±0.40^{a}
C20:1*n*9	0.45±0.02^{a}	0.30±0.02^{a}	0.15±0.01^{b}	0.38±0.02^{a}
∑MUFA	11.7±0.54^{b}	9.81±0.37^{b}	9.28±0.45^{b}	14.83±0.67^{a}
C18:2*n*6	0.89±0.04^{b}	0.26±0.01^{c}	0.76±0.03^{b}	1.34±0.04^{a}
C18:3*n*3	1.32±0.03^{a}	1.65±0.07^{a}	0.37±0.02^{b}	0.50±0.03^{b}
C20:2*n*6	0.12±0.01^{b}	0.10±0.01^{b}	0.25±0.02^{a}	0.12±0.01^{b}
C20:3*n*6	0.41±0.03^{c}	2.15±0.10^{a}	0.38±0.02^{c}	0.63±0.04^{b}
C20:4*n*6	5.16±0.18^{b}	9.03±0.46^{a}	9.61±0.39^{a}	6.03±0.27^{b}
C20:5*n*3	11.39±0.59^{b}	15.87±0.68^{a}	17.21±0.83^{a}	9.26±0.48^{b}
C22:5*n*3	3.36±0.11^{a}	3.0±0.12^{a}	3.72±0.17^{a}	2.32±0.08^{b}
C22:6*n*3	8.0±0.31^{b}	6.61±0.30^{b}	13.86±0.71^{a}	6.93±0.26^{b}
∑PUFA	30.65±1.45^{b}	38.67±1.67^{ab}	46.16±2.24^{a}	27.13±1.23^{b}
∑*n*3	24.07±1.14^{b}	27.13±1.25^{b}	35.16±1.60^{a}	19.01±1.08^{c}
∑*n*6	6.58±0.32^{b}	11.54±0.55^{a}	11.0±0.56^{a}	8.12±0.48^{b}
*n*3/*n*6	3.65±0.34^{a}	2.35±1.20^{b}	1.05±1.00^{c}	2.34±0.49^{b}
∑PUFA/∑SFA	0.53±0.04^{c}	0.75±0.03^{b}	1.04±0.04^{a}	0.47±0.21^{c}
AI	0.71±0.33^{a}	0.18±0.26^{d}	0.35±0.03^{c}	0.54±0.01^{b}
TI	0.66±0.03^{c}	0.54±0.45^{b}	0.37±0.32^{d}	0.80±0.08^{a}

Values reported are means ± standard deviation (n=3). Means followed by different letters in the same line are significantly different (p<0.05). SFA, saturated fatty acids; MUFA, monounsaturated fatty acids; PUFA, polyunsaturated fatty acids; AI, atherogenicity index; TI, thrombogenicity index.

(*Hippoglossus hippoglossus*) [Lie *et al*., 1992b] and horse mackerel (*Trachurus trachurus*) [Bandarra *et al*., 2001].

Phosphatidylinositol (PI) isolated from *C. regium* lipids contained mainly SFAs, which accounted for 44.47% to 57.98% of total FAs. The share of PUFAs was 27.13–46.16% of total FAs, and that of MUFAs ranged from 9.28% to 14.83% of total FAs (**Table 7**). The percentages of C16:0 and C18:0 were the lowest in PI of fish from November and January, respectively. Compared to the fatty acid composition of the phospholipid fraction (**Table 4**), contents of C18:0 and C20:4*n*6 were higher, but the share of C18:1*n*9, EPA (except sample from April), and DHA was lower in the PI (**Table 7**). The ∑PUFA/∑SFA ratio of PI was from 0.47 (April) to 1.04 (January) and AI ranged from 0.18 (November) to 0.71 (July). In turn, TI was found in the range of 0.37 (January) to 0.80 (April).

In general, when the water temperature was low in January, the share of PUFAs in PI was high compared to the other months, while the percentage of the predominant saturated fatty acids, C18:0 and C16:0, was low. The reason for this could be that membrane lipids have adapted to the cold environment. C18:0 and C20:4*n*6 were characteristics of the PI fraction. The same dominant fatty acids in the PI fraction have been found in previous studies [Lie *et al.,* 1992b; Kızmaz, 2021].

Analysis of the fatty acid composition of phosphatidylserine (PS) of *C. regium* muscle showed that the main FAs were C16:0, C18:0, C16:1*n*7, C18:1*n*9, EPA, and DHA (**Table 8**).

Table 8. Fatty acid composition (% of total fatty acids) and nutritional indices of phosphatidylserine of muscle of *Chondrostoma regium* collected in different seasons.

Fatty acid/Nutritional index	July	November	January	April
C14:0	3.35±0.12^{b}	2.12±0.08^{b}	2.63±0.11^{b}	4.60±0.25^{a}
C15:0	1.22±0.05^{a}	0.40±0.02^{b}	0.23±0.01^{c}	0.38±0.02^{c}
C16:0	18.91±0.74^{b}	20.74±0.92^{b}	17.47±0.60^{b}	24.08±1.22^{a}
C17:0	2.53±0.10^{a}	0.99±0.04^{b}	1.80±0.05^{ab}	1.13±0.05^{ab}
C18:0	20.49±1.07^{a}	7.5±0.35^{b}	6.29±0.28^{b}	9.19±0.42^{b}
∑SFA	46.5±2.14^{a}	31.75±1.72^{b}	28.42±1.30^{b}	39.38±2.02^{ab}
C16:1*n*7	13.96±0.54^{a}	7.70±0.37^{b}	10.89±0.56^{ab}	14.11±0.58^{a}
C18:1*n*9	16.5±0.70^{b}	15.62±0.63^{b}	23.44±1.10^{a}	24.5±1.05^{a}
C20:1*n*9	0.43±0.02^{c}	0.30±0.02^{c}	0.64±0.04^{b}	3.62±0.12^{a}
∑MUFA	30.89±1.13^{b}	23.62±1.18^{c}	34.97±1.56^{b}	42.23±2.14^{a}
C18:2*n*6	1.96±0.04^{b}	4.25±0.19^{a}	3.40±0.15^{ab}	2.58±0.10^{ab}
C18:3*n*3	0.76±0.03^{b}	1.30±0.05^{ab}	1.19±0.05^{ab}	2.36±0.10^{a}
C20:2*n*6	0.67±0.03^{a}	0.17±0.01^{b}	0.55±0.03^{a}	0.23±0.01^{b}
C20:3*n*6	0.24±0.02^{b}	0.70±0.03^{a}	0.64±0.03^{a}	0.21±0.01^{b}
C20:4*n*6	1.77±0.06^{b}	4.54±0.14^{a}	4.04±0.20^{a}	0.88±0.05^{b}
C20:5*n*3	7.16±0.35^{b}	10.66±0.54^{a}	9.47±0.47^{a}	5.23±0.30^{b}
C22:5*n*3	2.96±0.17^{b}	7.53±0.31^{a}	5.37±0.28^{a}	2.01±0.10^{b}
C22:6*n*3	7.01±0.36^{b}	15.4±0.73^{a}	11.86±0.52^{ab}	4.82±0.28^{c}
∑PUFA	22.53±1.13^{b}	44.55±2.10^{a}	36.52±1.72^{ab}	18.32±0.70^{b}
∑*n*3	17.89±0.74^{b}	34.89±1.55^{a}	27.89±1.58^{ab}	14.42±0.68^{b}
∑*n*6	4.64±0.15^{b}	9.66±0.55^{a}	8.63±0.41^{a}	3.90±0.13^{b}
*n*3/*n*6	3.85±0.05^{a}	3.61±0.08^{a}	3.23±0.11^{a}	3.69±0.67^{a}
∑PUFA/∑SFA	0.48±0.04^{b}	1.40±0.55^{a}	1.29±0.40^{c}	0.47±0.06^{b}
AI	0.60±0.34^{b}	0.43±0.05^{b}	0.39±0.10^{c}	0.70±0.07^{a}
TI	0.57±0.05^{a}	0.24±0.02^{b}	0.24±0.01^{b}	0.54±0.08^{a}

Values reported are means ± standard deviation (n=3). Means followed by different letters in the same line are significantly different (p<0.05). SFA, saturated fatty acids; MUFA, monounsaturated fatty acids; PUFA, polyunsaturated fatty acids; AI, atherogenicity index; TI, thrombogenicity index.

The contribution of C16:1*n*7 to total FAs of PS was the lowest in the sample from November (7.70% of total FAs) and the highest in that from April (14.11% of total FAs). Depending on the month of fishing, the ∑PUFA/∑SFA ratio ranged from 0.47 to 1.40, AI varied from 0.39 to 0.70, and TI was found in the range of 0.24 to 0.57. Interestingly, levels of EPA and DHA were lower, while these of C16:1*n*7 and C18:1*n*9 were higher in the PS than in the PL (**Table 4** and **8**). In the study conducted with tuna (*Thunnus obesus*), bluefin (*Thunnus thynnus*), bonito (*Sarda sarda*), frigate (*Auxis thazard*), skipjack (*Katsuwonus pelamis*), and yellowfin (*Thunnus albacares*) fishes, PS was the subclass with the highest contribution of SFAs among PC, PE and PI subclasses [Medina *et al*., 1995].

CONCLUSIONS

The findings demonstrated the high quality of lipids of *C. regium* because atherogenicity and thrombogenicity indices had low values, indicating no risk to human health. The *C. regium* muscle total lipid fraction was found to have a high *n3*/*n6* ratio and contain high levels of DHA and EPAs. The nutritional value of the fish species found in the Munzur River was high, as evidenced by the fact that this value was significantly greater than those of any other freshwater fish previously researched in Turkey.

The study results also showed that, in the reproductive period (January), the share of SFAs in total lipids increased and the share of MUFAs decreased compared to the other months. Season had an impact on the TAG, PL and PL subclass fatty acid (SFA, MUFA,

PUFA) levels as well. In summary, the fish of *C. regium* species are excellent sources of high quality, PUFA-rich lipids. As a result, it is stated that the consumption of *C. regium* is recommended for humans.

RESEARCH FUNDING

This research was financially supported by the Scientific Research Project of Dicle University (DUAPK-13-FF-75).

CONFLICT OF INTERESTS

The authors declare no conflict of interest.

ADDITIONAL INFORMATION

All applicable national guidelines for the care and use of animals were followed.

ORCID IDs

M. Başhan https://orcid.org/0000-0002-1228-9548
S. Kaçar https://orcid.org/0000-0002-9869-9045
H. Kaya Kayhan https://orcid.org/0000-0002-8656-8144

REFERENCES

1. Ackman, R.G. (1990). Seafood lipids and fatty acids. *Food Reviews International, 6*(4), 617–646. https://doi.org/10.1080/87559129009540896
2. Ackman, R.G., McLeod, C., Rakshit, S., Misra, K.K. (2002). Lipids and fatty acids of five freshwater food fishes of India. *Journal of Food Lipids, 9*(2), 127-145. https://doi.org/10.1111/j.1745-4522.2002.tb00214.x
3. Bandarra, N.M., Batista, I., Nunes, M.L., Empis, J.M. (2001). Seasonal variation in the chemical composition of Horse mackerel (*Trachurus trachurus*). *European Food Research Technology, 212*(5), 535–539. https://doi.org/10.1007/s002170100299
4. Biandolino, F., Prato, E., Grattagliano, A., Parlapiano, I. (2023). Effect of different cooking methods on lipid content and fatty acid profile of red mullet (*Mullus barbatus*). *Polish Journal of Food and Nutrition Sciences*, *73*(1), 59-69. https://doi.org/10.31883/pjfns/159651
5. Bušová, M., Kouřimská, L., Tuček, M. (2020). Fatty acids profile, atherogenic and thrombogenic indices in freshwater fish common carp (*Cyprinus carpio*) and rainbow trout (*Oncorhynchus mykiss*) from market chain. *Central European Journal of Public Health, 28*(4), 313-319. https://doi.org/10.21101/cejph.a5966
6. Caffrey, C., Leamy, A., O'Sullivan, E., Zabetakis, I., Lordan, R., Nasopoulou, C. (2023). Cardiovascular diseases and marine oils: A focus on omega-3 polyunsaturated fatty acids and polar lipids. *Marine Drugs*, *21*(11), art. no. 549. https://doi.org/10.3390/md21110549
7. Canhada, S., Castro, K., Perry, I.S., Luft, V.C. (2018). Omega-3 fatty acids' supplementation in Alzheimer's disease: A systematic review. *Nutritional Neuroscience, 21*(8), 529–538. https://doi.org/10.1080/1028415X.2017.1321813
8. Cengiz, E.İ., Ünlü, E., Başhan, M. (2010). Fatty acid composition of total lipids in muscle tissues of nine freshwater fish from the River Tigris (Turkey). *Turkish Journal of Biology, 34*(4), 433-438. https://doi.org/10.3906/biy-0903-19
9. D'Eliseo, D., Velotti, F. (2016). Omega-3 fatty acids and cancer cell cytotoxicity: Implications for multi-targeted cancer therapy. *Journal of Clinical Medicine, 5*(2), art. no. https://doi.org/10.3390/jcm5020015
10. Di Lena, G., Nevigato, T., Rampacci, M., Casini, I., Caproni, R., Orban, E. (2016). Proximate composition and lipid profile of red mullet (*Mullus barbatus*) from two sites of the Tyrrhenian and Adriatic seas (Italy): a seasonal differentiation. *Journal of Food Composition and Analysis, 45,* 121–129. https://doi.org/10.1016/j.jfca.2015.10.003
11. Emre, N., Uysal, K., Kavasoğlu, M., Emre, Y., Yalım, B., Pak, F. (2020). Seasonal variations of the fatty acid profiles in the edible portions of two freshwater fish species (*Pseudophoxinus fahrettini* and *Capoeta mauricii*). *Iranian Journal of Fisheries Sciences, 19*(2), 602-611. https://doi.org/10.22092/ijfs.2019.119242
12. Folch, J., Lees, M., Stanley, A. (1957). Simple method for the isolation and purification of total lipides from animal tissues. *Journal of Biological Chemistry, 226*(1), 497-509. https://doi.org/10.1016/S0021-9258(18)64849-5
13. Görgün, S., Akpınar, N., Dirican, S. (2014). A comparative study on the fatty acid profiles of total lipid, neutral and polar lipids in the liver and muscle of *Capoeta sieboldıı* (Steindachner, 1864) and *Capoeta baliki* (Turan, Kottelat, Ekmekçi, İmamoğlu, 2006) from Tödürge Lake (Sivas, Turkey). *Acta Alimentaria, 43*(1), 170–181. https://doi.org/10.1556/aalim.43.2014.1.17
14. Görgün, S., Akpınar, N., Zengin, G., Akpinar, M.A., Gunlu, A., Güler, G.O., Aktümsek, A. (2013). Determination of fatty acid profiles of total, neutral, and polar lipids in different tissues of *Vimba vimba* (L., 1758) from Eğirdir Lake (Isparta, Turkey). *Turkish Journal of Zoology, 37*(5), 627-634. https://doi.org/10.3906/zoo-1212-33.
15. Guerra, J.M.C., Fernandes, C.E., Vasconcelos, M.A.S., Ribeiro, M.A., Andrade, S.A.C., Sarubbo, L.A. (2022). Seasonal influence on lipid profiles of fish in Northeastern Brazil. *Aquaculture Reports, 24,* art. no. 101174. https://doi.org/10.1016/j.aqrep.2022.101174
16. Haliloğlu, H.I., Bayır, A., Sirkecioğlu, A.N., Aras, N.M., Atamanalp, M. (2004). Comparision of fatty acid composition in some tissues of rainbow trout (*Oncorhynchus mykiss*) living in seawater and freshwater. *Food Chemistry, 86*(1), 55-59. https://doi.org/10.1016/j.foodchem.2003.08.028
17. Henderson, R.J., Tocher, D.R. (1987). The lipid composition and biochemistry of freswater fish. *Progress Lipid Research, 26*(4), 281-347. https://doi.org/10.1016/0163-7827(87)90002-6
18. Kaçar, S., Başhan, M., Oymak, S.A. (2018). Fatty acid composition of total lipid, phospholipid and triacylglycerol in the muscle and gonad tissue of *Chondrostoma regium*. *Journal of Agriculture and Nautre, 21*(1), 20-25 (in Turkish, English abstract). https://doi.org/10.18016/ksudobil.292857
19. Kayhan, H., Başhan, M., Kaçar, S. (2015). Seasonal variations in the fatty acid composition of phospholipids and triacylglycerols of brown trout. *European Journal of Lipid Science and Technology, 117*(5), 738-744. https://doi.org/10.1002/ejlt.201400152
20. Kızmaz, V. (2021). Seasonal variation of fatty acid composition of phospholipid subclasses in muscle tissue in male, *Alburnus mussulensis*. *EJONS International Journal,* 5(17), 32–43. https://doi.org/10.38063/ejons.373
21. Kostetsky, E.Y., Velansky, P.V., Sanina, N.M. (2018). Thermal adaptation and fatty acid composition of major phospholipids in the plain sculpin *Myoxocephalus jaok* at different temperatures of natural habitat. *Journal of Evolutionary Biochemistry and Physiology, 54,* 205–215. https://doi.org/10.1134/S0022093018030055
22. Kostoglou-Athanassiou, I., Athanassiou, L., Athanassiou, P. (2020). The effect of omega-3 fatty acids on rheumatoid arthritis. *Mediterranean Journal of Rheumatology, 31(2)*, 190-194. https://doi.org/10.31138/mjr.31.2.190
23. Lemoine, S.C.M., Brigham, E.P., Woo, H., Hanson, C.K., McCormack, M.C., Koch, A., Putcha, N., Hansel, N.N. (2019). Omega-3 fatty acid intake and prevalent respiratory symptoms among U.S. adults with COPD. *BMC Pulmonary Medicine*, *19*(1), art. no. 97. https://doi.org/10.1186/s12890-019-0852-4
24. Li, J., Wang, X., Zhang, T., Wang, C., Huang, Z., Luo, X., Deng, Y. (2015). A review on phospholipids and their main applications in drug delivery systems. *Asian Journal of Pharmaceutical Sciences, 10*(2), 81-98. https://doi.org/10.1016/j.ajps.2014.09.004
25. Lie, Q., Hemre, G.H., Bjqrnsson, B. (1992b). Fatty acid composition of glycerolipids and neutral lipids in six different tissues of halibut (*Hippoglossus hippoglossus)* fedcapelin at constant temperature. *Fisk Dir Skr Ser Emering, 5*(2), 99-109.
26. Lie, Q., Hemre, G.L., Lambertsen, G. (1992a). Influence of dietary fatty acids on the glycerophospholipid composition in organs of cod (*Gadus morhua*). *Lipids, 27*(10), 770–775. https://doi.org/10.1007/BF02535847
27. Łuczyńska, J., Paszczyk, B., Borejszo, Z., Tarkowski, Ł. (2012). Fatty acid profile of muscles of freshwater fish from Olsztyn markets. *Polish Journal of Food and Nutrition Sciences, 62*(1), 51-55. https://doi.org/10.2478/v10222-011-0039-z
28. Medina, I., Aubourg, S.P., Perez Martin, R. (1995). Composition of phospholipids of white muscle of six tuna species. *Lipids, 30*(12), 1127-1135. https://doi.org/10.1007/BF02536613
29. Parzanini, C., Colombo, S.M., Kainz, M. J., Wacker, A., Parrish, C.C., Arts, M.T. (2020). Discrimination between freshwater and marine fish using fatty acids: ecological implications and future perspectives. *Environmental Reviews, 28*(4), 546-559. https://doi.org/10.1139/er-2020-0031
30. Rasoarahona, J.R.E., Ramanoelina, P.A.R., Bianchini, J.P., Gaydou, E.M. (2008). Muscle lipids and fatty acid profiles of the sea catfish (*Arius madagascariensis*) in Madagascar Inland Waters. *Journal of the American Oil Chemists' Society, 85*(5), 435-440. https://doi.org/10.1007/s11746-008-1211-4

31. Satar, E.İ., Uysal, E., Ünlü, E., Başhan, M., Satar, A. (2012). The effects of seasonal variation on the fatty acid composition of total lipid, phospholipid, and triacylglycerol in the dorsal muscle of *Capoeta trutta* found in the Tigris River (Turkey). *Turkish Journal of Biology, 36*(1), 113-123. **https://doi.org/10.3906/biy-1008-81**
32. Shirai, N., Suzuki, H., Tokairin, S., Ehara, H., Wada, S. (2002). Dietary and seasonal effects on the dorsal meat lipid composition of Japanese (*Silurus asotus*) and Thai catfish (*Clarias macrocephalus* and hybrid *Clarias macrocephalus* and *Clarias galipinus*). *Comparative Biochemistry and Physiology Part A: Molecular and Integrative Physiology, 132*(3), 609–619. **https://doi.org/10.1016/S1095-6433(02)00081-8**
33. Simopoulos, A.P. (2016). An increase in the omega-6/omega-3 fatty acid ratio increases the risk for obesity. *Nutrients*, *8*(3), art. no. 128. **https://doi.org/10.3390/nu8030128**
34. Sushchik, N.N., Zuev, I., Kalachova, G.S., Ageev, A.V., Gladyshev, M.I. (2018). Content of highly unsaturated fatty acids in fish from rivers of contrasting temperature: Fatty acids in fish from rivers of contrasting temperature. *River Research and Applications, 34*(6), 565-574. **https://doi.org/10.1002/rra.3286**
35. Tao, X., Yin, M., Lin, L., Song, R., Wang, X., Tao, N., Wang, X. (2024). UPLC-ESI-MS/MS strategy to analyze fatty acids composition and lipid profiles of Pacific saury (*Cololabis saira*). *Food Chemistry: X, 23*, art. no. 101682. **https://doi.org/10.1016/j.fochx.2024.101682**
36. Tellioğlu, A., Pala, G., Çoban, M.Z., Şen, D. (2004). The content of digestive system of *Chondrostoma regium* (Heckel, 1843) inhabiting in Keban Dam Lake. *Fırat* Üniversitesi *Fen ve Mühendislik Bilimleri Dergisi, 16*, 623-632 (in Turkish, English abstract).
37. Tocher, D.R., Bendıksen, E.A., Campbell, P.J., Bell, J.G. (2008). The role of phospholipids in nutrition and metabolism of teleost fish. *Aquaculture, 280*(1-4), 21–34. **https://doi.org/10.1016/j.aquaculture.2008.04.034**
38. Tommonaro, G., Paris, D., Guerriero, G., Majdoubi, F.Z., Grieco, G., Iodice, C., Caso, L., Ouizgane, A., El Moujtahid, A., El Ghizi, S., Bousseba, M., Hasnaoui, M., Iodice, A., Tramice, A. (2023). Fatty acids in waste tissues: the nutraceutical value of gonads and livers from the Moroccan *Hypophthalmichthys molitrix* and *Cyprinus carpio* fishes. *Marine Drugs*, *21*(3), art. no.188. **https://doi.org/10.3390/md21030188**
39. Uysal, K., Aksoylar, M.Y. (2005). Seasonal variations in fatty acid composition and the n-6/n-3 fatty acid ratio of pikeperch (*Sander lucioperca*) muscle lipids. *Ecology of Food and Nutrition, 44*(1), 23-35. **https://doi.org/10.1080/03670240590904308**
40. Vaden, D.L., Gohil, V.M., Gu, Z., Greenberg, M.L. (2005). Separation of yeast phospholipids using one-dimensional thin-layer chromatography. *Analytical Biochemistry, 338*(1), 162-164. **https://doi.org/10.1016/j.ab.2004.11.020**
41. Woloszyn, J., Haraf, G., Okruszek, A., Werenska, M., Goluch, Z., Teleszko, M. (2020). Fatty acid profiles and health lipid indices in the breast muscles of local Polish goose varieties. *Poultry Science, 99*(2), 1216–1224. **https://doi.org/10.1016/j.psj.2019.10.026**

ORIGINAL ARTICLE
http://journal.pan.olsztyn.pl

Polish Journal of Food and Nutrition Sciences
2024, Vol. 74, No. 4, 399–407
DOI: 10.31883/pjfns/195389
ISSN 1230-0322, e-ISSN 2083-6007

Seasonal Variations in Baltic Sprat (*Sprattus sprattus balticus*) Chemical Composition and Their Impact on Smoked Sprat Quality

Santa Puke, Ruta Galoburda*

Food Institute, Faculty of Agriculture and Food Technology, Latvia University of Life Sciences and Technologies, Rigas street 22, Jelgava, LV-3004, Latvia

This study aimed to evaluate the chemical composition of Baltic sprats throughout the fishing season (November-March) while examining the texture and color of smoked sprats produced after that. Smoked sprats were produced from fresh fish and fish from the same batches after one year of frozen storage and thawing. The protein content in raw sprats remained stable with lysine and leucine exhibiting the highest content among essential amino acids. The lipid content showed an inverse correlation with moisture content during fishing season. Throughout the fishing season, there was a notable reduction in fatty acid content, particularly in *n*3 fatty acids. The lowest values of atherogenicity and thrombogenicity indexes were recorded in the autumn sprats, while the hypocholesterolemic to hypercholesterolemic fatty acid ratio was the highest in this fish, indicating its higher nutritional value. The moisture content increased from 62.4 g/100 g in the fish from the autumn catch to 70.0 g/100 g in those from the spring; thereby, impacting the physical properties of smoked sprats such as texture, color, and pH. The observed decrease in hardness, as well as reduced redness and yellowness of smoked fish sourced from the spring catches was likely attributed to the higher moisture content. Smoked sprats produced from frozen sprats exhibited lower hardness and slightly darker color.

Keywords: color, seasonality, sprat, texture

ABBREVIATIONS

DL, drying loss; HH, hypocholesterolemic to hypercholesterolemic fatty acid ratio; IA, index of atherogenicity; IT, index of thrombogenicity; MUFA, monounsaturated fatty acids; PUFA, polyunsaturated fatty acids; SFA, saturated fatty acids; SL, smoking loss.

INTRODUCTION

Fish represents a vital source of nutrients essential for maintaining human health. Numerous scientific studies highlight the beneficial impact of fish consumption on various aspects of human well-being, particularly in cardiovascular disease prevention [Milićević *et al.*, 2022; Shalini *et al.*, 2021]. Among the range of fish products, smoked fish holds a prominent position due to its traditional appeal and widespread popularity. The quality of raw sprats is the primary factor affecting the quality of the smoked product. However, it is well-established that the quality of fish, particularly within the fishing season, is subject to fluctuations influenced not only by the inherent quality of the raw material but also by factors such as the method of catch and storage conditions preceding further processing [Sabu & Sasidharan, 2020].

Typically, in the Baltic Sea, the sprat fishing season starts in September or October and ends in April or May. Fish flesh quality parameters are influenced by seasonality, sex, age, size, skin properties, and geographical location, all contributing to

***Corresponding Author:**
Tel.: +371 29177803; e-mail: **ruta.galoburda@lbtu.lv** (R. Galoburda)

Submitted: 22 July 2024
Accepted: 29 October 2024
Published on-line: 21 November 2024

changes in its lipids and proteins [Abbas *et al*., 2008]. In the spring, the Baltic sprat lipid content is low, but in the autumn (October, November), it reaches its highest level. The lipid and moisture contents influence texture, while protein content remains stable throughout the fishing season, although amino acid composition varies [Usydus *et al*., 2012].

To ensure a year-round supply of raw material, sprats are frozen, but it is essential to maintain the stability of the nutritional composition in fish during freezing and storage. Freezing is a preservation method that ensures longer shelf-life of fish but causes structural damage to muscle cells, leading to changes in meat quality. Before use, frozen fish needs to be thawed, which alters its sensory attributes and nutritional value [Trigo *et al*., 2018]. Proper thawing aims to minimize quality changes, but impacts texture, moisture loss, and microbiological activity [Yang *et al*., 2019]. The pH of fresh fish or thawed fish is close to neutral. Babikova *et al.* [2020] reported a positive correlation between pH, moisture content, and textural properties. The pH is also responsible for changes in fish color. The main physical changes which occur in fish upon processing are those observed in texture and color, which are the main factors influencing consumer acceptance [Abraha *et al*., 2018].

While extensive literature exists regarding Atlantic fish and their processing techniques [Dawson *et al*., 2018; Fernandes *et al*., 2024; Jiang *et al.,* 2024], including smoking and quality enhancement methods [Güngören *et al*., 2023; Liu *et al*., 2023; Sutikno *et al*., 2019] and similar research on sardines and their practical applications [Scheuer *et al*., 2024; Serdaroglu *et al*., 2015], there is a dearth of data concerning Baltic sprats – a staple in many parts of Europe – and the seasonal variations in their quality. Sparse are also investigations on applying prior processing techniques to fresh and frozen fish for improvement of the production yield by mitigating smoking losses and minimizing drying in storage chambers while enhancing quality indicators such as texture, color, pH, sensory attributes, and microbiological safety.

In light of these gaps in knowledge, this study aimed to evaluate the chemical composition of Baltic sprats throughout the fishing season, while examining the texture and color of smoked sprats produced thereafter. Smoked sprats were produced from fresh fish and fish from the same batches after one year of frozen storage and thawing.

MATERIALS AND METHODS

Fish collection and processing

Fresh Baltic Sea sprats caught during the fishing season from November to March 2020 in the Baltic Sea FAO27, III.d.28.2 using a trawl were used in the present study. The fresh fish were transported to the producing company within 48 h, and the internal temperature of the fish was maintained at 2±2°C. The fish belonged to freshness category A and size category 1 for sprats described in Council Regulation (EC) No. 2406/96 [EC Regulation, 1996]. Sprats were stored until processing in a container covered with ice (in a proportion of fish to ice of 1:3) at 2±2°C in a refrigerated room. Fish from the same batches were frozen and packed in plastic bags, then placed inside cardboard boxes. To produce frozen sprats, fresh sprats were sorted by size and placed in polyethylene bags (with thickness not exceeding 0.15 mm) in 10-kg portions. These bags were placed on horizontal frames and quickly frozen at temperatures between –35°C and –39°C for at least 3 to 5 h using a tunnel freezer with periodic operation. The frozen sprats were then stored for one year at –18±2°C with a relative humidity above 85%.

Frozen sprats, packaged in blocks within plastic bags, were thawed in a defrost chamber using water spray and hot water steam until their internal temperature reached 2±2°C, a process took 1 to 2 h). Both fresh and frozen sprats were smoked in a batch-type hot smoking chamber (Reich Foodsystems, Urbach, Germany) using beech wood chips (with moisture below 15%, wood chip size 5–8 mm). Three independent batches of 300–350 g were prepared *per* sample type. The main parameters for the hot smoking process were 35–40 min of drying at 45 to 60°C, 10–12 min of cooking at 60 to 75°C, 2–5 min of steaming at 75 to 77°C, 10–15 min of adding smoke at 77 to 80°C and cooling to 10°C to facilitate cutting of heads or tails after smoking. All smoked fish samples were analyzed one day after smoking.

Analysis of fresh sprats

Moisture analysis of sprats was conducted following the method of International Organization for Standardization [ISO 1442:1997]. Briefly, a 3-g homogenized sample of fresh sprat carcass (without the head, blended into a paste) was mixed with 9 g of pre-heated sand. The mixture was dried at 150°C for 60 min until a constant weight was reached. After drying, the sample was placed in a desiccator to cool and then weighed.

The sprat pH analysis was performed using a pH meter (Jenway 3520, EU). To measure pH, a 1-g homogenized fish sample was mixed with 9 g of distilled water and immediately tested for pH.

The protein content was determined in triplicate using the Kjeldahl method [ISO 5983-2:2009], with 2 g of the sample analyzed on a Kjeltec 2300 automatic analyzer (Foss Analytical, Höganäs, Sweden). The protein content of sprats (g/100 g) was calculated using a nitrogen conversion factor of 6.25.

The lipid content of the raw fish was measured in triplicate *via* Soxhlet extraction using an Soxtec Avanti 2050 instrument (Foss Analytical, Höganäs, Sweden) and petroleum ether, following a standard procedure [ISO 1443:1973].

Amino acid and fatty acid profiles were analyzed in the accredited laboratory J. S. Hamilton Sp. z.o.o. (Gdynia, Poland). All results were expressed as g/100 g of product. The fatty acid profile was determined using gas chromatography after fatty acid transmethylation under alkaline conditions according to standard procedures [ISO 12966-1:2015-01; ISO 12966-2:2017-05; ISO 12966-4:2015-07].

The ratio between the saturated fatty acids (SFA) and the unsaturated fatty acids (UFA) was demonstrated by the index of atherogenicity (IA). This index was initially established in 1991 by Ulbricht & Southgate [1991], and can be calculated from Equation (1):

$$IA = \frac{4 \times C14:0 + C16:0}{MUFA + PUFAn6 + PUFAn3} \quad (1)$$

where: MUFA means the sum of monounsaturated fatty acids, PUFA*n*6 is the sum of *n*6 polyunsaturated fatty acids and PUFA*n*3 is the sum of *n*3 polyunsaturated fatty acids.

The index of thrombogenicity (IT) represents the ratio between pro-thrombogenic (SFA) and anti-thrombogenic fatty acids (MUFA, PUFA*n*6, and PUFA*n*3), and was calculated using Equation (2):

$$IT = \frac{C14:0 + C16:0 + C18:0}{0.5 \times MUFA + 0.5 \times PUFAn6 + 3 \times PUFAn3 + \frac{PUFAn3}{PUFAn6}} \quad (2)$$

The hypocholesterolemic to hypercholesterolemic fatty acid ratio (HH index), as detailed in the study by Chen & Liu [2020], interprets the dynamics of cholesterol metabolism and was calculated using Equation (3):

$$HH = \frac{C18:1n9 + C18:2n6 + C18:3n3}{C14:0 + C16:0} + \frac{C20:5n3 + C22:5n3 + C22:6n3}{C14:0 + C16:0} \quad (3)$$

Proteinogenic amino acid profile was analyzed as outlined in [PB-53/HPLC ed. II of 30.12.2008], where aspartic acid was the sum of asparagine, aspartic acid and its salts; glutamic acid was the sum of glutamine, glutamic acid and its salts; cysteine was the sum of cystine and cysteine.

Analysis of smoked sprats

Moisture content and pH of smoked sprats were evaluated according to the same methods as applied to fresh sprats.

The smoking losses (SL) were calculated using weight (W) in g before and after smoking, as shown in Equation (4):

$$SL\ (\%) = \frac{W_{before\ smoking} - W_{after\ smoking}}{W_{before\ pretreatment}} \times 100 \quad (4)$$

The drying losses (DL) are observed during smoked sprat cooling and storage. Therefore, for the study purposes, fish after smoking was stored in perforated plastic boxes at 2±1°C for cooling. The DL was determined 24 h after smoking and calculated according to the Equation (5):

$$DL\ (\%) = \frac{W_{before\ storage} - W_{after\ storage}}{W_{before\ storage}} \times 100 \quad (5)$$

The texture analysis was conducted using a Texture Analyzer TX. HD Plus, equipped with the Warner-Bratzler knife blade set (Stable Microsystems, Godalming, UK). Before analysis, each smoked fish specimen was cut to remove the bone, resulting in two separate pieces of smoked sprat fillet. The width of each fillet was measured before cutting and entered into the software. Subsequently, each fillet was placed longitudinally on the slotted platform of the texture analyzer. The blade was then set to move at a speed of 2 mm/s for a distance of 10 mm. This process yielded the cutting strength (measured in N/mm), indicating the firmness of the fish. Seven measurements were performed for each sample.

The color assessment was conducted using a ColorTec-PCM color meter (Accuracy Microsensors Inc., Vernon Hills, IL, USA) equipped with Color Tec-Color Soft QCW software. Color measurements were taken on the surface of 5 to 7 smoked fish specimens, with no more than two different locations measured on each fish side. A total of 10 measurements were obtained, capturing variations across the samples. In the CIE*L*a*b** system, the value *L** represents lightness on a scale from 0 to 100, ranging from black to white, while the value *a** indicates redness (+) or greenness (–), and the value *b** reflects yellowness (+) or blueness (–).

Statistical analysis

Samples underwent triplicate testing, except for color and textural parameters, which were analyzed with at least 7 repetitions. Means and standard deviations were calculated using MS Office Excel 2016 (Microsoft, Redmond, WA, USA) software. Analysis of variance (ANOVA) and *t*-tests were conducted using XLSTAT 2020 (Addinsoft, New York, USA). Comparisons were made at a significance level of $p \leq 0.05$. To investigate the relationship between chemical compositions and fishing periods, correspondence analysis (CA) was employed. Differences in categorical variables were analyzed using the *t*-test ($p \leq 0.05$).

RESULTS AND DISCUSSION

Composition of fresh Baltic sprats depending on the season

The nutritional composition of sprats varied significantly across individual periods of the fishing season (**Table 1**). This study revealed a high moisture content in the sprats caught during the spring, which was consistent with findings from other studies [Timberg *et al*., 2011; Usydus *et al*., 2012], while the highest lipid content was found in the sprats from the autumn catch when the moisture content was the lowest. Results showed that the protein content remained stable throughout the season. According to Rasul *et al*. [2021] the variations in fish composition are influenced by environmental factors such as water temperature, pH, salinity, and food availability during the season. The moisture content varies due to osmoregulation during the migration process. Regarding lipids, it is known that fish utilize those as an energy source during certain periods. Additionally, changes in fish composition are also affected by factors such as fish species, age, size, sex, habitat, and breeding season [Chen & Liu, 2020; Jiang *et al*., 2024; Usydus *et al*., 2012].

Sprats were recognized as a source of proteins with valuable amino acid profile. The highest contents among essential amino acids were found for lysine and leucine (**Table 2**). During the fishing seasons, noteworthy changes occurred in content of histidine, which decreased from 0.47 g/100 g in the autumn to 0.34 g/100 g in the spring. The highest contents were observed for non-essential amino acids such as aspartic acid and glutamic acid, which is consistent with the findings reported by Vázquez

Table 1. Fresh sprat composition across the fishing season.

Variable	Autumn	Winter	Spring
Protein content (g/100 g)	16.4±1.3[a]	14.9±1.2[a]	16.8±1.3[a]
Lipid content (g/100 g)	19.2±1.7[a]	12.9±1.1[b]	12.1±1.1[b]
Moisture (g/100 g)	62.4±1.2[b]	69.2±1.2[a]	70.0±1.2[a]

Average value (n=3) ± standard deviation. Different letters in the same row show significant differences at $p \leq 0.05$ (t-test).

Table 2. Amino acid content of sprats across the fishing season (g/100 g of product).

Amino acids	Autumn	Winter	Spring
Non-essential amino acids			
Arginine (Arg)	0.86±0.14[a]	0.92±0.15[a]	0.86±0.14[a]
Aspartic acid (Asp)	1.36±0.22[a]	1.16±0.19[a]	1.14±0.18[a]
Cysteine (Cys)	0.11±0.02[a]	0.10±0.02[b]	0.10±0.02[b]
Glutamic acid (Glu)	2.02±0.32[a]	2.13±0.34[a]	1.98±0.32[a]
Glycine (Gly)	0.73±0.12[a]	0.76±0.12[a]	0.74±0.12[a]
Serine (Ser)	0.57±0.09[a]	0.57±0.06[a]	0.56±0.09[a]
Essential amino acids			
Histidine (His)	0.47±0.08[a]	0.38±0.06[b]	0.34±0.05[b]
Isoleucine (Ile)	0.58±0.09[a]	0.59±0.09[a]	0.58±0.09[a]
Leucine (Leu)	1.07±0.17[a]	1.14±0.17[a]	1.11±0.18[a]
Lysine (Lys)	1.25±0.20[a]	1.25±0.21[a]	1.24±0.20[a]
Methionine (Met)	0.44±0.07[a]	0.46±0.08[a]	0.46±0.07[a]
Phenylalanine (Phe)	0.57±0.09[a]	0.58±0.09[a]	0.58±0.09[a]
Threonine (Thr)	0.65±0.10[a]	0.67±0.11[a]	0.64±0.10[a]

Average value (n=3) ± standard deviation. Different letters in a row show significant differences at $p \leq 0.05$ (t-test).

et al. [2023]. Sprats contain a significant amount of red muscle, which correlates with a higher content of free amino acids [Bodin *et al.*, 2022]. This is influenced by pH, which in fresh sprats is higher in the winter, resulting in reduced decarboxylation of certain amino acids [Jääskeläinen *et al.*, 2023].

Throughout the fishing season, there was a notable reduction in fatty acid content, particularly in *n*3 fatty acids, which exhibited a threefold decrease (**Table 3**, **Table S1** in Supplementary Materials). Specifically, total *n*3 fatty acids decreased from 6.3 g/100 g in the autumn to 1.9 g/100 g in the spring. As highlighted by Merdzhanova *et al.* [2018], sprats, being oily fish, are naturally rich in *n*3 fatty acids. The highest levels of *n*3 fatty acids were determined in the sprats caught in the autumn, indicating their elevated nutritional value during this period. This seasonal variation can be attributed to the weakening of protein-lipid linkages and reduction in lipid autoxidation as season progresses, as suggested by Beltrán & Moral [1991].

The primary fatty acids in sprats predominantly consist of *n*3 fatty acids, a finding consistent with previous research [Scheuer *et al.*, 2024]. In autumn, the fatty acid composition follows the pattern PUFA > MUFA >SFA. By spring, this pattern shifts, with MUFA becoming dominant followed by SFA and PUFA. This seasonal variation differed from the findings reported by Merdzhanova *et al.* [2018], but may be explained by changes in the sprat diet during spring, particularly a lower intake of lipids and a higher MUFA content. This suggests a reduced presence of cold-water copepods, which are typically part of the sprat diet in colder months. The seasonal changes in fatty acid composition were further confirmed by Jiang *et al.* [2024], reinforcing the idea that diet and environmental factors significantly influence the nutritional profile of sprats throughout the fishing season.

The plot diagram (**Figure 1**) illustrating the association between the analyzed periods of the fishing season and chemical composition shows that 97.87% of the variability was attributed to factor 1 (F1), while 2.13% was attributed to factor 2 (F2). Moisture and *n*3 fatty acid contents were the most important contributors to F1, each with a contribution of 0.252. In turn, protein content was the most significant contributor to F2, with a contribution of 0.522. The correspondence analysis indicates

Table 3. Fatty acid groups in sprats across the fishing season (g/100 g of product).

Variable	Autumn	Winter	Spring
Total saturated fatty acids (SFA)	4.9±0.6[a]	3.2±0.4[b]	2.3±0.3[c]
Total monounsaturated fatty acids (MUFA)	6.6±0.9[a]	4.6±0.6[b]	3.6±0.5[c]
Total polyunsaturated fatty acids (PUFA)	7.0±0.9[a]	3.6±0.5[b]	2.2±0.3[c]
Total *n*3 fatty acids	6.3±0.8[a]	3.1±0.4[b]	1.9±0.2[c]
Total *n*6 fatty acids	0.7±0.1[a]	0.4±0.1[b]	0.3±0.1[b]
Total *n*9 fatty acids	4.9±0.6[a]	3.5±0.5[b]	2.8±0.4[c]

Average value (n=3) ± standard deviation. Different letters in a row show significant differences at $p \leq 0.05$ (t-test).

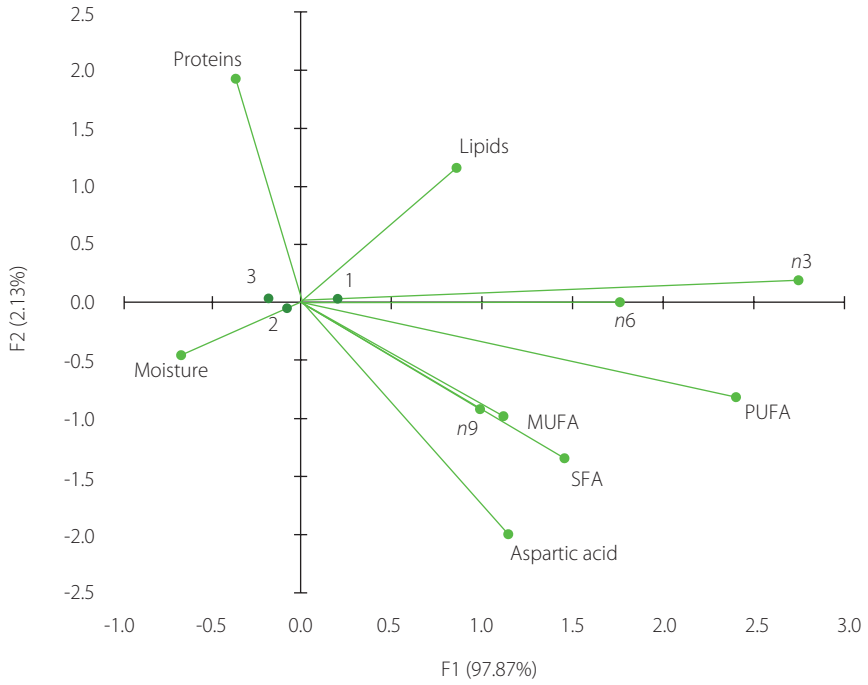

Figure 1. Correspondence analysis (CA) plot using chemical compositions and periods across the fishing season, including autumn (1), winter (2), and spring (3).

a linear relationship between moisture and lipid contents. Winter and spring fish were more similar in their chemical composition profiles, whereas the autumn fish showed more pronounced differences.

The nutritional value of fish is often assessed based on the PUFA/SFA ratio, which demonstrates the balance between polyunsaturated and saturated fatty acids. For sprats, this ratio ranged from 1.42 to 0.95 towards the end of the fishing season, while for other fish species, it varies from 0.5 to 1.62 [Chen & Liu, 2020]. The IA, which indicates the relationship between saturated and unsaturated fatty acids, increased from 0.43 to 0.66 during the whole fishing season (**Table 4**). Its lower value suggests a healthier lipid profile, implicated in a reduced risk of heart disease development. In turn, the IT of the sprats ranged from 0.14 to 0.21. This index, reflects the ratio between saturated fatty acids and the combined amount of monounsaturated fatty acids, *n*6, and *n*3 fatty acids. Lower IT values are associated with a reduced risk of cardiovascular problems due to reduced proportion of saturated fatty acids, which may increase the risk of clot formation. Łuczyńska *et al*. [2017] determined its values at 0.70 for herring and 0.31 for carp, with a range of 0.14 to 0.87 for most fish species. Furthermore, the HH index, which characterizes cholesterol metabolism, fluctuated throughout the fishing season (**Table 4**). Its higher value indicates a lipid profile that is more beneficial for lowering cholesterol levels, thus promoting better cardiovascular health.

The lowest values of atherogenicity and thrombogenicity indices were recorded in the autumn sprats, while the HH index was the highest in this season, indicating a higher nutritional value of the sprats. According to Chen & Liu [2020], IA and IT are the most commonly used to assess the composition of fatty acids. However, while these indices can be useful for comparing foods, no specific recommended values have been developed.

Table 4. Nutritional indices of sprats across the fishing season.

Index	Autumn	Winter	Spring
Index of atherogenicity (IA)	0.43±0.04^{b}	0.48±0.03^{b}	0.66±0.03^{a}
Index of thrombogenicity (IT)	0.14±0.04^{c}	0.15±0.02^{b}	0.21±0.02^{a}
Hypocholesterolemic to hypercholesterolemic fatty acid ratio (HH)	2.52±0.02^{a}	2.44±0.02^{b}	2.50±0.02^{a}

Average value (n=3) ± standard deviation. Different letters in a row show significant differences at $p \leq 0.05$ (t-test).

Table 5. The pH of raw sprats and physicochemical characteristics of smoked sprats across the fishing season.

Variable	Autumn		Winter		Spring	
	Fresh	Frozen	Fresh	Frozen	Fresh	Frozen
pH of raw sprats	6.70±0.02^{b}	6.24±0.02^{c}	6.98±0.02^{a}	6.50±0.03^{bc}	6.93±0.06^{a}	6.15±0.01^{c}
pH of smoked sprats	7.01±0.01^{a}	6.48±0.07^{b}	7.06±0.05^{a}	6.70±0.17^{b}	7.12±0.02^{a}	6.52±0.08^{b}
Moisture of smoked sprats (g/100 g)	62.4±0.01^{c}	62.5±0.05^{c}	65.0±0.03^{b}	61.6±0.05^{d}	67.50±0.03^{a}	62.20±0.02^{c}
Smoking losses (%)	29.57±0.06^{a}	22.30±0.03^{c}	25.90±0.04^{b}	17.30±0.03^{d}	22.10±0.02^{c}	17.30±0.04^{d}
Drying losses (%)	1.60±0.06^{a}	1.04±0.10^{c}	1.55±0.13^{a}	1.19±0.04^{c}	1.77±0.03^{a}	1.44±0.05^{b}

Average value (n=3) ± standard deviation. Different letters in a row show significant differences at $p \leq 0.05$ (t-test).

Physiochemical characteristics of smoked sprats

Similar to fresh fish, the significantly higher moisture content was determined in smoked sprats produced from the fish caught during the spring season and the highest lipid content in those from the autumn catch fish, when the moisture content was the lowest (**Table 5**). However, smoked sprats produced from frozen fish did not exhibit the same pattern. Reduced moisture content was observed in the smoked sprats produced from frozen winter and especially frozen spring fish compared to those produced from fresh fish. This difference may be related to the higher moisture content and distinctive water distribution patterns in raw fish tissue [Loje *et al*., 2007], coupled with increased tissue damage induced by ice crystals [Martinez *et al*., 2012; Ruiz-Alonso *et al*., 2021]. Our study results indicate that a higher moisture loss occurred during freezing, subsequent frozen storage, and thawing in the sprat samples with a higher initial moisture content. This resulted in lower smoking and drying losses in these samples compared to their fresh counterparts (**Table 5**).

The pH of sprats was affected by both frozen storage and smoking. Following one year of frozen storage, a decrease in pH was noted, with the most significant decline observed in the sprats caught in the spring season (**Table 5**). Conversely, smoking led to an increase in the pH of the sprats compared to that of raw fish. The impact of analyzed periods of the fishing season was evident in the moisture content of the smoked fish, as well as in smoking and drying losses. In production, smoking losses typically range from 35% to 50%. The results below 30% are considered excellent, while losses exceeding 50% are deemed unacceptable.

The color values L^*, a^*, and b^* determined for the smoked sprats changed throughout the fishing season, indicating differences in the product made from fresh or frozen fish (**Figure 2**). When comparing smoked sprats produced from fresh *vs*. frozen sources, distinct differences in redness (a^*) and yellowness (b^*) were evident. The color of the fish changes during heat treatment, primarily influenced by the non-enzymatic Maillard reaction [Liu *et al*., 2022]. During heat treatment, protein reduces the porosity in the product's structure and increases opacity, thereby enhancing light reflection. It is well known that opacity increases when myosin and actin denature [Valentim *et al*., 2024]. Smoking significantly decreases lightness and increases yellowness but has less impact on redness [Astruc *et al*., 2022]. The yellowness and redness were observed to be lower in smoked spring fish, likely due to the lower lipid content in raw fish, which may correlate with a reduced concentration of fat-soluble pigments [Nie *et al*., 2011]. Significantly lower redness was also found for Atlantic mackerel when comparing fresh and frozen fillets [Fernandes *et al*., 2024]. When comparing fresh and frozen sprats, the color changes as the sprats are frozen and during storage, pigments from fish surface are released from tissues and begin oxidation, causing the sprat tissue to darken and fade.

The smoked sprats produced from fresh sprats caught in the autumn exhibited higher hardness, measuring 0.99 N/mm, in contrast to those produced from fresh spring catch fish, for which 0.49 N/mm was recorded (**Figure 3**). Throughout the fishing season, texture parameters decreased by at least two times. Likewise, smoked sprats manufactured from frozen sprats demonstrated a decrease in hardness across the seasons.

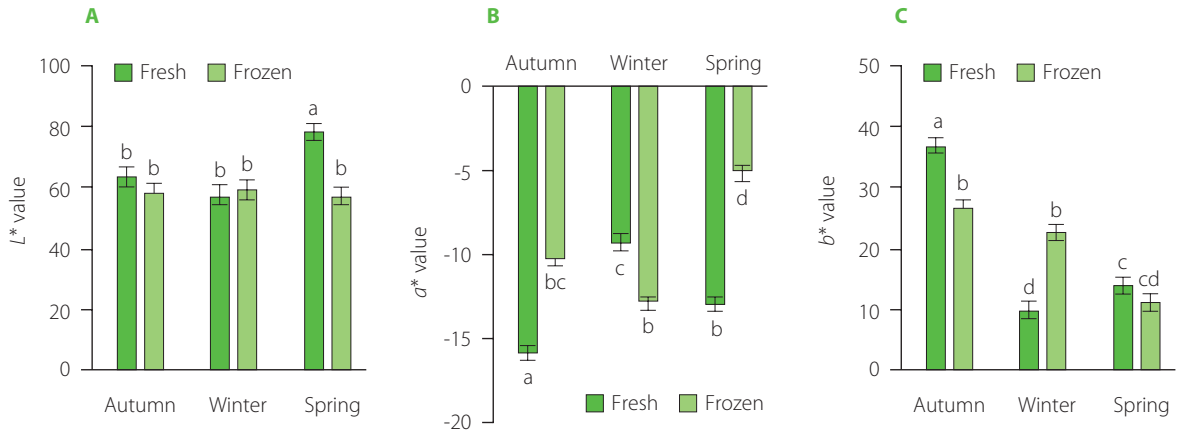

Figure 2. Color values determined for smoked sprats produced from fresh or frozen sprats: (**A**) lightness value, *L**; (**B**) redness value, *a**; (**C**) yellowness value, *b**. Bars show average value (n=7). Error bars represent standard deviation. Different letters above/below bars show significant differences $p \leq 0.05$ (*t*-test).

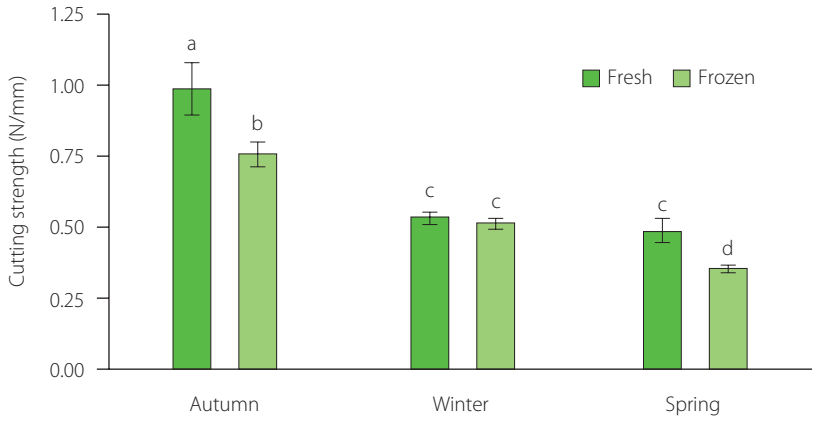

Figure 3. Texture of smoked sprats produced from fresh or frozen sprats.
Bars show average value (n=10). Error bars represent standard deviation. Different letters above bars show significant differences at $p \leq 0.05$ (*t*-test).

At the beginning of the fishing season, the hardness was at 0.77 N/mm, whereas by the fishing season's end, it decreased to 0.36 N/mm.

Our study results suggest that smoked sprats produced from the fresh autumn fish exhibited the highest texture values. Texture characteristics may be related to moisture and lipid content; as excessive lipid content can lead to decreased muscle strength [Jiang *et al*., 2024]. Changes in hardness can result from muscle shear resistance, protein extraction capacity, solubility, and viscosity changes during frozen storage [Xie *et al*., 2023]. Conversely, the reduced hardness observed in smoked sprats manufactured from the spring catch may be attributed to the higher moisture content in raw sprats. This increase in moisture could lead to a decrease in water-holding capacity due to protein denaturation and aggregation caused by ice crystals [Martinez *et al*., 2010]. To address this issue, various strategies can be employed to improve the water-holding capacity, such as salting and brining before smoking, which should be further investigated.

CONCLUSIONS

Baltic sprats are nutrient-rich fish, consistently high in protein throughout the fishing season. However, their lipid content undergoes significant changes over the season, significantly decreasing from autumn to spring. Autumn-caught sprats showed the highest $n3$ levels and the most favorable lipid profile, suggesting greater nutritional value during this period. In spring, the moisture content increased, which affected the physical characteristics of smoked sprats, including texture, color, and pH. The reduced hardness, along with reduced redness and yellowness in smoked sprats produced from the fish caught in the spring was likely a result of the increased moisture content. To ensure consistent quality in smoked sprats year-round, future research should focus on strategies to enhance the quality of spring catches.

SUPPLEMENTARY MATERIALS

The following are available online at **https://journal.pan.olsztyn.pl/Seasonal-Variations-in-Baltic-Sprat-Sprattus-sprattus-balticus-Chemical-Composition,195389,0,2.html**; **Table S1**. Fatty acid profile in Baltic sprats across the fishing season (g/100 g of product).

RESEARCH FUNDING

The research was financially supported by Latvia University of Life Sciences and Technologies (project Z43).

CONFLICT OF INTERESTS

The authors have no conflict of interest to declare.

ORCID IDs

R. Galoburda https://orcid.org/0000-0002-5804-516X
S. Puke https://orcid.org/0000-0003-1420-4760

REFERENCES

1. Abbas, K.A., Mohamed, A., Jamilah, B., Ebrahimian, M. (2008). A review on correlations between fish freshness and pH during cold storage. *American Journal of Biochemistry and Biotechnology*, *4*(4), 416–421. https://doi.org/10.3844/ajbbsp.2008.416.421
2. Abraha, B., Admassu, H., Mahmud, A., Tsighe, N., Shui, X. W., Fang, Y. (2018). Effect of processing methods on nutritional and physico-chemical composition of fish: a review. *MOJ Food Processing & Technology*, *6*(4), 376–382. https://doi.org/10.15406/mojfpt.2018.06.00191
3. Astruc, T., Vénien, A., Clerjon, S., Favier, R., Loison, O., Mirade, P.S., Portanguen, S., Rouel, J., Lethiec, M., Germond, A. (2022). Effect of dry salt versus brine injection plus dry salt on the physicochemical characteristics of smoked salmon after filleting. *Heliyon*, *8*(11), art. no. e11245. https://doi.org/10.1016/j.heliyon.2022.e11245
4. Babikova, J., Hoeche, U., Boyd, J., Noci, F. (2020). Nutritional, physical, microbiological, and sensory properties of marinated Irish sprat. *International Journal of Gastronomy and Food Science*, *22*, art. no. 100277. https://doi.org/10.1016/j.ijgfs.2020.100277
5. Beltrán, A., Moral, A. (1991). Changes in fatty acid composition of fresh and frozen sardine (*Sardina pilchardus* W.) during smoking. *Food Chemistry*, *42*(1), 99–109. https://doi.org/10.1016/0308-8146(91)90010-L
6. Bodin, N., Amiel, A., Fouché, E., Sardenne, F., Chassot, E., Debrauwer, L., Guillou, H., Tremblay-Franco, M., Canlet, C. (2022). NMR-based metabolic profiling and discrimination of wild tropical tunas by species, size category, geographic origin, and on-board storage condition. *Food Chemistry*, *371*, art. no. 131094. DOI: https://doi.org/10.1016/j.foodchem.2021.131094
7. Chen, J., Liu, H. (2020). Nutritional indices for assessing fatty acids: A mini-review. *International Journal of Molecular Sciences*, *21*(16), art. no. 5695. https://doi.org/10.3390/ijms21165695
8. Dawson, P., Al-Jeddawi, W., Remington, N. (2018). Effect of freezing on the shelf life of salmon. *International Journal of Food Science*, *2018*, 12, art. no. 1686121. https://doi.org/10.1155/2018/1686121
9. EC Regulation No 2406/96. Council Regulation (EC) No 2406/96 of 26 November 1996 laying down common marketing standards for certain fishery products. *Official Journal of the European Communities,* 23.12.96, No L 334/1.
10. Fernandes, C.M., Sveinsdóttir, H.I., Tómasson, T., Arason, S., Gudjónsdóttir, M. (2024). Impact of frozen storage on quality and cold storage stability of smoked deep-skinned fillets from well-fed Atlantic mackerel. *Journal of Food Composition and Analysis*, *125*, art. no. 105771. https://doi.org/10.1016/j.jfca.2023.105771
11. Güngören, A., Patir, B., Özpolat, E. (2023). The effect of propolis application on quality properties of vacuum-packed hot smoked rainbow trout (*Oncorhynchus Mykiss*, Walbaum 1792) fillets during cold storage. *LWT – Food Science and Technology*, *184*, art. no. 115084. https://doi.org/10.1016/j.lwt.2023.115084
12. ISO 1442:1997. Meat and meat products — Determination of moisture content (Reference method). The International Organization for Standardization.
13. ISO 1443:1973. Meat and meat products — Determination of total fat content. The International Organization for Standardization.
14. ISO 5983-2:2009. Animal feeding stuffs — Determination of nitrogen content and calculation of crude protein content. The International Organization for Standardization.
15. ISO 12966-1:2015-01. Animal and vegetable fats and oils — Gas chromatography of fatty acid methyl esters. Part 1: Guidelines on modern gas chromatography of fatty acid methyl esters. The International Organization for Standardization.
16. ISO 12966-2:2017. Animal and vegetable fats and oils — Gas chromatography of fatty acid methyl esters. Part 2: Preparation of methyl esters of fatty acids. The International Organization for Standardization.
17. ISO 12966-4:2015. Animal and vegetable fats and oils — Gas chromatography of fatty acid methyl esters Part 4: Determination by capillary gas chromatography. The International Organization for Standardization.
18. Jääskeläinen, E., Säde, E., Rönkkö, T., Hultman, J., Johansson, P., Riekkola, M.L., Björkroth, J. (2023). Marination increased tyramine levels in rainbow trout fillet strips packaged under modified atmosphere. *Food Microbiology*, *109*, art. no. 104099. https://doi.org/10.1016/j.fm.2022.104099
19. Jiang, Q., Chen, H., Gao, P., Yu, P., Yang, F., Wang, L., Xia, W. (2024). Seasonal variations in the channel catfish (*Ictalurus punctatus*): Nutritional composition, texture, and physicochemical properties of myofibrillar protein. *Food Bioscience*, *59*, art. no. 104034. https://doi.org/10.1016/j.fbio.2024.104034
20. Liu, L., Jiao, W., Xu, H., Zheng, J., Zhang, Y., Nan, H., Huang, W. (2023). Effect of rapid freezing technology on quality changes of freshwater fish during frozen storage. *LWT – Food Science and Technology*, *189*, art. no. 115520. https://doi.org/10.1016/j.lwt.2023.115520
21. Liu, S., Sun, H., Ma, G., Zhang, T., Wang, L., Pei, H., Li, X., Gao, L. (2022). Insights into flavor and key influencing factors of Maillard reaction products: A recent update. *Frontiers in Nutrition*, *9*, art. no. 973677. https://doi.org/10.3389/fnut.2022.973677
22. Loje, H., Jensen, K.N., Hyldig, G., Nielsen, N.H., Nielsen, J. (2007). Changes in liquid holding capacity, water distribution and microstructure during chill storage of smoked salmon. *Journal of the Science of Food and Agriculture*, 87(14), 2684-2691. https://doi.org/10.1002/jsfa.3031
23. Łuczyńska, J., Paszczyk, B., Nowosad, J., Łuczyński, M.J. (2017). Mercury, fatty acids content and lipid quality indexes in muscles of freshwater and marine fish on the polish market. Risk assessment of fish consumption. *International Journal of Environmental Research and Public Health*, *14*(10), art. no. 1120. https://doi.org/10.3390/ijerph14101120
24. Martinez, O., Salmerón, J., Guillén, M.D., Casas, C. (2010). Effect of freezing on the physicochemical, textural and sensorial characteristics of salmon (*Salmo salar*) smoked with a liquid smoke flavouring. *LWT – Food Science and Technology*, *43*(6), 910–918. https://doi.org/10.1016/j.lwt.2010.01.026
25. Martinez, O., Salmerón, J., Guillén, M.D., Pin, C., Casas, C. (2012). Physicochemical, sensorial and textural characteristics of liquid-smoked salmon (*Salmo salar*) as affected by salting treatment and sugar addition. *International Journal of Food Science and Technology*, *47*(5), 1086–1096. https://doi.org/10.1111/j.1365-2621.2012.02945.x
26. Merdzhanova, A., Dobreva, D.A., Panayotova, V. (2018). The comparison of proximate composition, fatty acids and fat- soluble vitamins content of the black sea sprat (*Sprattus Sprattus*) during catching seasons. *Annals Food Science and Technology*, *19*(2), 191–19.
27. Milićević, T., Romanić, S.H., Popović, A., Mustać, B., Đinović-Stojanović, J., Jovanović, G., Relić, D. (2022). Human health risks and benefits assessment based on OCPs, PCBs, toxic elements and fatty acids in the pelagic fish species from the Adriatic Sea. *Chemosphere*, *287*(Part 1), art. no. 132068. https://doi.org/10.1016/j.chemosphere.2021.132068
28. Nie, X.P., Zie, J., Häubner, N., Tallmark, B., Snoeijs, P. (2011). Why Baltic herring and sprat are weak conduits for astaxanthin from zooplankton to piscivorous fish. *Limnology and Oceanography*, *56*(3), 1155–1167. https://doi.org/10.4319/lo.2011.56.3.1155
29. PB-53/HPLC ed. II of 30.12.2008. Agriculture products. Amino acids profile. High performance liquid chromatography method with spectrophotometric detection (HPLC-UV/Vis) and diode array detection (HPLC-DAD).
30. Rasul, M., Jahan, I., Yuan, C., Sarkar, M., Bapary, M., Baten, M., Shah, A. (2021). Seasonal variation of nutritional constituents of some freshwater and marine fishes of South Asian Countries: A critical review. *Fundamental and Applied Agriculture*, *6*(2), 193–209. https://doi.org/10.5455/faa.65131
31. Ruiz-Alonso, S.A., Girón-Hernández, L.J., López-Vargas, J.H., Muñoz-Ramírez, A.P., Simal-Gandara, J. (2021). Optimizing salting and smoking conditions for the production and preservation of smoked-flavoured tilapia fillets. *LWT – Food Science and Technology*, *138*, art. no. 110733. https://doi.org/10.1016/j.lwt.2020.110733
32. Sabu, S., Sasidharan, A. (2020). Impact of fishing on freshness and quality of seafood: A review. *International Journal of Fisheries and Aquatic Studies*, *8*(2), 193–198.
33. Scheuer, F., Sterzelecki, F.C., Wagner, R., Xavier, A.C., de Souza, M.P., Brasil, E.M., Fracalossi, D., Cerqueira, V.R. (2024). Proximate and fatty acids composition in the muscle of wild and farmed sardine (*Sardinella brasiliensis*). *Food Chemistry Advances*, *4*, art. no. 100637. https://doi.org/10.1016/j.focha.2024.100637
34. Serdaroglu, M., Baris, P., Urgu, M., Doostifard, E., Yildiz-Turp, G. (2015). Quality changes of sardine fillets marinated with vinegar, grapefruit and pomegranate marinades. *Electronic Journal of Polish Agricultural Universities. Series Food Science and Technology*, *18*(4), art. no. 09.
35. Shalini, R., Jeyasekaran, G., Shakila, R.J., Sundhar, S., Arisekar, U., Jawahar, P., Aanand, S., Sivaraman, B., Malini, A.H., Surya, T. (2021). Dietary intake of trace elements from commercially important fish and shellfish of Thoothukudi along the southeast coast of India and implications for human health risk assessment. *Marine Pollution Bulletin*, *173*(Part A), art. no. 113020. https://doi.org/10.1016/j.marpolbul.2021.113020
36. Sutikno, L.A., Bashir, K.M.I., Kim, H., Park, Y., Won, N.E., An, J.H., Jeon, J.H., Yoon, S.J., Park, S.M., Sohn, J.H., Kim, J.S., Choi, J.S. (2019). Improvement in physicochemical, microbial, and sensory properties of common squid (*Todarodes pacificus* Steenstrup) by superheated steam roasting in combination with smoking treatment. *Journal of Food Quality*, *2019*, art. no. 8721725. https://doi.org/10.1155/2019/8721725

37. Timberg, L., Koppel, K., Kuldjärv, R., Paalme, T. (2011). Sensory and chemical properties of Baltic sprat (*Sprattus sprattus balticus*) and Baltic herring (*Clupea harengus membras*) in different catching seasons. *Agronomy Research*, *9*(SI II), 489–494.
38. Trigo, M., Rodríguez, A., Dovale, G., Pastén, A., Vega-Gálvez, A., Aubourg, S.P. (2018). The effect of glazing based on saponin-free quinoa (Chenopodium quinoa) extract on the lipid quality of frozen fatty fish. *LWT – Food Science and Technology*, *98*, 231–236. **https://doi.org/10.1016/j.lwt.2018.08.031**
39. Ulbricht, T.L.V., Southgate, D.A.T. (1991). Coronary heart disease: seven dietary factors. *The Lancet*, *338*(8773), 985–992. **https://doi.org/10.1016/0140-6736(91)91846-M**
40. Usydus, Z., Szlifder-Richert, J., Adamczyk, M. (2012). Variations in proximate composition and fatty acid profiles of Baltic sprat (*Sprattus sprattus balticus*). *Food Chemistry*, *130*(1), 97–103. **https://doi.org/10.1016/j.foodchem.2011.07.003**
41. Valentim, J., Afonso, C., Gomes, R., Gomes-Bispo, A., Prates, J.A.M., Bandarra, N. M., Cardoso, C. (2024). Influence of cooking methods and storage time on colour, texture, and fatty acid profile of a novel fish burger for the prevention of cognitive decline. *Heliyon*, *10*(5), art. no. 27171. **https://doi.org/10.1016/j.heliyon.2024.e27171**
42. Vázquez, J.A., Valcarcel, J., Sapatinha, M., Bandarra, N.M., Mendes, R., Pires, C. (2023). Effect of the season on the production and chemical properties of fish protein hydrolysates and high-quality oils obtained from gurnard (*Trigla spp.*) by-products. *LWT – Food Science and Technology*, 177, art. no. 114576. **https://doi.org/10.1016/j.lwt.2023.114576**
43. Xie, X., Zhai, X., Chen, M., Li, Q., Huang, Y., Zhao, L., Wang, Q., Lin, L. (2023). Effects of frozen storage on texture, chemical quality indices and sensory properties of crisp Nile tilapia fillets. *Aquaculture and Fisheries*, *8*(6), 626–633. **https://doi.org/10.1016/j.aaf.2022.11.007**
44. Yang, H., Chen, Q., Cao, H., Fan, D., Huang, J., Zhao, J., Yan, B., Zhou, W., Zhang, W., Zhang, H. (2019). Radiofrequency thawing of frozen minced fish based on the dielectric response mechanism. *Innovative Food Science and Emerging Technologies*, *52*, 80–88. **https://doi.org/10.1016/j.ifset.2018.10.013**

ORIGINAL ARTICLE
http://journal.pan.olsztyn.pl

Polish Journal of Food and Nutrition Sciences
2024, Vol. 74, No. 4, 408–418
DOI: 10.31883/pjfns/195594
ISSN 1230-0322, e-ISSN 2083-6007

Effect of Selected Drying Methods on the Cannabinoid Profile of *Cannabis sativa* L. var. *sativa* Inflorescences and Leaves

Joanna Kanabus*, Marcin Bryła, Marek Roszko

Department of Food Safety and Chemical Analysis, Prof. Waclaw Dabrowski Institute of Agricultural and Food Biotechnology – State Research Institute, Rakowiecka 36, 02-532 Warsaw, Poland

The hemp industry uses traditional drying methods based on ambient temperature. However, these methods do not guarantee a high-quality dried product due to the possibility of mold growth. The present study aimed to evaluate the effect of the drying method for parts of the *Cannabis sativa* L. var. *sativa* plant (ambient temperature drying without light, freeze-drying, and convective drying at 50, 60, and 70°C) on the content of 17 cannabinoids. The leaves were separated, and the inflorescences were subdivided according to size. Analyses were performed using UHPLC-HESI-MS. Traditional drying of the inflorescences increased the total cannabinoid content to 17.608–22.209 mg/g DM relative to fresh material (8.562–11.386 mg/g DM). Increasing the drying temperature by 10°C significantly enhanced cannabinoid degradation in the dried inflorescences. The most significant increase in cannabidiol and Δ^9-tetrahydrocannabinol content in the inflorescences was observed during traditional drying (up to 10 times). The greatest decrease in the content of the main acid precursors of cannabinoids, *i.e.*, cannabidiolic acid and Δ^9-tetrahydrocannabinolic acid A, was observed during convective drying (up to 3 times). The present study is one of the first to compare the effects of drying methods on the profile of cannabinoids in selected parts of the *Cannabis sativa* L. plant.

Keywords: cannabinoids, drying, hemp inflorescences, hemp leaves, UHPLC-HESI-MS

INTRODUCTION

Cannabis sativa L. var. *sativa* is one of the oldest cultivated plants in the world, while cannabinoids are one of the most essential bioactive substances of its plants [Kanabus *et al.*, 2021]. The most common cannabinoids include Δ^9-tetrahydrocannabinol (Δ^9-THC), cannabidiol (CBD), cannabigerol (CBG), and their acid forms [Aizpurua-Olaizola *et al.,* 2014; Pellati *et al.,* 2018], and can be found in both the inflorescences and the leaves [Knezevic *et al.,* 2021], *i.e.*, the parts of the plant where epidermal outgrowths called glandular trichomes are formed, which serve for the biosynthesis and storage of these compounds [Xie *et al.,* 2023]. In contrast, they are found in trace amounts in the seeds [Kanabus *et al.,* 2021]. The interest in hemp seeds as food to date has been mainly due to their high contents of protein (>20 g/100 g) and essential amino acids, and their unique and ideally balanced fatty acid composition (25–35 g/100 g) [Farinon *et al.,* 2020]. A potential benefit from consuming both the inflorescences and leaves of the *C. sativa* plant is the delivery of the cannabinoids to the body. When supplied to the body in adequate doses, cannabinoids exhibit many positive actions to support its functioning. The most important effects are analgesic, sedative, anti-anxiety, and anticonvulsant ones [Baker *et al.,* 2003]. One of the more interesting suggestions for the possible use of the dried extracts from this plant is to apply it as an ingredient in herbal teas or to add it to cakes or dairy products [Das *et al.,* 2022; Kanabus *et al.,* 2021]. However, due to very high psychoactive activity of cannabinoids, it was necessary to regulate their content in food, including in particular their most active

***Corresponding Author:**
Tel.: +48 606-39-40; e-mail: **joanna.kanabus@ibprs.pl** (J. Kanabus)

Submitted: 25 May 2024
Accepted: 5 November 2024
Published on-line: 2 December 2024

representative, *i.e.*, total Δ^9-THC, the maximum content of which in the dry matter of the plant has been set below 0.3% according the European Union (EU) Commission Regulation No. 2023/915 [Regulation EU 2023/915].

The cannabinoid content depends not only on the part of the plant, but also on its chemotypes, development stage [Aizpurua-Olaizola *et al*., 2016; Ubeed *et al.,* 2022], growth conditions (temperature, fertilization, humidity) [Park *et al*., 2022], and post-harvest treatments such as drying [Das *et al*., 2022]. Bioactive compounds are usually degraded during processing at elevated temperatures. It is known that acidic cannabinoids are decarboxylated by heating (even at ≥30°C) [Meija *et al*., 2022; Wang *et al*., 2016] or by the action of enzymes (*e.g.*, CBDA synthase) in the plant to produce CBDA from CBGA [Kanabus *et al.,* 2021]. However, there is little information on changes in the cannabinoid profile under the influence of the drying process. Determining the thermal stability of cannabinoids is important for handling plants and selecting the method of drying or processing of *C. sativa* plant parts for food production [Meija *et al.,* 2022]. Fresh fiber hemp is usually harvested at a high initial moisture content (MC) (usually 80 g/100 g) and should be dried to a safe MC value (10 g/100 g) to prevent the development of harmful microflora [Kwaśnica *et al.,* 2020]. The most common drying method is drying on hangers or trays. This process takes place at 15–20°C and lasts between 3 and 10 days. The structure of the hemp plant restricts airflow near the inflorescences, which can result in mold growth.

The drying of agricultural products is a complex process that involves heat and mass exchange phenomena, and can cause physical, chemical, and biochemical modifications [Addo *et al*., 2023; Kwaśnica *et al*., 2020]. Both traditional drying (with or without light at ambient temperature) and hot air-drying are widely used for various plant materials. The heat and moisture exchange rate during the hot air-drying is significantly better than natural air-drying due to forced air convection [Chen *et al*., 2021]. Convective drying at 40–60°C usually does not adversely affect the quality of the dried material. Still, the long drying time of this process does not guarantee the high quality of the dried plant material [Esfandi *et al*., 2024]. Freeze-drying is one of the latest methods used to dry plant material. It involves dehydration by sublimation and surface desorption of the frozen product. Freeze-dried products retain nutrients, bioactivity, and color compared to traditionally-dried products [Addo *et al*., 2023; Kiani *et al*., 2018]. By operating at low temperatures, freeze-drying potentially reduces the loss of bioactive compounds, thereby ensuring a higher-quality of the dried products [Challa *et al*., 2021].

The objective of the present study was to compare the profiles of cannabinoids of *C. sativa* var. *sativa* dried using different methods, including freeze-drying; drying at 20°C for 10 days; and convective drying at 50, 60, and 70°C to obtain MC of 10±1 g/100 g.

MATERIALS AND METHODS

Chemicals and reagents

The certified reference materials (CRMs) including cannabidiol (CBD), cannabidiolic acid (CBDA), cannabigerol (CBG), cannabichromene (CBC), cannabinol (CBN), cannabinolic acid (CBNA), cannabidivarinic acid (CBDVA), cannabicyclol (CBL), and cannabicyclic acid (CBLA) were purchased as solutions at the concentration of 1.0 mg/mL in methanol (MeOH) or acetonitrile (ACN) from Restek GmbH (Bad Homburg, Germany). Cannabigerolic acid (CBGA), cannabichromenic acid (CBCA), Δ^9-tetrahydrocannabinol (Δ^9-THC), Δ^8-tetrahydrocannabinol (Δ^8-THC), Δ^9-tetrahydrocannabinolic acid A (Δ^9-THCA-A), Δ^9-tetrahydrocannabivarinic acid (Δ^9-THCVA), and cannabidivarin (CBDV) were provided by LGC Standards (Teddington, UK). The solution of Δ^9-tetrahydrocannabivarin (Δ^9-THCV) in MeOH (1.0 mg/mL) was obtained from Cerilliant Corporation (Round Rock, TX, USA). The CRMs had a certified purity value of >98.00%. Quality control material (QCM) HEMP-1 in ground hemp form (National Research Council Canada) was used for validation. Solvents of purity for liquid chromatography-mass spectrometry (LC-MS) analysis of water, ACN, and MeOH were purchased from Witko (Łódź, Poland), whereas HCOOH and HCO_2NH_4 (LC-MS grade) were purchased from Sigma Aldrich (St. Louis, MO, USA).

Plant material

The *Cannabis sativa* L. var. *sativa* 'Białobrzeskie' plants were selected for analysis. This variety has a documented history of human consumption and has been used for years for CBD extraction. Plants were obtained from the Institute of Natural Fibres and Herbaceous Plants in Poznań, located in Pętkowo, Poland (52°12'32"N 17°15'17"E). They were harvested at the peak of flowering, specifically between twenty days after the start of flowering and ten days after the end of flowering [Regulation EU 2017/1155]. After harvesting, the plants were divided according to the size of the inflorescences (small (<10 cm), medium (10–20 cm), and large (>20 cm)). Then, the inflorescences (S, M and B groups, respectively) and leaves (L) were collected, and the remaining plant parts (roots and stems) were removed. The samples were then frozen and stored at –60°C.

Drying methods

The drying conditions were chosen based on the usual conditions for this plant material type and the literature [Kwaśnica *et al.,* 2020; Thamkaew *et al*., 2021]. Each time, the drying process was carried out to achieve MC of approximately 10±1 g/100 g. The drying of the samples was carried out in triplicate, and the sample weight was 50±0.2 g each time. The traditional drying of fresh plant material was carried out on thin blotting paper in a ventilated room without light, with low air humidity (52±2%) [Das *et al*., 2022]. The ambient temperature in the room was 20±2°C. The moisture content of the samples was checked every 24 h during 10 days. The freeze-drying of frozen samples (–60°C) was performed at 25°C for 24 h in the Alpha 1-4 LSC plus lyophilizer unit (Martin Christ Gefriertrocknungsanlagen GmbH, Osterode am Harz, Germany). A KBC G-100/250 laboratory dryer (Warsaw, Poland) with natural air circulation was used to carry out convective drying at 50, 60, and 70°C, and the temperature was checked each time for uniform process conditions. Sample weights were recorded every 1 h for the first 12 h. After obtaining

MC of 10 g/100 g, all dried samples were ground into a fine powder using a Grindomix GM200 grinder (Retsch, Haan, Germany) and stored until analyzed.

Preparation of extracts

Samples of both fresh and dried hemp material (0.1 g) were extracted using MeOH (fresh material – 5 mL, dried material – 2×10 mL) at 25±1°C for 2 min. Mixtures of solids in solvent were homogenized (2 min, 5000 rpm) using a Unidrive X 1000 homogenizer (CAT Scientific Inc., Paso Robles, CA, USA) and then centrifuged (2 min; 10,000×*g*) using an MPW-380R centrifuge (MPW Med. Instruments, Warsaw, Poland). Sample preparation procedure was described in detail in our previous publication [Kanabus *et al.,* 2023]. The extracts were filtered through a 0.22 µm (13 mm filter diameter) syringe filter (LLG Labware, Meckenheim, Germany) and directly subjected to cannabinoid analysis.

Determination of cannabinoids

Identification and quantification of the cannabinoids were performed using an ultra-high-performance liquid chromatography-Q-Exactive Orbitrap mass spectrometry setup operating with a heated electrospray interface (UHPLC-HESI-MS) (Thermo Fisher Scientific, Waltham, MA, USA). Chromatographic separation was performed using a 2.1×100 mm, C18 Cortecs, 1.6 µm column (Waters, Milford, MA, USA). The mobile phase used in the isocratic mode (0.3 mL/min, 10 min) was a mixture of ACN and an aqueous 0.02% HCOOH and 5 mM HCO_2NH_4 solution (75:25, *v/v*). Chromatographic and spectral data and spectrometer operation parameters were described in detail in our previous work [Kanabus *et al.*, 2023].

Standard solutions of all 17 cannabinoids with the concentration of 100 µg/mL were prepared by dissolving 1.0 mL of the compound reference standard in ACN or MeOH using 10-mL volumetric flasks separately. This step was repeated as it was necessary to prepare higher dilutions for most compounds except CBD and CBDA. All solutions were stored at –80°C. Calibration curves in the relevant ranges for the compound were generated using Thermo TraceFinderTM software, version 5.1 (Thermo Fisher Scientific, Pleasanton, CA, USA).

Validation of the method was described in detail in our previous publication [Kanabus *et al.,* 2023]. To confirm and maintain the method's validity, a Certified Reference Material (HEMP-1) analysis was performed for each series of cannabinoid analyses (unpublished data). The recoveries achieved were within the 80–120% target range and fulfilled the guidelines included in ICH 2005 and AOAC 2002 [Kanabus *et al.*, 2023].

The cannabinoid content was determined using a WPS 30S balance dryer (Radwag, Radom, Poland), and respective results were expressed on a dry matter basis (mg/g DM). In addition, total Δ^9-THC content was calculated Δ^9-THC and Δ^9-THCA-A following Equation (1) [Regulation EU 2023/915]:

$$\text{Total } \Delta^9\text{-THC} = \Delta^9\text{-THC} + (0.877 \times \Delta^9\text{-THCA-A}) \quad (1)$$

Statistical analysis

Data were analyzed statistically using Statistica 13 software (Statsoft, Carlsbad, CA, USA). A one-way analysis of variance (one-way ANOVA) was used to determine significant differences ($p<0.01$) between the mean contents of individual cannabinoids and their sum in the fresh plant material and dried using different methods. The homogeneity of the groups was determined using the Tukey's honestly significant difference (HSD) test.

RESULTS AND DISCUSSION

This study discusses the effect of selected drying methods on the stability of 17 cannabinoids (listed in M&M - Chemicals and reagents) found in the *Cannabis sativa* L. var. *sativa* 'Białobrzeskie' plant. The chromatographic and spectral data used to identify these compounds were presented in our previous study [Kanabus *et al.*, 2023]. The conditions of the drying methods and the time required to obtain the MC of the samples at the level of 10 g/100 g are presented in the Supplementary Materials (**Table S1**). The contents of individual cannabinoids and their sums in fresh inflorescences and leaves, and after their drying by the chosen methods are presented in **Table 1** and **Figures 1–4**. The paper also presents results of determinations of the total Δ^9-THC content, which was designed to represent the sum of Δ^9-THC and Δ^9-THCA-A equivalents in a given product [Regulation EU 2023/915].

Effect of drying method on total cannabinoid content

The total cannabinoid content determined in the fresh material ranged from 4.516 mg/g DM (leaves) to 11.386 mg/g DM (medium inflorescences) (**Table 1**). Freeze-drying and convective drying at low temperature (50°C) allowed the preservation of the total content of cannabinoids except for the medium-sized inflorescences. In contrast, inflorescences dried at 60 and 70°C contained less ($p<0.01$) total cannabinoids than the fresh material. In general, the higher the drying temperature was, the lower was the content of the total cannabinoids in inflorescences. For leaves, a significantly ($p<0.01$) lower total cannabinoid content was determined in the samples dried *via* all methods compared to that in the fresh material. Among dried leaves, those obtained by convective drying (50°C and 70°C) had the highest content of total cannabinoids (3.062–3.418 mg/g DM). Compared to the fresh material, the cannabinoid content of leaves dried by traditional drying and freeze-drying decreased around 1.8-fold. The differences in the total cannabinoid content of materials obtained by different methods may result from the different thermal stability of individual cannabinoids and from possible conversions between them, primarily non-enzymatic decarboxylation of acidic cannabinoids to their neutral forms and isomeric forms occurring under the influence of heating and aging [García-Valverde *et al.,* 2022; Grafström *et al.,* 2016; Meija *et al.,* 2022; Wang *et al.,* 2016]. The effects of each drying method used in our study on individual cannabinoid contents were described below in separate subsections concerning drying at ambient temperature, freeze-drying, and convective drying.

Table 1. Cannabinoid content (mg/g dry matter) of fresh *Cannabis sativa* L. var. *sativa* small (S), medium (M) and large (B) inflorescences and leaves (L) and after their drying by selected methods.

Cannabinoid	Part of plant	Fresh material	Traditional drying	Freeze-drying	Convective drying		
					50°C	60°C	70°C
CBC	S	0.168±0.010^{fA}	1.444±0.150^{aA}	0.565±0.020^{bA}	0.431±0.030^{dB}	0.538±0.038^{bcA}	0.208±0.010^{eC}
	M	0.125±0.006^{fB}	1.154±0.048^{aB}	0.471±0.022^{cB}	0.850±0.059^{bA}	0.424±0.029^{dC}	0.301±0.048^{eAB}
	B	0.104±0.013^{fC}	1.470±0.039^{aA}	0.291±0.001^{eC}	0.422±0.030^{cC}	0.535±0.010^{bB}	0.366±0.054^{dA}
	L	0.003±0.001^{eD}	0.066±0.003^{cC}	0.020±0.005^{dD}	0.141±0.003^{bD}	0.167±0.012^{aD}	0.175±0.004^{aD}
CBDV	S	0.001±0.001^{eA}	0.125±0.014^{aB}	0.020±0.001^{dA}	0.068±0.005^{bA}	0.041±0.003^{cA}	0.063±0.004^{bA}
	M	0.001±0.001^{eA}	0.150±0.009^{aA}	0.018±0.008^{dA}	0.052±0.004^{bB}	0.027±0.002^{cB}	0.029±0.004^{cB}
	B	0.001±0.001^{eA}	0.125±0.011^{aB}	0.009±0.002^{cdB}	0.009±0.006^{cdD}	0.023±0.002^{bC}	0.007±0.002^{dC}
	L	0.001±0.001^{fA}	0.008±0.002^{dC}	0.003±0.001^{eC}	0.015±0.002^{cC}	0.022±0.002^{abC}	0.029±0.007^{aB}
CBG	S	0.025±0.007^{eB}	1.040±0.026^{aA}	0.280±0.015^{bA}	0.107±0.008^{dA}	0.195±0.014^{cA}	0.201±0.023^{cA}
	M	0.040±0.001^{eA}	0.627±0.045^{aC}	0.193±0.022^{bB}	0.080±0.006^{cB}	0.193±0.011^{bA}	0.053±0.008^{dC}
	B	0.043±0.004^{eA}	0.970±0.023^{aB}	0.203±0.005^{bB}	0.085±0.006^{dB}	0.126±0.017^{cB}	0.134±0.006^{cB}
	L	0.006±0.003^{cC}	0.087±0.003^{aD}	0.018±0.003^{bC}	0.026±0.008^{bC}	0.083±0.004^{aC}	0.019±0.009^{bD}
CBL	S	< LOD^{dA}	0.550±0.015^{aC}	0.311±0.030^{bA}	0.023±0.002^{cA}	0.022±0.001^{cAB}	0.022±0.001^{cA}
	M	< LOD^{eA}	0.687±0.011^{aB}	0.261±0.040^{bAB}	0.025±0.002^{cA}	0.026±0.003^{cA}	0.021±0.002^{dA}
	B	< LOD^{cA}	0.846±0.015^{aA}	0.166±0.020^{bC}	0.019±0.001^{bB}	0.021±0.002^{bAB}	0.020±0.002^{bA}
	L	< LOD^{dA}	0.037±0.004^{aD}	0.011±0.001^{cD}	0.020±0.003^{bB}	< LOD^{dC}	< LOD^{dB}
CBN	S	< LOD^{eA}	0.033±0.001^{aA}	0.017±0.002^{bA}	0.003±0.001^{dA}	0.014±0.001^{cB}	0.014±0.001^{cA}
	M	< LOD^{eA}	0.022±0.002^{aB}	0.013±0.001^{cB}	0.002±0.001^{dAB}	0.017±0.001^{bA}	0.013±0.001^{cA}
	B	< LOD^{dA}	0.030±0.001^{aA}	0.014±0.003^{bAB}	0.002±0.001^{cAB}	0.013±0.003^{bB}	0.012±0.001^{bAB}
	L	< LOD^{cA}	0.004±0.001^{aC}	0.005±0.002^{aC}	0.003±0.001^{bA}	< LOD^{cC}	< LOD^{cC}
CBNA	S	0.002±0.001^{aAB}	0.002±0.001^{aB}	0.001±0.001^{aB}	0.003±0.001^{aB}	0.001±0.001^{aA}	0.001±0.001^{aA}
	M	0.003±0.001^{bA}	0.018±0.001^{aA}	0.001±0.001^{cB}	0.003±0.001^{bB}	0.001±0.001^{cA}	0.001±0.001^{cA}
	B	0.002±0.001^{abAB}	0.002±0.002^{abB}	0.001±0.001^{bB}	0.004±0.001^{aAB}	0.002±0.001^{abA}	0.001±0.001^{bA}
	L	0.004±0.002^{abA}	0.001±0.001^{bcB}	0.008±0.001^{aA}	0.006±0.002^{aA}	0.002±0.001^{bA}	0.001±0.001^{bcA}
Δ^9-THC	S	0.012±0.001^{cB}	1.136±0.170^{aA}	0.405±0.035^{bA}	0.398±0.027^{bA}	1.046±0.073^{aAB}	0.440±0.016^{bA}
	M	0.017±0.001^{fA}	0.576±0.021^{bC}	0.350±0.004^{cB}	0.287±0.020^{dB}	1.230±0.031^{aA}	0.200±0.007^{eD}
	B	0.015±0.001^{dA}	1.071±0.025^{aAB}	0.179±0.003^{cC}	0.219±0.015^{bC}	1.153±0.080^{aA}	0.232±0.006^{bC}
	L	0.005±0.001^{eC}	0.148±0.075^{bcD}	0.038±0.002^{dD}	0.189±0.004^{bD}	0.267±0.021^{aC}	0.267±0.004^{aB}
Δ^9-THCV	S	0.001±0.001^{dB}	0.020±0.002^{aA}	0.006±0.001^{cA}	0.013±0.001^{bA}	0.014±0.002^{bA}	0.018±0.003^{aA}
	M	0.001±0.001^{cB}	0.007±0.001^{bB}	0.004±0.002^{bA}	0.011±0.002^{aA}	0.012±0.001^{aA}	0.006±0.001^{bB}
	B	0.001±0.001^{cB}	0.018±0.003^{aA}	0.002±0.001^{cB}	0.002±0.002^{cB}	0.006±0.001^{bB}	0.001±0.001^{cC}
	L	0.006±0.003^{aA}	0.002±0.002^{abC}	0.001±0.001^{bB}	0.004±0.002^{aB}	0.005±0.001^{aB}	0.006±0.001^{aB}
CBDVA	S	0.721±0.079^{abA}	0.575±0.059^{cA}	0.806±0.033^{aA}	0.472±0.033^{dB}	0.733±0.057^{abA}	0.416±0.033^{dB}
	M	0.665±0.071^{bAB}	0.510±0.087^{cAB}	0.521±0.042^{cB}	0.587±0.041^{bcA}	0.429±0.050^{dB}	0.925±0.040^{aA}
	B	0.385±0.038^{cC}	0.511±0.036^{aB}	0.198±0.014^{eC}	0.280±0.054^{dC}	0.440±0.030^{bB}	0.250±0.017^{dC}
	L	0.092±0.014^{aD}	0.046±0.009^{cC}	0.017±0.002^{dD}	0.082±0.008^{abD}	0.020±0.003^{dC}	0.021±0.002^{dD}
CBD	S	0.061±0.003^{fB}	5.996±0.136^{aA}	1.575±0.080^{eB}	3.450±0.458^{bA}	1.947± 0.137^{dA}	2.977±0.159^{bcA}
	M	0.066±0.007^{fB}	4.443±0.161^{aC}	3.890±0.186^{bA}	2.450±0.171^{cB}	1.849±0.170^{dA}	0.864±0.021^{eC}

Table 1 cont. Cannabinoid content (mg/g dry matter) of fresh *Cannabis sativa* L. var. *sativa* small (S), medium (M) and large (B) inflorescences and leaves (L) and after their drying by selected methods.

Cannabinoid	Part of plant	Fresh material	Traditional drying	Freeze-drying	Convective drying		
					50°C	60°C	70°C
CBD	B	0.045±0.002^{cC}	5.348±0.192^{aB}	1.149±0.131^{bC}	1.640±0.111^{bC}	1.007±0.102^{bB}	1.058±0.134^{bB}
	L	1.680±0.230^{aA}	0.483±0.015^{dD}	0.105±0.013^{eD}	1.280±0.125^{bD}	0.848±0.094^{cC}	1.020±0.133^{bB}
CBGA	S	0.152±0.016^{aB}	0.027±0.002^{cB}	0.053±0.013^{bB}	0.020±0.001^{dA}	0.008±0.002^{eB}	0.005±0.001^{eA}
	M	0.190±0.026^{aA}	0.058±0.004^{bA}	0.058±0.003^{bB}	0.017±0.002^{cB}	0.014±0.005^{cA}	0.006±0.002^{dA}
	B	0.151±0.013^{aB}	0.020±0.006^{cB}	0.071±0.001^{bA}	0.016±0.002^{cB}	0.006±0.004^{dB}	0.002±0.001^{eC}
	L	0.172±0.012^{aA}	0.002±0.001^{bC}	0.002±0.001^{bC}	0.002±0.001^{bC}	0.004±0.002^{bBC}	0.004±0.001^{bB}
Δ^9-THCVA	S	0.048±0.007^{aA}	0.011±0.002^{dB}	0.011±0.001^{dA}	0.008±0.001^{eA}	0.020±0.002^{bA}	0.015±0.002^{cA}
	M	0.027±0.010^{aB}	0.018±0.002^{bA}	0.006±0.002^{dB}	0.008±0.001^{dA}	0.012±0.001^{cB}	0.013±0.002^{cA}
	B	0.025±0.003^{aB}	0.010±0.002^{bB}	0.004±0.001^{dB}	0.008±0.001^{bcA}	0.002±0.001^{eD}	0.001±0.001^{eC}
	L	0.006±0.001^{aC}	0.001±0.001^{cC}	0.002±0.001^{cC}	0.002±0.001^{cB}	0.005±0.001^{abC}	0.006±0.001^{aB}
CBLA	S	0.018±0.003^{aB}	0.015±0.001^{aB}	0.004±0.002^{bB}	0.017±0.002^{aB}	0.004±0.001^{bC}	0.003±0.001^{bC}
	M	0.018±0.002^{aB}	0.017±0.002^{aB}	0.006±0.002^{cB}	0.011±0.001^{bC}	0.002±0.001^{dC}	0.002±0.001^{dC}
	B	0.015±0.002^{aBC}	0.011±0.003^{bC}	0.004±0.001^{dB}	0.017±0.001^{aB}	0.013±0.001^{abB}	0.009±0.001^{cB}
	L	0.032±0.005^{aA}	0.025±0.002^{bA}	0.036±0.004^{aA}	0.037±0.004^{aA}	0.033±0.002^{aA}	0.032±0.008^{aA}
CBCA	S	1.371±0.087^{aA}	1.113±0.129^{bA}	0.736±0.081^{cA}	0.486±0.034^{dB}	0.388±0.027^{eA}	0.355±0.023^{eB}
	M	0.592±0.028^{aC}	0.480±0.036^{cC}	0.540±0.019^{abB}	0.414±0.038^{dC}	0.256±0.018^{fB}	0.370±0.012^{eB}
	B	0.818±0.075^{aB}	0.660±0.024^{bB}	0.428±0.022^{cC}	0.638±0.037^{bA}	0.401±0.028^{cA}	0.416±0.036^{cA}
	L	0.276±0.017^{aD}	0.279±0.025^{aD}	0.228±0.035^{bD}	0.172±0.023^{cD}	0.079±0.012^{dC}	0.079±0.004^{dC}
Δ^9-THCA-A	S	0.420±0.017^{aC}	0.390±0.011^{bB}	0.360±0.016^{cC}	0.275±0.025^{dC}	0.289±0.027^{dB}	0.264±0.021^{dB}
	M	0.600±0.023^{aB}	0.500±0.064^{bcA}	0.541±0.032^{bA}	0.550±0.029^{bA}	0.478±0.017^{cA}	0.281±0.018^{dB}
	B	0.840±0.077^{aA}	0.279±0.013^{dC}	0.451±0.080^{bAB}	0.440±0.051^{bB}	0.464±0.028^{bA}	0.345±0.069^{cA}
	L	0.240±0.017^{aD}	0.220±0.024^{aC}	0.230±0.025^{aD}	0.241±0.013^{aC}	0.079±0.013^{bC}	0.080±0.015^{bC}
CBDA	S	8.146±0.305^{bB}	9.750±0.758^{aA}	8.420±0.514^{bA}	6.427±0.450^{cA}	2.785±0.195^{dA}	2.092±0.108^{eB}
	M	9.047±0.347^{aA}	9.140±0.284^{aA}	8.490±0.448^{abA}	6.977±0.551^{cA}	2.512±0.176^{dA}	2.063±0.116^{dB}
	B	6.122±0.863^{aC}	6.427±0.223^{aB}	5.450±0.227^{bB}	5.446±0.381^{bB}	1.547±0.104^{dB}	3.220±0.144^{cA}
	L	1.992±0.285^{aD}	1.060±0.121^{cC}	1.863±0.281^{aC}	1.199±0.192^{bcC}	1.070±0.073^{cC}	1.328±0.071^{bC}
Total cannabinoids	S	11.127±0.778^{bcA}	22.209±1.554^{aA}	13.461±0.942^{bB}	12.183±0.852^{bA}	8.043±0.563^{dA}	7.163±0.501^{dA}
	M	11.386±0.796^{cA}	18.403±1.288^{aB}	15.362±1.075^{bA}	12.124±0.848^{cA}	7.478±0.523^{dA}	5.147±0.360^{eC}
	B	8.562±0.599^{bB}	17.608±1.232^{aB}	8.619±0.603^{bC}	9.245±0.647^{bB}	5.564±0.389^{cB}	6.077±0.425^{cB}
	L	4.516±0.316^{aC}	2.472±0.173^{cC}	2.587±0.181^{cD}	3.418±0.239^{bC}	2.687±0.188^{cC}	3.062±0.214^{bD}

Results are shown as mean ± standard deviation (n=3). Values in the rows marked with different letters (a–f) differ significantly (p<0.01). Values in the columns (separately for each compound) marked with different letters (A–D) differ significantly (p<0.01). LOD, limit of detection. The full names of the compounds are listed in the "Chemicals and reagents" subsection.

Effect of traditional drying on cannabinoid profile

The total content of cannabinoids in the inflorescences decreased slightly during the initial period of the process, reaching a minimum value after 2 (small and large inflorescences) or 4 (medium inflorescences) days of drying, and then began to increase successively until the 10th day (**Figure 1**). In the case of leaves, the decrease in the total content lasted longer, until the 5th day of drying, and was definitely greater (more than 2-fold), whereas the further increase was less spectacular than in the case of inflorescences (**Figure 2**). The highest increase, up to 100-fold, in the content after traditional drying was determined for CBC, CBG, CBD, and Δ^9-THC (**Table 1**). The content of CBD increased the most and the final content of this compound in inflorescences ranged from 4.443 to 5.348 mg/g DM.

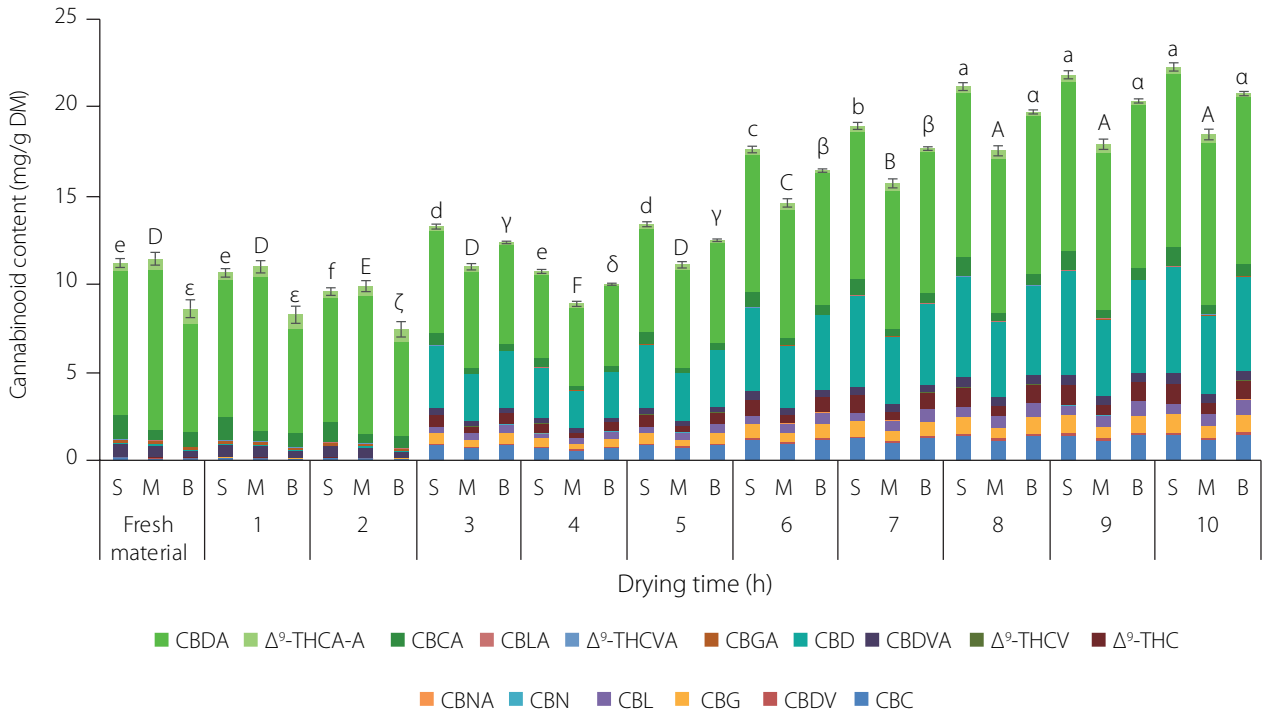

Figure 1. Changes in the cannabinoid profile during traditional drying (20°C, 10 days, without access to light) of *Cannabis sativa* L. var. *sativa* small (S), medium (M) and large (B) inflorescences.
Values marked with different letters (a–f for S, A–F for M, α–ζ for B inflorescences) differ significantly ($p<0.01$). The full names of the compounds are listed in the "Chemicals and reagents" subsection.

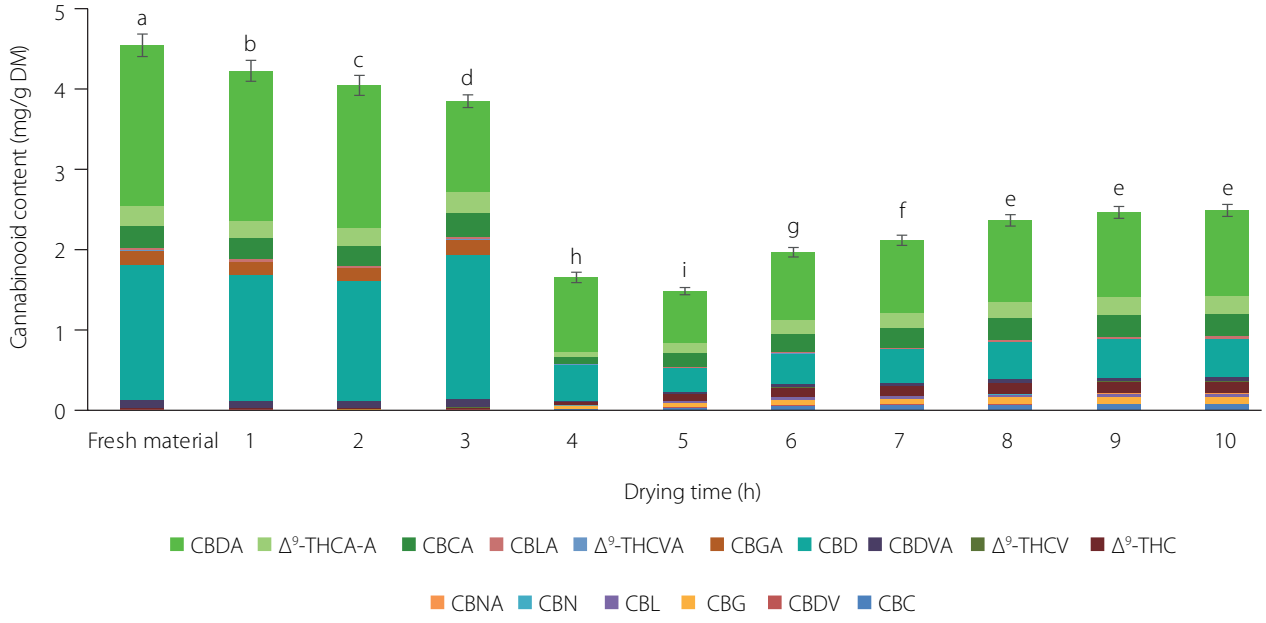

Figure 2. Changes in the cannabinoid profile during traditional drying (20°C, 10 days, without access to light) of *Cannabis sativa* L. var. *sativa* leaves.
Values marked with different letters (a–i) differ significantly ($p<0.01$). The full names of the compounds are listed in the "Chemicals and reagents" subsection.

The Δ^9-THC content during drying of the inflorescences at 20°C increased from 0.012–0.017 mg/g DM to 0.576–1.136 mg/g DM. The main acidic cannabinoids in the fresh samples were CBDA, CBCA, CBDVA, and Δ^9-THCA-A. The content of the Δ^9-THC precursor, Δ^9-tetrahydrocannabinolic acid (Δ^9-THCA-A), in fresh inflorescences ranged from 0.420–0.840 mg/g DM and decreased after 10 days of drying at ambient temperature (0.279–0-500 mg/g DM). A decrease was also recorded in the contents of CBCA and CBDVA in inflorescences as well as CBDVA and CBDA in leaves. Our study results were in line with those of Esfandi *et al.* [2024], who dried parts of the *C. sativa* L. plant at ambient temperature without light. These authors compared changes in CBD

and Δ^9-THC contents in fresh and dried material and showed successively more than 7-fold and 10-fold increases in the content of these compounds after drying. A higher Δ^9-THC content in traditionally dried inflorescences compared to the fresh material was also reported by Uziel *et al*. [2024]. In turn, Das *et al*. [2024] dried hemp samples at 30°C and observed a 0.30-fold increase in Δ^9-THC content. The content of Δ^9-THCA-A decreased 0.25-fold relative to fresh material. Similar results were obtained in the present study, and a decrease in the content of this compound was observed as well.

In the case of *C. sativa* inflorescences and leaves, a decrease in CBGA content was observed compared to the fresh material, with a simultaneous increase in CBG content (**Table 1**). Moreover, an increase in CBDA content and a simultaneous increase in CBD content were noted in small and large inflorescences. Based on these observations, it can be assumed that CBGA was converted at 20°C by enzymes, such as cannabidiolic acid synthase, allowing the formation of CBDA and then both compounds underwent non-enzymatic decarboxylation to the neutral forms CBG and CBD. The enzymatic inter-conversion of CBGA to CBDA is well established in the biosynthesis pathway of cannabinoids during plant growth [Kim *et al*., 2022; Taura *et al*., 2007]. In turn, Meija *et al*. [2022] reported that decarboxylation of CBDA to CBD was likely to occur even during storage of dried inflorescences at ambient temperature.

CBL and CBN, which were absent in the fresh material (<limit of detection, LOD), were determined in the inflorescences dried at ambient temperature in the range of 0.550–0.846 mg/g DM and 0.022–0.033 mg/g DM, respectively; for the leaves, the values were lower at 0.037 mg/g DM and 0.004 mg/g DM (**Table 1**). The Δ^8-THC was not determined in any of the samples analyzed.

After 10 days of drying at 20°C without light, the total Δ^9-THC content was 1.478, 1.015, and 1.246 mg/g DM in the small, medium and large inflorescences, respectively, and 0.341 mg/g DM in the leaves, indicating that this drying method poses no risk of exceeding the total Δ^9-THC content in the dried matter of plants according to the Commission Regulation (EU), which is 0.3% [Regulation EU 2023/915].

Effect of freeze-drying on cannabinoid profile

After freeze-drying of different-sized inflorescences and leaves of *C. sativa*, no Δ^8-THC was detected in any sample. Of all the cannabinoids identified in inflorescences of different sizes, the highest content was found for CBDA (5.450–8.490 mg/g DM), which was approximately 0.1 times lower than its content in the fresh material (6.122–9.047 mg/g DM) (**Table 1**). When the inflorescences were subjected to freeze-drying, the content of CBD increased from 0.045–0.066 mg/g DM to 1.149–3.890 mg/g DM (depending on the size of inflorescences). The opposite observation was noted for the leaf samples. Drying by this method resulted in a more than 16-fold decrease in CBD content, *i.e.*, from 1.680 to 0.105 mg/g DM. Both CBN and CBL, which were not detected in the fresh plant material (<LOD), were found in the freeze-dried material (at 0.005–0.017 mg/g and 0.011–0.311 mg/g, respectively), probably due to the decarboxylation of their acidic precursors (CBNA and CBLA, respectively). In freeze-dried inflorescence and leaf samples, the total Δ^9-THC content did not exceed the target level of 0.3% of plant dry matter, but its values were relatively high: 0.721 mg/g DM (small inflorescence), 0.824 mg/g DM (medium inflorescence), 0.575 mg/g DM (large inflorescence), and 0.240 mg/g DM (leaves).

Several literature reports suggest that freeze-drying retains more aromatic and bioactive compounds in dried plants than other drying methods especially those involving heating [Di Cesare *et al.*, 2003; Thamkaew *et al.*, 2021]. While most of the works focus on the freeze-drying of herbs, there is a lack of information on the bioactive compound profile of *C. sativa* individual plant parts dried using this method. One of the first studies carried out by Addo *et al.* [2023] reported that the freeze-drying increased the contents of CBDA, CBGA, and CBG in dried samples by up to 3-fold compared to the fresh material. The contents of the listed cannabinoids after drying were in the range of 0.380–0.450 mg/g, 2.870–4.910 mg/g, and 0.570–1.330 mg/g, respectively. In our study, the contents of the cannabinoids in question fell within the ranges of 1.863–8.490 mg/g DM, 0.002–0.071 mg/g DM, and 0.018–0.280 mg/g DM, respectively.

Effect of convective drying on cannabinoid profile

The convective drying of inflorescences of different sizes and leaves was carried out using three temperatures: 50°C, 60°C, and 70°C. The changes in the total and individual cannabinoid contents during the drying of the inflorescences and leaves are shown in **Figures 3** and **4**, respectively. The total cannabinoid content of the small, medium and large inflorescences dried at 70°C decreased during the initial period of the process, reaching a minimum value after 2 h of drying. In the case of drying at 50°C and 60°C, the content of cannabinoids remained similar throughout the drying period. The most significant decrease in cannabinoid content was observed in all inflorescences dried at 60°C after the 8th h of drying. In the case of leaves dried at 50°C, an increase in the total content of cannabinoids was recorded up to 10 h of drying, while a further two-hour drying under these conditions resulted in a decrease in the total content of these compounds. For leaves dried at 60°C and 70°C, cannabinoid degradation was noted after 4 h of drying. The predominant cannabinoid in the dried inflorescences in each temperature variant was CBDA (1.070–6.977 mg/g DM), the content of which decreased up to fivefold compared to the fresh material (**Table 1**). Convective drying at 50°C resulted in inflorescences having a significantly higher CBD content than the samples dried at the other temperatures tested. On the other hand, the convective drying of leaves at all temperatures decreased CBD content by up to half. In the dried inflorescences (all condition variants), the occurrence of CBL (0.019–0.083 mg/g DM) and CBN (0.002–0.017 mg/g DM), which were not detected in the fresh material, was observed. In contrast, in leaves, these compounds were present only in the samples dried at 50°C (0.020 and 0.003 mg/g DM, respectively). The content of CBGA in the inflorescences decreased after drying at all temperatures and was the lowest after drying at 70°C (0.002–0.006 mg/g DM). The convective drying did

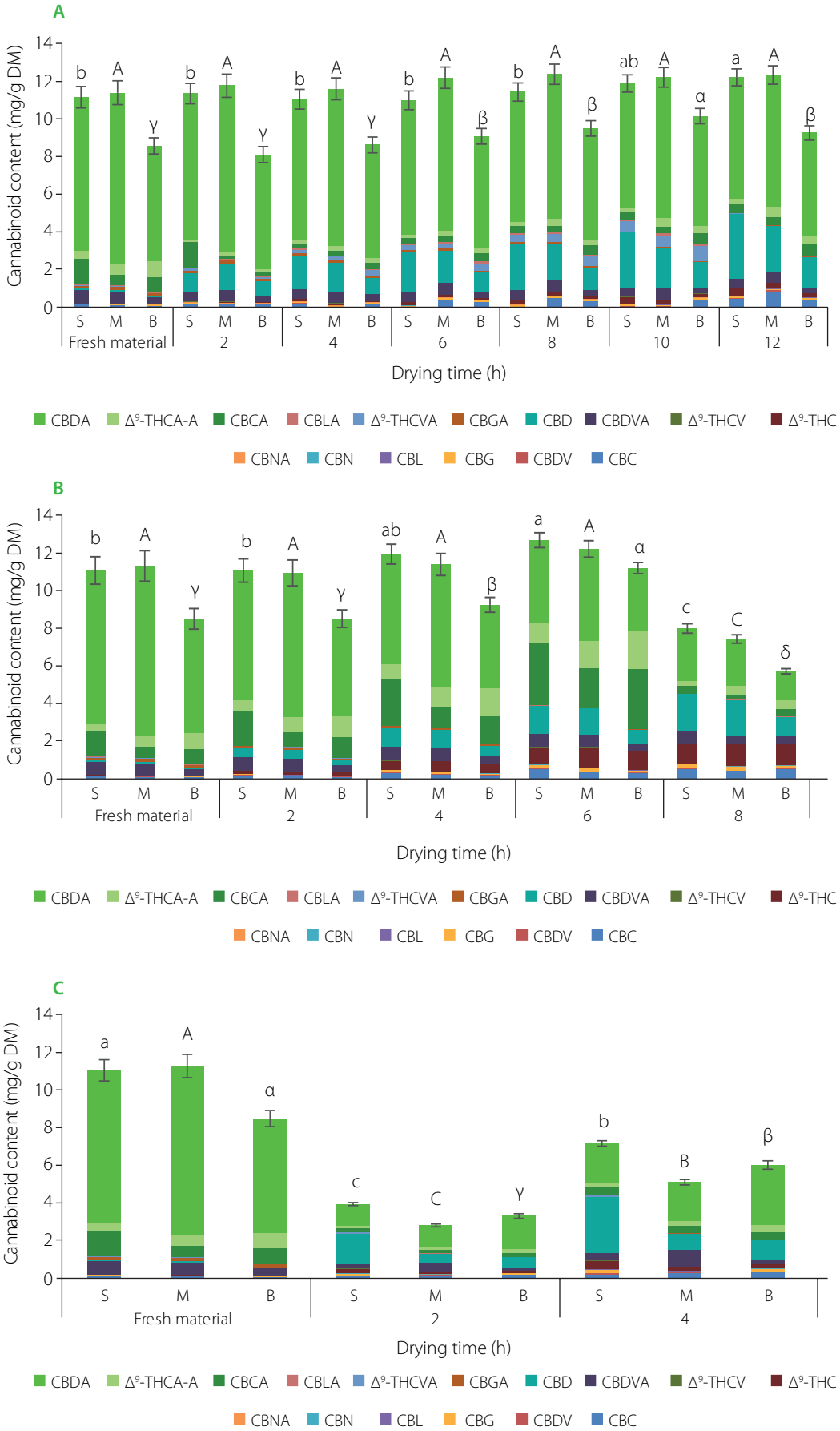

Figure 3. Changes in the cannabinoid profile during convective drying at 50°C (**A**), 60°C (**B**), and 70°C (**C**) of *Cannabis sativa* L. var. *sativa* small (S), medium (M) and large (B) inflorescences.
Values marked with different letters (a–c for S, A–C for M, α–δ for B inflorescences) differ significantly ($p<0.01$). The full names of the compounds are listed in the "Chemicals and reagents" subsection.

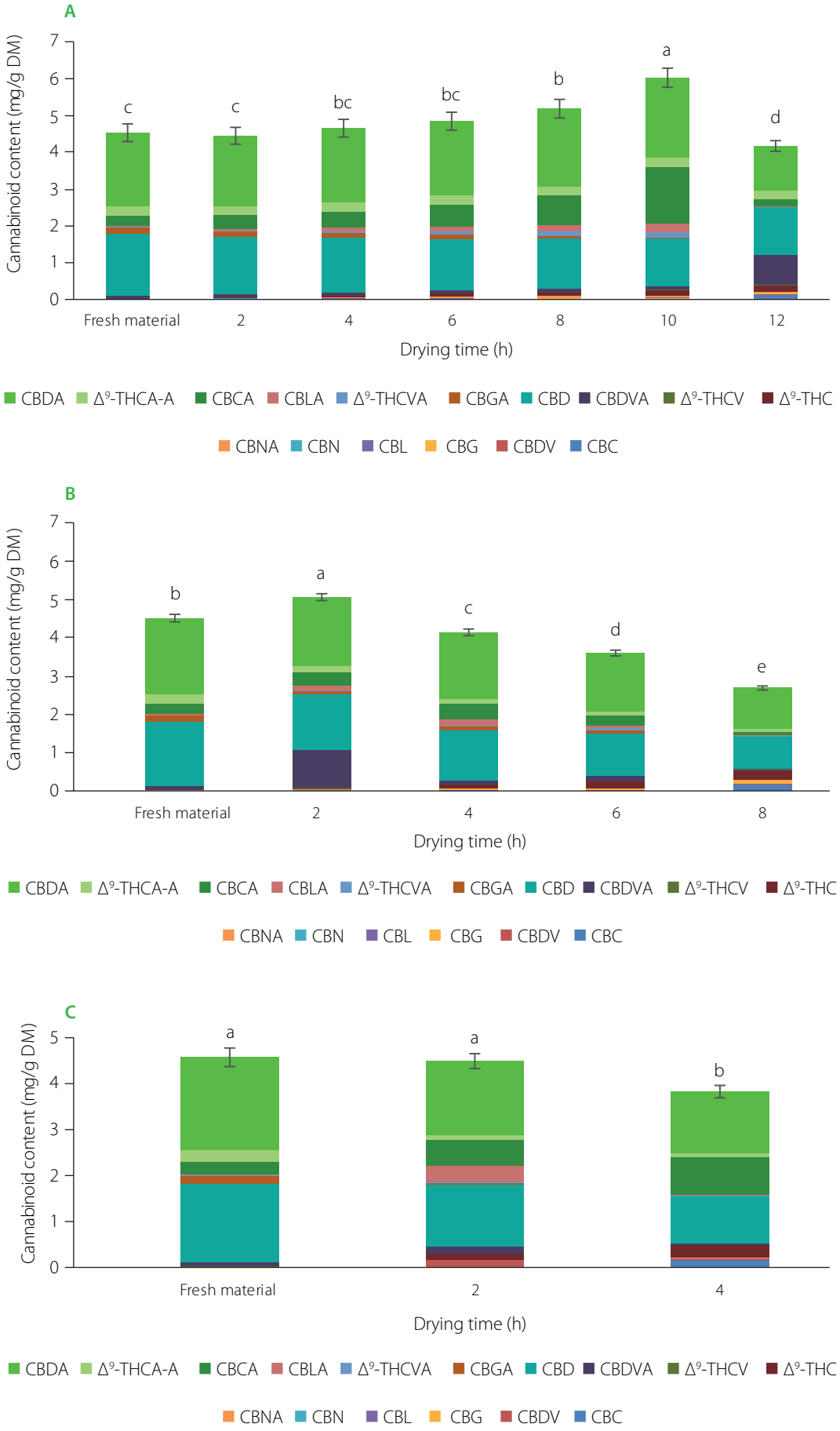

Figure 4. Changes in the cannabinoid profile during convective drying at 50°C (**A**), 60°C (**B**), and 70°C (**C**) of *Cannabis sativa* L. var. *sativa* leaves. Values marked with different letters (a–e) differ significantly ($p<0.01$). The full names of the compounds are listed in the "Chemicals and reagents" subsection.

not affect the formation of Δ^8-THC in either inflorescences or leaves. The dominant cannabinoid in leaves was CBDA, whose content was recorded at 1.328 mg/g DM after processing at 70°C. In the variant at 60°C, the final content of this compound in the dried material was significantly lower.

The convective drying at different temperatures also significantly affected the levels of Δ^9-THC, Δ^9-THCA-A, and total Δ^9-THC in the dried samples (**Table 1**, **Figures 3** and **4**). The highest content of Δ^9-THC was recorded for medium inflorescences dried at 60°C (1.230 mg/g DM). Among the dried leaves, those processed at 60 and 70°C had the highest Δ^9-THC content (0.267 mg/g DM). The convective drying of inflorescences and leaves at 70°C resulted in the samples having the lowest content of Δ^9-THCA-A (0.080–0.345 mg/g DM). The values of total Δ^9-THC calculated for the samples dried at 50°C were in the range of 0.400–0.769 mg/g DM, for these dried at 60°C the range was 0.336–1.560 mg/g DM, and content in materials dried at 70°C ranged from 0.337 to 0.671 mg/g DM. The total Δ^9-THC contents determined in all analyzed samples were within the safe limit stipulated in the Commission Regulation (EU) [Regulation EU 2023/915].

Literature data on the effect of the drying process on cannabinoid content/degradation rates indicate that levels of neutral cannabinoids increase after drying. One of the first reports on drying plant parts was presented by Turner & Mahlberg [1984], who dried leaf samples of *C. sativa* L. for 24 h at 37°C, at room temperature (2 weeks), and at 60°C (oven drying – 12 h). In the samples dried at both 37°C and 60°C, a 2-fold higher amount of neutral cannabinoids was recorded compared to the fresh material, indicating that the decarboxylation process was already occurring at 37°C. Chen *et al.* [2021] used hot air drying (40, 50, 60, 70, 90°C) and infrared drying (40 and 60°C) to dry the inflorescences of *C. sativa* L. var. *sativa* plants. They showed that increasing the ambient temperature to 90°C significantly facilitated the decarboxylation of CBDA (from 0.2% to 14.1%) and also that the use of infrared drying resulted in a higher loss of cannabinoids compared to hot air drying by 16.2% and 72.3% on average, respectively. Uziel *et al.* [2024] compared microwave drying of hemp with conventional drying. Microwave drying was carried out at 4 temperature variants (40, 50, 60 and 80°C). The authors showed that the use of microwaves in drying hemp significantly shortened the drying time (<4.5 h depending on the temperature used) compared to traditional drying (10 days). They also confirmed that the use of high drying temperatures in cannabis caused changes in the composition of the cannabinoids present in the dried material. The cited article showed that the highest contents of CBDA and Δ^9-THCA-A decarboxylation products were determined in the samples dried at 80°C, whereas in our study – in the samples dried at 50°C. These differences may be due to the initial content of these cannabinoids and their precursors in the fresh material. As confirmed by Esfandi *et al.* [2024], temperature (45, 55, 65°C) as well as drying method type (drying with or without light, oven drying, vacuum drying or microwave drying) used to dry *C. sativa* L. samples, affect the increase in on the contents of selected cannabinoids (CBD and Δ^9-THC) in the dried plant material. There are also data indicating that the drying process did not affect the cannabinoid content of the dried material. The study presented by Kwaśnica *et al.* [2023] compared the 50, 60, and 70°C convective method, the vacuum-microwave method, and combination thereof used to dry the leaves of *C. sativa* L. and showed that the drying method did not affect changes in the profile of the cannabinoids analyzed. The results we obtained and those cited above confirm the need to control the drying processes of the *C. sativa* L. plant parts, as there is a risk of exceeding the acceptable level of Δ^9-THC in the dried samples. This poses a severe risk in terms of ensuring the safety of the food produced from the dried plants. The chosen drying process conditions may not have been sufficient to inhibit the activity/activity of the enzymes by which the precursors of the selected cannabinoids are synthesised, and thus changes in the the sum and the profile of individual cannabinoids. Acidic cannabinoids can also be synthesised. The higher temperature of the drying process results in enhanced water diffusion from the dried material, thus resulting in a shorter drying time. Intense evaporation of water from the plant material may have resulted in a lower temperature of the material (not measured during the experiment), which affected the profile of the cannabinoid compounds. In addition, a greater loss of water results in a slower rate of decarboxylation. To confirm this, it would be necessary to determine the changes/kinetics of enzymatic activity during the drying process in order to find conditions (time and water content) that cause a reduction in enzyme activity and accompanying chemical reactions.

CONCLUSIONS

The study highlights the influence of the size (small, medium, large inflorescences) and parts (inflorescences and leaves) of *Cannabis sativa* L. var. *sativa* and the effect of the drying process on the cannabinoid content of the dried materials. The use of higher temperatures, *i.e.*, 50°C, 60°C and 70°C, made it possible to determine differences in the content changes of cannabinoids during drying. It was found that increasing the drying temperature by 10°C contributed to greater degradation of the analyzed compounds. Traditional drying resulted in dried inflorescences containing up to 2 times more of the analyzed compounds compared to the fresh material. In the case of leaf samples, drying *via* all methods tested resulted in a decrease in the total cannabinoid contents (up to 2-fold). Appropriately selected drying conditions of the *C. sativa* L. var. *sativa* plant parts make it possible to obtain safe (containing an acceptable total Δ^9-THC content) raw material, which can be used to produce hemp-containing foods or dietary supplements.

SUPPLEMENTARY MATERIALS

The following are available online at **https://journal.pan.olsztyn.pl/Effect-of-Selected-Drying-Methods-on-the-Cannabinoid-Profile-of-Cannabis-sativa-L,195594,0,2.html; Table S1**. Conditions and time of drying by the chosen method necessary to obtain moisture content of 10±1 g/100 g in the dried parts of the plant

RESEARCH FUNDING

The research has not received external funding.

CONFLICT OF INTERESTS

The authors declare no competing financial interest.

ORCID IDS

M. Bryła https://orcid.org/0000-0002-1855-3610
J. Kanabus https://orcid.org/0000-0001-9804-5570
M. Roszko https://orcid.org/0000-0003-1848-2100

REFERENCES

1. Addo, P.W., Chouvin-Bosse, T., Taylor, N., Macpherson, S., Paris, M., Lefsrud, M. (2023). Freeze-drying *Cannabis sativa* L. using real-time relative humidity monitoring and mathematical modeling for the cannabis industry. *Industrial Crops Products*, *199*, art. no. 116754. https://doi.org/10.1016/j.indcrop.2023.116754
2. Aizpurua-Olaizola, O., Omar, J., Navarro, P., Olivares, M., Etxebarria, N., Usobiaga, A. (2014). Identification and quantification of cannabinoids in *Cannabis sativa* L. plant by high performance liquid chromatography-mass spectrometry. *Analytical and Bioanalytical Chemistry*, *406*, 7549-7560. https://doi.org/10.1007/s00216-014-8177-x
3. Aizpurua-Olaizola, O., Soydaner, U., Öztürk, E., Schibano, D., Simsir, Y., Navarro, P., Etxebarria, N., Usobiaga, A. (2016). Evolution of the cannabinoid and terpene content during the growth of *Cannabis sativa* plant from different chemotypes. *Journal of Natural Products*, *79*(2), 324-331. https://doi.org/10.1021/acs.jnatprod.5b00949
4. Baker, D., Pryce, G., Giovannoni, G., Thompson, A.J. (2003). The therapeutic potential of *Cannabis*. *The Lancet Neurology*, *2*(5), 291-298. https://doi.org/10.1016/S1474-4422(03)00381-8
5. Challa, S.K.R., Misra, N.N., Martynenko, A. (2021). Drying of cannabis – state of the practices and future needs. *Drying Technology*, *39*(14), 2055–2064. https://doi.org/10.1080/07373937.2020.1752230
6. Chen, C., Wongso, I., Putnam, D., Khir, R., Pan, Z. (2021). Effect of hot air and infrared drying on the retention of cannabidiol and terpenes in industrial hemp (*Cannabis sativa* L.). *Industrial Crops Products, 172*, art. no. 114051. https://doi.org/10.1016/j.indcrop.2021.114051
7. Das, P.C., Vista, A.R., Tabil, L.G., Baik, O. (2022), Postharvest operations of *Cannabis* and their effect of cannabinoid content: A review. *Bioengineering*, *9*(8), art. no. 364. https://doi.org/10.3390/bioengineering9080364
8. Das, P.C., Bail, O.D., Tabil, L.G. (2024). Microwave-infrared drying of cannabis (*Cannabis sativa* L.): Effect on drying characteristics, energy consumption and quality. *Industrial Crops and Products*, 211, 118215. https://doi.org/10.1016/j.indcrop.2024.118215
9. Di Cesare, L.F., Forni, E., Viscardi, D., Nani, R.C. (2003). Changes in the chemical composition of basil caused by different drying procedures. *Journal of Agricultural and Food Chemistry, 51*(12), 3575–3581. https://doi.org/10.1021/jf021080o
10. Esfandi, A., Mehrafarin, A., Jari, S.K., Badi, H.N., Larijani, K. (2024). Variability in color and phytochemical properties of hemp (*Cannabis sativa* L.) upon drying techniques; an opportunity for industrial products. *Journal of Medicinal Plants and By-products*, *13*(1), 79-86. https://doi.org/10.22034/JMPB.2023.128276
11. Farinon, B., Molinari, R., Costantini, L., Merendino, N. (2020). The seed of industrial hemp (*Cannabis sativa* L.): Nutritional quality and potential functionality for human health and nutrition. *Nutrients,* 12(7) art. no. 1935. https://doi.org/10.3390/nu12071935
12. García-Valverde, M.T., Sánchez-Carnerero Callado, C., Díaz-Liñán, M.C., Sánchez de Medina, V., Hidalgo-García, J., Nadal, X., Hanuš, L., Ferreiro-Vera, C. (2022). Effect of temperature in the degradation of cannabinoids: From a brief residence in the gas chromatography inlet port to a longer period in thermal treatments. *Frontiers in Chemistry*, *10,* art. no. 1038729. https://doi.org/10.3389/fchem.2022.1038729
13. Grafström, K., Andersson, K., Pettersson, N., Dalgaard, J., Dunne, S.J. (2019). Effects of long term storage on secondary metabolite profiles of cannabis resin. *Forensic Science International*, *301*, 331-340. https://doi.org/10.1016/j.forsciint.2019.05.035
14. Kanabus, J., Bryła, M., Roszko, M., Modrzewska, M., Pierzgalski, A. (2021). Cannabinoids – Characteristics and potential for use in food production. *Molecules, 26*(21), art. no. 6723. https://doi.org/10.3390/molecules26216723
15. Kanabus, J., Bryła, M., Roszko, M. (2023). The development, validation, and application of a UHPLC-HESI-MS method for the determination of 17 cannabinoids in *Cannabis sativa* L. *var. sativa* plant material. *Molecules*, *28*(23), art. no. 8008. https://doi.org/10.3390/molecules28248008
16. Kiani, S., Minaei, S., Ghasemi-Varnamkhasti, M. (2018). Real-time aroma monitoring of mint (*Mentha spicata* L.) leaves during the drying process using electronic nose system. *Measurement*, *124*, 447-452. https://doi.org/10.1016/j.measurement.2018.03.033
17. Kim, A.L., Yun, Y.J., Choi, H.W., Hong, Ch.H., Shim, H.J., Lee, J.H., Kim, Y.Ch. (2022). Profiling cannabinoid contents and expression levels of corresponding biosynthetic genes in commercial *Cannabis* (*Cannabis sativa* L.) cultivars. *Plants*, 11(22), art. no. 3088. https://doi.org/10.3390/plants11223088
18. Knezeivc, F., Nikolai, A., Marchart, R., Sosa, S., Tubaro, A., Novak, J. (2021). Residues of herbal hemp leaf teas – How much of the cannabinoids remain? *Food Control*, *127*, art. no. 108146. https://doi.org/10.1016/j.foodcont.2021.108146
19. Kwaśnica, A., Pachura, N., Masztalerz, K., Figiel, A., Zimmer, A., Kupczyński, R., Wujcikowska, K., Carbonell-Barrachina, A.A., Szumny, A., Różański, H. (2020). Volatile composition and sensory properties as quality attributes of fresh and dried hemp flowers (*Cannabis sativa* L.). *Foods*, *9*(8), art. no. 1118. https://doi.org/10.3390/foods9081118
20. Kwaśnica, A., Pachura, N., Carbonell-Barrachina, Á.A., Issa-Issa, H., Szumny, D., Figiel, A., Masztalerz, K., Klemens, M., Szumny, A. (2023). Effect of drying methods on chemical and sensory properties of *Cannabis sativa* leaves. *Molecules*, *28*(24), art. no. 8089. https://doi.org/10.3390/molecules28248089
21. Meija, J., McRae, G., Miles, Ch.O., Melanson, J.E. (2022). Thermal stability of cannabinoids in dried cannabis: a kinetic study. *Analytical and Bioanalytical Chemistry*, *414*(1), 377-384. https://doi.org/10.1007/s00216-020-03098-2
22. Pellati, F., Borgonetti, V., Brighenti, V., Biagi, M., Benvenuti, S., Corsi, L. (2018). *Cannabis sativa* L., and non psychoactive cannabinoids: The chemistry and role against oxidative stress, inflammation, and cancer. *BioMed Research International*, *2018*, art. no. 1691428. https://doi.org/10.1155/2018/1691428
23. Park, S.H., Pauli, C.S., Gostin, E.L., Staples, S.K., Seifried, D., Kinney, C., Vanden Heuvel, B.D. (2022). Effects of short-term environmental stresses on the onset of cannabinoid production in young immature flowers of industrial hemp (*Cannabis sativa* L.). *Journal of Cannabis Research*, *4*, art. no. 1. https://doi.org/10.1186/s42238-021-00111-y
24. Regulation EU 2021/2115 of the European Parliament and of the Council of 2 December 2021 establishing rules on support for strategic plans to be drawn up by Member States under the common agricultural policy (CAP Strategic Plans) and financed by the European Agricultural Guarantee Fund (EAGF) and by the European Agricultural Fund for Rural Development (EAFRD) and repealing Regulations (EU) No 1305/2013 and (EU) No 1307/2013. https://eur-lex.europa.eu/eli/reg/2021/2115/oj
25. Regulation EU 2023/915 of 25 April 2023 on maximum levels for certain contaminants in food and repealing Regulation (EC) No 1881/2006. https://eur-lex.europa.eu/eli/reg/2023/915/oj
26. Taura, F., Sirikantaramas, S., Shoyama, Y., Yoshikai, K., Shoyama, Y., Morimoto, S. (2007). Cannabidiolic-acid synthase, the chemotype-determining enzyme in the fiber-type *Cannabis sativa*. *FEBS Letters*, *581*(16), 2929-2934. https://doi.org/10.1016/j.febslet.2007.05.043
27. Thamkaew, G., Sjoholm, I., Galindo, F.G. (2021). A review of drying methods for improving the quality of dried herbs. *Critical Reviews in Food Science and Nutrition*, *61*(11), 1763-1786. https://doi.org/10.1080/10408398.2020.1765309
28. Turner, J.C., Mahlberg, P.G. (1984). Effects of sample treatment on chromatographic analysis of cannabinoids in *Cannabis sativa* L. (Cannabaceae). *Journal of Chromatography A, 283*, 165–171. https://doi.org/10.1016/S0021-9673(00)96251-4
29. Ubeed, H.M.S.A.L., Wills, R.B.H., Chandrapala, J. (2022). Post-harvest operations to generate high-quality medicinal cannabis products: a systematic review. *Molecules*, *27*(5), art. no. 1719. https://doi.org/10.3390/molecules27051719
30. Uziel, A., Milay, L., Procaccia, S., Cohen, R., Burstein, A., Sulimani, L., Shreiber-Livne, I., Lewitus, D., Meiri, D. (2024). Solid-state microwave drying for medical cannabis inflorescences: A rapid and controlled alternative to traditional drying. *Cannabis and Cannabinoid Research*, *9*(1), 397-408. http://doi.org/10.1089/can.2022.0051
31. Wang, M., Wang, Y.H., Avula, B., Radwan, M.M., Wanas, A.S., van Antwerp, J., Parcher, J.F., ElSohly, M., Khan, I.A. (2016). Decarboxylation study of acidic cannabinoids: A novel approach using Ultra-High-Performance Supercritical Fluid Chromatography/Photodiode Array-Mass Spectrometry. Cannabis and Cannabinoid Research, 1(1), 262–271. https://doi.org/10.1089/can.2016.0020
32. Xie, Z., Mi, Y., Kong, L., Gao, M., Chen, S., Chen, W., Meng, X., Sun, W., Chen, S., Xu, Z. (2023). Cannabis sativa: Origin and history, glandular trichome development, and cannabinoid biosynthesis. Horticulture Research, 10(9), art. no. 150. https://doi.org/10.1093/hr/uhad150

INSTRUCTIONS FOR AUTHORS

SUBMISSION. Original contributions relevant to food and nutrition sciences are accepted on the understanding that the material has not been, nor is being, considered for publication elsewhere. All papers should be submitted and will be processed electronically via Editorial Manager system (available from PJFNS web site: http://journal.pan.olsztyn.pl). On submission, a corresponding author will be asked to provide: Cover letter; Files with Manuscripts, Tables, Figures/Photos; and Names of two potential reviewers (one from the author's homeland – but outside author's Institution, and the other from abroad). All papers which have been qualified as relevant with the scope of our Journal are reviewed. All contributions, except the invited reviews are charged. Proofs will be sent to the corresponding author and should be returned within one week since receipt. No new material may be inserted in the text at proof stage. It is the author's duty to proofread proofs for errors.

Authors should very carefully consider the preparation of papers to ensure that they communicate efficiently, because it permits the reader to gain the greatest return for the time invested in reading. Thus, we are more likely to accept those that are carefully designed and conform the instruction. Otherwise, papers will be rejected and removed from the online submission system.

SCOPE. The Polish Journal of Food and Nutrition Sciences publishes original, basic and applied papers, and reviews on fundamental and applied food research, preferably these based on a research hypothesis, in the following Sections:

Food Technology:
- Innovative technology of food development including biotechnological and microbiological aspects
- Effects of processing on food composition and nutritional value

Food Chemistry:
- Bioactive constituents of foods
- Chemistry relating to major and minor components of food
- Analytical methods

Food Quality and Functionality:
- Sensory methodologies
- Functional properties of food
- Food physics
- Quality, storage and safety of food

Nutritional Research:
- Nutritional studies relating to major and minor components of food (excluding works related to questionnaire surveys)

"News" section:
- Announcements of congresses
- Miscellanea

OUT OF THE SCOPE OF THE JOURNAL ARE:
- Works which do not have a substantial impact on food and nutrition sciences
- Works which are of only local significance i.e. concern indigenous foods, without wider applicability or exceptional nutritional or health related properties
- Works which comprise merely data collections, based on the use of routine analytical or bacteriological methods (i.e. standard methods, determination of mineral content or proximate analysis)
- Works concerning biological activities of foods but not providing the chemical characteristics of compounds responsible for these properties
- Nutritional questionnaire surveys
- Works related to the characteristics of foods purchased at local markets
- Works related to food law
- Works emphasizing effects of farming / agricultural conditions / weather conditions on the quality of food constituents
- Works which address plants for non-food uses (i.e. plants exhibiting therapeutic and/or medicinal effects)

TYPES OF CONTRIBUTIONS. *Reviews*: (at least: 30 pages and 70 references) these are critical and conclusive accounts on trends in food and nutrition sciences; *Original papers*: (maximally: 30 pages and 40 references) these are reports of substantial research; *Reports on post and forthcoming scientific events, and letters to the Editor* (all up to three pages) are also invited (free of charge).

REVIEW PROCESS. All scientific contributions will be peer-reviewed on the criteria of originality and quality. Submitted manuscripts will be preevaluated by Editor-in-Chief and Statistical Editor (except for review articles), and when meeting PJFNS' scope and formal requirements, they will be sent to a Section Editor who upon positive preevaluation will assign at least two reviewers from Advisory Board Members, reviewers suggested by the author or other experts in the field. Based on the reviews achieved, Section Editor and Editor-in--Chief will make a decision on whether a manuscript will be accepted for publication, sent back to the corresponding author for revision, or rejected. Once a manuscript is sent back to the corresponding author for revision, all points of the reviews should be answered or rebuttal should be provided in the Explanation letter. The revised manuscripts will be checked by Section Editor and by the original reviewers (if necessary), and a final decision will be made on acceptance or rejection by both Section Editor and Editor-in-Chief.

Polish Journal of Food and Nutrition Sciences uses CrossCheck's iThenticate software to detect instances of similarity in submitted manuscripts. In publishing only original research, PJFNS is committed to deterring plagiarism, including self-plagiarism.

COPYRIGHT LICENSE AGREEMENT referring to Authorship Responsibility and Acknowledgement, Conflict of Interest and Financial Disclosure, Copyright Transfer, are required for all authors, i.e. *Authorship Responsibility and Acknowledgement*: Everyone who has made substantial intellectual contributions to the study on which the article is based (for example, to the research question, design, analysis, interpretation, and written description) should be an author. It is dishonest to omit mention of someone who has participated in writing the manuscript ("ghost authorship") and unfair to omit investigator who have had important engagement with other aspects of the work. All contributors who do not meet the criteria for authorship should be listed in an Acknowledgments section. Examples of those who might be acknowledged include a person who provided purely technical help, writing assistance, or a department chairperson who provided only general support. Any financial and material support should also be acknowledged. *Conflict of Interest and Financial Disclosure*: Authors are responsible for disclosing financial support from the industry or other conflicts of interest that might bias the interpretation of results. *Copyright License Agreement*: Authors agree to follow the Creative Commons Attribution-Non--Commercial-NoDerivs 4.0 License.

A manuscript will not be published once the signed form has not been submitted to the Editor with the manuscript revised after positive reviews.

CHANGES TO AUTHORHIP. Authors are expected to consider carefully the list and order of authors before submitting their manuscript and provide the definitive list of authors at the time of the original submission. Any addition, deletion or rearrangement of author names in the authorship list should be made only before the manuscript has been accepted and only if approved by the journal Editor. To request such a change, the Editor must receive the following from the corresponding author: (a) the reason for the change in author list and (b) written confirmation (e-mail, letter) from all authors that they agree with the addition, removal or rearrangement. In the case of addition or removal of authors, this includes confirmation from the author being added or removed.

ETHICAL APPROVAL OF STUDIES AND INFORMED CONSENT. For all manuscripts reporting data from studies involving human participants or animals, formal approval by an appropriate institutional review board or ethics committee is required and should be described in the Methods section. For those investigators who do not have formal approval from ethics review committees, the principles outlined in the Declaration of Helsinki should be followed. For investigations of humans, state in the Methods section the manner in which informed consent was obtained from the study participants (i.e., oral or written). Editors may request that authors provide documentation of the formal review and recommendation from the institutional review board or ethics committee responsible for oversight of the study.

UNAUTHORIZED USE. Unauthorized use of the PJFNS name, logo, or any content for commercial purposes or to promote commercial goods and services (in any format, including print, video, audio, and digital) is not permitted by IAR&FR PAS.

MANUSCRIPTS. A manuscript in English must be singlesided, preferably in Times New Roman (12) with 1.5-point spacing, without numbers of lines. The Editor reserves the right to make literary corrections and to make suggestions to improve brevity. English is the official language. The English version of the paper will be checked by Language Editor. Unclear and unintelligible version will be returned for correction.

Every paper should be divided under the following headings in this order: a **Title** (possibly below 150 spaces); the **Name(s)** of the author(s) in full. In paper with more than one author, the asterisk indicates the name of the author to whom correspondence and inquiries should be addressed, otherwise the first author is considered for the corre-spondence. Current full postal address of the indicated corresponding author or the first author must be given in a footnote on the title page; the **Place(s)** where the work was done including the institution name, city, country if not Poland. In papers originated from several institu-tions the names of the authors should be marked with respective superscripts; the **Key words** (up to 6 words or phrases) for the main topics of the paper; an **Abstract** (up to 250 words for regular papers and reviews) summarizing briefly main results of the paper, no literature references; an **Introduction** giving essential background by saying why the research is important, how it relates to previous works and stating clearly the objectives at the end; **Materials and Methods** with sufficient experimental details permitting to repeat or extend the experiments. Literature references to the methods, sources of material, company names and location (city, country) for specific instruments must be given. Describe how the data were evaluated, including selection criteria used; **Results and Discussion** presented together (in one chapter). Results should be presented concisely and organized to supplement, but not repeat, data in tables and figures. Do not display the data in both tabular and graphic form. Use narrative form to present the data for which tables or figures are unnecessary. Discussion should cover the implications and consequences, not merely recapitulating the results, and it must be accomplished with concise **Conclusions**; **Acknowledgements** should be made to persons who do not fill the authorship criteria (see: Authorship forms); **Research funding** should include financial and material support; **Conflict of Interests**: Authors should reveal any conflicts of interest that might bias the interpretation of results; and **References** as shown below.

REFERENCES each must be listed alphabetically at the end of the paper (each should have an Arabic number in the list) in the form as follows: **Periodicals** – names and initials of all the authors, year of publication, title of the paper, journal title as in Chemical Abstracts, year of publication, volume, issue, inclusive page numbers, or article id.; **Books** – names and initials of all the authors, names of editors, chapter title, year of publication, publishing company, place of publication, inclusive page numbers; **Patents** – the name of the application, the title, the country, patent number or application number, the year of publication.

For papers published in language other than English, manuscript title should be provided in English, whereas a note on the original language and English abstract should be given in parentheses at the end.

The reference list should only include peer-reviewed full-text works that have been published or accepted for publication. Citations of MSc/PhD theses and works unavailable to international Editors, Reviewers, and Readers should be limited as much as possible.

References in the text must be cited by name and year in square parentheses (e.g.: one author – [Tokarz, 1994]; two authors – [Słonimski & Campbell, 1987]; more than two authors – [Amarowicz *et al*., 1994]). If more than one paper is published in the same year by the same author or group of authors use [Tokarz, 1994a, b]. Unpublished work must only be cited where necessary and only in the text by giving the person's name.

Examples:

Article in a journal:

Słonimski, B.A., Campbell, L.D., Batista, E., Howard B. (2008). Gas chromatographic determination of indole glucosinolates. Journal of Science and Food Agriculture, 40(5), 131–143.

Asher, A., Tintle, N.L., Myers, M., Lockshon, L., Bacareza, H., Harris, W.S. (2021). Blood omega-3 fatty acids and death from COVID-19: A pilot study. *Prostaglandins, Leukotrienes and Essential Fatty Acids, 166*, art. no. 102250.

Book:

Weber, W., Ashton, L., Milton, C. (2012). Antioxidants – Friends or Foes? 2nd edition. PBD Publishing, Birmingham, UK. pp. 218–223.

Chapter in a book:

Uden, C., Gambino, A., Lamar, K. (2016). Gas chromatography. In M. Queresi, W. Bolton (Eds.), CRC Handbook of Chromatography, CRC Press Inc., Boca Raton, Florida, USA, pp. 44–46.

ABBREVIATIONS AND UNITS. Abbreviations should only be used when long or unwieldy names occur frequently, and never in the title; they should be given at the first mention of the name. Metric SI units should be used. The capital letter L should be used for liters. Avoid the use of percentages (% g/g,% w/w; Mol%; vol%), ppm, ppb. Instead, the expression such as g/kg, g/L, mg/kg, mg/mL should be used. A space must be left between a number and a symbol (e.g. 50 mL not 50mL). A small x must be used as multiplication sign between numeric values (e.g. 5 × 102 g/mL). Statistics and measurements should be given in figures, except when the number begins a sentence. Chemical formulae and solutions must specify the form used. Chemical abbreviations, unless they are internationally known, Greek symbols and unusual symbols for the first time should be defined by name. Common species names should be followed by the Latin at the first mention, with contracting it to a single letter or word for subsequent use.

FIGURES should be submitted in separate files. Each must have an Arabic number and a caption. Captions of all Figures should be provided on a separate page "Figure Captions". Figures should be comprehensible without reference to the text. Self-explanatory legend to all figures should be provided under the heading "Legends to figures"; all abbreviations appearing on figures should be explained in figure footnotes. Three-dimensional graphs should only be used to illustrate real 3D relationships. Start the scale of axes and bars or columns at zero, do not interrupt them or omit missing data on them. Figures must be cited in Arabic numbers in the text.

TABLES should be submitted in separate files. They should be as few in number and as simple as possible (like figures, they are expensive and space consuming), and include only essential data with appropriate statistical values. Each must have an Arabic number and a caption. Captions of all Tables should be provided on a separate page "Table Captions". Tables should be self-explanatory; all abbreviations appearing in tables should be explained in table footnotes. Tables must be cited in Arabic numbers in the text.

PAGE CHARGES. A standard publication fee has been established at the rate of 450 EUR + tax (if applicable, e.g. for private persons) irrespective of the number of pages and tables/figures. For Polish Authors an equivalent fee was set at 1950 PLN + VAT. Payment instructions will be sent to Authors via e-mail with acceptance letter.

Information on publishing and subscription is available from:

Ms. Joanna Molga
Editorial Office of Pol. J. Food Nutr. Sci.
Institute of Animal Reproduction and Food Research Tuwima 10 Str., 10–748 Olsztyn 5, Poland
phone (48 89) 523–46–70, fax (48 89) 523–46–70;
e-mail: pjfns@pan.olsztyn.pl; http://journal.pan.olsztyn.pl

Nutrition